(3)

The Thorium Benzyne
and
The Cerium(IV)-Nitrogen Bond

by

Anthony F. England

Submitted to the Department of Chemistry
in Partial Fulfillment of the Requirements for the Degree of

DOCTOR OF PHILOSOPHY
in Organic Chemistry

at the

Massachusetts Institute of Technology

June, 1995

© 1995 Massachusetts Institute of Technology

All rights reserved
The author hereby grants to MIT permission to reproduce and to distribute
publicly paper and electronic copies of this thesis document in
whole or in part

Signature of Author . . . . . .
Department of Chemistry
February 18th, 1995

Certified by . . . . . .
Stephen L. Buchwald
Department of Chemistry
Thesis Supervisor

Accepted by . . . . . .
Dietmar Seyferth
Chairman, Departmental Committee on Graduate Students

Science
MASSACHUSETTS INSTITUTE
OF TECHNOLOGY

JUN 12 1995

This doctoral thesis has been examined by a Committee of the Department of Chemistry as follows:

Professor Gregory C. Fu . . . . . .
Chairman

Professor Stephen L. Buchwald . . . . . .
Thesis Supervisor

Professor Alan Davison. . . . . .

and

Dr. Carol J. Burns . . . . . .
Los Alamos National Laboratory External Committee Member

The Thorium Benzyne
and
The Cerium(IV)-Nitrogen Bond
by
Anthony F. England

Submitted to the Department of Chemistry on February 18th, 1995 in partial fulfillment of the requirements for the Degree of Doctor of Philosophy in Organic Chemistry

Abstract:

The chemistry of transiently stable benzyne complexes of thorium(IV) has been investigated. An efficient Grignard reagent mediated procedure for the synthesis of the diphenyl precursor complex, and new methyl aryl derivatives has been developed. *Ortho*-methyl substituted aryl complexes of this type also undergo facile generation of benzyne intermediates, whereas intramolecular C-H activation chemistry is limited in analogous *ortho*-methoxy substituted species. Solution and solid state structural evidence suggests that geometrical constraints and chelation effects are responsible for these observations.

Novel regioselective ligand activation processes occur when the benzyne intermediate is generated in the presence of selected Lewis bases. Product analysis suggests that substrate precoordination is important to the reaction outcome. Examples of aromatic and benzylic carbon-hydrogen activation, along with phosphorus-oxygen bond cleavage have been demonstrated by this highly reactive organoactinide species.

Simple amide complexes of cerium(IV) have been synthesized and structurally characterized for the first time. Silicon stabilized amide ligands have been employed to support the tetravalent lanthanide; primary and dialkyl substituted bases promote redox chemistry. Ligand redistribution processes are also common in these systems, typically serving to reduce the metal center, although tetravalent rearrangement products have also been generated.

Thesis Supervisor: Dr. Stephen L. Buchwald
Title: Professor of Chemistry

So, yes, fair enough, a Ph.D. requires quite an effort for a few years
But it doesn't amount to a lifetime of hard work and devotion
Dedicated to two people that have really earned this degree

To Mum and Dad

Mary Teresa England
February 24th, 1942 - October 14th, 1993

My Mother's love never to be replaced,
I miss you Mum - Love Anthony

But then to me, she was only my Mother.

And to Granny and Mike on the occasion
of your 97th and 30th Birthdays, twelve days ago

Acknowledgment

More so than particular individuals I would like to thank anyone and everyone that has given their time to help me in whatever way, knowingly so, or not. To those that did not feel appreciated at the time - I apologize; Thanks a lot.

Specifically, I am indebted to my supervisor, Professor Steve Buchwald, for the interactions which have taught me so much throughout my time in his research group. Furthermore for his patience, allowing me time when I most needed it. I am also thankful to Steve for the rare opportunity handed to me to take time away from Cambridge, traverse the continent and pursue research goals in Los Alamos. In addition, random acts of silliness will be fondly remembered - Cuny's ant pheromone stands out.

In Los Alamos, I would first like to thank Shannon Burns for allowing me to borrow her mom at times over the last couple of years. It has been a pleasure to have Dr. Carol Burns as an advisor at LANL, both while in New Mexico and more recently throughout a continued collaboration at MIT. Truly a motivational and inspirational relationship.

Cheers to the Buchwald group past and present (spanning Donald to Udo), Bob the glassblower and LANL's INC-4/-1/CST-3/-18, or whatever it is called this week, for making work a little less such. To Rick Broene, the definitive postdoc/ski partner - just about the best introduction to a foreign situation a new group member could ask for.

Cheers also to the lads, to Linda too, responsible for most of the laughs outside of the lab, for the coffees, beers and the rest. To various alarm clocks, cowboy doctors, all at BU from IR to Soc, Sergeant Eddie, the 380 and staff of 500 Mem. Dr. To roommates in Los Alamos: Susan for the free cash and Dave for actually being around; Jim and Margo, the blue fox, the piñata rabbits, and the other Dave in New York.

Table of Contents

Chapter One 15

The Thorium Benzyne: Grignard Reagent Mediated Syntheses of $Cp^*_2Th(Phenyl)_2$ and $Cp^*_2Th(Methyl)(Aryl)$ Derivatives

Introduction 17

Results and Discussion 19

Summary 25

Experimental 26

References 30

Chapter Two 33

The Thorium Benzyne: Structure-Reactivity Relationships in Precursor Complexes: Solution and Solid State Structures of $Cp_2Zr(Me)(o\text{-}MeOC_6H_4)$ and $Cp^*_2Th(Me)(o\text{-}MeOC_6H_4)$

Introduction 35

Results and Discussion 38

Summary 58

Experimental 59

References 61

Chapter Three 65

The Thorium Benzyne: Reactivity of the $Cp^*_2Th(C_6H_4)$ Moiety with Lewis Bases

Introduction 67

Results and Discussion 71

Summary 123

Experimental 124

References 128

Chapter Four 135

The Cerium(IV)-Nitrogen Bond: Studies into the Synthesis of Simple Amide Complexes of Cerium(IV)

Introduction 137

Results and Discussion 147

Summary 190

Experimental 191

References 203

Appendix

Appendix to Chapter Two 211

Appendix to Chapter Three 231

Appendix to Chapter Four 273

CHAPTER ONE[1]

The Thorium Benzyne: Grignard Reagent Mediated Syntheses of $Cp^*_2Th(Phenyl)_2$ and $Cp^*_2Th(Methyl)(Aryl)$ Derivatives

Introduction

Organometallic complexes of the Group 4 metals are of considerable utility in organic synthesis, and are important reagents in such varied reactions as the hydrometallation,[2] olefin polymerization,[3,4] and reductive coupling[5-11] of unsaturated substrates. The bis(cyclopentadienyl) zirconium systems $Cp_2Zr(C_6H_5)_2$ and $Cp_2Zr(CH_3)(Ar)$ (Cp = η^5-cyclopentadienyl; Ar = e.g., *o*-tolyl, *o*-anisyl, 2-naphthyl) have been employed as general precursors to zirconocene aryne complexes by means of thermally induced intramolecular C-H activation reaction.[12-16] Thermally stable adducts of the benzyne complexes may be obtained by conducting these eliminations in the presence of a stabilizing Lewis base such as trimethylphosphine (eq 1). The resultant adducts are isolable, and are useful as reagents for subsequent organic transformations.[17]

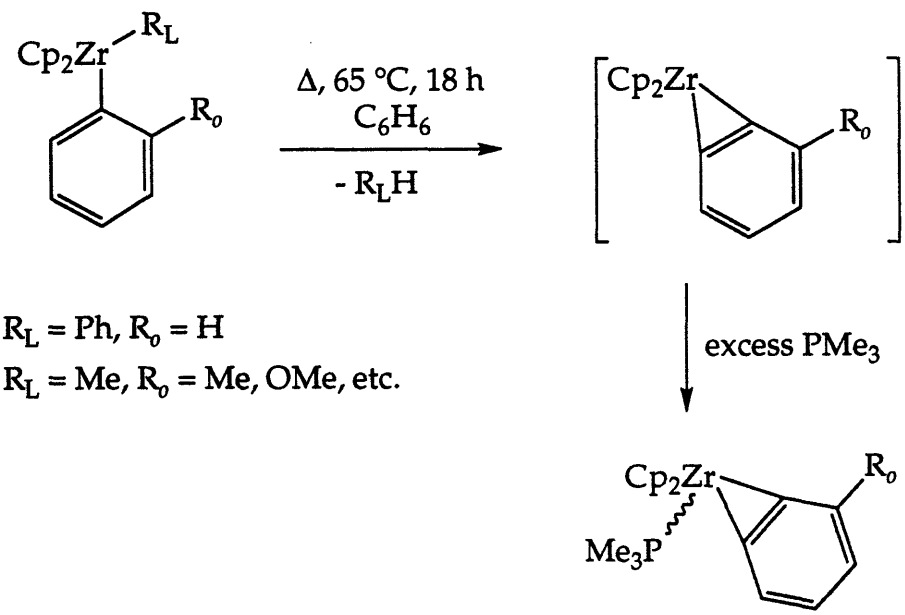

R_L = Ph, R_o = H
R_L = Me, R_o = Me, OMe, etc.

(1)

Tetravalent early actinide (i.e. Th and U) complexes often display chemistry similar to that of the Group 4 metals.[18-20] The large ionic radius and electropositive nature of the heavy elements, however, enables elimination reactions, proceeding by way of intramolecular C-H or N-H activation, to occur more readily than analogous reactions in the *d*-transition series.[21-25] It has previously been reported that solutions of the complexes $Cp^*_2An(C_6H_5)_2$ (Cp^* = η^5-pentamethylcyclopentadienyl; An = Th, U) eliminate benzene at or above room temperature. The formation of benzyne

intermediates in this system has been postulated from deuterium labeling experiments, and in the case of uranium, a uranaindene complex was prepared from the insertion of diphenylacetylene into one of the two U-C bonds of the transient Cp^*_2U(benzyne) species (Scheme 1).[22] As part of a

Scheme 1

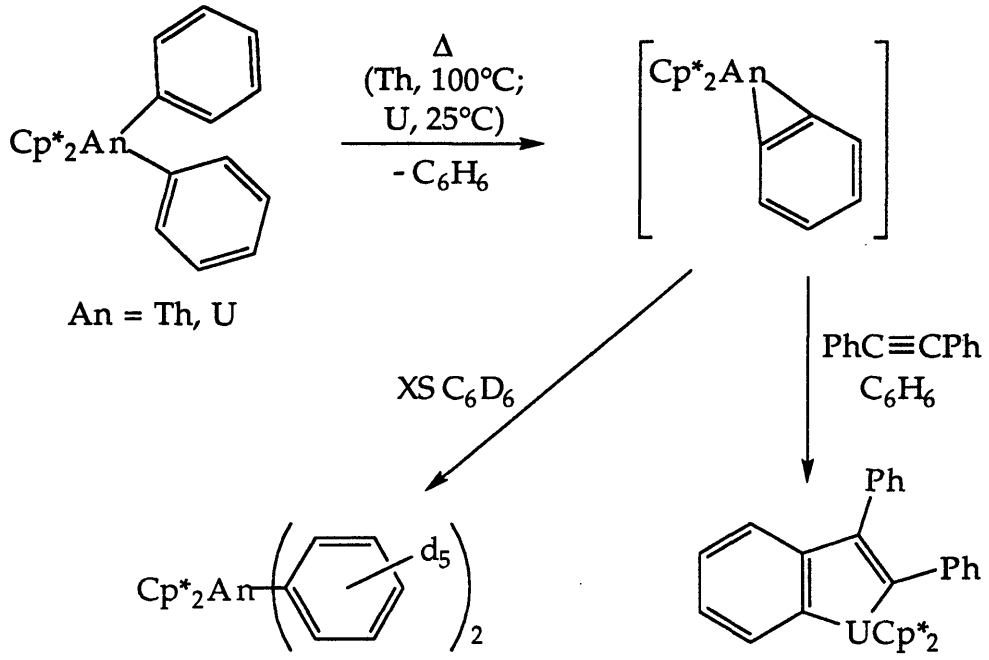

study of the generation and reactivity of actinide benzyne complexes,[26] we have developed a general synthetic route to a series of alkyl-aryl complexes of thorium. To the best of our knowledge, there are no previous reports of mixed alkyl-aryl complexes. Such complexes could prove to be suitable precursors to benzyne species, in analogy with Group 4 chemistry. A modified procedure provides a simple, high yield route to the diphenyl complex $Cp^*_2ThPh_2$ (**1**).

Results and Discussion

Extensive studies of the ligand metathesis chemistry of $Cp^*_2ThCl_2$ have been conducted by Marks and coworkers.[21,22] These investigations have demonstrated the utility of alkyllithium reagents in the preparation of the dialkyl derivatives $Cp^*_2ThR_2$ (e.g. R = Me, CH_2CMe_3, CH_2SiMe_3, CH_2Ph, Ph). Yields realized using this synthetic route are, however, only moderate. For example, the reaction of $Cp^*_2ThCl_2$ with phenyllithium (Et_2O, -78 °C, 5h) is reported to produce the diphenyl complex, $Cp^*_2Th(C_6H_5)_2$ (**1**) in 32-40% yield.[22]

In order to prepare sufficient quantities of this and related complexes needed for our investigation of actinide benzyne complexes, we sought to improve upon this method by developing a high yield route to both the diphenyl complex and its monoalkyl-monoaryl analogues **2-4**. We have found that the use of Grignard reagents as the alkylating agent provides a convenient and reliable means for the preparation of **1**. Grignard reagents have frequently been used in the preparation of Group 4 metallocene alkyl-halide and some homoleptic dialkyl complexes, although reported preparations of mixed dialkyl derivatives most commonly employ organolithium reagents in the second step.[6,27-30] Magnesium reagents have similarly been employed in organoactinide chemistry, both in the preparation of $Cp^*_2AnCl_2$ (An = Th, U) from the tetrachlorides, $AnCl_4$,[22] and in the further alkylation of $Cp^*_2AnCl_2$ to generate the dialkyls $Cp^*_2An(\eta^4\text{-}C_4H_6)$ [31,32] and $Cp^*_2Th(CH_2CH_2CH_3)_2$.[22] Currently, the scope of the use of Grignard reagents in the synthesis of titanocene alkyl-aryl complexes is under further investigation, with the preparation of differentially substituted benzyne precursors directly from commercially available air-stable metallocene dichloride starting materials.[33] This methodology has allowed for the preparation of derivatives not previously accessible by organolithium routes,[33] as well as improved syntheses of known complexes.[34]

A rapid reaction takes place upon addition of phenylmagnesium bromide solution to a toluene solution of $Cp^*_2ThCl_2$ at room temperature. Within minutes after the Grignard addition, the starting dichloride is no longer detectable in the ^1H NMR spectrum of the reaction mixture. The reaction product is not solely the diphenyl complex, however, but rather a mixture of **1** and the intermediate phenyl-halide complex.[22] Complete

conversion to form the diphenyl complex does not occur utilizing extended reaction times, elevated reaction temperatures, or an excess of Grignard reagent.

The addition of *p*-dioxane to the reaction mixture is key in the preparation of pure **1**. The room temperature reaction between $Cp^*_2ThCl_2$ (1 equiv), PhMgBr (≥ 2 equiv) and *p*-dioxane (≥ 2 equiv) provides a convenient preparation of $Cp^*_2ThPh_2$ in greater than 80% isolated yield (eq 2). A

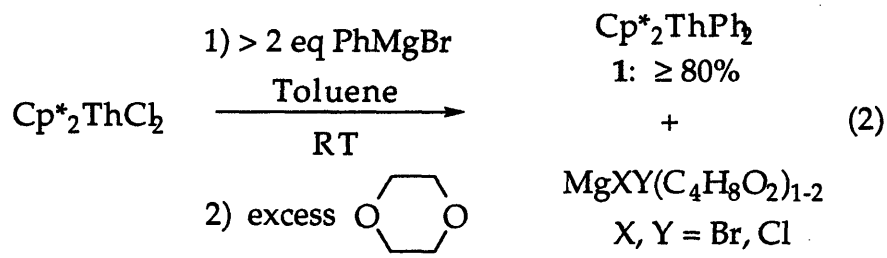

(2)

comparison of the ^1H NMR spectra of the product with that described in the literature illustrates the high degree of conversion achieved, even after only a short reaction time. By-products comprise only a small fraction of the reaction product (≤ 5%).

In the absence of dioxane, incomplete alkylation is likely due to back reaction between the product diphenyl thorium complex and solubilized magnesium salts. Electropositive metal complexes are known to participate in Schlenk-type equilibria with magnesium halides; halide exchange and the formation of complex mixed-metal halide complexes is well documented.[35-38] Halogen exchange reactions mediated by Grignard reagents have also been observed in Group 4 chemistry.[39]

Addition of *p*-dioxane permits removal of precipitated $MgX_2(dioxane)_x$ adducts from solution[40] and eliminates the possibility of back-reaction, driving the equilibrium toward the formation of **1** (Scheme 2). This simple methodology has been extended to the stepwise double alkylation of $Cp^*_2ThCl_2$, providing a direct route to the methyl-aryl complexes $Cp^*_2Th(Me)(o\text{-}Ar)$ (*o*-Ar = *o*-$MeOC_6H_4$ (**2**), *o*-MeC_6H_4 (**3**), 2, 5-$Me_2C_6H_3$ (**4**)) (Scheme 3). The preparation of **2-4** has been successful both with and without isolation of the respective aryl-halide intermediates, **5-7**.

Unlike the preparation of **1**, the syntheses of the methyl substituted aryl complexes **3** and **4** are adversely affected by the use of an excess of Grignard reagent, resulting in reduced product purity. However, a similar

Scheme 2

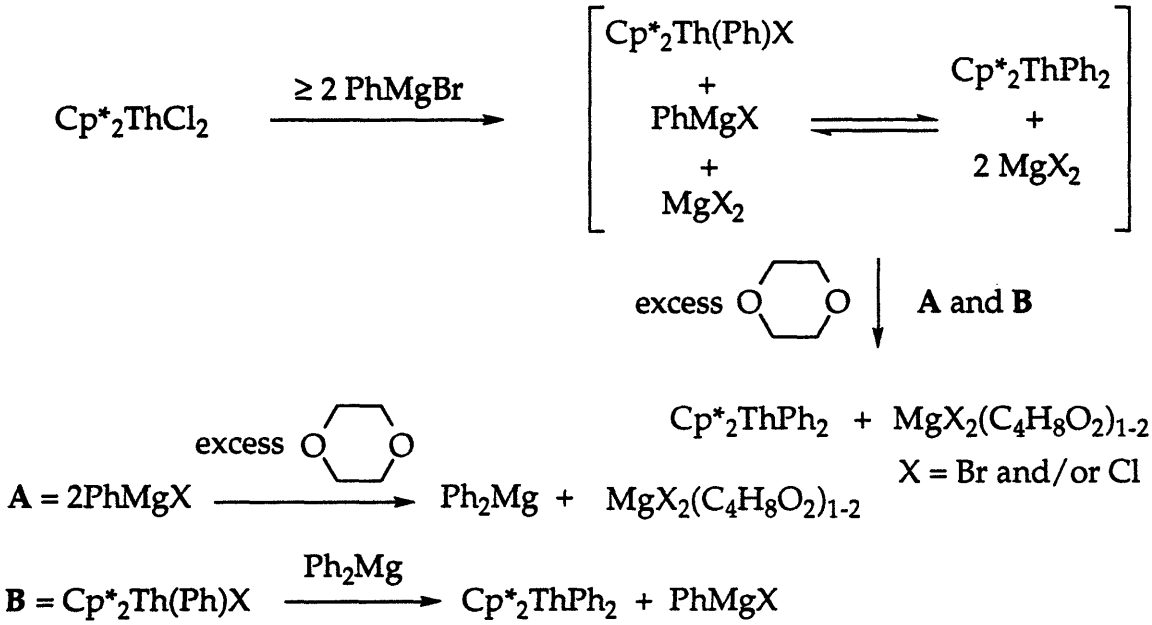

Scheme 3

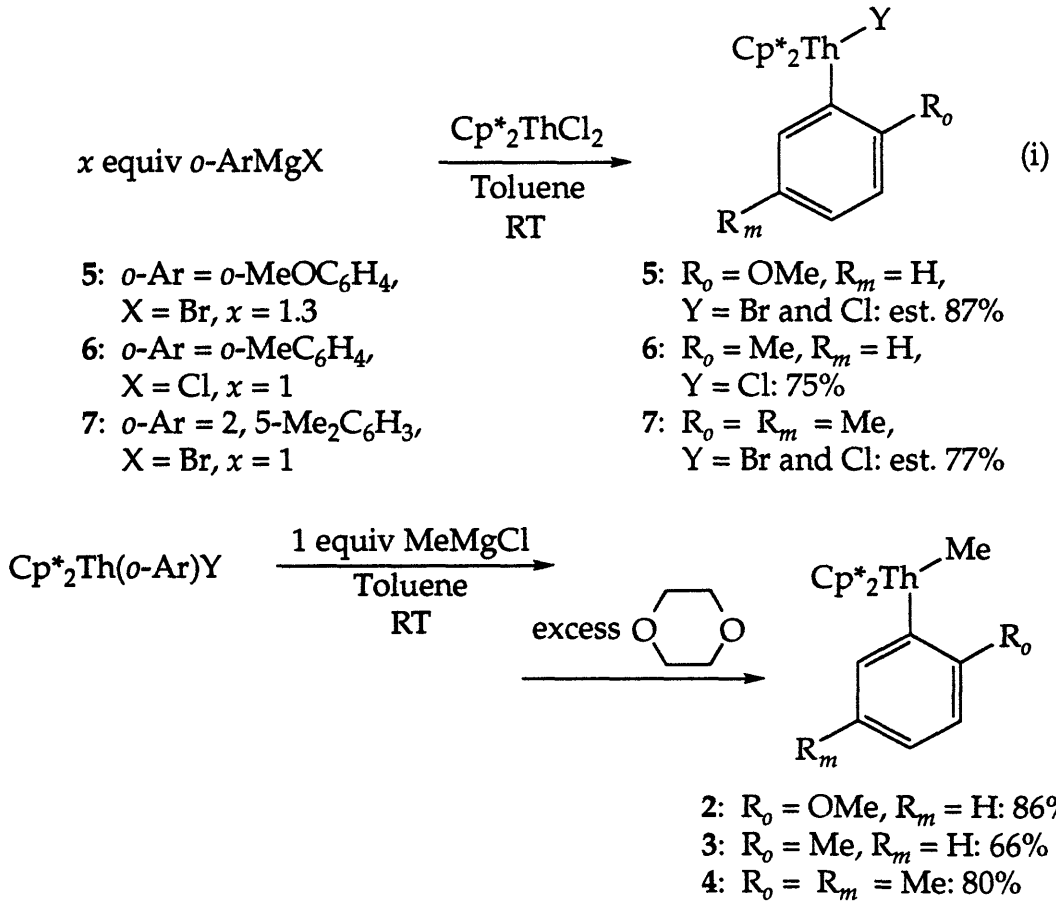

effect is not observed in the preparation of the *o*-anisyl derivative, **2**, and an excess of Grignard is generally employed to achieve the best possible conversion.

In the procedures to prepare **2-4** from the respective aryl halides, *p*-dioxane is again added to the reaction mixtures. Experiments with the *o*-anisyl halide system have indicated that, in the absence of the complexing agent, conversion to the methyl-aryl species is limited; significant quantities of unreacted **5** are observed in the ^{1}H NMR spectrum of the reaction mixture.

The presence of THF (THF = tetrahydrofuran) in the preparations of **6** and **7** also results in the formation of significantly less pure products (the preparation of the *o*-anisyl derivative, **5**, is again less sensitive to variations in reaction conditions). The cleanest products are generally obtained upon removal of the THF solvent from the Grignard reagent prior to reaction with $Cp^*_2ThCl_2$. When the reaction is carried out in the presence of THF, ^{1}H NMR spectra of the crude reaction mixtures of **3** and **4** clearly indicate the presence of significant quantities of coordinated THF. The introduction of impurities in both cases is likely due to the presence of solubilized magnesium species, whether free or associated with the thorium complex. THF adducts of both magnesium halides[41,42] and bis(alkyl)magnesium species[43] are known to exist, and may be carried through in the isolation of the thorium complexes. The tolerance of the *o*-anisyl system to variation in stoichiometry may be due to intra- or intermolecular magnesium-oxygen interactions which affect the solubility characteristics of the dialkyl species and/or inhibit THF coordination.[41]

The complexes **6** and **7** exist as pairs of rotamers (**I** and **II**). The *ortho*-methyl substituent of the aryl group in each is sufficiently bulky to inhibit free rotation about the metal-aryl bond. Variable temperature ^{1}H NMR

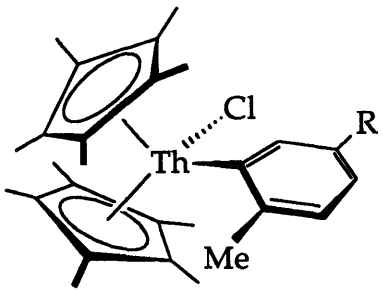

I

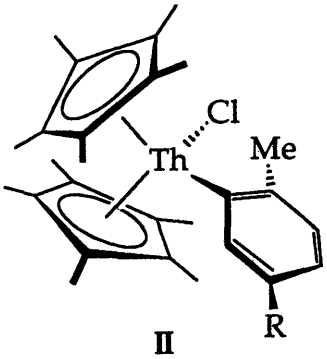

II

R = H, Me

experiments performed on **6** and **7** have verified this phenomenon, since the rotameric pairs are observed to coalesce at elevated temperatures (≈ 85-100 °C). This hindered rotation is not unexpected, judging from reports of similar barriers to rotation for the complexes $Cp^*_2U(C_6H_5)_2$,[22] and related bis(pentamethylcyclopentadienyl) actinide systems.[22,24,44] Rotamers are not, however, observed for **5**. The possibility of free rotation in the *o*-anisyl system exists, although it is far more likely that the molecule is observed in one conformation only, due to being constrained by a significant intramolecular thorium-oxygen interaction.[45]

The situation for complex **7** is further complicated in that the alkylation of $Cp^*_2ThCl_2$ by 2-(*p*-xylyl)magnesium bromide results in the formation of a mixture two pairs of aryl-halide rotamers, i.e $Cp^*_2Th(2, 5\text{-}Me_2C_6H_3)(X)$ (X = Br, Cl). Mixtures of the chloride and bromide derivatives are generated in alkylations to prepare both **5** and **7** as the result of the halide-exchange equilibrium between the actinide metal center and solvated magnesium species. The bromide derivative appears to be favored, with product ratios ranging from near parity to almost two to one (Br/Cl), depending on both the aryl substituent and exact reaction stoichiometries. We have been able to successfully distinguish between the two halide derivatives $Cp^*_2Th(o\text{-}Ar)X$ (*o*-Ar =*o*-$MeOC_6H_4$, 2, 5-$Me_2C_6H_3$; X = Br, Cl) by selectively enhancing the chloride component of the halide mixtures. The room temperature reaction between $Cp^*_2Th(o\text{-}Ar)X$ and an excess of $MgCl_2(THF)_2$[43] in toluene greatly increases the $Cp^*_2Th(o\text{-}Ar)Cl$ fraction. The observed halide ratios in the mixed species **5** and **7** may also be perturbed by the addition of *p*-dioxane. The presence of a large excess of *p*-dioxane results in the formation of product mixtures comprised of at least 90% chloride. The use of arylmagnesium chloride reagents in alkylation, as in the preparation of **6**, assures the formation of only one halide product.

Reaction of the aryl-halide complexes with MeMgCl in toluene results in the preparation of the methyl-aryl complexes, $Cp^*_2Th(Me)(o\text{-}Ar)$ (*o*-Ar = *o*-$MeOC_6H_4$ (**2**), *o*-MeC_6H_4 (**3**), 2, 5-$Me_2C_6H_3$ (**4**)). The dimethyl compound, $Cp^*_2ThMe_2$, is a common side-product in the methylation of the aryl-halide species, and results by way of displacement of the aryl substituent from the starting $Cp^*_2Th(o\text{-}Ar)X$ (X = Br, Cl) and/or product $Cp^*_2Th(Me)(o\text{-}Ar)$. $Cp^*_2ThMeCl$ has also been observed to form.[44] Any further reduction in the

purity of the products from the preparation of **2-7** are seemingly due to unreacted starting materials and solvated magnesium species.

Steric congestion about the actinide center may be responsible for the failure to observe the *ortho*-substituted diaryl complexes, even in the presence of excess aryl Grignard. Spectroscopic investigations of $Cp^*_2U(C_6H_5)_2$ suggest that the phenyl rings are required to be juxtaposed in a canted manner.[22] *Ortho*-substitution of these aryl ligand would be expected to exacerbate steric constraints within the tight framework. Although the Group 4 analog, di-*o*-tolyl zirconocene is known to exist transiently, this complex contains a less bulky bis(cyclopentadienyl) (Cp_2) ligand set, and decomposes readily, even at low temperatures.[13]

Summary

A simple Grignard alkylation strategy has been employed to prepare the known complex **1** and the previously unreported complexes **2-7**. All of the reported alkylation reactions occur readily in non-coordinating solvents at room temperature, and provide the desired products in moderate to high yields. Similarly, the alkyl-aryl systems **2-4** have been prepared in good yield by a one-pot method from $Cp^*_2ThCl_2$. Methylation of the intermediate aryl-halide complexes **5-7** is readily achieved, but attempts to prepare the bis-*o*-substituted aryl derivatives have proven unsuccessful. Formation of these complexes is doubtless prevented by unfavorable steric interactions.

In the absence of *o*-substituted diaryl complexes analogous to the diphenyl complex, preliminary studies have demonstrated the utility of complexes **2-4** as suitable alternate precursors in the preparation of substituted benzyne complexes. Studies of the thermal reactions of these species have provided insight into the mechanism of formation and reactivity of the thorium benzyne species.[45] Further, the unsubstituted diphenyl complex **1**, a known benzyne precursor, has been the subject of a comparison study of actinide and Group 4 benzyne reactivity.[26,45] In all cases, it has proven unnecessary to further purify these materials to ensure successful reactivity.

These procedures for the preparation of **1-7** demonstrate the facile nature of metathesis reactions between actinide halides and Grignard reagents. Using this methodology, second alkylations of the metal center proceed readily. Magnesium mediated alkyl and halide redistribution equilibria have been observed; these can result in "over-methylation" to yield $Cp^*_2ThMe_2$ in the preparation of **2-4**, or in halide exchange equilibria in the preparation of the aryl halide precursors **5** and **7**.

Experimental

General Procedures. All manipulations were conducted under an atmosphere of helium in a Vacuum Atmospheres Co. drybox. Nuclear Magnetic Resonance (NMR) spectra were recorded on an IBM (Bruker) AF-250 MHz spectrometer. NMR chemical shifts were determined in benzene-d_6, and are internally referenced to the solvent (^{1}H, δ 7.15; ^{13}C, δ 128.0). Elemental analyses were performed in our laboratory using a Perkin-Elmer 2400 CHN analyzer.[46] Solvents were distilled from sodium/benzophenone ketyl (*p*-dioxane, hexane, diethyl ether, and toluene). Benzene-d_6 was vacuum transferred, after drying over calcium hydride. $Cp^*_2ThCl_2$ was prepared according to the published procedure.[22] Stock solutions of *o*-anisylmagnesium bromide and 2-(*p*-xylyl)magnesium bromide were prepared, using standard Schlenk techniques, from the respective arylbromides and magnesium in THF. The concentrations of prepared Grignard reagents were determined after titration with *sec*-butanol, in toluene, using 1,10-phenanthroline as the indicator.[47] Methylmagnesium chloride (3.0 M in THF, d = 1.013 g/mL), phenylmagnesium bromide (3.1 M in Et_2O, d = 0.939 g/mL), *o*-tolylmagnesium chloride (1.0 M in THF, d = 0.956 g/mL) solutions, 2-bromoanisole and 2-bromo-*p*-xylene were purchased from Aldrich and used as received. The purity of isolated powders was determined by integration of methyl resonances in the product ^{1}H NMR spectrum of a weighed sample against a known quantity of hexamethylbenzene internal standard.

$Cp^*_2Th(C_6H_5)_2$ (1). Phenylmagnesium bromide (1.48 g, 4.89 mmol) was added to a stirred solution of $Cp^*_2ThCl_2$ (1.03 g, 1.80 mmol) in toluene (20 mL) at room temperature, resulting in the formation of a yellow suspension. After 40 min of stirring, *p*-dioxane (0.435 g, 4.94 mmol) was added to the reaction mixture, giving rise to an immediate precipitation of solids and the formation of a thick cream-colored suspension. Stirring was continued for 2 h, during which time the suspension turned yellow in color. The volatiles were removed under reduced pressure to yield a cream colored product powder. The solid was extracted with toluene (4 x 15 mL) and filtered through Celite to remove insoluble salts. Toluene was removed under reduced pressure to yield **1** as an off-white powder. Isolated solid: 970 mg

(82%; estimated purity: 97% **1**; yield of **1**: 80%). The identity of the product was confirmed by comparison of the ^1H NMR spectrum with that in the literature.[22] Recrystallization of the product from toluene or hexane affords **1** as colorless crystals. Alternate reactions were carried out using diphenylmagnesium (generated *in situ* by the addition of *p*-dioxane to phenylmagnesium bromide) as the alkylating agent. These did not yield significantly different results.

Representative Procedure for the Preparation of Aryl-Halide Complexes $Cp^*_2Th(o\text{-}Ar)X$ (X = Br and/or Cl): $Cp^*_2Th(o\text{-}MeOC_6H_4)X$ (X = Br, Cl) (5). The solvent was removed from a solution of *o*-anisylmagnesium bromide (0.5 mL, 0.96 M in THF, 0.48 mmol) under reduced pressure. The resultant oily residue was dissolved in toluene (10 mL), at room temperature. Solid $Cp^*_2ThCl_2$ (222 mg, 0.39 mmol) was then added to the stirred solution. Shortly after addition, a white precipitate formed. The reaction mixture was stirred for 75 min before being taken to dryness *in vacuo*. The residue was extracted with toluene (15 mL), and the solution filtered to remove magnesium salts. Compound **5** was isolated as a white powder after removal of the solvent. Isolated solid: 280 mg (107%; purity: 81% **5**; yield of **5**: 228 mg (87%); Br/Cl ratio = 2.62 : 1). The mixture of halides may be recrystallized from ether. ^1H NMR (250 MHz, C_6D_6) $Cp^*_2Th(o\text{-}MeOC_6H_4)Cl$ δ 1.95 (s, 30H), 3.64 (s, 3H); $Cp^*_2Th(o\text{-}MeOC_6H_4)Br$ δ 1.97 (s, 30H), 3.70 (s, 3H); unassigned aromatic protons δ 6.38 (m, 2 x 1H), 7.03 (m, 2 x 1H), 7.17 (m, 2 x 1H), 7.78 (m, 2 x 1H). ^{13}C NMR (62.9 MHz, C_6D_6) $Cp^*_2Th(o\text{-}MeOC_6H_4)Cl$ δ 11.6, 53.9, 107.1, 123.5, 125.0, 127.1, 138.2, 166.3, 196.6; $Cp^*_2Th(o\text{-}MeOC_6H_4)Br$ 12.0, 55.0, 107.5, 123.4, 125.4, 127.2, 138.1, 166.6, 195.8.

$Cp^*_2Th(2, 5\text{-}Me_2C_6H_3)X$ (X = Br, Cl) (7). Reagents: 2-(*p*-xylyl)magnesium bromide solution (0.50 mL, 1.16 M in THF, 0.58 mmol), toluene solvent (10 mL), $Cp^*_2ThCl_2$ (332 mg, 0.58 mmol), toluene extractant (15 mL). Isolated solid: 340 mg (88%; purity: 84% **7**; yield of **7**: 285 mg (74%); Br/Cl ratio = 1.44 : 1). The product may be recrystallized as a mixture, from ether or hexane. ^1H NMR (250 MHz, C_6D_6) $Cp^*_2Th(2, 5\text{-}Me_2C_6H_3)Cl$ major rotamer: δ 1.95 (s, 30H), δ 2.29 (s, 3H), 2.53 (s, 3H); $Cp^*_2Th(2, 5\text{-}Me_2C_6H_3)Cl$ minor rotamer: δ 1.92 (s, 30H), 2.31 (s, 3H), 2.62 (s, 3H); $Cp^*_2Th(2, 5\text{-}Me_2C_6H_3)Br$ major rotamer: δ 1.96 (s, 30H), 2.32 (s, 3H), 2.54 (s, 3H); $Cp^*_2Th(2, 5\text{-}Me_2C_6H_3)Br$ minor rotamer: δ

1.94 (s, 30H), 2.30 (s, 3H), 2.65 (s, 3H); unassigned aromatic protons: δ 6.09 (s), 6.19 (s), 6.83 (m), 7.18 (m), 7.59 (s), 7.69 (s). ^{13}C NMR (62.9 MHz, C_6D_6) $Cp^*_2Th(2, 5\text{-}Me_2C_6H_3)Cl$ major rotamer: δ 11.6, δ1.8, 26.2, 126.2, 224.5; $Cp^*_2Th(2, 5\text{-}Me_2C_6H_3)Cl$ minor rotamer: δ 11.7, 21.4, 25.6, 126.6, 214.8; unassigned aromatic carbons of both chloride rotamers: δ 123.8, 128.3, 129.2, 130.1, 130.3.131.2, 132.1, 132.5, 133.4, 141.7, 142.8.

$Cp^*_2Th(o\text{-}MeC_6H_4)Cl$ (6). Reagents: *o*-tolylmagnesium chloride (411 mg, 0.39 mmol), toluene solvent (10 mL), $Cp^*_2Cl_2$(250 mg, 0.44 mmol), toluene extractant (15 mL). Isolated solid: 270 mg (98%; estimated purity: 76% **6**; yield of **6**: 205 mg (75%)). Analytically pure **6** was obtained with recrystallization from toluene/hexane (≈ 1:1). ^1H NMR (250 MHz, C_6D_6) major rotamer: δ 1.93 (s, 30H), 2.52 (s, 3H); minor rotamer: δ 1.92 (s, 30H), 2.62 (s, 3H); unassigned aromatic protons δ 6.58 (d, J = 6.6 Hz, 1H (minor rotamer)), 6.99-7.08 (m, 2 x 1H), 7.21-7.31 (m, 2 x 2H), 7.73 (d, J = 6.7 Hz, 1H (major)). ^{13}C NMR (62.9MHz, C_6D_6) major rotamer: δ 11.6, 26.7, 126.3, 224.8; minor rotamer: δ 11.7, 26.0, 126.7, 216.1; unassigned aromatic carbons of both rotamers: δ 122.4, 123.3, 123.8, 128.2, 129.3.131.1, 131.5, 132.2, 144.9, 145.5. Anal. Calcd for $C_{27}H_{37}ClTh$: C, 51.55; H, 5.93. Found: C, 51.41; H, 5.76.

Representative Procedure for One-Pot Preparation Methyl-Aryl Complexes $Cp^*_2Th(Me)(o\text{-}Ar)$: $Cp^*_2Th(Me)(o\text{-}MeOC_6H_4)$ (2). *o*-Anisylmagnesium bromide (0.5 mL, 0.96 M in THF, 0.48 mmol) and $Cp^*_2ThCl_2$ (225 mg, 0.39 mmol) were reacted together, in toluene (10 mL), exactly as in the preparation of **5**. The reaction mixture was stirred for 75 min before being taken to dryness *in vacuo*. The residue was extracted with toluene (15 mL), and the solution filtered to remove magnesium salts.

Methylmagnesium chloride solution (126 mg, 0.37 mmol) was then added to the stirred solution of $Cp^*_2Th(o\text{-}MeOC_6H_4)X$ (X = Br, Cl) (**5**). *p*-Dioxane (90 mg, 1.02 mmol) was added to the clear reaction solution, initiating the precipitation of a white solid. The resulting suspension was stirred for further 45 min, and the solvents were removed *in vacuo*. The solid was extracted with toluene (15 mL), and the solution filtered. Toluene was then removed under reduced pressure, to yield the crude product as a white powder. Isolated solid: 240 mg (98%; purity: 87% **2**; yield of **2**: 210 mg (86%)). Analytically pure **2** may be obtained with recrystallization from ether

or toluene. ^{1}H NMR (250 MHz, C_6D_6) δ -0.10 (s, 3H), 1.91 (s, 30H), 3.30 (s, 3H), 6.35 (d, J = 8.0Hz, 1H), 7.05 (dt, J^1 = 1.7Hz, J^2 = 7.7Hz, 1H), 7.20 (t, J = 6.9Hz, 1H), 7.75 (dd, J^1 = 1.6Hz, J^2 = 6.6Hz, 1H). ^{13}C NMR (62.9 MHz, C_6D_6) δ 11.4, 52.0, 68.4, 106.9, 122.2, 123.3, 126.8, 138.4, 170.0, 198.4. Anal. Calcd for $C_{28}H_{40}OTh$: C, 53.84; H, 6.45. Found: C, 54.23; H, 5.77.

$Cp^*_2Th(Me)(o\text{-}MeC_6H_4)$ (3). Reagents: *o*-tolylmagnesium chloride (1000 mg, 0.96 mmol), toluene solvent (20 mL), $Cp^*_2ThCl_2$ (606 mg, 1.06 mmol), toluene extractant/solvent (25 mL), MeMgCl solution (337 mg, 1.00 mmol), *p*-dioxane (238 mg, 2.70 mmol), toluene extractant (25 mL). Isolated solid: 586 mg (91%; purity: 73% **3**; yield of **3**: 427 mg (66%)). Recrystallization of **3** was achieved from hexane, at -40 °C. ^{1}H NMR (250 MHz, C_6D_6) δ 0.51 (s, 3H), 1.87 (s, 30H), 2.56 (s, 3H), 7.05 (m, 2H), 7.24 (d, J = 7.4 Hz, 1H), 7.38 (t, J = 6.9 Hz, 1H). ^{13}C NMR (62.9 MHz, C_6D_6) δ 11.4, 52.0, 68.4, 106.9, 122.2, 123.2, 126.8, 138.4, 170.0, 198.4. Anal. Calcd for $C_{28}H_{40}Th$: C, 55.25; H, 6.62. Found: C, 54.32; H, 6.39.

$Cp^*_2Th(Me)(2,5\text{-}Me_2C_6H_3)$ (4). Reagents: 2-(*p*-xylyl)magnesium bromide solution (1.6 mL, 0.36 M in THF, 0.58 mmol), toluene solvent (10 mL), $Cp^*_2ThCl_2$ (336 mg, 0.59 mmol), toluene extractant/solvent (15 mL), MeMgCl solution (176 mg, 0.52 mmol), *p*-dioxane (125 mg, 1.42 mmol), toluene extractant (15 mL). Isolated yield: 381 mg (104%; purity: 77% **4**; overall yield of **4**: 292 mg (80%)). Analytically pure **4** was obtained with recrystallization from hexane, at -40 °C. ^{1}H NMR (250 MHz, C_6D_6) δ 0.55 (s, 3H), 1.88 (s, 30H), 2.30 (s, 3H), 2.56 (s, 3H), 6.87 (m, 2H), 7.21 (d, J = 7.3 Hz, 1H). ^{13}C NMR (62.9 MHz, C_6D_6) δ 11.3, 22.1, 25.9, 56.5, 118.8, 123.2, 129.7, 131.7, 141.6, 221.5. Anal. Calcd for $C_{29}H_{42}Th$: C, 55.94; H, 6.80. Found: C, 55.31; H, 6.51.

References

(1) Adapted from an article co-written by the author: England, A. F.; Burns, C. J.; Buchwald, S. L. *Organometallics*, **1994**, *13*, 3491-3495.

(2) Schwartz, J.; Labinger, J. A. *Angew. Chem. Int. Ed. Engl.* **1976**, *15*, 333-340.

(3) Collman, J. P.; Hegedus, L. S.; Norton, J. R.; Finke, R. G. *Principles and Applications of Organotransition Metal Chemistry*; University Science: Mill Valley, CA, 1987, Chapter 11.

(4) Jordan, R. F. *Adv. Organomet. Chem.* **1991**, *32*, 325-387.

(5) Buchwald, S. L.; Watson, B. T.; Wannamaker, M. W.; Dewan, J. C. *J. Am. Chem. Soc* **1989**, *111*, 4486-4494.

(6) Buchwald, S. L.; Nielsen, R. B. *J. Am. Chem. Soc.* **1989**, *111*, 2870-2874.

(7) Negishi, E. *Chem. Scr.* **1989**, *29*, 457-468.

(8) Negishi, E.; Miller, S. R. *J. Org. Chem.* **1989**, *54*, 6014-6016.

(9) Takahashi, T.; Seki, T.; Nitto, Y.; Saburi, M.; Rousset, C. J.; Negishi, E. *J. Am. Chem. Soc.* **1991**, *113*, 6266-6268.

(10) Grossman, R. B.; Davis, W. M.; Buchwald, S. L. *J. Am. Chem. Soc.* **1991**, *113*, 2321-2322.

(11) Rousset, C. J.; Negishi, E.; Suzuki, N.; Takahaski, T. *Tetrahedron* **1992**, *33*, 1965-1968.

(12) Erker, G. *J. Organomet. Chem.* **1977**, *134*, 189-202.

(13) Buchwald, S. L.; Fisher, R. A.; Foxman, B. M. *Angew. Chem. Int. Ed. Engl.* **1990**, *29*, 771-772.

(14) Buchwald, S. L.; King, S. M. *J. Am. Chem. Soc.* **1991**, *113*, 259-265.

(15) Cuny, G. D.; Gutiérrez, A.; Buchwald, S. L. *Organometallics* **1991**, *10*, 537-539.

(16) Tidwell, J. H.; Senn, D. R.; Buchwald, S. L. *J. Am. Chem. Soc.* **1991**, *113*, 4685-4686.

(17) Buchwald, S. L.; Lucas, E. A.; Davis, W. M. *J. Am. Chem. Soc.* **1989**, *111*, 397-398.

(18) Smith, G. M.; Sabat, M.; Marks, T. J. *J. Am. Chem. Soc.* **1987**, *109*, 1854-1856.

(19) Ciliberto, E.; Condorelli, G.; Fagan, P. J.; Manriquez, J. M.; Fragala, I.; Marks, T. J. *J. Am. Chem. Soc.* **1981**, *103*, 4755-4759.

(20) Beshouri, S. M.; Fanwick, P. E.; Rothwell, I. P.; Huffman, J. C. *Organometallics* **1987**, *6*, 2498-2501.

(21) Bruno, J. W.; Smith, G. M.; Marks, T. J.; Fair, C. K.; Schultz, A. J.; Williams, J. M. *J. Am. Chem. Soc.* **1986**, *108*, 40-56.

(22) Fagan, P. J.; Manriquez, J. M.; Maatta, E. A.; Seyam, A. M.; Marks, T. J. *J. Am. Chem. Soc.* **1981**, *103*, 6650-6667.

(23) Fendrick, C.; Marks, T. J. *J. Am. Chem. Soc.* **1986**, *108-437*, 425-437.

(24) Hall, S. W.; Huffman, J. C.; Miller, M. M.; Avens, L. R.; Burns, C. J.; Arney, D. S. J.; England, A. F.; Sattelberger, A. P. *Organometallics* **1993**, *12*, 752-758.

(25) Watson, P. J. In *Selective Hydrocarbon Activation*; Davies, J. A.; watson, P. J.; Liebman, J. F.; Greenberg, A, Ed.; VCH: New York, NY, 1990

(26) See Chapter Three.

(27) Collier, M. R.; Lappert, M. F.; Pearce, R. *J. Chem. Soc., Dalton Trans.* **1973**, 445-451.

(28) Jeffrey, J.; Lappert, M. F.; Luong-Thi, N. T.; Webb, M.; Atwood, J. L. *J. Chem. Soc., Dalton Trans.* **1981**, 1593-1605.

(29) Lappert, M. F.; Pickett, C. J.; Riley, P. I.; Yarrow, P. I. W. *J. Chem. Soc., Dalton Trans.* **1981**, 805-813.

(30) Brindley, P. P.; Scotton, M. J. *J. Chem. Soc., Perkin Trans. 2* **1981**, 419-423.

(31) Erker, G.; Mühlenbernd, T.; Benn, R.; Ruflinska, A. *Organometallics* **1986**, *5*, 402-404.

(32) Smith, G. M.; Suzuki, H.; Sonnenberger, D. C.; Day, V. W.; Marks, T. J. *Organometallics* **1986**, *5*, 549-561.

(33) Aoki, K.; Buchwald, S. L.; Work in progress.

(34) Campora, J.; Buchwald, S. L. *Organometallics* **1993**, *12*, 4182-4187.

(35) Abis, L.; Bacchilega, G.; Spera, S.; Zucchini, U.; Dall'Occo, T. *Makromol. Chem.* **1991**, *192*, 981-988.

(36) Salyulev, A. B.; Vovkotrub, E. G.; Strekalovskii, V. N. *Zh. Neorg. Khim* **1990**, *35*, 902-904.

(37) Sobota, P.; Utko, J.; Janas, Z. *J. Organomet. Chem.* **1986**, *316*, 19-23.

(38) Sobota, P. *Pure Appl. Chem.* **1989**, *61*, 861-866.

(39) Rausch, M. D. *Inorg. Chem.* **1964**, *3*, 300-301.

(40) Cope, A. C. *J. Am. Chem. Soc.* **1935**, *57*, 2238-2240.

(41) Markies, P. R.; Altink, R. M.; Villena, A.; Akkerman, O. S.; Bickelhaupt, F.; Smeets, W. J. J.; Spek, A. L. *J. Organomet. Chem.* **1991**, *402*, 289-312.

(42) Handlir, K.; Holecek, J.; Benes, L. *Collect. Czech. Chem. Commun.* **1985**, *50*, 2422-2430.

(43) Screttas, C. G.; Micha-Screttas, M. *J. Organomet. Chem.* **1985**, *292*, 325-333.

(44) Fagan, P. J.; Manriquez, J. M.; Marks, T. J.; Vollmer, S. H.; Day, C. S.; Day, V. W. *J. Am. Chem. Soc.* **1981**, *103*, 2206-2220.

(45) See Chapter Two.

(46) Satisfactory elemental analyses were obtained for compounds **2**, **3**, **4**, and **6**, however consistent analyses could not be obtained for halide mixtures **5** and **7**.

(47) Watson, S. C.; Eastham, J. F. *J. Organomet. Chem.* **1967**, *9*, 165-168.

CHAPTER TWO

The Thorium Benzyne: Structure-Reactivity Relationships in Precursor Complexes: Solution and Solid State Structures of $Cp_2Zr(Me)(o\text{-}MeOC_6H_4)$ and $Cp^*_2Th(Me)(o\text{-}MeOC_6H_4)$

Introduction

The advent of practical routes to early transition metal complexes of unsaturated organic fragments has enabled significant advances in approaches to the preparation of synthetically challenging organic and organometallic species, including complexes of alkenes, alkynes, benzyne (benzyne = C_6H_4, 1, 2-didehydrobenzene, *ortho*-phenylene) and aryne derivatives and and heterosubstituted derivatives.[1-5] Although the first fully characterized example of a transition metal benzyne complex was the tantalum species $Cp^*Ta(C_6H_4)Me_2$,[6] (Cp^* = η^5-pentamethycyclo-pentadienyl) there have been few studies since which have concentrated on the preparation and reactivity of similar systems other than those of the group 4 elements.

In a study of the thermochemistry of actinide alkyl complexes, Marks and co-workers did however discuss the close relationship between group 4 and early actinide systems with the preparation of the transient benzyne complexes $Cp^*_2An(C_6H_4)$ (An = Th, U).[7] As their position in the periodic table implies, these elements are among the most electropositive and oxophilic of the transition series (Table 1). Complexes of zirconium, hafnium and thorium, all form stable tetrapositive ions, whereas titanium, cerium, and uranium are subject to redox chemistry in reducing ligand environments. Furthermore, all of the tetravalent ions, save for the lanthanide,[8] form strong bonds to carbon, and as a result an extensive array of σ- and π-bonded organometallic chemistry is known for each.[9-11] In this study we aim to examine the relationship between the chemistry of the benzyne complexes tetravalent zirconium and thorium.

Due to the size of the actinide metal centers, the vast majority of the metallocene (e.g., bis(cyclopentadienyl)) chemistry of these elements is centered around the permethylated derivatives Cp^*_2An. Since smaller unsubstituted bis(Cp) ligand sets are unstable with respect to redistribution to mono- and tris(cyclopentadienyl) frameworks.[18]

In addition to the increased size of the metal center, the thorium system also differs from the zirconocene derivatives by virtue of more bulky, more electron donating bis(Cp^*) ancillary ligand set. Although bis(pentamethylcyclopentadienyl) ligation typically effects reduction in strongly oxidizing metal centers,[8,19-21] this ligand environment imparts

Table 1. Group 4 Extended Triad

M	Z	EC[a]	IR/Å[b]	Electronegativity[c]	$E^0(M^{IV}/M^n)$[d]
Ti	22	[Ar] $3d^2 4s^2$	0.745	1.54 (Ti^{II})	+ 0.01 V (Ti^{III})
Zr	40	[Kr] $4d^2 5s^2$	0.86	1.33 (Zr^{II})	- 1.53 V (Zr^0)
Ce	58	[Xe] $4f^1 5d^1 6s^2$	1.01	1.12	+ 1.61 V (Ce^{III})
Hf	72	[Xe] $4f^{14} 5d^2 6s^2$	0.85	1.3	- 1.70 V (Hf^0)
Th	90	[Rn] $6d^2 7s^2$	1.08	1.3	- 1.90 V (Th^0)
U	92	[Rn] $5f^3 6d^1 7s^2$	1.03	1.7	- 0.61 V (U^{III})

[a]EC = Electron configuration of metal: Ti, Zr, Hf reference[12]; Ce, Th, U reference[13].

[b]IR = Shannon and Prewitt crystal radii for tetravalent ions in coordination number 6.[14]

[c]Electronegativity = Calculated Pauling electronegativity: Ti, Zr, Hf reference[15]; Ce, Th, U reference[16].

[d]$E^0(M^{IV}/M^n)$ = Standard reduction potential for tetravalent ions to most accessible oxidation state.[17]

stability to numerous mid to high oxidation state organoactinide species.[9,22-27] Furthermore, the difference in ionic radii between zirconium and the actinide elements compensates for the additional bulk of the Cp* ligands in the coordination sphere.[14]

The benzyne intermediates of interest are generated by the thermally induced decomposition of diphenyl precursor complexes Cp'_2MPh_2 (M = Ti,[28] Zr;[29] Cp' = Cp; M = Th, U, Cp' = Cp*[7]) (eq 1).

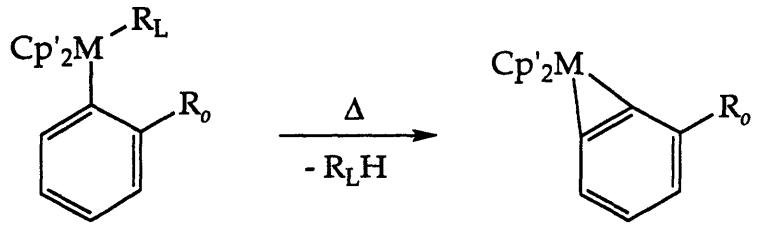

(1)

M = Ti, Zr; Cp' = Cp; R_L = Ph, R_o = H

M = Th, U; Cp' = Cp*; R_L = Ph, R_o = H

M = Ti, Zr; Cp' = Cp; R_L = Me, R_o = Me, OMe, etc.

Given that steric constraints control the extent to which substituted diaryl complexes may be employed, the potential applications of such complexes are not without severe limitations. With this in mind, the σ-bond metathesis chemistry of zirconocene, and more recently titanocene, complexes has been elaborated for alkyl-aryl complexes (e.g., eq 1: R_L = Me). Herein we describe an investigation into the thermodynamic stability of the recently prepared analogous thorium methyl-aryl derivatives $Cp'_2M(Me)$(*o*-Ar) (Cp' = Cp*; M = Th; *o*-Ar = *o*-tolyl, *o*-anisyl; Cp' = Cp*; M = Zr; *o*-Ar = *o*-anisyl). In most cases, the overall reactivity of these group 4 and actinide systems is very similar. However, this study concentrates on the surprising differences in stability of the methyl-(*ortho*-anisyl) analogs Cp_2ZrMe(*o*-$MeOC_6H_4$) and Cp^*_2ThMe(*o*-$MeOC_6H_4$). Further, conformational analyses in both solution and the solid state have been utilized to decipher the structural features responsible for the observed differences in reactivity.

Results and Discussion

Preparation of $Cp_2ZrMe(o\text{-}MeOC_6H_4)$ (1). Preparation of this zirconocene (methyl)(*o*-anisyl) complex is readily achieved by the reaction of $Cp_2Zr(Me)Cl$ with the respective Grignard reagent (eq 2). Complex **1** is the sole metallocene derived species evident in the product mixture, and may be isolated by

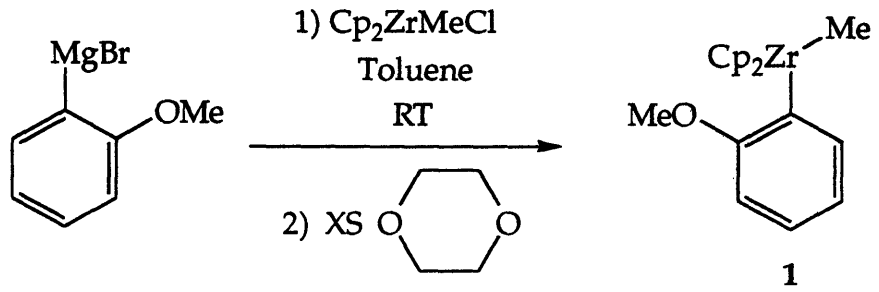

(2)

recrystallization from hexane, in greater than 69% yield. The synthesis follows a similar strategy to that employed for the preparation of the actinide analog $Cp^*_2Th(Me)(o\text{-}MeOC_6H_4)$ (**2**).[30]

Thermal Stability of $Cp_2Zr(Me)(o\text{-}MeOC_6H_4)$ (1) and $Cp^*_2Th(Me)(o\text{-}MeOC_6H_4)$ (2) in Solution. The thermally induced intramolecular C-H activation chemistry of **1**[3,5], other related group 4 metallocene (methyl)(aryl)[3,5,31-35] and diphenyl complexes[28,29,36,37] is well established. Likewise, the analogous actinide complexes $Cp^*_2AnPh_2$ (An = Th, U) undergo a similar mode of decomposition to generate transient benzyne intermediates.[7] The chemistry of benzyne complexes of the actinides had not, however been extended beyond the parent diphenyl system, although several examples regarding C-H activation/elimination chemistry of reactive actinide dialkyl species have been reported.[22,23,38-40] Although suitable bis(Cp*)Th alkyl-aryl complexes had not been prepared until recently,[30] derivatives of this type were expected to undergo similar decomposition pathways to that seen for group 4 analogs (eq 3). An examination of the intramolecular C-H activation chemistry of thorium methyl-aryl complexes demonstrates that this assumption is only partially correct. A study of differentially substituted aryl derivatives demonstrates that the nature of the *ortho*-substituent (R_o) proves to be crucial to the intrinsic stability of the methyl-aryl precursors in the thorium system, ultimately determining if C-H activation and

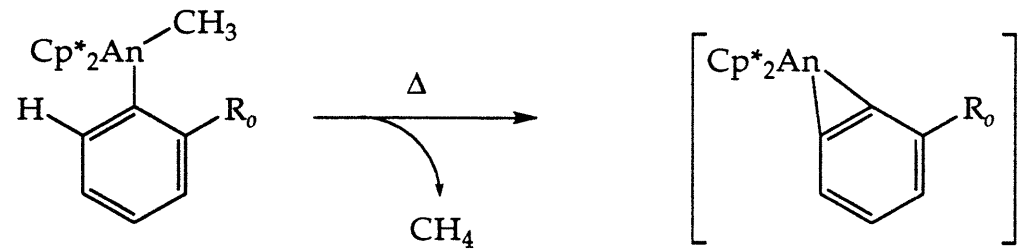

(3)

R_o = Me, OMe, etc.

elimination of methane occurs to a significant extent. Although relative reaction rates naturally differ among variously substituted group 4 analogs,[3,5,41] there are no instances in which benzyne generation is curtailed by the effects of the *ortho*-substituent. This is, however, observed to be the case with the *ortho*-methoxy group of $Cp^*_2ThMe(o\text{-}MeOC_6H_4)$ (**2**). Lengthy periods of thermolysis for **2** are required in order to effect decomposition of this particular methyl-aryl derivative (100 °C, $t_{1/2} \approx 25$ h). Conversely, the zirconium analog $Cp_2ZrMe(o\text{-}MeOC_6H_4)$ (**1**) is known to decompose readily under milder conditions (85 °C, $t_{1/2} \approx 42$ min). The ultimate reaction product of the decomposition of **2** is $Cp^*_2ThPh_2$, seemingly indicating that the mode of reactivity of the actinide is ultimately conserved, with intramolecular C-H activation ultimately resulting in the loss of an equivalent of methane and generation of the respective benzyne intermediate.

Alkyl substitution of the aromatic ring at the *ortho*-position has been shown to considerably enhance the rate of methane elimination. The anticipated C-H activation of the aryl substituent is facile in the *ortho*-methylated thorium derivatives $Cp^*_2Th(Me)(o\text{-}Ar)$ (o-Ar = $o\text{-}MeC_6H_4$ (**3**), 2, 5-$Me_2C_6H_3$ (**4**)), even at ambient temperature (90%, 3 days).[42] The typical benzyne-derived metallacycle or perdeuterodiphenyl complexes have been identified as the reaction products generated through decomposition of the methyl-(*ortho*-tolyl) derivatives in the presence of 3-hexyne and benzene-d_6, respectively (Scheme 1).[3,5,7,29,42] These experimental observations are a result of the range of different intramolecular interactions apparent in seemingly closely related systems. Solution state NMR and NOE difference spectra, and solid state X-ray crystallographic data provide insight into the structural features responsible for the observed differences in reactivity of the differentially substituted actinide species.

Scheme 1

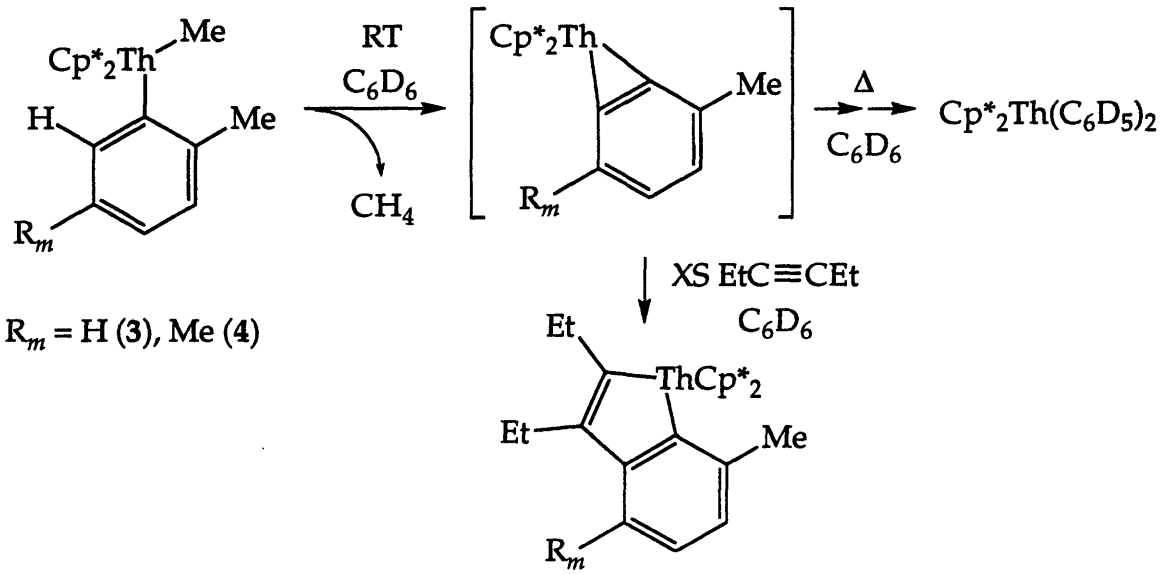

R_m = H (**3**), Me (**4**)

Solution NMR Characterization and Conformational Analysis of 1-7. ^{1}H and ^{13}C NMR spectra of $Cp_2ZrMe(o\text{-}MeOC_6H_4)$ (**1**) and $Cp^*_2ThMe(o\text{-}MeOC_6H_4)$ (**2**) are typical of diamagnetic metallocene complexes (Figure 1). The ^{1}H NMR chemical shifts of the methoxy groups of both **1** and **2** (^{1}H NMR, C_6D_6: δ 3.20 and δ 3.30, respectively) are somewhat surprising since the resonance for each does not move appreciably from that observed in anisole itself (^{1}H δ 3.28). There is a detectable change in the ^{13}C shift of the methoxy carbon atom of the metal-bound system, however (^{13}C NMR, C_6D_6: **1**, δ 53.2; **2**, δ 68.4; anisole, δ 53.5). That this is the case is particularly interesting for **2**, and especially so after further investigation of the molecular structure of the thorium complex (*vide infra*). Both **1** and **2** manifest a single set of resonances in the ^{1}H NMR spectrum, showing the presence of either rapid rotation about the metal-aryl linkage or hindered rotation giving rise to predominantly one geometric isomer. Additional NMR studies show the latter to be the case, with both complexes existing as single rotamers in solution at room temperature. A study of **2**, the *ortho*-methyl analogs $Cp^*_2Th(Me)(o\text{-}Ar)$ (o-Ar = $o\text{-}MeC_6H_4$ (**3**), 2, 5-$Me_2C_6H_3$ (**4**)) and the alkyl-halide precursors $Cp^*_2Th(o\text{-}Ar)(X)$ (o-Ar = $o\text{-}MeOC_6H_4$, X = Br (**5a**), Cl (**5b**); o-Ar = $o\text{-}MeC_6H_4$, X = Cl (**6**); o-Ar = 2, 5-$Me_2C_6H_3$, X = Br (**7a**), Cl (**7b**)) reveals that this preference for a single isomer is

Figure 1. ^1H and ^{13}C NMR Data for $Cp_2Zr(Me)(o\text{-}MeOC_6H_4)$ (1) and $Cp^*_2ThMe)(o\text{-}MeOC_6H_4)$ (2)

	1		2	
	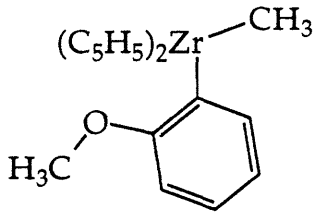		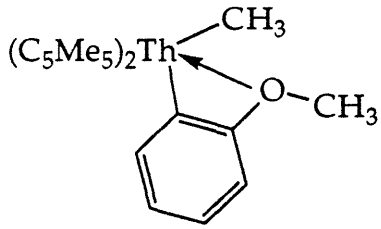	
Methyl				
CH_3	0.21	(s, 3H)	-0.10	(s, 3H)
CH_3	34.4		52.0	
Methoxy				
OCH_3	3.20	(s, 3H)	3.30	(s, 3H)
OCH_3	53.2		68.4	
Cp Ring				
C_5H_5	5.81	(s, 10H)	-	
$C_5(CH_3)_5$	-		1.91	(s, 30H)
C_5R_5	110.5		122.2	
$C_5(CH_3)_5$	-		11.4	
Aromatic Ring				
4 x *H*	6.42	(d, J = 8.0 Hz, 1H)	6.35	(d, J = 8.0 Hz, 1H)
	6.98	(t, J = 7.0 Hz, 1H)	7.05	(dt, J^1 = 1.7 Hz,
	7.09	(dd, J^1 = 1.5 Hz,		J^2 = 7.7 Hz, 1H)
		J^2 = 7.0 Hz, 1H)	7.20	(t, J = 6.9 Hz, 1H)
	7.13	(dt, J^1 = 1.5 Hz,	7.75	(dd, J^1 = 1.6 Hz,
		J^2 = 7.8 Hz, 1H)		J^2 = 6.6 Hz, 1H)
6 x C	107.6, 121.6		106.9, 123.3	
	127.0, 136.1		126.8, 138.4	
	165.3, 168.5		170.0, 198.4	

Figure 2. Selected ^{1}H NMR Data for 2-7 with Corresponding Rotational Equilibria

	2	5a	5b	3	4
Cp* Rings					
$C_5(CH_3)_5$	1.91	1.97	1.95	1.87	1.88
Th-Methyl					
CH_3 (s, 3H)	-0.10	-	-	0.51	0.55
Aromatic Ring Substituents					
OCH_3	3.30	3.70	3.64	-	-
CH_3	-	-	-	2.56	2.56
CH_3	-	-	-	2.30	-

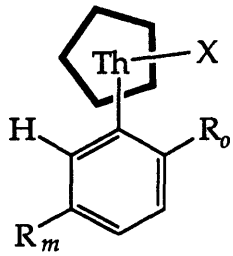

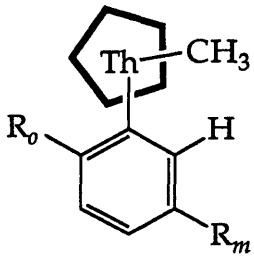

R_o = OMe, R_m = H
X = Me (**2**), Br (**5a**), Cl (**5b**)

R_o = Me
R_m = H (**3**), Me (**4**)

		6	7a	7b
Cp* Rings				
$C_5(CH_3)_5$	major	1.93	1.96	1.95
	minor	1.92	1.94	1.92
Aromatic Ring Substituents				
CH_3	major	2.52	2.32	2.29
	minor	2.62	2.30	2.31
CH_3	major	-	2.54	2.53
	minor	-	2.65	2.62

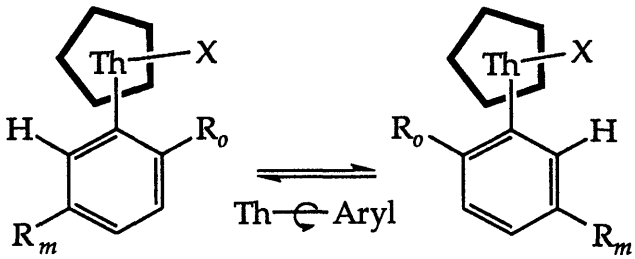

R_o = Me, R_m = H, X = Cl (**6**)
R_o = R_m = Me, X = Br (**7a**), Cl (**7b**)

not always the case for *ortho*-substituted aryl derivatives (Figure 2). At room temperature, on the NMR time-scale, the complexes **3**, **4** and **5** also show a single set of resonances in the ^{1}H NMR spectrum, while the halo-(*ortho*-tolyl) derivatives **6** and **7** exist as discrete rotameric pairs (Figure 2). Coalesence of the pairs of rotamers has been observed at elevated temperatures (≈ 100 °C). It is not realistic to expect that rapid rotation about the metal-aryl axis occurs in the *ortho*-tolyl complexes **3** and **4**, when the same mode is precluded in the presence of the sterically less imposing halide subtituents (Van der Waals radii: Cl = 1.70-1.90 Å; Br = 1.80-2.00 Å; CH_3 = 2.00Å).[16,43] Previously, it has been determined that related actinide diphenyl[7] and bisamide[44] systems also exhibit barriers to rotation in complexes containing the bulky bis(Cp*) ancillary ligand set. Rather, it is believed that **1-4** all primarily exist in singular locked conformations in solution, and that the geometry of the thorium methyl-(*ortho*-anisyl) derivative differs significantly from that of the zirconocene or methyl-(*ortho*-tolyl) analogs, such as to render **2** comparatively unreactive with respect to intramolecular C-H activation.

The mechanism of C-H activation and elimination of methane from alkyl-aryl complexes of this type is proposed to proceed via a multi-centered pathway, necessitating the formation of a four-membered transition state (Scheme 2: **III**).[29] The formation of such a species is likely only accessible from one of the two possible conformations of these methyl-aryl precursor complexes (Scheme 2: **I**). In systems adopting the conformation **II**, the nature of the intramolecular activation necessitates rotation to an intermediate with the geometry **I**. However, if rotation about the metal-aryl linkage, past the bulky bis(cyclopentadienyl) framework, is inhibited, the intermediate **II** is unable to achieve formation of the requisite transition state and enable activation the aromatic hydrogen atom. Conversely, if rotation about the metal-aryl bond is rapid or if an intermediate with the geometry **I** predominates, then the proposed C-H activation is facile. The parent methyl-aryl species $Cp^*_2Th(Me)(Ph)$ demonstrates considerable thermal stability by comparison with the *ortho*-alkyl substituted analogs **3** and **4**, demonstrating that additional factors may be required in order to drive the elimination reaction.[45] This observation is consistent the premise that steric crowding of the metal center assists the C-H activation pathway.[46]

Scheme 2

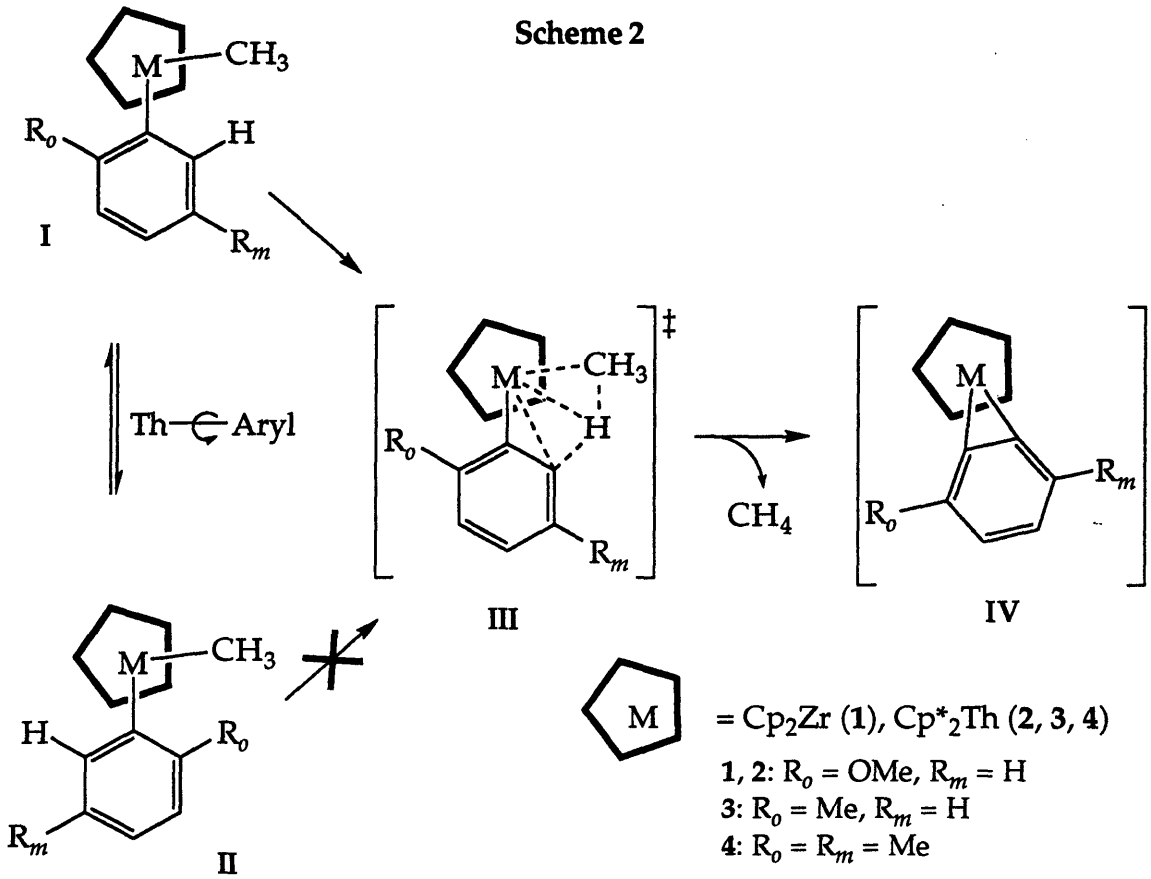

The restricted rotation observed for **3** and **4**, and the facile room temperature methane elimination is further consistent with the complexes being constrained to the geometry represented by **I**. Steric repulsion between the thorium-methyl and (*ortho*-tolyl) methyl substitutents of **3** and **4** in the geometry **I** is apparently substantial, such that the favored geometry of these complexes is believed to be one in which the thorium bound methyl group is directed toward the metallocene framework (Figure 3: **I**). However, without additional structural information it is not possible to exclude **II** from consideration as the favored conformer for either **3** or **4**, since in both cases it is conceivable that the elimination of methane proceeds from the rotamer **I**, present as a minor species.

An examination of the relative tendencies of **1** and **2** to undergo intramolecular C-H activation has therefore led us to postulate that the difference in solution state structure between these two species is responsible for determining the respective rates of decomposition. It has been proposed that ready C-H activation chemistry is undertaken by the zirconium system

Figure 3

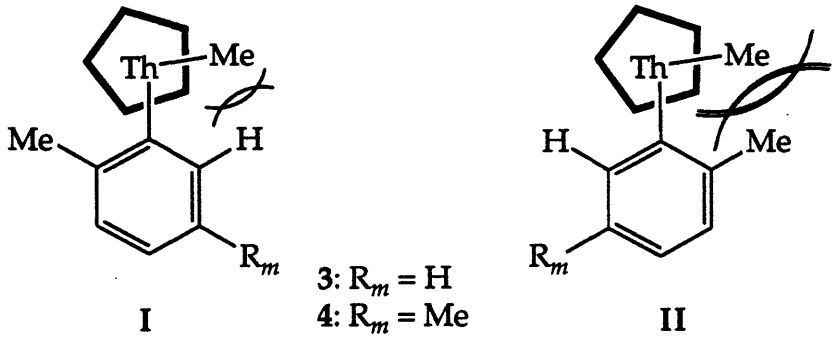

since the metal-bound methyl group and the 'leaving' *ortho*-hydrogen atom are situated in a geometry which relates closely to the requisite transition state (Scheme 2: **I**). Conversely, in **2**, the *ortho*-anisyl moiety is believed to orient such that the methoxy group occupies the centermost coordination site in the equatorial plane of the metallocene wedge (i.e., Scheme 2: **II**). Since methane elimination is only viable from an intermediate of geometry **I**, it is therefore necessary that the rotational equilibrium of **2** be driven in favor of the reactive species in order to effect the C-H activation. Solution and solid state structural determinations have confirmed that this indeed proves to be the case in both complexes, and that the reactivity of the actinide complex is further reduced by the presence of a significant thorium-oxygen donor interaction.

Solution State Structures of $Cp_2ZrMe(o\text{-}MeOC_6H_4)$ (1) and $Cp^*_2ThMe(o\text{-}MeOC_6H_4)$ (2). The nuclear Overhauser effect (NOE) has proven to be an extremely useful technique for the elucidation of the solution molecular structures of complicated organic structures. Likewise, the standard NOE experiment has been successfully employed here for providing conformational data regarding the coordination mode of the *ortho*-anisyl moiety in the metallocene frameworks of **1** and **2**.

Spectrometric determinations were performed in J. Young sealed NMR tubes under rigorously anaerobic conditions, in benzene-d_6. NOE enhancements due to the irradiation of the methyl, methoxy and aromatic protons of the analogous zirconium and thorium methyl-(*ortho*-anisyl) complexes have been recorded (Figure 4; **1**: Table 2; Appendices 2.1-2.5. **2**: Table 3; Appendices 2.6 and 2.7). Large positive enhancements are

Table 2. ^1H NMR NOE Data for $Cp_2ZrMe(o\text{-}MeOC_6H_4)$ (1)

Percent relative observed NOE	^1H Nucleus irradiated				
	CH_3	OCH_3	H_A	H_B	$H_{(C+D)}$
CH_3 (3H)	-	+1	0	0	+2
OCH_3 (3H)	+1	-	+4	0	0
C_5H_5 (10H)	+5	+1	-1	-1	0
H_A (1H)	-1	+32	-	-2	+10
H_B (1H)	-3	+2	-1	-	+30
$H_{(C+D)}$ (2H)	+9	-3	+2	+7	-

Table 3. ^1H NMR NOE Data for $Cp^*_2ThMe(o\text{-}MeOC_6H_4)$ (2)

Percent relative observed NOE	^1H Nucleus irradiated	
	CH_3	OCH_3
CH_3 (3H)	-	+6
OCH_3 (3H)	+ 6	-
H_X	+ 48	0

Figure 4

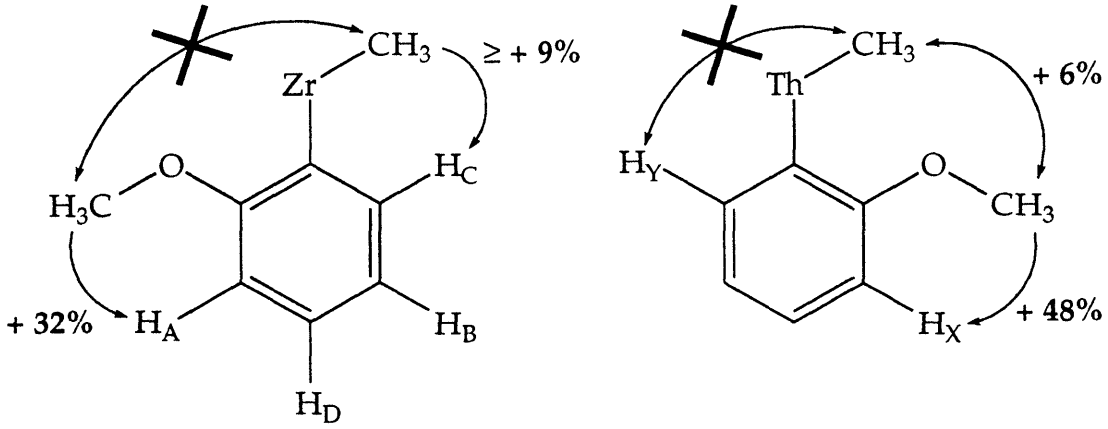

1-NOE **2-NOE**

experienced between pairs of adjacent protons or groups of protons due to their close proximity and limited relaxation pathways (e.g., (aryl-H)-(aryl-H), (OCH_3)-(aryl-H)).[47] Smaller negative NOE values are observed as the result of

three-spin systems, and zero values are recorded for internuclear distances out of the detection range of the experiment (i.e., longer than ≈ 4 Å).[47] Similar negative values due to the Cp and Cp* ligands are also conceivable, however, the largest decrease in NOE as a result of such a three spin system (i.e., Me(irr)-(Cp or Cp*)$_{(obs^1)}$-(aryl-H or MeO)$_{(obs^2)}$) will also be observed at the point of the largest positive enhancement, and therefore cannot invoke an alternative interpretation of the data.

In the conformations proposed for **1** and **2**, enhancement should be observed upon irradiation of the thorium bound methyl group, corresponding to either the *ortho*-proton (H_C (Figure 4: **1-NOE**) or methoxy group (Figure 4: **2-NOE**), respectively, which is indeed observed to be the case (**1**: $Me_{(irr)}$-$H_{(C+D)(obs)}$ = + 9%; **2**: $Me_{(irr)}$-$OMe_{(obs)}$ = + 6%). The similarity of the chemical shifts of H_C and H_D precludes an accurate determination of the NOE signal due to these protons independently. For the purpose of this investigation it is not, however, important to distinguish between these two aromatic signals. The nature of the NOE experiment is such that enhancement observed for aromatic protons adjacent to H_C (i.e. H_B) upon irradiation of the thorium-bound methyl group is observed as a relaxation pathway of the aromatic hydrogen atom. As a result, a negative value is recorded for $H_{B(obs)}$. The observed $Me_{(irr)}$-$H_{C(obs)}$ value actually may be somewhat more positive than the observed + 9%, given that this value potentially also incorporates a negative result due to $Me_{(irr)}$-$H_{B(obs)}$. Nonetheless, the recorded value is significant, clearly implicating the proposed conformation for **1** (Figure 4: **1-NOE**).

The presence of an equilibrium between the two possible structures would be observed as a positively enhanced signals for both of the proximate groups (OMe and *ortho*-H (**1**: H_C; **2**: H_Y)) in either of the methyl-(*ortho*-anisyl) species **1** or **2**, upon irradiation of the methyl group. In such an instance the equilibrium ratio may be determined from a comparison of the relative enhancements observed. Here, at room temperature at least, any enhancement due to the minor species proves small enough such as to be undetectable, which is consistent with both **1** and **2** adopting non equilibrating conformations.

Solid State Structures of $Cp_2ZrMe(o\text{-}MeOC_6H_4)$ (1) and $Cp^*_2ThMe(o\text{-}MeOC_6H_4)$ (2). The key to the difference between the solution state structures of **1** and **2** becomes clear from an examination of the X-ray crystallographically determined structures of the two species (1: Figures 5-13; Appendices 2.8-2.14). The structures reveal the opposing orientation of the anisyl substituents, and a significant thorium-oxygen interaction in **2** (Figure 5). Coordination of the

Figure 5

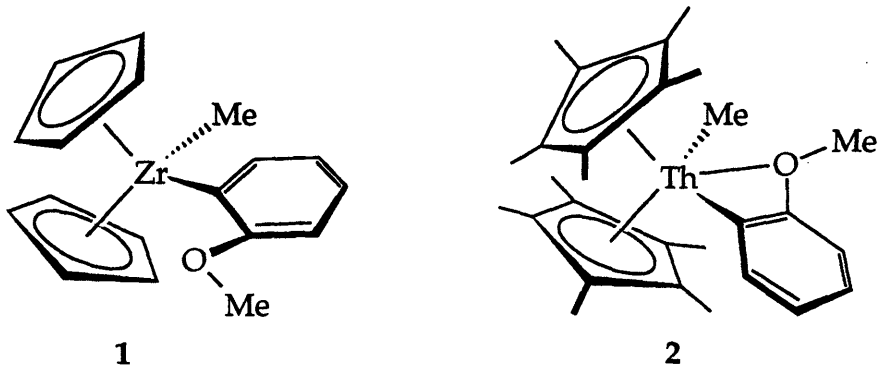

ether oxygen to the thorium center occurs in the equatorial plane bisecting the metallocene wedge. The resultant coordinative interaction is long (2.627(15) Å) relative to either traditional 'covalent' thorium-oxygen interactions (e.g., Chapter 3: **5**: Th-O(4) = 2.138(7) Å) or coordinate bonds (e.g., Chapter 3: **4**: Th-O = 2.421(12) Å; **5**: Th-O(1) = 2.456 Å) (Figure 6). The anisole

Figure 6

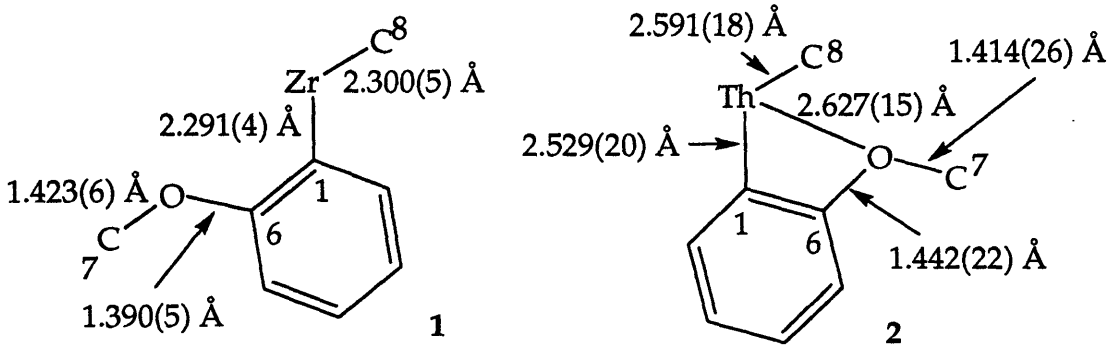

oxygen atom is considerably less basic than that of aliphatic ethers (e.g., THF, Et_2O), or phosphoryl ligands (e.g. Chapter 3: **4** and **5**). Nonetheless, coordination of the *ortho*-substituent to the metal center effects considerable deformation of the thorium-aryl angle (i.e. Th-C(1)-C(2)/C(6) =

147.1(14)°/101.5(12)°) from that which would otherwise be expected (trigonal sp^2: C-C-C ≈ 120°) (Figure 7). A small, but significant deformation of this

Figure 7

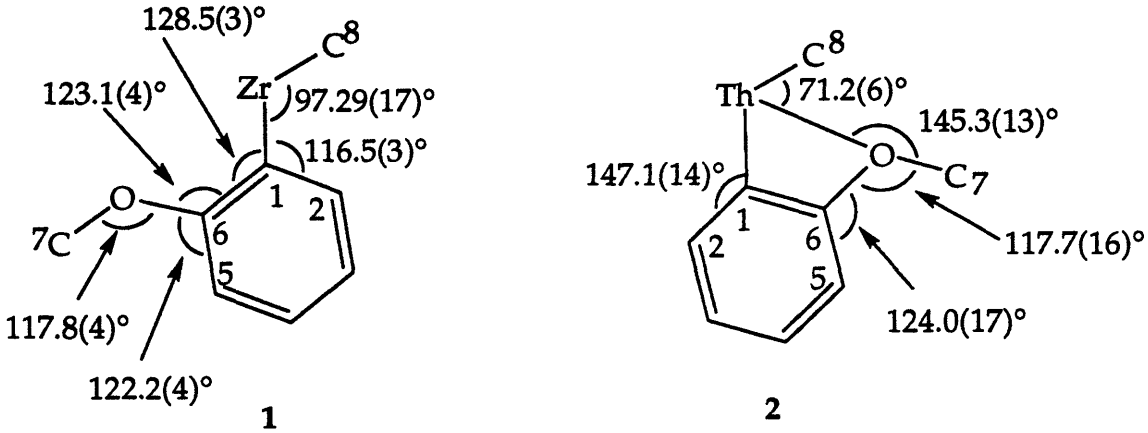

∠ O-Th-C1 = 53.6(6)° ∠ Th-O-C6 = 97.0(10)°
∠ C1-Th-C8 = 124.8(7)° ∠ O-C6-C1 = 107.9(15)°
∠ Th-C(1)-C6 = 101.5(12)°

angle is also observed in **1**, although in the opposite sense (i.e. Zr-C(1)-C(2)/C(6) = 128.5(3)°/116.5(3)°). Similar angular distortions have previously been proposed to be the result of orbital considerations in related zirconocene species.[48]

Figure 8. ORTEP Plot of $Cp_2Zr(Me)(o\text{-}MeOC_6H_4)$ (1)

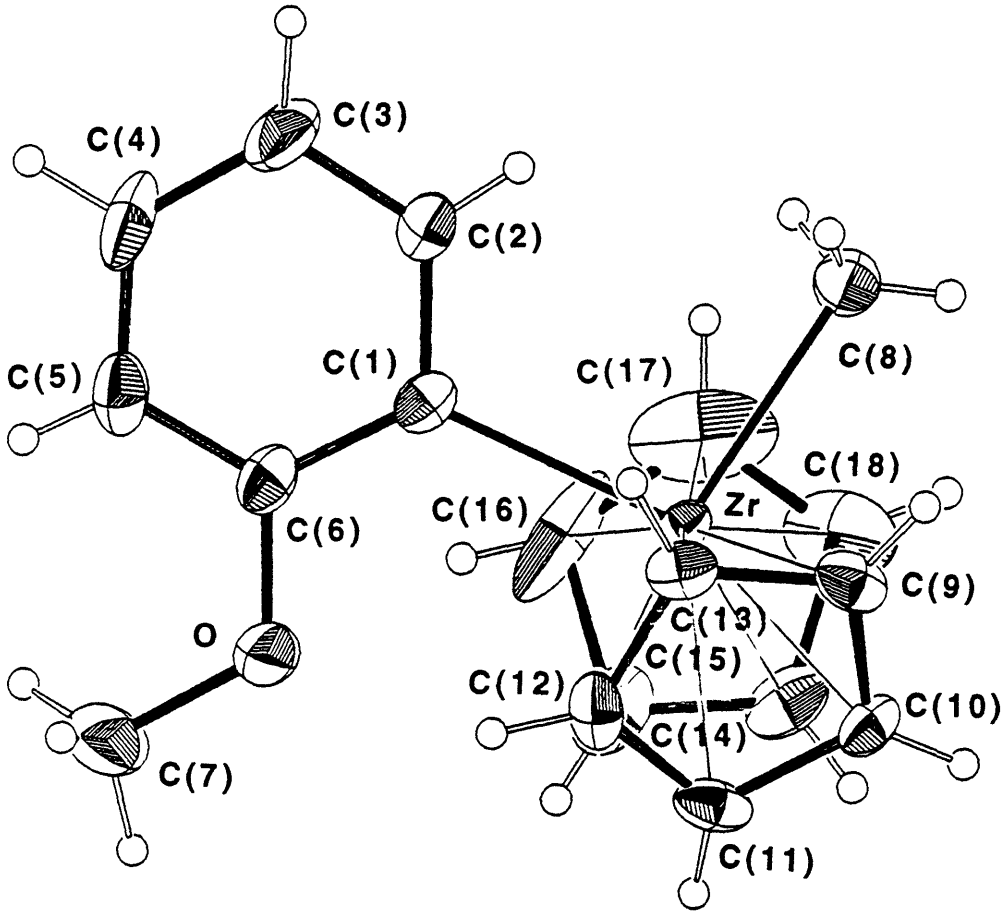

Figure 9. ORTEP Plot of $Cp^*_2Th(Me)(o\text{-}MeOC_6H_4)$ (2)

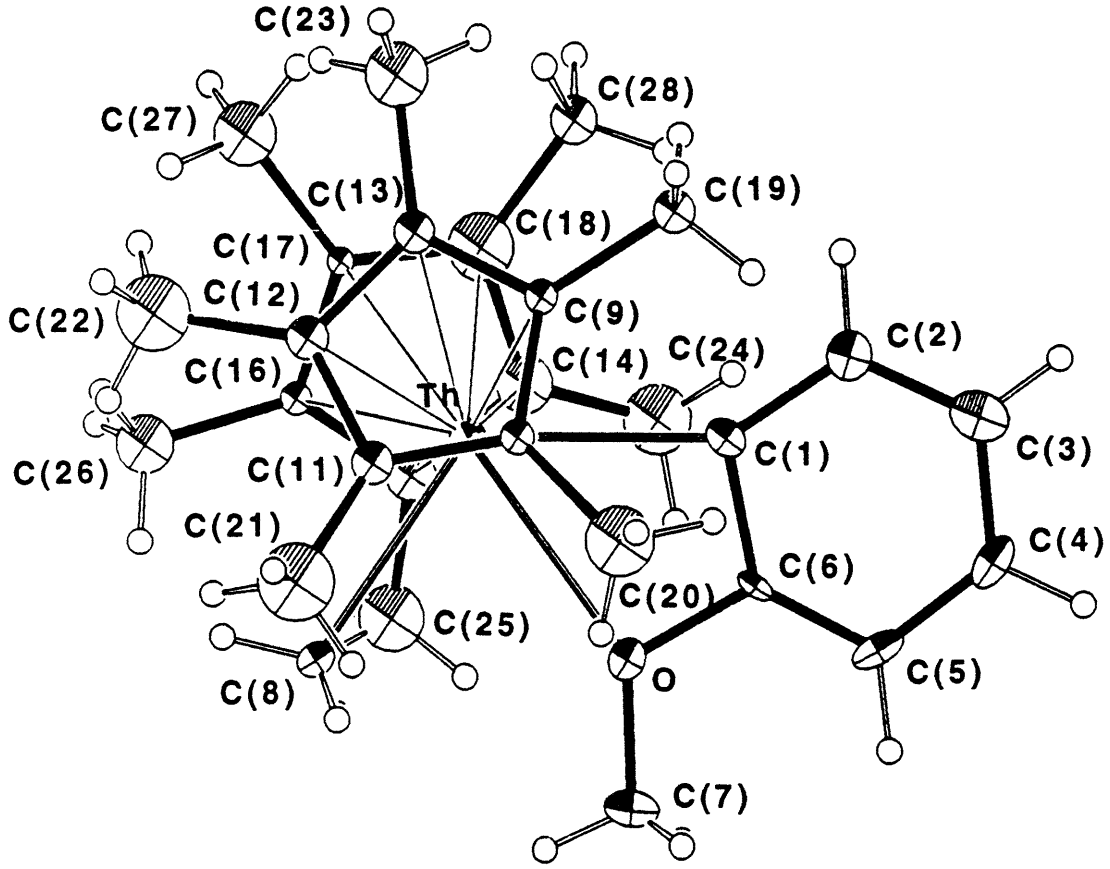

Figure 10. ORTEP Plot and Space-filling Diagram of $Cp_2Zr(Me)(o\text{-}MeOC_6H_4)$ (1)

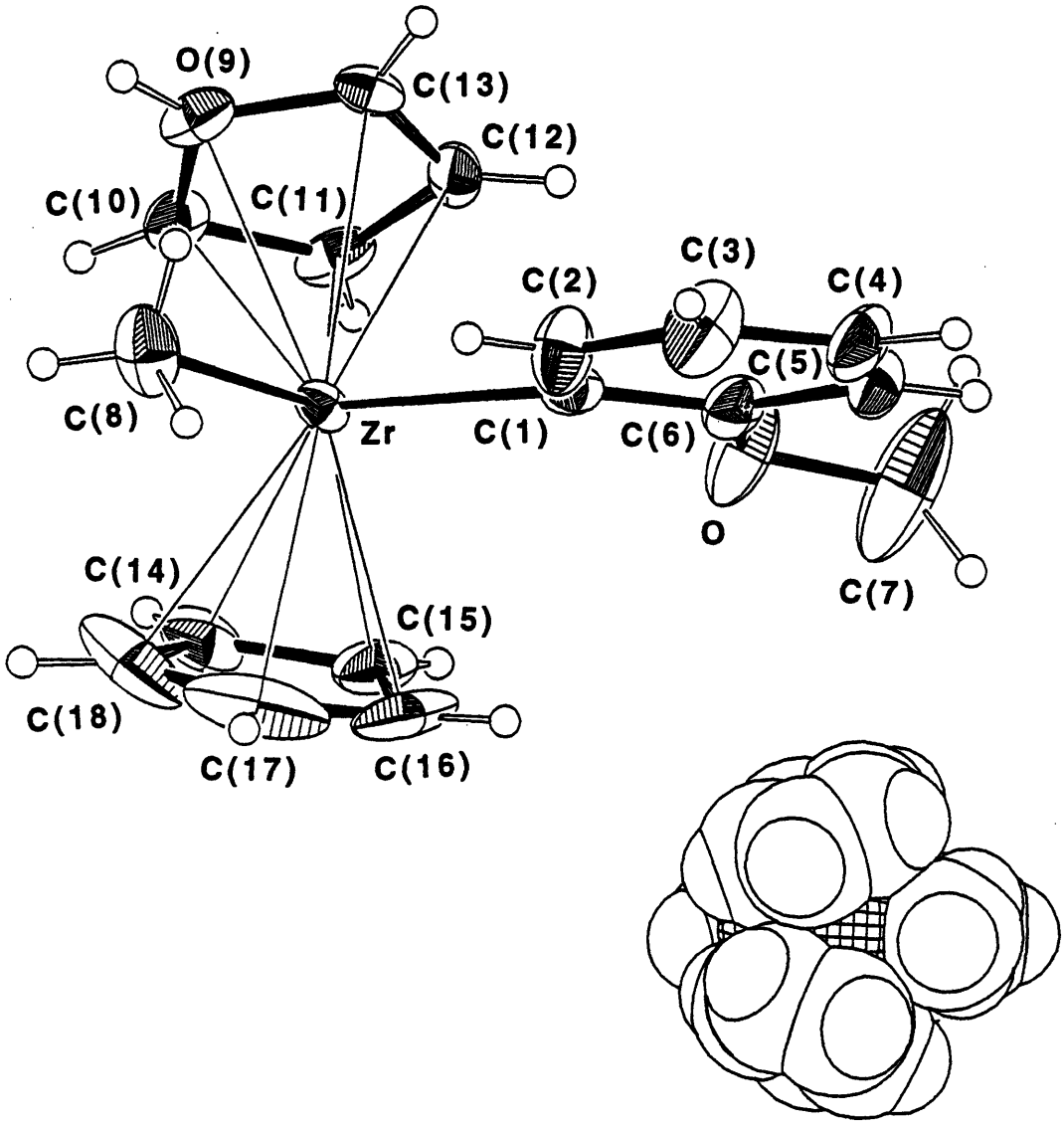

Figure 11. ORTEP Plot and Space-filling Diagram of $Cp^*_2Th(Me)(o\text{-}MeOC_6H_4)$ (2)

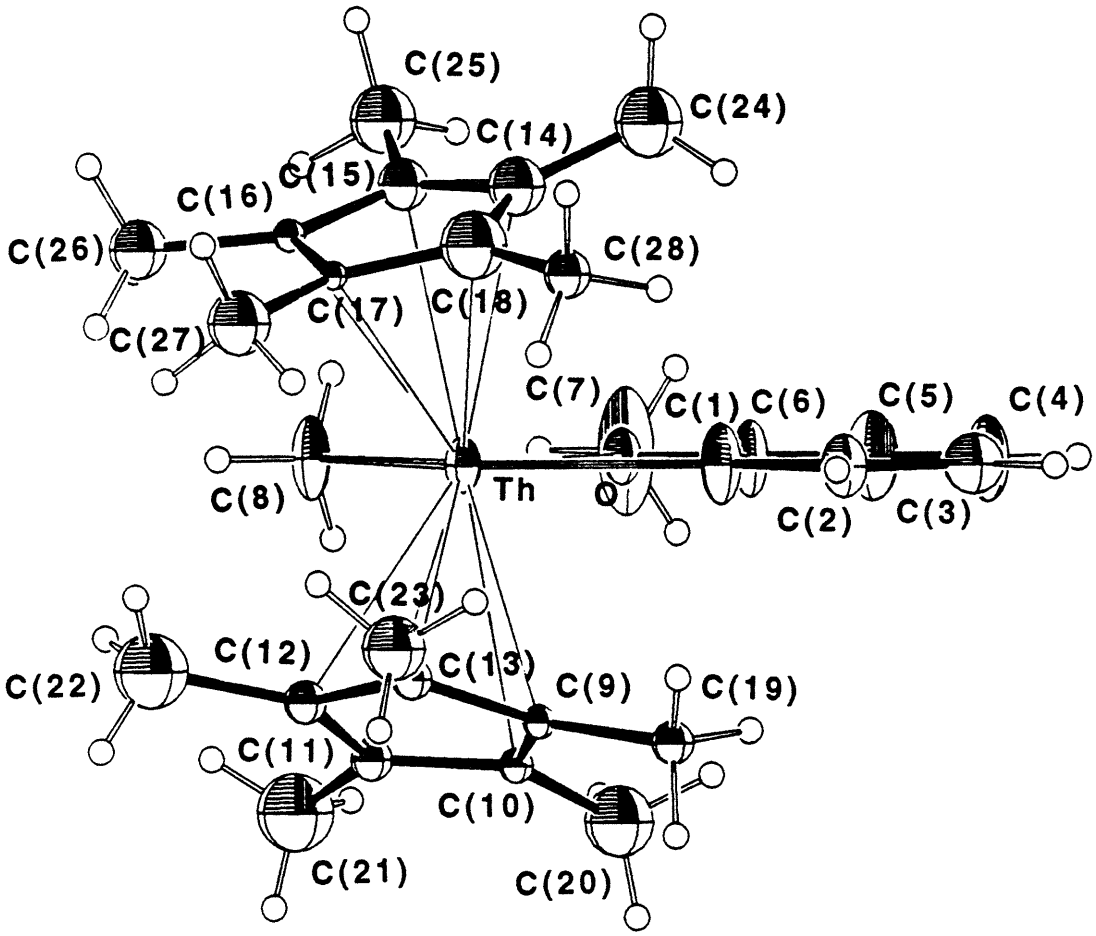

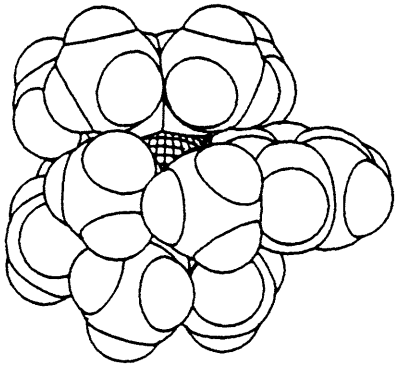

Figure 12. Selected Bond Lengths for Common Atoms of $Cp_2Zr(Me)(o\text{-}MeOC_6H_4)$ (1) and $Cp^*_2Th(Me)(o\text{-}MeOC_6H_4)$ (2)

atom	atom	1	2
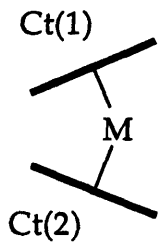		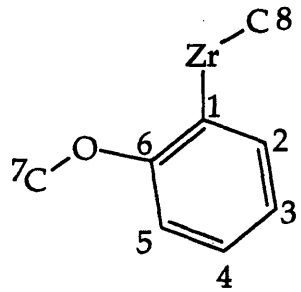	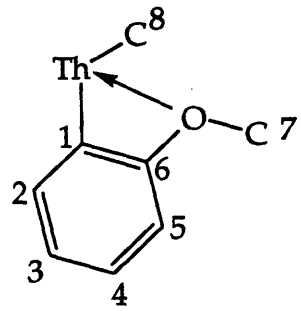
Metal, Methyl and Methoxy			
M	O	-	2.627(15)
M	C(1)	2.291(4)	2.529(20)
M	C(8)	2.300(5)	2.591(18)
O	C(6)	1.390(5)	1.442(22)
O	C(7)	1.423(6)	1.414(26)
Metal-Cp(Centroid)			
M	Ct(1)	2.210	2.614
M	Ct(2)	2.203	2.463
Metal-Cp(sp^2-C)			
M	Cp(1) (ave)	2.507	2.885
M	Cp(2) (ave)	2.499	2.743
Aromatic Ring			
C(1)	C(2)	1.392(6)	1.434(3)
C(1)	C(6)	1.394(6)	1.437(27)
C(2)	C(3)	1.392(6)	1.386(3)
C(3)	C(4)	1.372(7)	1.386(3)
C(4)	C(5)	1.375(6)	1.405(3)
C(5)	C(6)	1.376(6)	1.335(3)

Figure 13. Selected Bond Angles for Common Atoms of $Cp^*_2Th(Me)(o\text{-}MeOC_6H_4)$ (1) and $Cp_2Zr(Me)(o\text{-}MeOC_6H_4)$ (2)

atom	atom	atom	1	2
			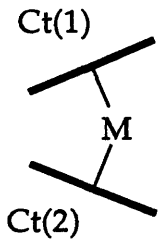	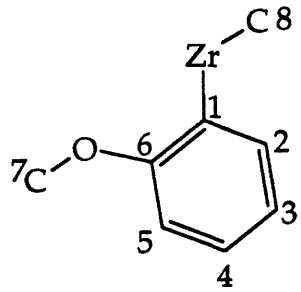	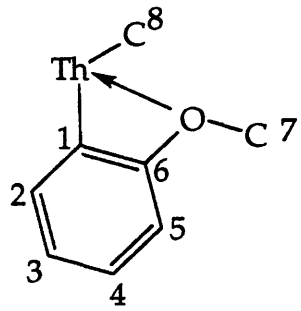
Metal, Methyl and Methoxy				
O	M	C(1)	-	53.6(6)
O	M	C(8)	-	71.2(6)
C(1)	M	C(8)	124.8(7)	97.3(17)
M	O	C(6)	-	97.0(10)
M	O	C(7)	-	145.3(13)
C(6)	O	C(7)	117.8(4)	117.7(16)
M	C(1)	C(2)	116.5(3)	147.1(14)
M	C(1)	C(6)	128.5(3)	101.5(12)
O	C(6)	C(1)	123.1(4)	107.9(15)
O	C(6)	C(5)	122.2(4)	124.0(17)
Metal-Cp(Centroid)				
Ct(1)	M	Ct(2)	132.59	138.1
Aromatic Ring				
C(2)	C(1)	C(6)	115.0(4)	111.4(17)
C(1)	C(2)	C(3)	123.2(4)	123.2(20)
C(2)	C(3)	C(4)	118.9(5)	119.3(21)
C(3)	C(4)	C(5)	120.2(4)	121.5(20)
C(4)	C(5)	C(6)	119.5(4)	116.5(19)
C(1)	C(6)	C(5)	123.1(4)	128.1(18)

Structural Analysis of $Cp_2Zr(Me)(o\text{-}MeOC_6H_4)$ (1) and $Cp^*_2Th(Me)(o\text{-}MeOC_6H_4)$ (2). Several different steric and electronic arguments may be employed to explain the differences between the molecular structures of these seemingly closely related systems. Steric arguments may be drawn from a consideration of the size of the specific metal ion and the effects of the differentially subtituted cyclopentadienyl ligand sets working in conjunction with the methyl and *ortho*-anisyl ligands. The tetravalent actinide is considerably larger than the zirconium equivalent (Th^{IV} = 1.08 Å, Zr^{IV} = 0.86 Å).[14] The difference in ionic radii amounts to a significant decrease in the available space in the coordination sphere of the zirconium nucleus with respect to that of the actinide. Coordination of the oxygen, and the formation of an electronically satisfied eighteen electron zirconium complex may further be precluded by the overwhelming steric constraints at or about the group 4 metal center. The recent expansion of work in the area of Lewis base stabilized adducts of metallocene complexes containing unsaturated σ-bonded fragments has demonstrated the ease with which stable '$Cp_2M^{IV}(X)_2L$' frameworks may be prepared.[3,5,35,49,50] Although to date the only structurally characterized examples of species at all related to **1** are the methoxymethyl derivatives $(C_5H_4R)_2M(CH_2OMe)(Cl)$ (M = Ti, R = Me[51]; M = Zr, R = H[52]) and the zirconocene alkoxyalkyl complexes $Cp_2Zr(Cl)(R)$ (R = CH(Me)OEt,[53] CH_2OCH_2Ph) (Figure 14).[54] Here, the titanocene complex demonstrates monodentate coordination, while all of the related zirconocene species adopt an η^2-oxygen inside conformation. In the case of the zirconocene species, the formation of such bidentate complexes is consistent with the previously determined crystal structures for η^2-acyl[55] and formaldehyde[56,57] derivatives.

Figure 14

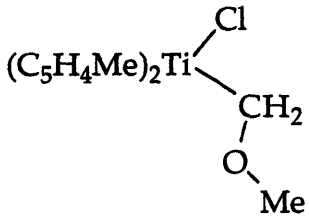

Erker *et al*,**1988**

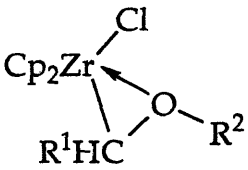

Erker *et al*,**1986**
Buchwald *et al*, **1988, 1989**

Here, the unexpected structural differences in these group between analogous titanium and zirconium species are postulated to be a result of differences in

the Lewis acidities of the first and second row metal ions, since the respective crystal structures reveal no obvious steric barriers.[51] The differences between the Lewis acidity and oxophilicity of tetravalent zirconium and thorium may be a contributing factor in determining the molecular structures of **1** and **2**.[58,59]

Summary

The zirconocene methyl *ortho*-anisyl complex $Cp_2Zr(Me)(o\text{-}MeOC_6H_4)$ (**1**) readily undergoes thermal decomposition by way of intramolecular C-H activation to yield the transient benzyne species $Cp_2Zr(o\text{-}MeOC_6H_3)$ (85 °C, $t_{1/2} \approx 42$ min). Unlike this and the *ortho*-methylated derivatives $Cp^*_2Th(Me)(o\text{-}MeC_6H_3R)$ (R = H, 5-Me), the actinide analog $Cp^*_2Th(Me)(o\text{-}MeOC_6H_4)$ (**2**) does not demonstrate a comparable level of reactivity (100 °C, $t_{1/2} \approx 25$ h).

An examination of the solution and solid state structures of the *ortho*-methoxy substituted derivatives provides a rationale for the differential stabilities of these two species. X-ray crystallography illustrates that the orientation of the *ortho*-anisyl moiety in **1** is opposite to that of **2**. The crystal structure of **2** also reveals the existence of a significant methoxy-thorium donor interaction which is presumably responsible for the inherent stability of the actinide complex. No such zirconium-oxygen bond is observed in **1**. The conformation of the zirconocene species is thus believed to approximate the intermediate required for the formation of the transition state for methane elimination. Room temperature ^1H NMR NOE difference spectra confirm similar geometries in solution also, and the existence of only a single rotameric form for each complex.

A comparison of the ^1H NMR spectra of **2** with those of *ortho*-methylated actinide analogs and related species exemplifies the strong influence of the *ortho*-substituent on the favored geometries of such complexes, ultimately serving to either assist or inhibit intramolecular C-H activation processes.

Experimental

General Procedures. All manipulations were conducted under an atmosphere of argon or helium in a Vacuum Atmospheres Co. drybox. Nuclear Magnetic Resonance (NMR) spectra were recorded on a IBM (Bruker) AF 250, Bruker AMX 500, Varian XL-300, UN-300 or VXR-500 spectrometer. NMR chemical shifts were determined in benzene-d_6 , and are internally referenced to the solvent (^{1}H, δ 7.15; ^{13}C, δ 128.0). The elemental analysis of $Cp_2ZrMe(o\text{-}MeOC_6H_4)$ was performed by Oneida Research Services, Inc., Whitesboro, New York. Solvents were either dried over sodium/benzopheneone ketyl and subsequently distilled (hexane and THF) or vacuum transferred (benzene-d_6), or distilled after drying over sodium (toluene). *p*-Dioxane was degassed, stirred over 4Å molecular seives, and passed through a plug of alumina prior to use. $Cp_2Zr(Me)Cl$[60] and **2-7**[30,42] were prepared according to published procedures. A solution of *o*-anisylmagnesium bromide was prepared in the glove box, from 2-bromoanisole (Aldrich) and an excess of magnesium, in THF, at room temperature. The concentration of the Grignard reagent was determined to be 0.88 M, upon titration with *sec*-butanol, in THF, using 1,10-phenanthroline as the indicator.[61]

The thermally induced decomposition of **1** and **2** were carried out in benzene-d_6, in J. Young valve sealed NMR tubes, under an atmosphere of argon and helium, respectively. Relative sample concentrations were determined by a comparison of the ^{1}H NMR spectral integrals with those of the internal standard hexamethylbenzene (δ 2.12, s, 18H).

Preparation of $Cp_2ZrMe(o\text{-}MeOC_6H_4)$ (1). Under reduced pressure THF was removed from a solution of *o*-anisylmagnesium bromide (7.0 mL, 6.18 mmol). Subsequently, the oily residue was dissolved in toluene (20 mL). To the vigorously stirred Grignard solution was next added a solution of $Cp_2ZrMeCl$ (1.46 g, 5.37 mmol, also in toluene (20 mL). This effected an immediate color change to a pale yellow, shortly followed by the precipitation of a small quantity of by-product salts. Further precipitation was induced by the addition of *p*-dioxane (1.18 g, 13.4 mmol) to the reaction mixture. The resultant off-white suspension was allowed to stir for 90 minutes before removing the solvent *in vacuo*. The dried product was subsequently

extracted with hexane (140 mL), and filtered through a Celite-topped glass frit, to remove insoluble salts. Analytically pure **1** was obtained as X-ray quality colorless crystals after reducing the solvent volume by half, and cooling, to -40 °C. Combined yield of the first two crops: 1.28 g (69%). ^{1}H NMR (500 MHz, C_6D_6) *d* 0.21 (s, 3H), 3.19 (s, 3H), 5.80 (s, 10H), 6.42 (d, J = 8.0 Hz, 1H), 6.98 (t, J = 7 Hz, 1H), 7.09 (dd, J^1 = 1.5 Hz, J^2 = 7.0Hz, 1H), 7.09 (dd, J^1 = 1.5 Hz, J^2 = 7.8 Hz, 1H). ^{13}C NMR (75.0 MHz, C_6D_6) δ 34.4, 53.2, 107.6, 110.5, 121.6, 127.0, 136.1, 165.3, 168.5. Anal. Calcd for $ZrC_{18}H_{20}O$: C, 62.93; H, 5.87. Found: C, 62.97; H, 5.82.

NMR Data for Thorium (Methyl)(*o*-Aryl) Derivatives 2-7 (^{1}H NMR (250 MHz, C_6D_6). **Cp*$_2$Th(Me)(*o*-MeOC$_6$H$_4$) (2).** δ -0.10 (s, 3H), 1.91 (s, 30H), 3.30 (s, 3H), 6.35 (d, J = 8.0 Hz, 1H), 7.05 (dt, J^1 = 1.7 Hz, J^2 = 7.7 Hz, 1H), 7.20 (t, J = 6.9 Hz, 1H), 7.75 (dd, J^1 = 1.6 Hz, J^2 = 6.6 Hz, 1H). ^{13}C NMR (62.9 M Hz, C_6D_6) δ 11.4, 52.0, 68.4, 106.9, 122.2, 123.3, 126.8, 138.4, 170.0, 198.4.

Cp*$_2$Th(Me)(*o*-MeC$_6$H$_4$) (3). δ 0.51 (s, 3H), δ 1.87 (s, 30H), δ 2.56 (s, 3H), δ 7.05 (m, 2H), δ 7.24 (d, J = 7.4 Hz, 1H), δ 7.38 (t, J = 6.9 Hz, 1H).

Cp*$_2$Th(Me)(2, 5-Me$_2$C$_6$H$_3$) (4). δ 0.55 (s, 3H), δ 1.88 (s, 30H), δ 2.30 (s, 3H), δ 2.56 (s, 3H), δ 6.87 (m, 2H), δ 7.21 (d, J = 7.3 Hz, 1H).

Cp*$_2$Th(*o*-MeOC$_6$H$_4$)Br (5a). δ 1.97 (s, 30H), δ 3.70 (s, 3H). **Cp*$_2$Th(*o*-MeOC$_6$H$_4$)Cl (5b).** δ 1.95 (s, 30H), δ 3.64 (s, 3H). Unassigned aromatic protons for both **5a** and **5b** δ 6.38 (m, 2 x 1H), δ 7.03 (m, 2 x 1H), δ 7.17 (m, 2 x 1H), δ 7.78 (m, 2 x 1H).

Cp*$_2$Th(*o*-MeC$_6$H$_4$)Cl (6). major rotamer: δ 1.93 (s, 30H), δ 2.52 (s, 3H); minor rotamer: δ 1.92 (s, 30H), δ 2.62 (s, 3H). Unassigned aromatic protons δ 6.58 (d, J = 6.6 Hz, 1H (minor rotamer)), δ 6.99-7.08 (m, 2 x 1H each), δ 7.21-7.31 (m, 2 x 2H each), δ 7.73 (d, J = 6.7 Hz, 1H (major rotamer)).

Cp*$_2$Th(2, 5-Me$_2$C$_6$H$_3$)Br (7a) major rotamer: δ 1.96 (s, 30H), δ 2.32 (s, 3H), δ 2.54 (s, 3H); minor rotamer: δ 1.94 (s, 30H), δ 2.30 (s, 3H), δ 2.65 (s, 3H); unassigned aromatic protons: δ 6.09 (s), δ 6.19 (s),δ 6.83 (m), δ 7.18 (m), δ 7.59 (s), δ 7.69 (s). **Cp*$_2$Th(2, 5-Me$_2$C$_6$H$_3$)Cl (7b).** ^{1}H NMR (250 MHz, C_6D_6) major rotamer: δ 1.95 (s, 30H), δ 2.29 (s, 3H), δ 2.53 (s, 3H); minor rotamer: δ 1.92 (s, 30H), δ 2.31 (s, 3H), δ 2.62 (s, 3H).

References

(1) Negishi, E.; Takahashi, T. *Aldrichimica Acta* **1985**, *18*, 31-47.

(2) Negishi, E.; Takahashi, T. *Synthesis* **1988**, 1-19.

(3) Buchwald, S. L.; Nielsen, R. N. *Chem. Rev.* **1988**, *88*, 1047-1058.

(4) Negishi, E. *Chem. Scr.* **1989**, *29*, 457-468.

(5) Broene, R. D.; Buchwald, S. L. *Science (Washington, D. C.)* **1993**, *261*, 1696-1701.

(6) McLain, S., J; Schrock, R. R.; Sharp, P. R.; Churchill, M. R.; Youngs, W. J. *J. Am. Chem. Soc.* **1979**, *99*, 263-265.

(7) Fagan, P. J.; Manriquez, J. M.; Maatta, E. A.; Seyam, A. M.; Marks, T. J. *J. Am. Chem. Soc.* **1981**, *103*, 6650-6667.

(8) See Chapter Four.

(9) *Fundamental and Technological Aspects of Organo-f-Element Chemistry*; Marks, T. J.; Fragalà, I. L., Ed.; Reidel: Dordrecht, Holland, 1984, 49-76.

(10) Cardin, D. J.; Lappert, M. F. *Chemistry of Organo-Zirconium and -Hafnium Compounds*; Wiley: New York, N. Y., 1986.

(11) Collman, J. P.; Hegedus, L. S.; Norton, J. R.; Finke, R. G. *Principles and Alications of Organotransition Metal Chemistry*; University Science: Mill Valley, CA, 1987, Chapter 11.

(12) Moore, C. E. *Ionization Potentials and Ionization Limits Derived from the Analyses of Optical Spectra*; NSRDS-NBS 34, National Bureau of Standards: Washington, D.C., 1970.

(13) Cotton, S. *Lanthanides and Actinides*; Oxford University: New York, NY, 1991.

(14) Shannon, R. D. *Acta Crystallogr., Sect A: Cryst. Phys., Diffr., Theor. Gen. Crystallogr.* **1976**, *A32*, 751-767.

(15) Allred, A. L. *J. Inorg. Nucl. Chem.* **1961**, *17*, 215-221.

(16) Pauling, L. *The Nature of the Chemical Bond, 3d Ed.*; Cornell University: Ithaca, N.Y., 1960, 93.

(17) de Bethune, A. J.; Loud, N. A. S. *Standard Aqueous Electrode Potentials and Temperature Coefficients at 25 °C*; C. A. Hampel: Skokie, IL, 1964.

(18) Secaur, C. A.; Day, V. W.; Ernst, R. D.; Kennelly, W. J.; Marks, T. J. *J. Am. Chem. Soc.* **1976**, *98*, 3713-3715.

(19) Tilley, T. D.; Andersen, R. A.; Spencer, B.; Ruben, H.; Zalkin, A.; Templeton, D. H. *Inorg. Chem.* **1980**, *19*, 2999-3003.

(20) Evans, W. J.; Deming, T. J.; Ziller, J. W. *Organometallics* **1989**, *8*, 1581-1583.

(21) Evans, W. J.; Shreeve, J. L.; Ziller, J. W. *Organometallics* **1994**, *13*, 731-733.

(22) Fendrick, C. M.; Marks, T. J. *J. Am. Chem. Soc.* **1986**, *108*, 425-437.

(23) Bruno, J. W.; Smith, G. M.; Marks, T. J.; Fair, C. K.; Schultz, A. J.; Williams, J. M. *J. Am. Chem. Soc.* **1986**, *108*, 40-56.

(24) Marks, T. J. *Inorg. Chim. Acta* **1987**, *140*, 1-2.

(25) Arney, D. S. J.; Burns, C. J.; Smith, D. C. *J. Am. Chem. Soc.* **1992**, *114*, 10068-10069.

(26) Hall, S. W.; Huffman, J. C.; Miller, M. M.; Avens, L. R.; Burns, C. J.; Arney, D. S. J.; England, A. F.; Sattelberger, A. P. *Organometallics* **1993**, *12*, 752-758.

(27) Arney, D. S. J.; Burns, C. J. *J. Am. Chem. Soc.* **1993**, *115*, 9840-9841.

(28) Boekel, C. P.; Teuben, J. H.; de Liefde Meijer, H. J. *J. Organomet. Chem.* **1975**, *102*, 161-165.

(29) Erker, G. *J. Organomet. Chem.* **1977**, *134*, 189-202.

(30) England, A. F.; Burns, C. J.; Buchwald, S. L. *Organometallics* **1994**, *13*, 3491-3495.

(31) Buchwald, S. L.; Lucas, E. A.; Dewan, J. C. *J. Am. Chem. Soc.* **1987**, *109*, 4396-4397.

(32) Buchwald, S. L.; Lucas, E. A.; Davis, W. M. *J. Am. Chem. Soc.* **1989**, *111*, 397-398.

(33) Buchwald, S. L.; Fisher, R. A.; Foxman, B. M. *Angew. Chem. Int. Ed. Engl.* **1990**, *29*, 771-772.

(34) Buchwald, S. L.; King, S. M. *J. Am. Chem. Soc.* **1991**, *113*, 259-265.

(35) Campora, J.; Buchwald, S. L. *Organometallics* **1993**, *12*, 4182-4187.

(36) Buchwald, S. L.; Watson, B. T. *J. Am. Chem. Soc.* **1986**, *108*, 7411-7413.

(37) Schock, L. E.; Brock, C. P.; Marks, T. J. *Organometallics* **1987**, *6*, 232-241.

(38) Bruno, J. W.; Marks, T. J.; Day, V. W. *J. Am. Chem. Soc.* **1982**, *104*, 7357-7356.

(39) Bruno, J. W.; Marks, T. J.; Morss, L. R. *J. Am. Chem. Soc.* **1983**, *105*, 6824-6832.

(40) Fendrick, C. M.; Marks, T. J. *J. Am. Chem. Soc.* **1984**, *106*, 2214-2216.

(41) Lucas, E. A.; Buchwald, S. L. Unpublished work; (methyl)(1-naphthalyne) zirconocene complexes have been shown to eliminate methane at, or below, room temperature.
(42) See Chapter One.
(43) Bondi, A. *J. Phys. Chem.* **1964**, *68*, 441-451.
(44) Fagan, P. J.; Manriquez, J. M.; Marks, T. J.; Vollmer, S. H.; Day, C. S.; Day, V. W. *J. Am. Chem. Soc.* **1981**, *103*, 2206-2220.
(45) Interpretation of the thermolytic decomposition of the methy-phenyl $Cp^*_2Th(Me)(Ph)$ complex is difficult, since separation of the product away from impurities ($Cp^*_2ThPh_2$ (≈ 10%), $Cp^*_2ThMe_2$ (≈ 10 %)) after synthesis has so far proven impossible. Although little change in the ^1H NMR resonances due to the $Cp^*_2Th(Me)(Ph)$ species is observed, it remains unclear as to whether any or all thermal decomposition derives from the diphenyl precursor following ligand redistribution processes.
(46) Buchwald, S. L.; Lum, R. T.; Fisher, R. A.; Davis, W. M. *J. Am. Chem. Soc.* **1989**, *111*, 9113-9114.
(47) Neuhaus, D.; Williamson, M. P. *The Nuclear Overhauser Effect in Structural and Conformational Analysis*; VCH: New York, NY, 1989, 23-101.
(48) Hofmann, P.; Stauffert, P.; Schore, N. *Chem. Ber.* **1982**, *115*, 2153-2174.
(49) Van Wagenen, B. C.; Livinghouse, T. *Tetrahedron Lett.* **1989**, *30*, 3495-3498.
(50) Takagi, K.; Rousset, C. J.; Negishi, E. *J. Am. Chem. Soc.* **1991**, *113*, 1440-1442.
(51) Erker, G.; Schlund, R.; Krüger, C. *J. Organomet. Chem.* **1988**, *338*, C4-C6.
(52) Erker, G.; Schlund, R.; Krüger, C. *J. Chem. Soc., Chem. Commun.* **1986**, 1403-1404.
(53) Buchwald, S. L.; Nielsen, R. B.; Dewan, J. C. *Organometallics* **1988**, *7*, 2324-2328.
(54) Buchwald, S. L.; Nielsen, R. B.; Dewan, J. C. *Organometallics* **1989**, *8*, 1593-1598.
(55) Tatsumi, K.; Nakamura, A.; Hofmann, P.; Stauffert, P.; Hoffman, R. *J. Am. Chem. Soc.* **1985**, *107*, 4440-4451.
(56) Kro, K.; Skibbe, V.; Erker, G.; Krüger, C. *J. Am. Chem. Soc.* **1983**, *105*, 3353-3354.
(57) Gambarotta, S.; Floriani, C.; Chiesi-Villa, A.; Guastini, G. *J. Am. Chem. Soc.* **1983**, *105*, 1690-1691.

(58) Satchell, D. P. N.; Satchell, R. S. *Chem. Rev.* **1969**, *69*, 251-278.
(59) Satchell, D. P. N.; Satchell, R. S. *Q. Rev., Chem. Soc.* **1971**, *25*, 171-199.
(60) Wailes, P. C.; Weigold, H.; Bell, A. P. *J. Organomet. Chem.* **1971**, *33*, 181-188.
(61) Watson, S. C.; Eastham, J. F. *J. Organomet. Chem.* **1967**, *9*, 165-168.

CHAPTER THREE

The Thorium Benzyne:
Reactivity of the $Cp^*_2Th(C_6H_4)$ Moiety with Lewis Bases

Introduction

Transition metal complexes of high energy organic molecules have received considerable attention over the last twenty years.[1-23] Activity in this field has been extensive, such that there have been a large number of reports encompassing complexes of a wide variety of organic substrates. In the past, we have primarily been interested in the preparation of complexes of group 4 metals of polyunsaturated hydrocarbons for applications in organic synthesis. At the center of these investigations has often been the zirconium complex of benzyne $Cp_2Zr(C_6H_4)$ (benzyne = η^2-didehydrobenzene, *o*-phenylene) (Cp = η^5-cyclopentadienyl), which is known to exist as a short-lived intermediate. Although formally a π-bonded complex of zirconium(II) (eq 1: **I**), both the reactivity and structure of early transition metal complexes of this type bear a much closer relationship to that of its σ-bonded zirconium(IV) *ortho*-phenylene resonance structure (eq 1: **II**).[20,24,25]

The parent benzyne complex is generated by thermally induced abstraction of a hydrogen atom from Cp_2ZrPh_2, with concomitant elimination of an equivalent of benzene. This method for the generation of group 4 benzyne complexes has been expanded to related methyl-aryl systems (eq 1: R_L = Me).[17,26]

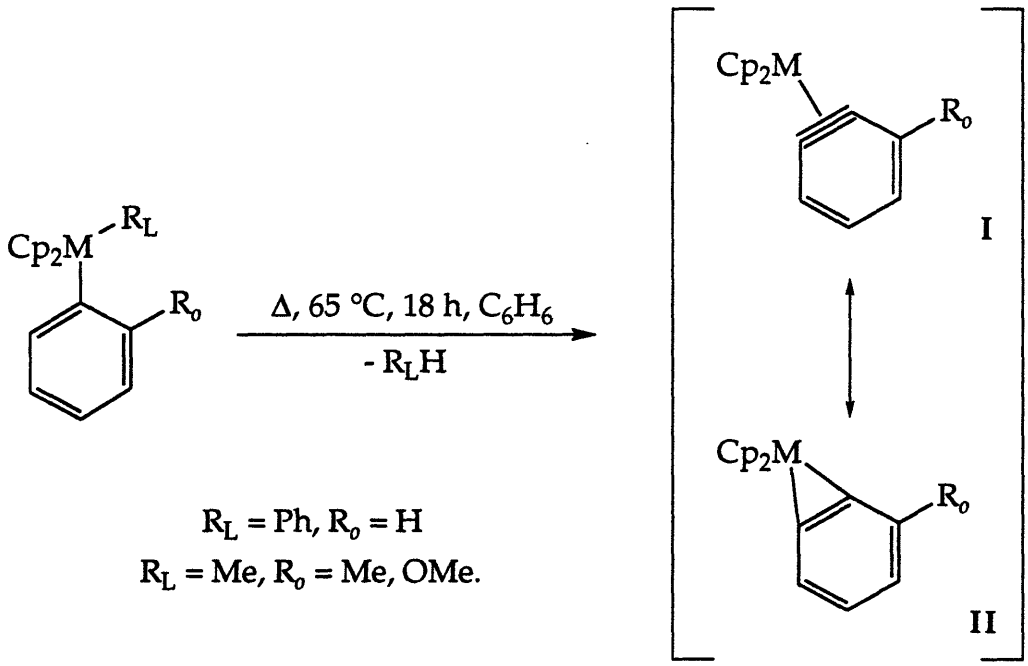

(1)

Numerous examples of benzyne complexes of group 4[18,20,24,25,27] and other metals[20,28] have now been isolated and structurally characterized. The first such species reported was the fourteen electron complex $Cp^*Ta(Me)_2(C_6H_4)$, prepared by Schrock and co-workers.[10] The intrinsic reactivity of group 4 benzyne complexes precluded their isolation for sometime.[1,2,4] Isolation of the first example of a group 4 benzyne complex was ultimately achieved with steric and electronic saturation of the metal center with formation a zirconium benzyne-trimethylphosphine adduct $Cp_2Zr(C_6H_4)(PMe_3)$ (eq 2). A variety of alkene, alkyne and aryne complexes of

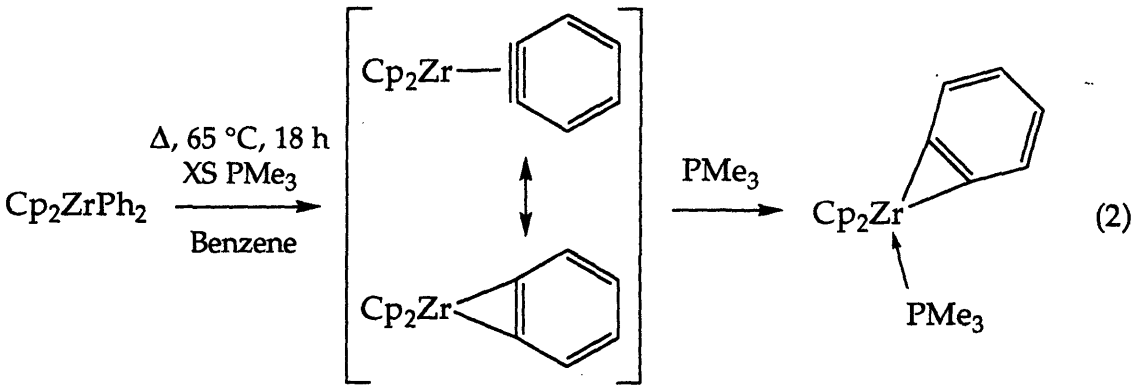

(2)

zirconium, titanium and hafnium complexes have since been prepared and characterized as Lewis base adducts.[18,19,24,25,27,29-32] Both adducts of this type and intermediates generated *in situ* generated have been successfully employed in effecting numerous organic transformations.[17,18,21,22,26]

In many respects, the chemistry of the early actinide elements may be considered as an extension of that of the group 4 metals.[33] However, due to the size of the actinide metal centers, the vast majority of the metallocene (i.e. biscyclopentadienyl) chemistry of these elements revolves around the permethylated derivatives Cp^*_2An (Cp^* = η^5-pentamethylcyclopentadienyl) since smaller unsubstituted bis(Cp) ligand sets commonly employed in group 4 chemistry are unstable with respect to redistribution to mono- and tris-cyclopentadienyl frameworks among larger more electropositive metal ions.[34] Subsequently, in a study of the C-H activation chemistry of thorium and uranium alkyl species. Marks and co-workers reported that the generation of the actinide benzyne benzyne moieties $Cp^*_2An(C_6H_4)$ (An = Th, U) may also be readily achieved upon thermolysis of the respective diphenyl precursors $Cp^*_2AnPh_2$. The existence of transient complexes was proposed

based on spectroscopic, kinetic and labeling studies, and trapping experiments.[11]

Aside from the move to a significantly larger, more electropositive metal center, the thorium system also differs from the zirconocene derivatives by virtue of the more bulky, more electron donating bisCp* ancillary ligand set. Notwithstanding, although this change effects reduction in some strongly oxidizing metal centers,[35-38] this ligand environment is conducive to stability in numerous mid to high oxidation state organoactinide species.[39-45] Furthermore, the difference in ionic radius between the zirconium and the actinide elements all but accounts for the additional bulk of the Cp* ligands in the coordination sphere.[46]

Prior to undertaking an investigation of these systems, it is perhaps also fitting to consider the relationship of the Cp^*_2Th system with direct group 4 analogs. Thermolytic studies have not been performed on the $Cp^*_2TiPh_2$ system, however, formation of the permethylated zirconium benzyne species, from the diphenyl precursor, has been shown to be facile.[47] The reactive benzyne intermediate may be trapped in the presence of ethylene to form a zirconaindan complex.[47] The insertion of unsaturated molecules into alkene/alkyne complexes is well precedented in the literature. However, in the absence of substrate, C-H activation of the Cp*-ring methyl protons is observed to take place, resulting in the formation of the η^6-fulvene complex, $Cp^*_2Zr(\eta^1\text{-}CH_2\text{-}\eta^5\text{-}C_5Me_4)(Ph)$. Although activation of the ancillary ligand set is cited to occur upon thermolysis of the actinide dialkyl $Cp^*_2Th(CH_2Si(CD_3)_2)_2$, to form the fulvene species $Cp^*_2Th(\eta^1\text{-}CH_2\text{-}\eta^5\text{-}C_5Me_4)(CH_2Si(CD_3)_2)$,[42] there is no evidence to suggest the existence of similar phenomena in the benzyne system.[11] In aromatic solvents, and in the absence of a trapping alkene or alkyne the Cp_2M(benzyne) and Cp^*_2An(benzyne) intermediates react similarly to regenerate the respective diphenyl species, by activation of the solvent. After initial studies, there have been no follow-up reports regarding the reactivity of actinide benzyne systems until this point. Equally, there have been no efforts reported to isolate and structurally characterize actinide benzyne complexes. Herein, we report a comprehensive study of the reactivity of the $Cp^*_2Th(C_6H_4)$ moiety with a variety of Lewis bases. One of the original objectives prior to undertaking this research was the preparation and characterization of the first example of a high energy organic species to be stabilized by an actinide metal center; a

thorium complex of benzyne. This goal has so far proven an elusive one. However, although it has not proven possible to isolate a stable benzyne complex, a wealth of novel ligand activation processes have been uncovered from a study of the reactivity of this system. The following results serve to exemplify reasons for difficulties in this respect, and also illustrate the extremely nucleophilic character of the benzyne fragment, and especially in conjunction with an electropositive actinide metal center. An examination of a range of reaction products formed from the thermolysis of $Cp^*_2ThPh_2$ in the presence of differentially substituted donor substrates gives rise to a better understanding of the regioselective nature of the reactivity of nascent Lewis acid-base adducts of this organoactinide intermediate. This work serves to demonstrate not only the apparent similarities between neutral actinide and group 4 systems, but the sometimes significant disparities as well. As a result, some of the chemistry presented relates much more closely to that known cationic zirconium and lanthanide systems, and in some cases, the reactivity unearthed is so far unique to the thorium system.

Results and Discussion

Thermal Decomposition of $Cp^*_2ThPh_2$. Generation of the Transient Thorium Benzyne Intermediate $Cp^*_2Th(C_6H_4)$. The thermolysis of solutions of the bis(pentamethylcyclopentadienyl) actinide diphenyl complexes $Cp^*_2AnPh_2$ (An = Th, U) in aromatic solvents generates the transiently stable actinide stabilized benzyne complexes $Cp^*_2An(C_6H_4)$ (An = Th, U).[11] The short-lived intermediates react too rapidly to be observed by standard NMR techniques, but their identity may be deduced on the basis of deuterium cross-over experiments.[11] Further evidence is provided by a study of the reaction products generated from the reaction of the intermediate with trapping agents.[11] Thermal activation of the uranium derivative proceeds rapidly at room temperature, however, elevated temperatures are required in order to yield similar reaction rates for the thorium system.[11] In this present study, all of the thermolysis reactions were conducted as solutions in benzene or toluene in Schlenk flasks, sealed under an atmosphere of helium, and heated for 4-5 h in a silicon oil bath maintained at 100 °C. In the absence of a more reactive substrate, the highly reactive benzyne complex rapidly activates the solvent, and in benzene-d_6 quantitatively generates the perdeuterated diphenyl derivative (eq 3).[11] Activation of both the aromatic and benzylic

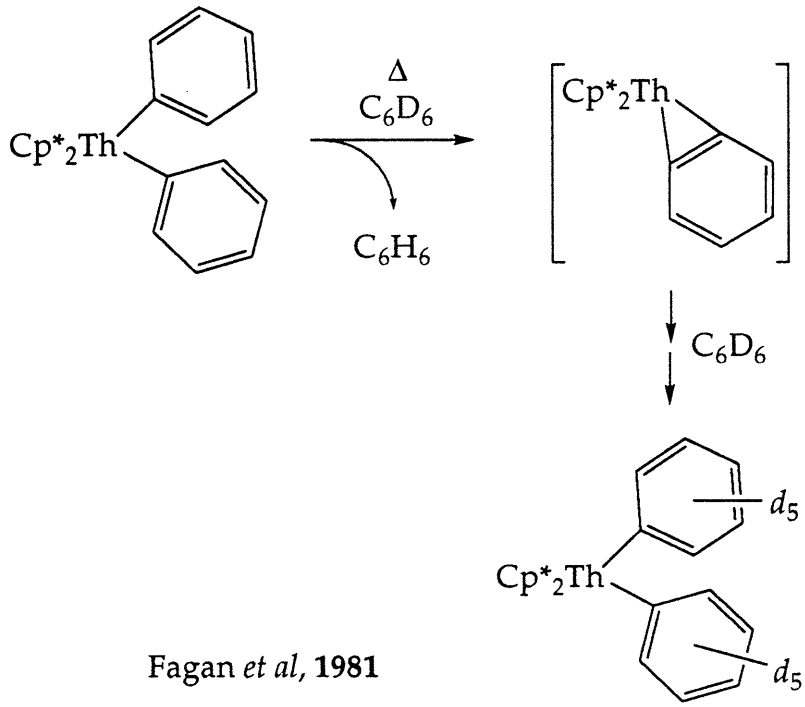

(3)

Fagan *et al*, **1981**

hydrogen atoms of toluene in related systems is known to result in the formation of a complicated mixture of *ortho-*, *meta-* and *para*-tolyl and benzyl species.[1,11]

Reaction of $Cp^*_2Th(C_6H_4)$ with 3-Hexyne. Preparation of $Cp^*_2Th(C_6H_4C(C_2H_5)=C(C_2H_5))$ (1). The insertion of alkynes and alkenes into metal-carbon bonds has previously been shown to be facile in complexes of the *d*- and *f*-transition series of benzyne and other unsaturated ligands.[13,14,16,17,26] The synthesis of an earlier example of a uraniaindene complex from the insertion of diphenylacetylene into the analogous uranium benzyne species was reported.[11] The preparation of metallacycles has often been used as supporting evidence for the existence of proposed intermediates of high energy unsaturated ligands. Insertions of this type typically proceed quantitatively, and the products are readily identifiable. Ethylene itself proves not to undergo clean insertion into the metal-carbon bonds of the benzyne moiety. NMR experiments show the formation of distinct triplet resonances presumably due to the metallindane product $Cp^*_2Th((C_6H_4)CH_2CH_2)$ after only brief periods of thermolysis. However, with extended heating, the signals due to the initial species give way to decomposition products. Although the cyclic geometry of any such thoraindane product likely precludes decomposition via intramolecular C-H activation and the formation of a benzyne intermediate,[33] activation of the ancillary ligand set is conceivable.[42] By analogy with the reported uranium system, the unsaturated thoraindene complex $Cp^*_2Th(C_6H_4C(C_2H_5)=C(C_2H_5))$ (**1**) is however readily prepared from the thermolysis of $Cp^*_2ThPh_2$ in the presence of an excess of 3-hexyne (eq 4). Preparation of the analogous

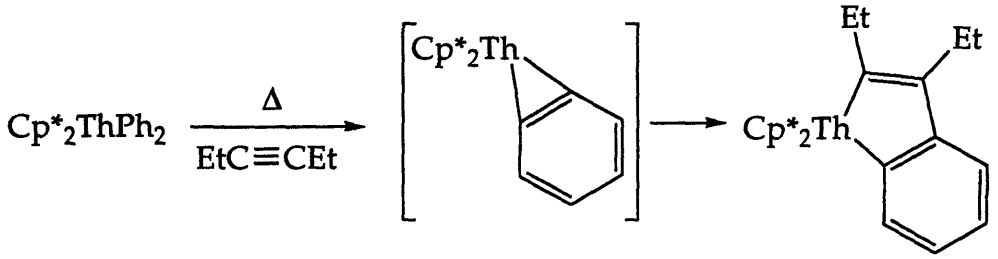

(4)

1

diphenylacetylene-derived metallacycle of thorium has not, however, been attempted. Insertion of this substrate into a Th-C bond of the

metallacyclopropene expected to be facile, although it proves too sterically demanding for the synthesis of the analogous zirconocene metallacycle.[47] The rate of insertion of the alkyne into the metal-carbon bond, is fast enough that deuterium exchange with the solvent is not detected.[11] The use of an excess of the volatile alkyne in the reaction mixture ensures complete conversion to the metallacycle, but does not yield products of multiple insertion. By ^{1}H NMR spectroscopy, the metallaindene **1** is determined to be the sole product of the reaction. The pure crystalline product may be obtained following extraction into, and recrystallization from hexane, with cooling to -40 °C (yield: 69%) The diamagnetic NMR spectra (^{1}H, ^{13}C) of **1** are as expected, and consistent with those previously reported for other diamagnetic thorium(IV) alkyl derivatives.[11,42,44,48-53]

Solid State Structure of $Cp^*_2Th(C_6H_4C(C_2H_5)=C(C_2H_5))$ (1). The results of an X-ray crystallographic determination of a suitable crystal of **1** illustrates the nature of the thoraindene framework (Figures 1-3; Appendices 3.12, 3.14-3.16). The hydrocarbon framework that constitutes the metallaindene lies in the equatorial plane that bisects the metallocene wedge. As is clear from the crystal structures of **3**, **4** and **5**, (*vide infra*) the increase in bulk due to the incorporation of a third σ-bonded species effects a significant decrease in the Cp(1)-Th-Cp(2) angle creating a more divergent wedge with increased Th-Cp* bond distances. The thorium alkyl distances in the metallaindene (Th-C(21) = 2.486(10); Th-C(29) = 2.502(9) Å) are as expected for a bis(Cp*) thorium dialkyl species (e.g., $Cp^*_2Th(CH_2SiMe_2(o\text{-}C_6H_4))$ = 2.493(11), 2.449(12) Å;[40] $Cp^*_2Th(CH_2CMe_3)_2$ = 2.543(4), 2.456(4) Å;[40] $Cp^*_2Th(CH_2SiMe_3)_2$ = 2.463(13), 2,485(14) Å;[49] $Cp^*_2Th(CH_2CMe_3)(CH_2SiMe_3)$ = 2.47(3), 2.44(3) Å);[40] $[Cp^*_2Th(Me)(THF)_2]^+(BPh_4)^-$ = 2.49(1) Å;[54] $[Cp^*_2Th(Me)]^+[B(C_6F_5)_4]^-$ = 2.399(8) Å)[55] The angles of the metallacycle are distorted somewhat from that expected for a five-membered ring system by the small angle about the metal center (C(21)-Th-C(29) = 73.6(3)°; cf. $Cp^*_2Th(CH_2SiMe_2(o\text{-}C_6H_4))$ = 86.3(4)°,[40] $Cp^*_2Th(CH_2CMe_3)_2$ = 98.1(1)°,[40] $Cp^*_2Th(CH_2SiMe_3)_2$ = 96.8(4)°;[49] $Cp^*_2Th(CH_2CMe_3)(CH_2SiMe_3)$ = 101(3)°).[40]

Figure 1. ORTEP Plot and Space-filling Diagram of $Cp^*_2Th(C_6H_4C(C_2H_5)=C(C_2H_5))$ (1)

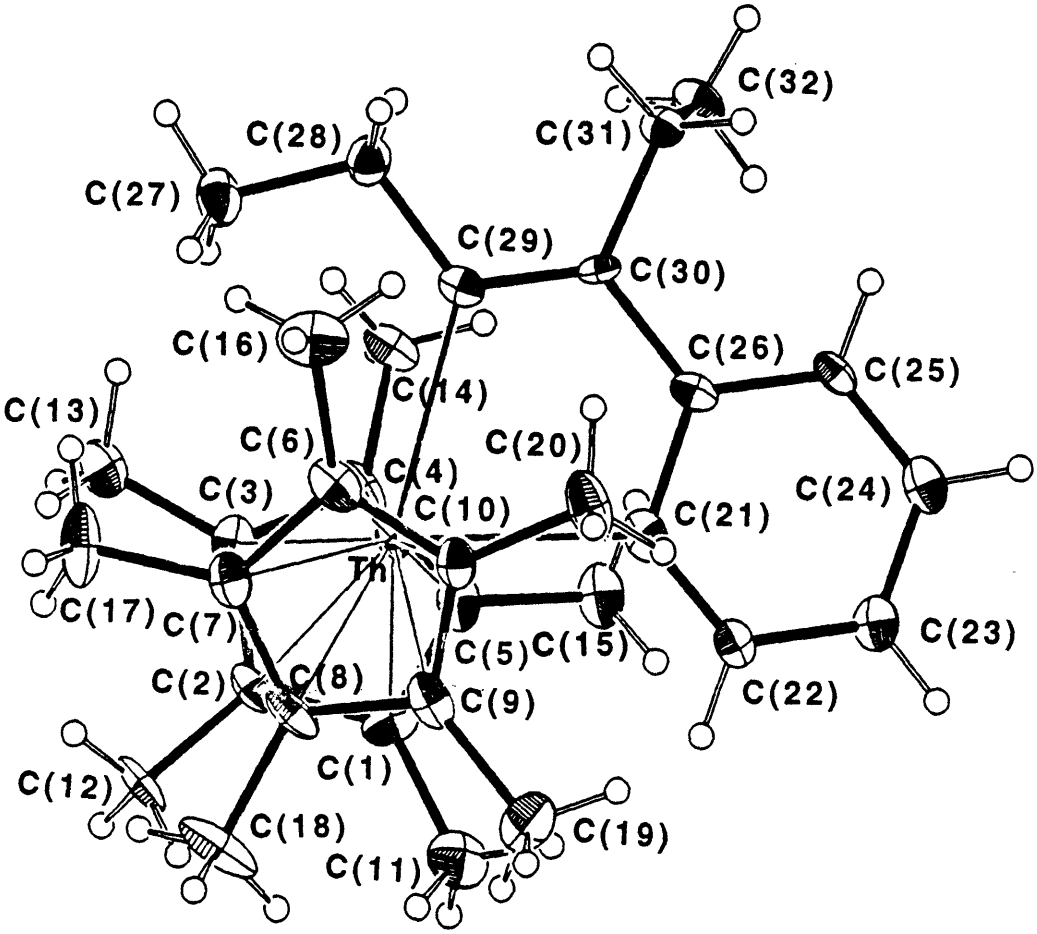

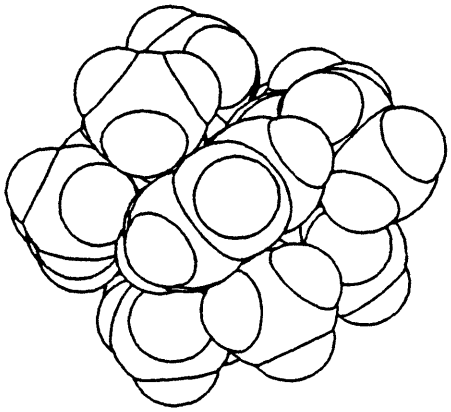

Figure 2. Selected Bond Distances and Angles for $Cp^*_2Th(C_6H_4C(C_2H_5)=C(C_2H_5))$ (1)

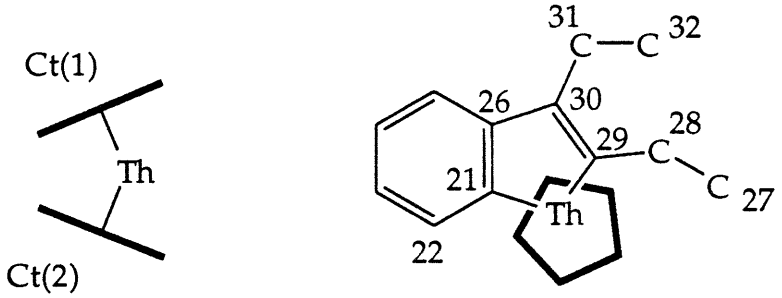

Bond Lengths (Å)

Th	Ct(1)	2.528	C(26)	C(30)	1.505(12)
Th	Ct(2)	2.528	C(28)	C(29)	1.507(13)
Th	C(21)	2.486(10)	C(29)	C(30)	1.371(13)
Th	C(29)	2.502(9)	C(30)	C(31)	1.508(12)
C(21)	C(26)	1.448(12)			

Bond Angles (deg)

Ct(1)	Th	Ct(2)	142.06	Th	C(29)	C(28)	127.2(6)
C(21)	Th	C(29)	73.6(3)	Th	C(29)	C(30)	112.4(6)
Th	C(21)	C(22)	130.1(7)	C(28)	C(29)	C(30)	120.1(8)
Th	C(21)	C(26)	110.2(6)	C(26)	C(30)	C(29)	121.4(8)
C(21)	C(26)	C(30)	122.0(8)	C(26)	C(30)	C(31)	116.6(8)
C(25)	C(26)	C(30)	121.1(8)	C(29)	C(30)	C(31)	122.0(8)

Figure 3. ORTEP Plot of $Cp^*_2Th(C_6H_4C(C_2H_5)=C(C_2H_5))$ (1)

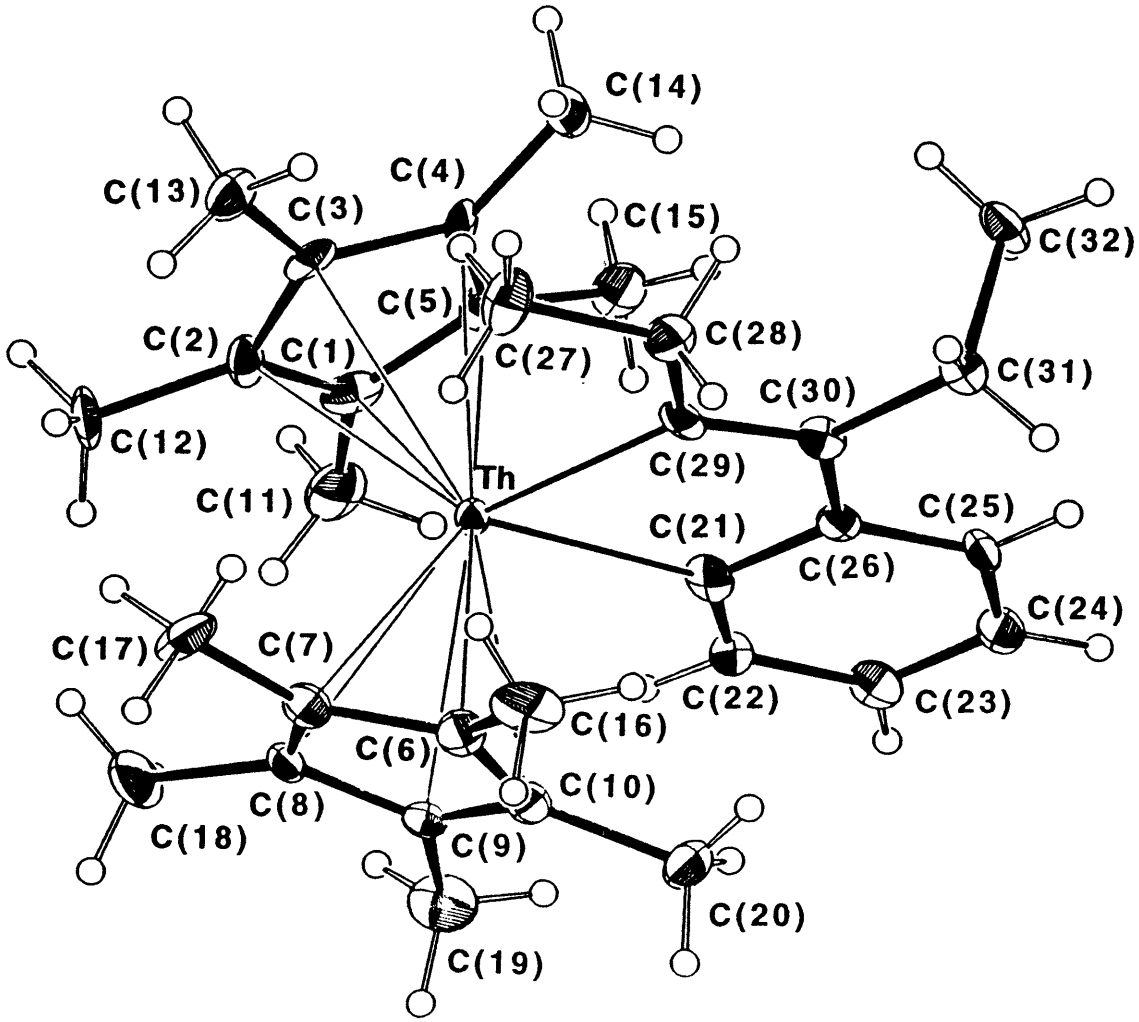

Reaction of $Cp^*_2Th(C_6H_4)$ with 4-Dimethylaminopyridine. Preparation of $Cp^*_2Th(Ph)((4\text{-}NMe_2)C_5H_3N)$ (2). Pyridine ligands have recently been employed successfully as stabilizing Lewis bases in the preparation of adducts of group 4 alkyne[21,22] and benzyne[56] complexes. However, attempts to utilize this strategy for the preparation of an isolable adduct of the thorium benzyne intermediate were unsuccessful. Rather, a study of the reactivity of pyridine ligands towards the thorium benzyne serves as an introduction to a range of regioselective benzyne mediated intermolecular ligand activation processes, all of which are unique among the actinides.

When heated in the presence of one or more equivalents, of 4-dimethylaminopyridine (DMAP), the diphenyl precursor $Cp^*_2ThPh_2$ generates the pyridyl complex $Cp^*_2Th(Ph)((4\text{-}NMe_2)C_5H_3N)$ (**2**) (eq 5). The presence of two inequivalent thorium bound *ipso*-carbon atoms (phenyl and 2-pyridyl) at low-field (^{13}C, C_6D_6: δ 215.0, 231.3) and three aromatic protons imply this structure. Analytically pure colorless crystals of **2** may be isolated

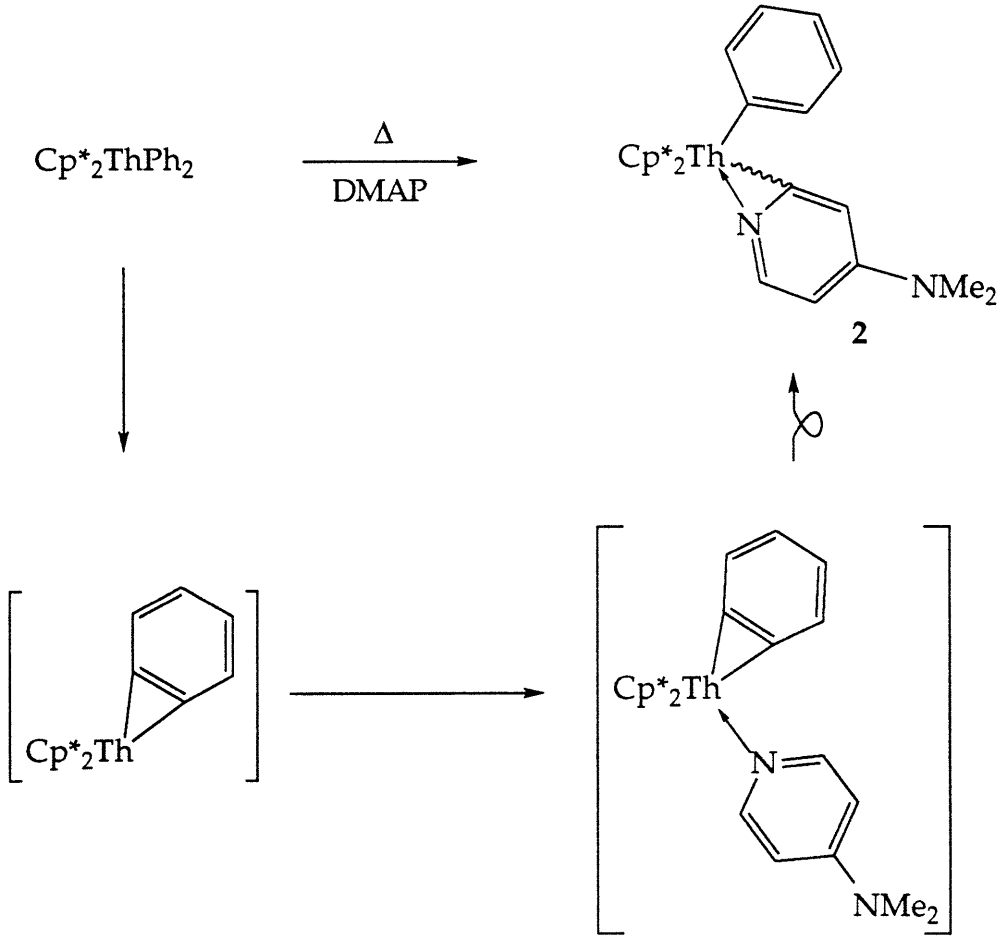

(5)

by recrystallization from hexane at -40 °C (yield: 45%). ^1H NMR experiments reveal that the synthesis of **2** from $Cp^*_2ThPh_2$ and DMAP is essentially quantitative. The molecular structure of **2** is expected to include chelation through the pyridine nitrogen atom, in agreement with related systems.[57-62] Other than enhancing the basicity of the pyridine, the *para*-dimethylamino substituent of DMAP is not believed to have any effect on the course of the reaction. Here, DMAP is simply employed rather than pyridine itself in order to aid isolation and characterization of the product. Preliminary experiments suggest that the reactivity of $Cp^*_2Th(C_6H_4)$ with pyridine or α-picoline is identical.

Intramolecular coordination of the pyridine nitrogen has been observed in all of the crystal structures of related pyridyl systems determined to date.[59-61,63] In a species such as **2**, with potentially three σ-bonded ligands there are three possible modes of coordination which the pyridyl moiety may adopt. In an η^2 fashion, the ligand may either be oriented with the nitrogen bonded to the central coordination site (Scheme 1: **I**) or one of the outer

Scheme 1

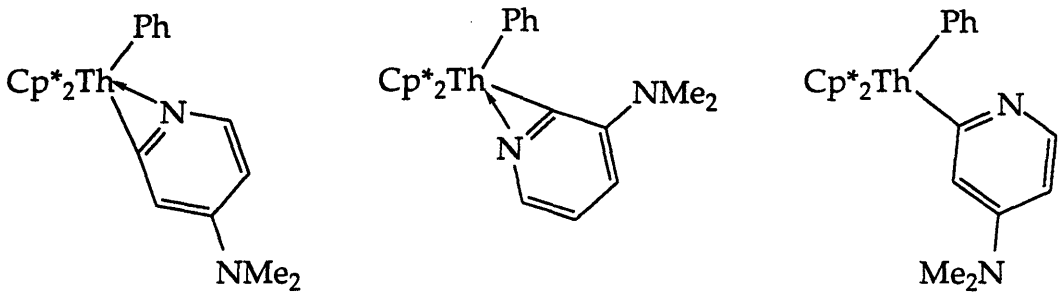

I **II** **III**

positions (**II**). The kinetic product on formation of the zirconocene cation $[Cp_2Zr(\eta^2\text{-}N, C\text{-}(6\text{-Me})C_5H_3N)(THF)]^+$ comprises both rotameric forms, which are observed to slowly convert to a single thermodynamic product.[63] The pyridyl moiety is also known to bind only in a monodentate fashion, however, this is unlikely in the case of the large, electropositive actinide metal center. Although it is expected that **2** adopts a chelated structure, it is not possible to determine which of the two possible geometrical isomers is observed (Scheme 1: **I** or **II**). Furthermore, without low temperature NMR data it is not possible to discount the possibility of the occurrence of rapid

equilibration between conformers at room temperature on the NMR timescale.

The formation of the observed complex necessitates selective C-H activation of the pyridine at the α-position (*ortho*-, 2-H) Activation of either the β-, γ- or *N*-methyl positions is not observed to occur to any significant extent. The regiospecific nature of these reactions suggests that the ligand activation step is preceeded by some degree of coordination of the pyridine nitrogen to the metal center. A highly reactive transient benzyne-DMAP adduct is therefore implicated as the intermediate generated immediately prior to the activation step. This is in stark contrast with related stable group 4 systems.[21,22,56] Presumably coordinative and electronic saturation in eighteen electron group 4 complexes, and the lack of low-lying vacant orbitals in such *d*-series systems precludes intramolecular C-H activation processes. Trivalent titanium pyridine adducts are, however, known to demonstrate similar reactivity to the actinide species to yield η^2-pyridyl derivatives.[57]

The rapid decomposition of the proposed transient adduct of the thorium benzyne, $Cp^*_2Th(C_6H_4)(DMAP)$, leads to the question as to whether analogous zirconocene benzyne-pyridine adducts are indefinitely stable with respect to intramolecular C-H activation and rearrangement to pyridyl derivatives. Both steric and electronic factors suggest generation of the actinide pyridyl to be considerably more favorable than in group 4 systems. The size of the thorium center allows for ease of orientation of both the benzyne and pyridine ligands into the requisite transition state geometry in order to facilitate ligand activation. Further, the actinide species is ultimately better able to accomodate the bulk of the phenyl-pyridyl system, and in so doing maximize stabilization through nitrogen.

Although this is believed to be the first example of pyridine activation by an actinide complex, this mode of reactivity is common for other *d*- and *f*-transition series complexes. Several reports have, however, previously been made regarding the activation of pyridine ligands by lanthanides,[58,59] group 3[61,64] and group 4 systems.[57,62] The η^2-pyridyl complex $Cp^*HfCl_2(C_5H_4N)$ has been prepared by a metathesis route as part of a study into the mechanism of reaction of η^2-silaacyl complexes with pyridine.[60] This hafnium species is the only fully characterized example of a neutral group 4 η^2-pyridyl complex.

While stable and isolable, lanthanide hydride and alkyl complexes demonstrate considerable reactivity toward Lewis bases such as pyridine to

yield η^2-pyridyl derivatives.[58] Group 3 derivatives are also known to react similarly to analogous lanthanide complexes.[61,64] The preparation of such complexes is proposed to proceed following the formation of Lewis acid-base adducts, which have been observed in certain instances.[57,58,65] Subsequently, intramolecular hydrogen abstraction in the bis(pentamethylcyclopentadienyl) derivatives effects formation of the η^2-pyridyl species. In addition, the trivalent titanium alkyl species $Cp_2Ti(R)$ (R = Me, Et, *n*-Bu) undergo similar reactivity with substituted α-pyridine ligands.[57] Conversley, where the η^2-pyridyl complex of yttrium $Cp^*_2Y(C_5H_4N)$ is readily generated from the reaction between pyridine and a dihydride precursor,[59] the less bulky analogs $[(C_5H_4R)_2YH(THF)]$ (R = H, Me) generate pyridine adducts, which have been shown to be stable in pentane solution.[65] Adducts of this type are known to decompose by way of intramolecular hydride transfer in THF solution, to give rise to the formation of the yttrium amide species $(C_5H_4R)_2Y(C_5H_6N)$.[65]

A comparison of the reactivity of the thorium benzyne complex and the zirconocene methyl cation systems with α-substituted pyridine ligands also reveals many similarities. Jordan has demonstrated the facile nature with which the η^2-pyridyl system may be prepared from the interaction of pyridine with $[Cp_2ZrMe(THF)]^+$ (THF = tetrahydrofuran).[62,63,66,67] The mechanism of this reaction is suspected to involve displacement of the coordinated THF by pyridine, followed by a subsequent C-H activation of the pyridine to form the η^2-pyridyl moiety with loss of an equivalent of methane. Likewise, α-picoline (2-methylpyridine) reacts similarly to generate the η^2-(α-picolyl) cation $[Cp_2Zr(6\text{-}Me\text{-}C_5H_3N)]^+$.[63]

It is clear from X-ray crystallographic determinations, that η^2-coordination of the pyridyl moiety is common, although this is not necessarily the case in solution. Recent efforts have been made to establish the presence of such phenomena by solution NMR techniques. The observed NMR (^1H, ^{13}C) spectra of **2** are as expected for a diamagnetic f^0-metal complex, and are consistent with those previously reported for other η^2-pyridyl systems, although these data do not conclusively confirm the chelating nature of the pyridyl moiety in solution.[57-59,61,62,64] A recent report by Teuben and co-workers utilized the chemical shift of the residual *ortho*-hydrogen atom (6-H) of the pyridyl ligand as an indicator for identifying chelation through the nitrogen in related pyridyl systems. This proton, observed at lowest field (^1H, C_6D_6: pyridine δ 8.53; DMAP δ 8.43) in simple

pyridine ligands, has been proposed to shift significantly with coordination of the nitrogen atom upon formation of an η^2-pyridyl moiety.[64] The NMR spectrum of **2** compares favorably with that of other η^2-pyridyl complexes recorded, although the chemical shift observed for the tell-tale proton is the closest so far recorded for that of the free base (Table 1). These data illustrate

Table 1. ^{1}H NMRChemical Shift Data for Low-field 6-H Hydrogen Atom of 2 and Related Pyridyl Species

compound	solvent	*ortho*-H/ δ (ppm)	reference
2	Benzene-d_6	8.45	this work
$Cp^*_2Y(2\text{-}C_5H_4N)$	Benzene-d_6	8.02	64
$Cp^*_2Y(2\text{-}C_5H_4N)(THF)$	Benzene-d_6	8.08	59
$Cp^*_2YCH_2CH_2(2\text{-}C_5H_4N)$	Toluene-d_8	7.45	64
$Cp^*_2Lu(2\text{-}C_5H_4N)$	Cyclohexane-d_{12}	8.23	58
$Cp^*_2Sc(2\text{-}C_5H_4N)$	Benzene-d_6	7.93	61
$Cp^*HfCl_2(2\text{-}C_5H_4N)$	Benzene-d_6	7.92	60
Pyridine	Benzene-d_6	δ 8.53	this work
DMAP	Benzene-d_6	δ 8.43	this work

the difficulties in predicting the solution state structure of **2**, or other derivatives by relying on a comparison of the spectra of related species, since the specific nature of the metal center and auxiliary ligands may strongly influence the resonance frequency of neighboring nuclei. This is further exemplified by a study of the solution and solid state structures of the bis(Cp*) thorium dialkyl complex $Cp^*_2Th(Me)(o\text{-}MeOC_6H_4)$. ^{1}H NOE and X-ray crystal structure evidence categorically show the existence of a significant thorium-oxygen interaction. Notwithstanding, the chemical shift of the tightly held methoxy group protons (^{1}H, C_6D_6: δ 3.30) is effectively unchanged from that of anisole (δ 3.28).[68] equally, this chemical shift is not significantly different from that observed for the zirconium analog $Cp_2Zr(Me)(o\text{-}MeOC_6H_4)$ (δ 3.20), in which a strong donor interaction does not occur.[68]

Perhaps the closest known relatives to the phenyl-pyridyl derivative **2** are uranium imino derivatives $Cp^*_2U(CR{=}N^tBu)(X)$ (R = X = Me; R = Me, X = Cl; R = n-Bu, X = Cl)[69] (Scheme 2: **I**), and the triscyclopentadienyl analogs $Cp_3U(CR^1{=}NR^2)$ (R^1 = Me, R^2 = c-C_6H_{11}; R^1 = n-Bu, R^2 = ^{t}Bu, 2, 6-$Me_2C_6H_3$)[70]

Scheme 2

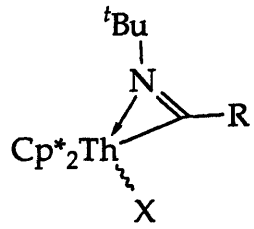

I

R = X = Me
R = Me, X = Cl
R = *n*-Bu, X = Cl

Dormond *et al*, **1984**

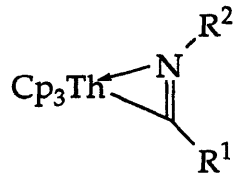

II

R^1 = Me, R^2 = *c*-C_6H_{11}
R^1 = *n*-Bu, R^2 = 2, 6-$Me_2C_6H_3$

Marks *et al*, **1984**

(Scheme 2: **II**). Variable temperature NMR evidence suggests that all of the aforementioned complexes exist as η^2-imino species, since hindered rotation about the uranium-carbon bond is observed (Scheme 2).

In the absence of more concrete structural evidence, it is therefore reasonable to propose that the molecular structure of **2** also involves chelation through the pyridyl nitrogen. Additional support for this hypothesis may be drawn from the crystallographically determined structures of known pyridyl complexes.[59-61,63] Complex **2** may therefore exist in one of two possible geometric forms. NMR studies (^1H, ^{13}C) clearly show the presence of a single species in solution at or above room temperature, which is consistent with either rapid or frozen-out rotation about the thorium-pyridyl linkage. A comparison of the molecular structures of known pyridyl systems[57-59,61,62,64] would seem to indicate that rapid rotation of the η^2-pyridyl moiety is unlikely although rotameric equilibria have been demonstrated in related species.[71] The apparent rigidity of the thorium-nitrogen interaction is further emphasized by the thermal stability of the complex. In the absence of a permanent donor contact, the phenyl-pyridyl would be expected to decompose at a rate comparable to that of $Cp^*_2ThPh_2$.

Kinetic and Mechanistic Analysis of the Formation of 2. Marks and co-workers reported on the rates of formation of $Cp^*_2An(C_6D_5)_2$ from $Cp^*_2An(C_6H_5)_2$ (An = Th, U) during thermolysis in benzene-d_6. In order to corroborate the fact that the rate determining step in the preparation of the ligand activated species under study here also involves the formation of the

same benzyne intermediate, the preparation of **2** from $Cp^*_2Th(C_6H_5)_2$ and DMAP was monitored by ^1H NMR. Thermolysis of the diphenyl precursor was subsequently carried out in the presence of different concentrations of DMAP, and over a range of temperatures in order to determine activation parameters for this process (Appendices 3.1-3.11). Control experiments demonstrate that Lewis acid-base complexes of the precursor complex, e.g. $Cp^*_2Th(Ph)_2(DMAP)$, are not formed either at ambient or elevated temperatures, although such adducts have been observed as intermediates for other η^2-pyridyl precursors.[58,61]. At least one equivalent of ligand is required for conversion to the desired product. The observed rate of the reaction is independent of the concentration of DMAP, and dependent only on that of reactive actinide species. These results are consistent with the previously proposed mechanism, with formation of a highly reactive benzyne complex as an intermediate upon thermolysis of $Cp^*_2ThPh_2$ as the rate determining step of the reaction. Since activation of the Lewis base does not prove to be the rate determining step, it is only possible to speculate on the details of the requisite transition state for the activation step. The regioselectivity of the activation of DMAP supports the idea that precoordination of the pyridine nitrogen to the actinide center is necessary prior to activation, resulting in the formation of the transiently stable adduct $Cp^*_2Th(C_6H_4)(DMAP)$. It is not inconceivable that activation occurs specifically at the α-position of DMAP due to the steric imposition of the dimethylamino group, however, seemingly analogous reactivity with pyridine and α-picoline suggests that this is not the only important consideration. It remains uncertain, however, as to whether coordination of the pyridine nitrogen persists throughout the transition state. The failure of analogous group 4 species to decompose similarly suggests that this is likely the case. It is plausible that the nature of the transition state is one in which activation of the adduct occurs immediately at the point of association or dissociation of the Lewis base. A DMAP adduct of the thorium benzyne complex does not inherently appear to be unstable given that such a species is both coordinatively saturated and electronically satisfied. Since the exact position of the transition state on the reaction coordinate is not known, both of the extremes of Lewis base coordination are presented as potential intermediates (Scheme 3: a: dissociated; b: coordinated). The presence of a significant coordinative interaction between nitrogen and thorium may conceivably only add to the

tight geometrical constraints imposed on the atoms involved in the transition state.

Scheme 3

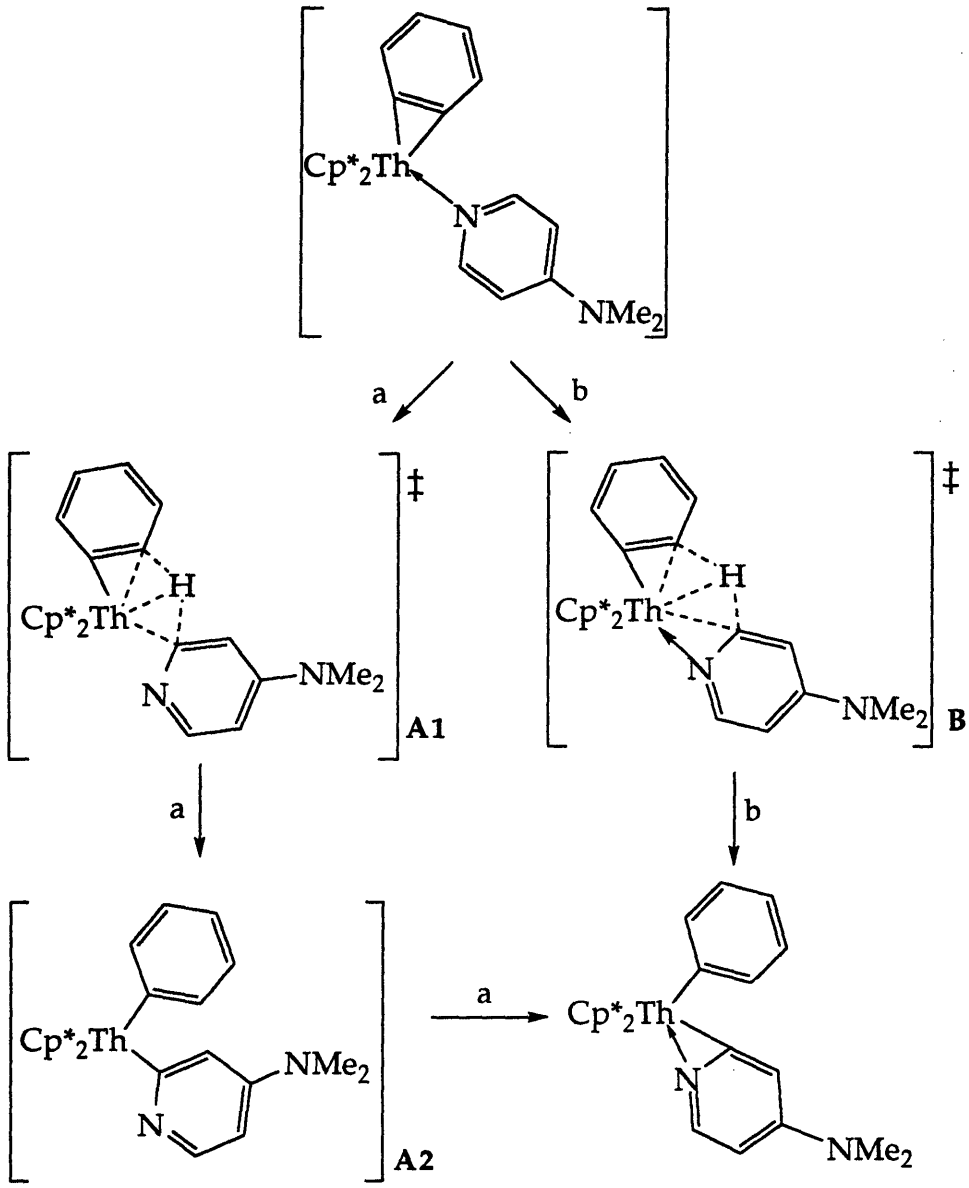

There is no evidence to suggest that deuterium is incorporated into the cyclopentadienyl methyl groups to any significant extent, providing no reason to suggest the formation of an η^6-fulvene complex as an intermediate in the preparation of **2**.[11] Fulvene derivatives have previously been implicated as the active species in C-H activation processes of related thorium[42] and group 4[12,19,47] alkyl species.

The observed rate constants have been used to calculate a set of activation parameters for the preparation of **2**: E_a = 29.7 (9) kcal/mole; $\Delta H^{\ddagger}$ = 28.9 (9) kcal/mole; 5.5 (4) eu; $\Delta G^{\ddagger}$ = 26.9 (10) kcal/mole (Tables 2 and 3). The derived values fall well within the range expected for a unimolecular process involving formation of $Cp^*_2Th(C_6H_4)$ from $Cp^*_2ThPh_2$, with concomitant elimination of an equivalent of benzene. The statistics also compare favorably with those determined for related systems (Table 4)[11,72]. The rate constants determined herein are comparable to that established for the $Cp^*_2ThPh_2/Cp^*_2Th(C_6H_4)$ system, obtained in the absence of a trapping ligand.[11]

Table 2. Observed Rate Constants and Half-lives for Kinetic Studies

sample	temperature/°C	k_{obs} x 10^{-5} (σ)/s-1	$t_{1/2}$/min
A1	72.7	6.66 (0.5)	173
A2	72.7	5.18 (0.8)	223
B1	78.2	16.13 (0.7)	720
B2	78.2	15.05 (1.9)	764
C1	89.0	42.83 (2.9)	270
C2	89.0	43.35 (2.3)	266

Table 3. Calculated Rate Constants at 25, 70, and 100 °C

temperature	k_{calc} x 10^{-5} (σ)/s^{-1}	$t_{1/2}$/min
25	0.00576	2.01 x 10^5
70	4.08	283
100	135	8.53

Table 4. Activation Parameters and Rate Constants (at 70 °C) for the Thermolysis of $Cp^*_2ThPh_2$ and Related Compounds

compound	10^5k, s-1	Ea, kcal/mole	$\Delta H^{\ddagger}$, kcal/mole	$\Delta S^{\ddagger}$, eu	$\Delta G^{\ddagger}_{25\,°C}$, kcal/mole	reference
$Cp^*_2Th(C_6H_5)_2$	4.08	29.7 ± 9	28.9 ± 9	5.5 ± 4	26.9 ± 10	this work
$Cp^*_2Th(C_6H_5)_2$	≈ 3[b]					11
$Cp^*_2U(C_6H_5)_2$	≥170	-	-	-	-	11
$Cp^*_2Zr(C_6H_5)_2$	9.2	23.1 (3)[a]	22.5 (3)[a]	-11.8 (3)[a]	26.0 (4)[a]	47
$Cp^*_2Zr(C_6D_5)_2$	-	26.5 (4)[a]	25.8 (4)[a]	-5.8 (15)[a]	27.5 (8)[a]	47
$Cp_2Zr(C_6H_5)_2$	3.0	-	-	-	-	1
$Cp_2Zr(p\text{-}MeC_6H_4)_2$	2.8	-	-	-	-	1
$Cp_2Zr(o\text{-}MeC_6H_4)_2$	4.2	-	-	-	-	1
$Cp_2Ti(C_6H_5)_2$	6.2	22	20.9	1.0	20.6	73
$Cp^*_2Ti(C_6H_5)Cl$	11.5	29	27.7	4.0	26.5	74
$Cp^*_2TiMe_2$	1.4	28.36	27.6 (3)[a]	-2.9 (7)[a]	28.4	75
$Cp^*_2Th(R)_2$[c]	-	-	25.4 (13)[a]	-14.4 (4)[a]	29.6	40
$Cp^*_2Th(R)_2$[d]	-	-	28.5 (11)[a]	-3 (3)[a]	29.4	40

[a]Numbers in parentheses are estimated confidence limits

[b]Estimated from data in reference[11]

[c]R = $CH_2Si(CD_3)_3$; thermolysis of $Cp^*_2Th\text{-}[CH_2Si(CD_3)CD_2]\text{-}$ via γ-H abstraction

[d]R = $CH_2Si(CD_3)_3$; thermolysis of $Cp^*_2Th\text{-}[CH_2Si(CD_3)CD_2]\text{-}$ via ring H abstraction

A comparison of the entropies of activation ($\Delta S^{\ddagger}$) in the thermolysis of $Cp^*_2ThPh_2$, $Cp^*_2ZrPh_2$ and Cp_2TiPh_2, is particularly informative. The estimated value for the activation of the zirconium species is negative (-11.8 eu), whereas both of the thorium and titanium complexes are positive (5.5 eu and 1.0 eu, respectively). The decrease in entropy is consistent with a loss of rotational degrees of freedom on moving to the transition state.[47] The transition state geometries for all three of these species are expected to be identical, the observed entropic differences may be attributed to the ancillary ligand set working in conjunction with the respective metal centers. The effects of the difference in electronegativity of these metal centers may be discounted as an important factor here, since the observed trend is the reverse of that which would be expected based on such an argument (Table 4). The combination of two Cp* ligands and the zirconium ion creates a tighter ligand framework, with a higher degree of steric saturation than for either of the Cp^*_2Th or Cp_2Ti systems. This is as expected for a case in which a small metal ion (crystal radius in coordination number six: Ti (0.745 Å) < Zr (0.86 Å) < Th (1.08 Å))[46] is placed in a bulky ligand environment (Cp^*_2 >> Cp_2).

Reaction of $Cp^*_2Th(C_6H_4)$ with α-Substituted Pyridines. Derivatives of bases other than DMAP have been employed, in an effort to prepare an intermediate similar to that responsible for the generation of **2** (i.e. $Cp^*_2Th(C_6H_4)$(DMAP)) which is stable with respect to intramolecular C-H activation (e.g., eq 6). Substitution at the *ortho*-position of the pyridine ring

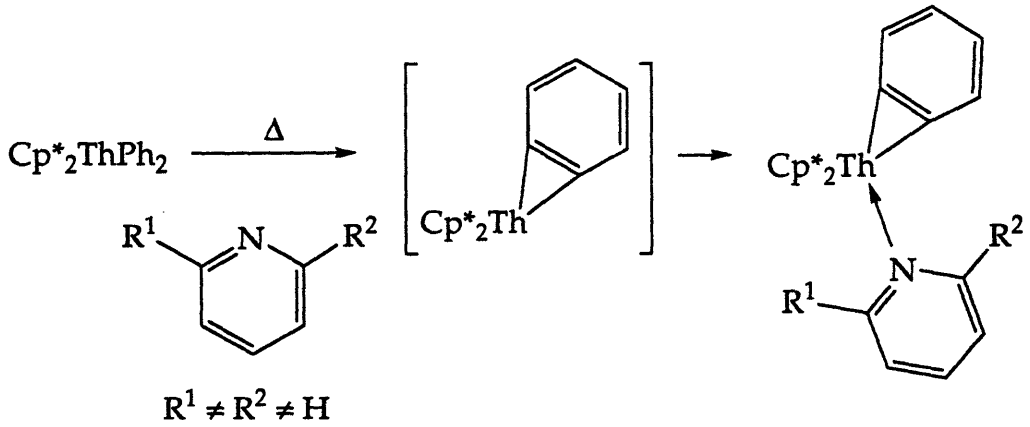

(6)

in some cases dramatically affects the reactivity of the thorium benzyne moiety towards the heterocyclic bases.

Reaction with α-Picoline. The activation of α-picoline (2-methylpyridine) is believed to proceed solely by aromatic C-H activation, as per the preparation of **2**, even though benzylic activation has been shown to be a viable pathway in certain instances (*vide infra*). This is not surprising, since hydrogen abstraction processes are considerably more facile for aromatic systems, than with benzylic or aliphatic substrates. Several examples of η^2-picolyl derivatives have previously been reported among the *d*-transition series.[57,60,62] Furthermore, the large number of examples of L_nM(alkene), L_nM(alkyne), L_nM(benzyne), and L_nM(pyridyl) complexes demonstrates the tendency of the *f*- and early *d*-series complexes to form small rings over larger metallacycles. This is not observed to be the case for late transition metal systems, however, in which the formation of larger rings is often favored.[76-80]

Reaction of $Cp^*_2Th(C_6H_4)$ with α, α′-Disubstituted Pyridines. 2, 6-Lutidine. Preparation of $Cp^*_2Th(Ph)(2\text{-}CH_2\text{-}6\text{-}MeC_5H_3N)$ (3). In the absence of *ortho*-hydrogen atoms, the thermally generated thorium benzyne intermediate reacts cleanly with 2, 6-dimethylpyridine (2, 6-lutidine) to generate $Cp^*_2Th(Ph)(2\text{-}CH_2\text{-}6\text{-}MeC_5H_3N)$ (**3**) by abstraction of one of the benzylic methyl hydrogen atoms (eq 7). The pyridylmethyl-phenyl complex **3**

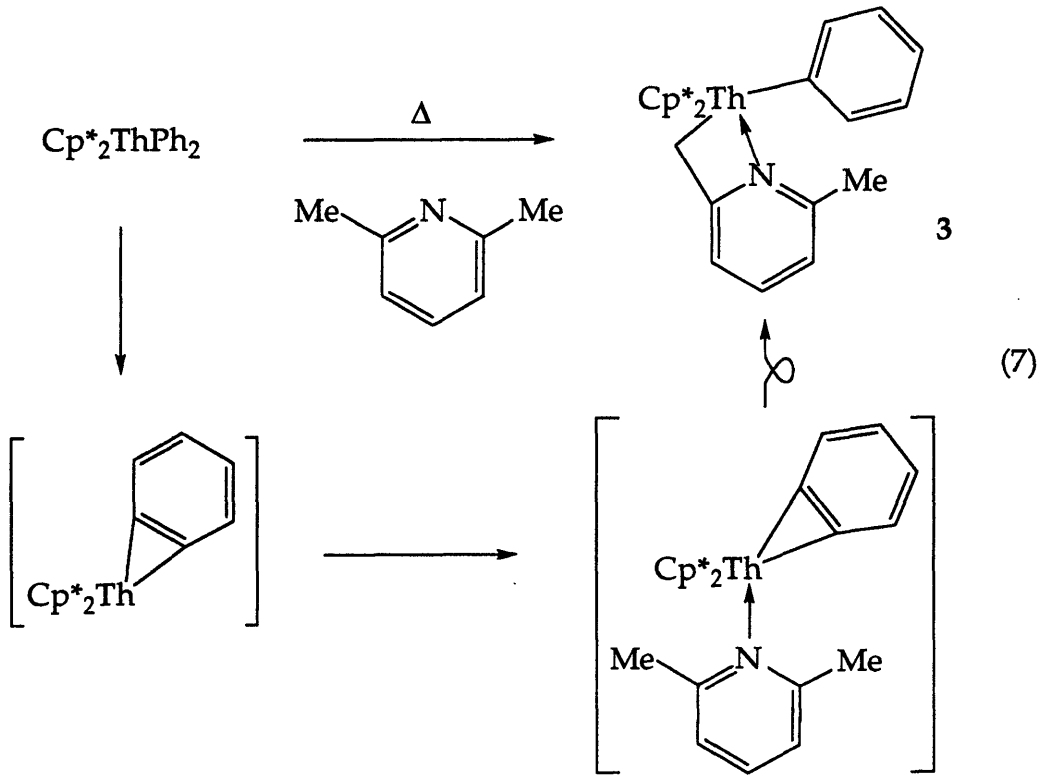

(7)

is generated quantitatively, and may be isolated in pure form as yellow crystals by recrystallization from hexane at -40 °C (yield: 70%). This species is observed to slowly decompose with extended periods of thermolysis, or at elevated temperatures. The mechanistic details of this transformation have not been examined, however, the formation of a single regioisomer of the observed products suggests that C-H activation of a benzylic hydrogen proceeds after initial formation of a transient Lewis base adduct of the thorium benzyne complex. Again, as with the pyridyl derivative, although the donor atom appears to direct the reaction, it is not possible to implicate thorium-nitrogen interaction in the active species (cf. Scheme 3).

The presence of the pyridylmethyl ligand of **3** is readily established from analysis of the $^{13}C\{^1H\}$ NMR spectrum. Activation of the α-methyl group of 2, 6-lutidine is indicated by the the new-found asymmetry of the base, with a low-field triplet (δ 59.7, J_{CH} = 133Hz) for the methylene group and a quartet for the methyl group (δ 25.3, J_{CH} = 126Hz) (Figure 4: **3-η¹**).

Figure 4

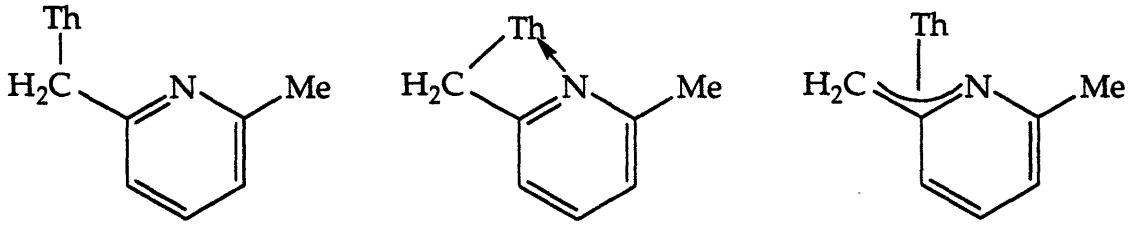

3-η¹ **3-η²** **3-η³**

Bonding of the ligand through the methylene carbon is further supplemented by coordination of the pyridine nitrogen, generating a four-membered chelate. A coupling constant (J_{CH}) of 133Hz for methylene resonance is entirely consistent with the values recorded for other complexes containing the η^2-pyridylmethyl moiety (Figure 4: **3-η²**).[62,81-84] in a cyclobutane-like geometry.[85] Although solution characterization of this complex suggests that the pyridylmethyl fragment is chelated, the full extent of the bonding interaction between the ligand and the actinide is only revealed by the crystal state structure of **3**.

The singlet resonance (THF-d_8, 245 K δ 2.11, 2H) for the methylene group, in the ^1H NMR spectrum of **3** is indicative of equivalence between

protons which prove to be diastereotopic in the solid state. This suggests that in solution the pyridylmethyl fragment is either symmetrically disposed or rapidly flipping between the two possible enantiomeric chelate complexes.[81] The absence of distinct signals for the phenyl aryl protons of **3** reveals that the rate of rotation about the thorium-carbon bond is slow on the NMR timescale. Five discrete resonances are observed at 245 K, in THF-d_8, demonstrating that rotation is effectively frozen-out at this temperature.

There have been several reports regarding the preparation of complexes containing chelating lutidyl (η^2-CH_2{6-Me-C_5H_3N}) fragments. All of the examples so far studied, except for one, have utilized metathetical syntheses.[81-83,86-88] These include the bis(pyridylmethyl) complex Th(2, 6-^{t}Bu$_2$OC$_6$H$_3$)$_2$(CH$_2$-6-MeC$_5$H$_3$N)$_2$, which has been crystallographically characterized.[81] Activation of the α-methyl substituents of 2, 6-dialkylpyridines, $R_2C_5H_3N$ (R = Me, Et) has only recently been demonstrated for the first time by Jordan.[84,89,90]

Solid State Structure of Cp*$_2$Th(Ph)(2-CH$_2$-6-MeC$_5$H$_3$N) (3). The solid state structure of **3** has been determined by X-ray crystallography (Figures 5 and 6; Appendices 3.13, 3.17-3.19). Unfortuantely the poor quality of the data set obtained (R = 5.37%; R_W = 8.46%) from the diffraction experiment precludes the use of the solution for a detailed analysis of the bond distance and angles in the pyridylmethyl complex. The exceptionally long C(27)-C(28) bond distance (1.819(23) Å)is a clear indicator of the error in the refinement of the structure. However, the structure does clearly indicate the connectivity and geometry of the metallocene and organic fragments. In this lutidine derived species, the pyridylmethyl and phenyl ligands occupy three sites in the wedge of the metallocene framework, in which the pyridine nitrogen occupies the central coordination site. The geometry of the pyridylmethyl ligand in **3** is of an η^3-azaallyl complex (Figure 4: **3**-η^3). The conventional thorium-methylene interaction is supplemented by chelation through the pyridyl nitrogen, resulting in the formation of a four-membered metallacycle, and the distance between the metal center and *ipso*-carbon is estimated to be within the range expected for an η^3-allylic interaction. Furthermore, the pyridine ring is tilted considerably out of the equatorial plane bisecting the

Figure 5. ORTEP Plot of $Cp^*_2Th(Ph)(2\text{-}CH_2\text{-}6\text{-}MeC_5H_3N)$ (3)

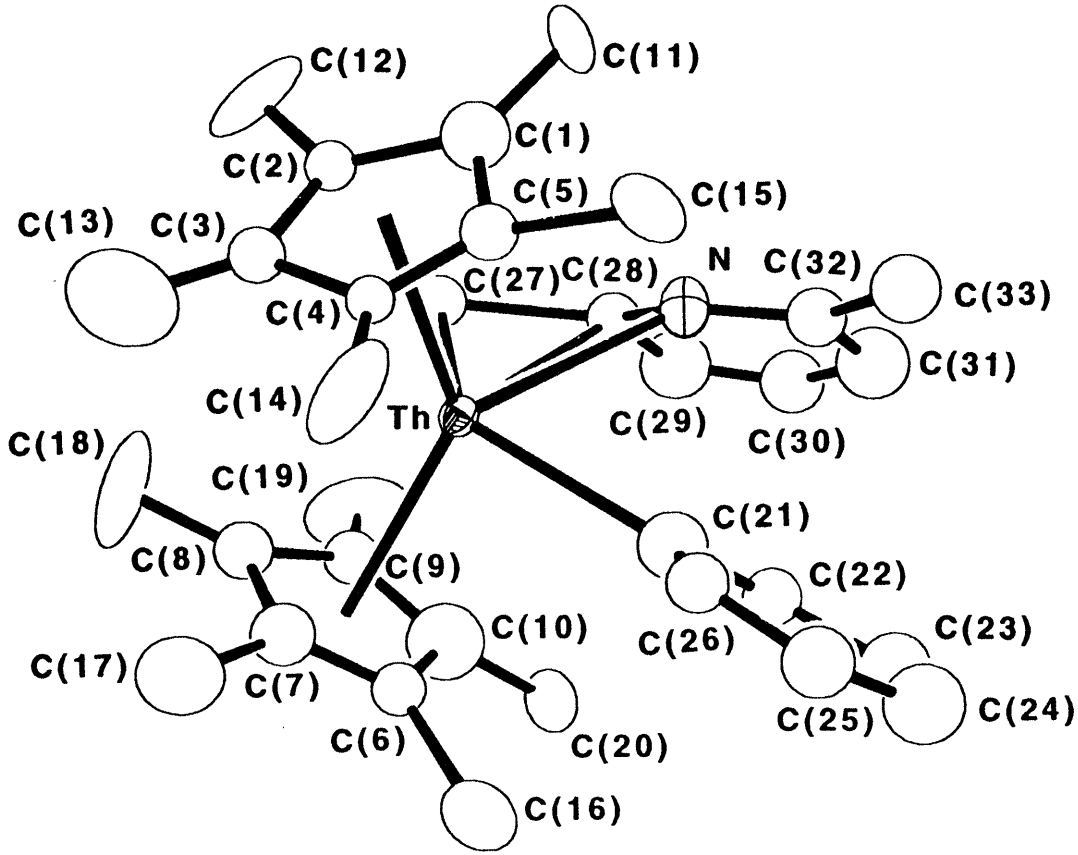

Figure 6. Selected Bond Distances and Angles for $Cp^*_2Th(Ph)(2\text{-}CH_2\text{-}6\text{-}MeC_5H_3N)$ (3)

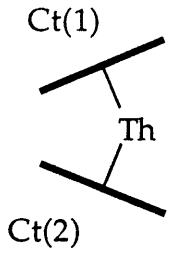

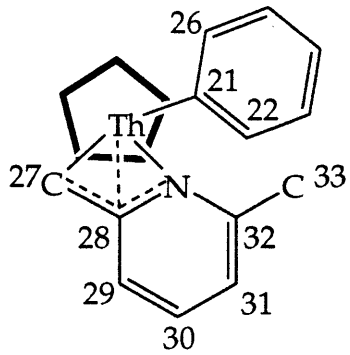

Bond Lengths (Å)

Th	Ct(1)	2.587	N	C(32)	1.335(22)
Th	Ct(2)	2.489	C(27)	C(28)	1.819(23)
Th	N	2.721(14)	C(28)	C(29)	1.438(34)
Th	C(21)	2.597(19)	C(29)	C(30)	1.276(31)
Th	C(27)	2.617(15)	C(30)	C(31)	1.437(34)
Th	C(28)	2.985(19)	C(31)	C(32)	1.416(35)
N	C(28)	1.418(24)	C(32)	C(33)	1.476(29)

Bond Angles (deg)

N	Th	C(21)	73.8(5)	Th	C(28)	C(27)	60.4(7)
N	Th	C(27)	62.5(6)	Th	C(28)	C(29)	139.6(11)
N	Th	C(28)	28.3(5)	N	C(28)	C(27)	117.3(15)
C(21)	Th	C(27)	131.0(6)	N	C(28)	C(29)	119.4(15)
C(21)	Th	C(28)	94.5(6)	C(27)	C(28)	C(29)	121.8(16)
C(27)	Th	C(28)	37.2(5)	C(28)	C(29)	C(30)	117.2(23)
Th	N	C(28)	86.3(9)	C(29)	C(30)	C(31)	124.6(25)
Th	N	C(32)	139.6(11)	C(30)	C(31)	C(32)	118.1(20)
C(28)	N	C(32)	121.4(17)	N	C(32)	C(31)	118.0(19)
Th	C(27)	C(28)	82.5(8)	N	C(32)	C(33)	122.6(19)
Th	C(28)	N	65.5(9)	C(31)	C(32)	C(33)	119.3(17)

metallocene wedge. Although the steric demands of the bulky phenyl, pyridylmethyl and bisCp* moieties cannot be ruled out, this observation suggests that the organic fragment orients in such a way as to maximize overlap between the metal center and the *ipso*-carbon atom of the heterocycle. Tridentate coordination of the pyridylmethyl ligand of **3** is not unexpected, since analogous pyridylmethyl complexes of zirconium[84] and thorium[81] and thorium benzyl[51] systems are known to bind similarly in the solid state.

α, α′-Disubstituted Pyridines, $R_2C_5H_3N$ (R > Me). Exploratory NMR scale experiments show no reaction between the thorium benzyne intermediate and bulky pyridine ligands. Thermolysis of $Cp^*_2ThPh_2$, in benzene-d_6, and in the presence of any of the α, α′-disubstituted bases 2, 6-$R_2C_5H_3N$ (R = Et, ^{i}Pr, ^{t}Bu, *p*-tolyl) simply results in quantitative conversion to the perdeuterodiphenyl derivative $Cp^*_2Th(C_6D_5)_2$ (Scheme 4). Of these bulky

Scheme 4

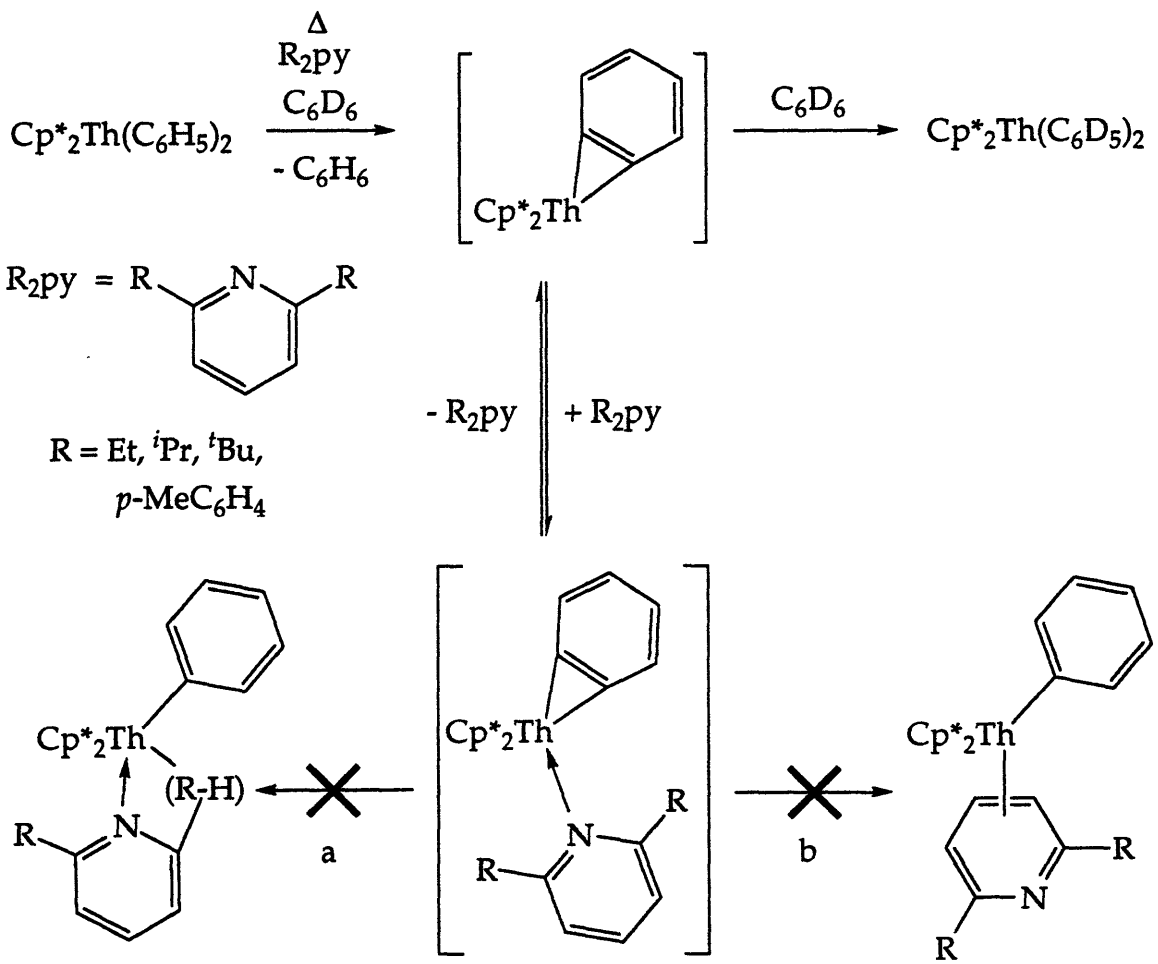

pyridine derivatives, the most imposing di-*tertiary*-butyl system lacks benzylic hydrogens. Subsequently, the most closely related activation of this particular substrate would necessitate abstraction of an aliphatic hydrogen from one of the *tertiary*-butyl methyl groups. Steric factors aside, σ-bonded activation of aliphatic substrates is observed to be extremely slow relative to that of aromatic species in related related systems.[42] In the case of other pyridine ligands containing benzylic hydrogen atoms (e.g. R = Et, ^{i}Pr), there is no evidence to suggest that C-H activation occurs to form analogs of **3**, or other pyridyl derivatives (Scheme 4: a). Equally, hydrogen atom abstraction from the γ- and hindered β-positions of the pyridine ring is not observed to take place to any significant extent (Scheme 4: b). Bulkier pyridines than 2, 6-lutidine are not intrinsically poor substrates for this type of process in *d*-transition metal chemistry. Only recently the metalation of 2, 6-diethylpyridine and 2, 6-lutidine was achieved by activation through the use of cationic zirconium complexes, yielding the zirconocene η^2-pyridylmethyl cations $[Cp_2Zr(2\text{-}CHR\text{-}6\text{-}R'C_5H_3N)(THF)]^+$ (R= H, R′ = Me; R = Me, R′ = Et) the result.[84,89,90]

The failure of the thorium benzyne complex to activate bulkier disubstituted pyridine ligands is simply due to overwhelmingly unfavorable steric constraints effecting the stability of the transition state geometry of the requisite activation step. Since precoordination is implicated in the regioselective activation of the Lewis base, it is conceivable that the bulky pyridine ligands 2, 6-$R_2C_5H_3N$ (R = Et, ^{i}Pr, ^{t}Bu) are simply too large to enable sufficient donation from the nitrogen lone pair to the empty metal based orbital. However, this is not believed to offer a complete explanation for the observed phenomenon, and especially not with 2, 6-diethylpyridine, a ligand that has already demonstrated considerable reactivity.[84] A better understanding of the failure of these ligands to react with the thorium benzyne may be perhaps be drawn from a consideration of the relationship of the actinide species and pyridine ligand in the transition state geometry required for the activation process (Scheme 5: **IV**). Since hydrogen abstraction via a σ-bond metathesis pathway necessitates the formation of a constructive agostic interaction, the other two substituents of the α-carbon have the capacity to strongly influence the stability of the requisite intermediate (Scheme 5: **IV**: X and Y). The planar nature of the transition state thus unavoidably directs both groups toward the bis(Cp*) framework.

Scheme 5

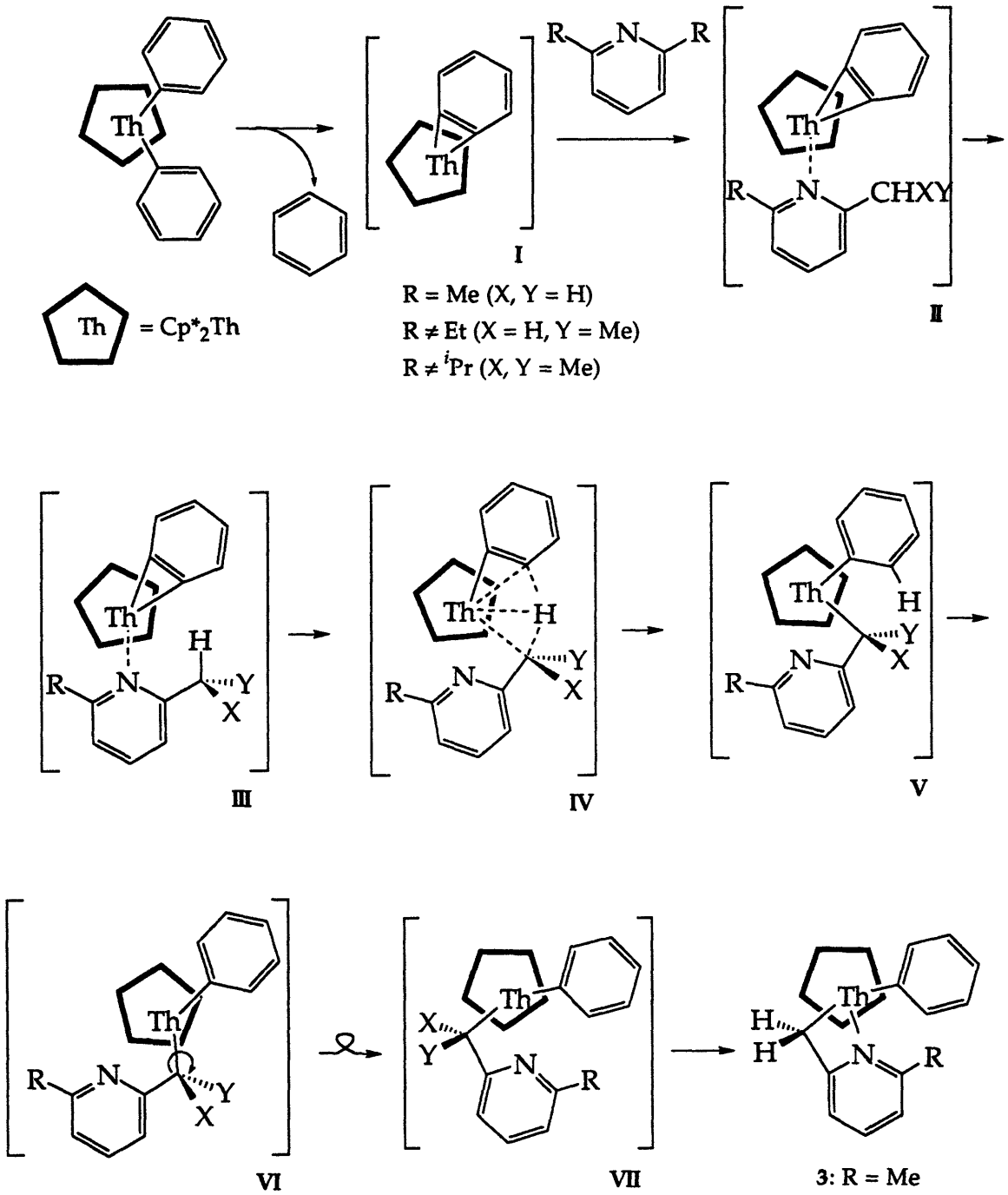

Hence, the steric imposition of bulky α-substituents (X and/or Y ≥ Me) on the Cp* methyl groups prevents formation of the essential agostic overlap. This interaction does not, however, prove unfavorable such as to influence the reactivity of plain ring cyclopentadienyl systems.[84]

Reaction of $Cp^*_2Th(C_6H_4)$ with Triphenylphosphine Oxide. Preparation of $Cp^*_2Th(Ph)(o\text{-}C_6H_4P(O)Ph_2)$ (4). Facile C-H activation also occurs from the reaction of the $Cp^*_2Th(C_6H_4)$ with triphenylphosphine oxide. The observed product of the *ortho*-metaltion process is formation of the phenyl-diphenylphosphinoyl complex $Cp^*_2Th(Ph)(o\text{-}C_6H_4P(O)Ph_2)$ (4) (eq 8).

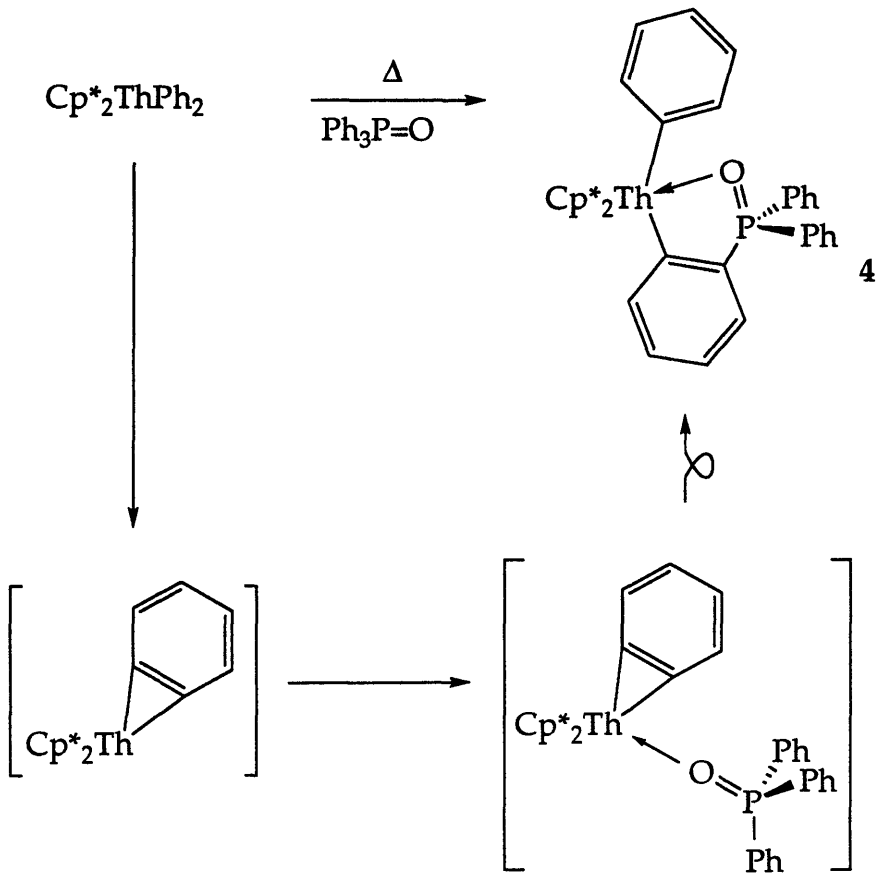

(8)

The sole product of the reaction, **4** may be isolated as colorless crystals with recrystallization from a hot concentrated solution of hexane (60% isolated yield). The complicated nature of the phenyl and *ortho*-phenylene rings precludes identification of the molecular structure of **4** by standard solution NMR methods. It is however clear through the ^{31}P NMR and infrared spectra that the product maintains an interaction between the metal center and phosporyl oxygen in both the solution and solid states. As expected, coordination of the oxygen to the actinide metal center effects a move of the ^{31}P signal to lower field (^{31}P NMR, C_6D_6 δ 58.3) relative to free triphenylphosphine oxide (δ 23.0-27.0).[91]

Although many differentially substituted Lewis bases have been employed as substrates in orthometalation processes, phosphine oxide ligands have effectively been ignored.[92] This is not unexpected, since the vast majority of activation processes of this type have utilized late transition metal systems. A search of the literature reveals the presence of only three species with similar structural feature to those observed in **4**, and subsequently **5**. Of these, the only report of direct regiospecific activation of triphenylphosphine oxide proves to be deprotonation with phenyllithium, yielding Li(*o*-$C_6H_4P(O)Ph_2$), in good yield.[93] Otherwise phosphinoyl complexes have been prepared following the oxidation of *in situ* generated phosphinyl derivatives.[94,95]

Although intramolecular activation processes with ligands of this type have not previously been observed among the actinides, similar reactivity is demonstrated by the lanthanide species Cp^*_2LuR (R = H, Me) (eq 9). The

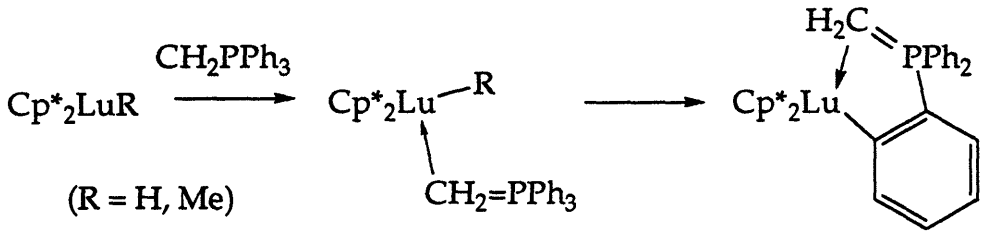

(9)

Watson, **1983**

reaction of the unstabilized phosphaylide CH_2PPh_3 with the lutetium alkyl or hydride complex, initially generates the Lewis base adducts $Cp^*_2LuR(CH_2PPh_3)$ (R = H, Me). Subsequent C-H activation of an aromatic *ortho*-hydrogen atom brings about formation of the observed phosphametallacycle and concomitant elimination of an equivalent of hydrogen/methane.[58]

Adducts analogous to those observed in this lutetium system are not, however, visible as intermediates in the preparation of **4**. A phosphine adduct of the initially generated benzyne species $Cp^*_2Th(C_6H_4)$ is proposed to form, at least transiently, immediately prior to the activation steps, however; this, together with activation of the pyridine moiety exemplifies the similarities that exist between the reactivity patterns observed for the thorium benzyne and lanthanide hydride/alkyl species.

The mechanism of formation of **4** is believed to follow a similar pathway to that observed for the formation of the other activation products (**2** and **3**; *vide supra*). The observed complex is therefore believed to be the thermodynamic product of the activation reaction, which results following rearrangement of an initially generated species, by rotation about the thorium-aryl linkage, and subsequent coordination of the phosphoryl oxygen.

As in the preparation of **2** and **3**, the primary unknown in the mechanism of formation of **4** remains the disposition of the donor oxygen, during the transition state (Scheme 6: a, coordinated; b, dissociated). Without

Scheme 6

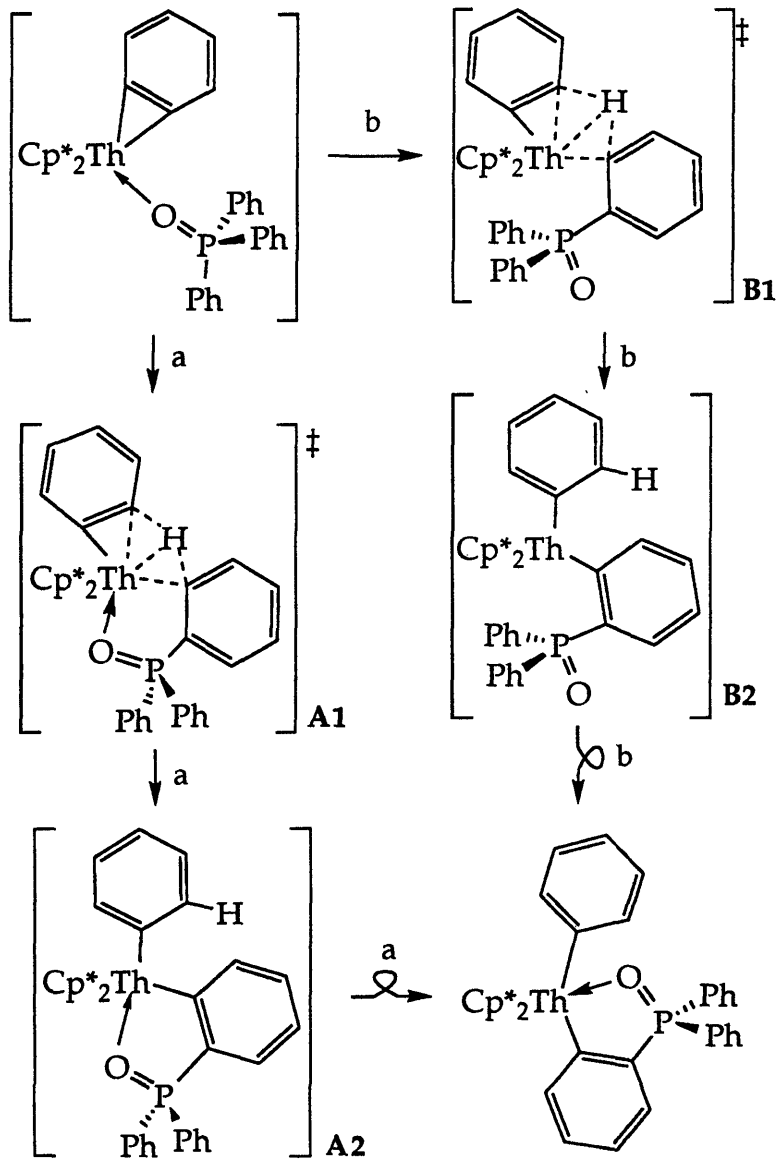

additional insight provided by a thorough investigation of the mechanism of this process, it is possible only to speculate on the exact nature of the geometry of the active species. However, the regioselectivity observed in the preparation of **4** suggests that precoordination of the oxygen is crucial to the outcome of the reaction.

Precoordination of the basic site to the metal center eliminates any possibility of competition in the activation step by the solvent. More importantly though, this contact is believed to target the reaction between the organoactinide intermediate and the *ortho*-hydrogens of the phosphine oxide.

Solid State Structure of $Cp^*_2Th(Ph)(o\text{-}C_6H_4P(O)Ph_2)$ (4). The solid state structure of 4 has been determined by X-ray crystallography (Figures 7-9; Appendices 3.13, 3.20-3.22). The refinement of this structure proved to be extremely problematical, since in the sample analyzed, one of the pair of independent molecules in the unit cell demonstrated considerable disorder in the both the cyclopentadienyl and phenyl substitutents. Therefore, here, an analysis of the solid state structure of **4** is presented, based solely on the parameters determined for the well ordered molecule. Bond distances and angles exhibited by the two different molecules have, however, been determined to be well within the acceptable error ($\pm 3\sigma$) for disparities.

In the solid state the phenyl and diphenylphosphinoyl ligands are almost exactly coplanar, situated in the equatorial plane bisecting the wedge of the metallocene framework. The phosphoryl oxygen atom of the bidentate moiety coordinates the metal center centrally, flanked on either side by the aryl substituents. This orientation is however the reverse of that expected from a consideration of the requisite transition state for the formation of **4** from triphenylphosphine oxide, demonstrating the occurrence of a rearrangement process between the initially generated activation product and the observed species.

The thorium-Cp bond distances (Th-Cp = 2.573, 2.583 Å) and the angle defining the metallocene wedge are as expected for a bulky $Cp^*_2Th(X)_2L$ system (Cp(1)-Th-Cp(2) = 135.5°) (cf. **2**, **3**, **5**; *vide infra*). Consequently, the observed thorium-aryl interactions are both significantly longer (Th-C(21) = 2.634(17) Å; Th-C(39) = 2.591(18) Å) than those in either the dialkyl derivatives **1** (Th-C(21) = 2.486(10) Å) or $Cp^*_2Th(CH_2SiMe_2(o\text{-}C_6H_4))$ (2.449(12) Å) The

Figure 7. ORTEP Plot of $Cp^*_2Th(Ph)(o\text{-}C_6H_4P(O)Ph_2)$ (4): Molecule A

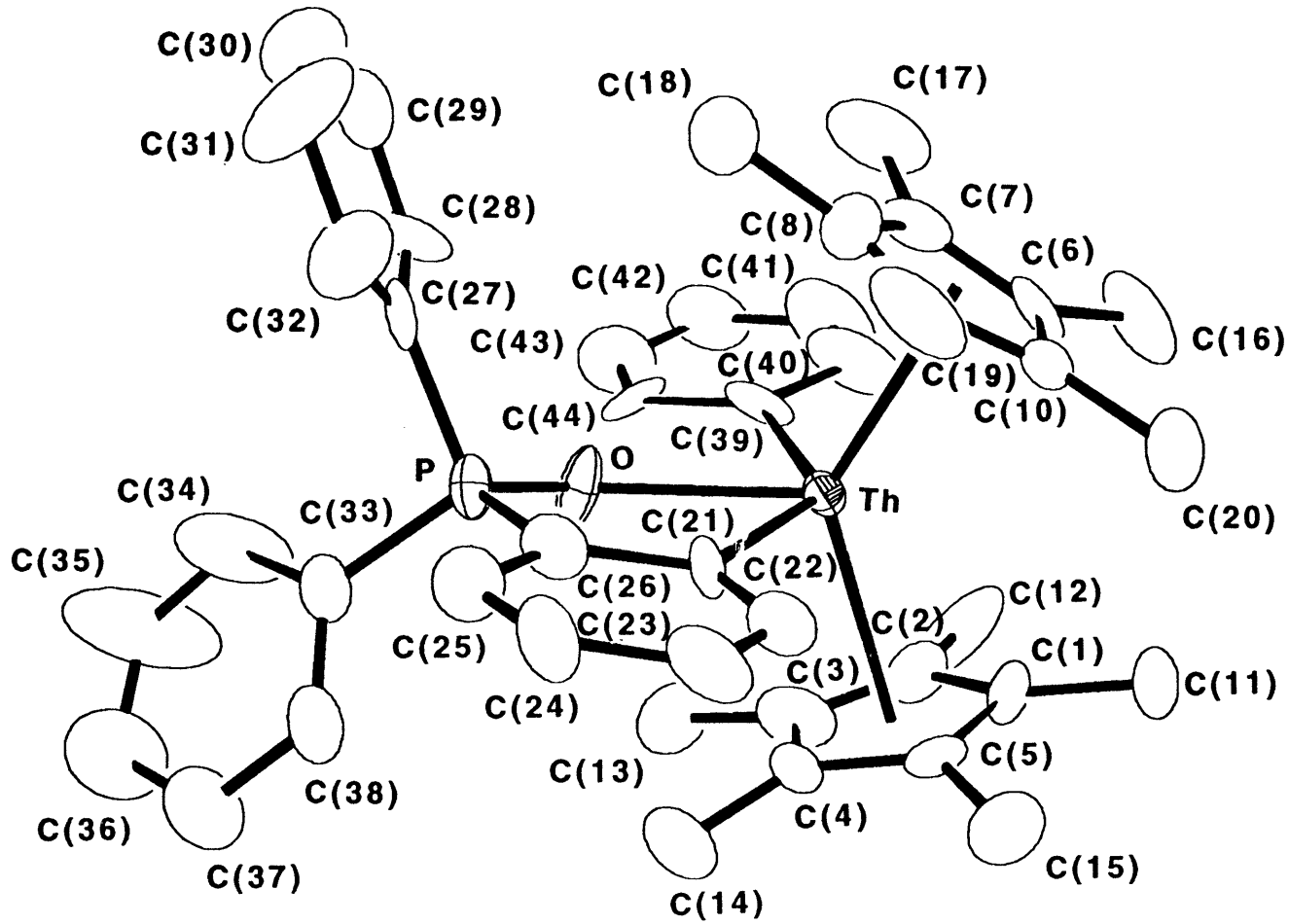

Figure 8. Selected Bond Distances and Angles for $Cp^*_2Th(Ph)(o\text{-}C_6H_4P(O)Ph_2)$ (4): Molecule A

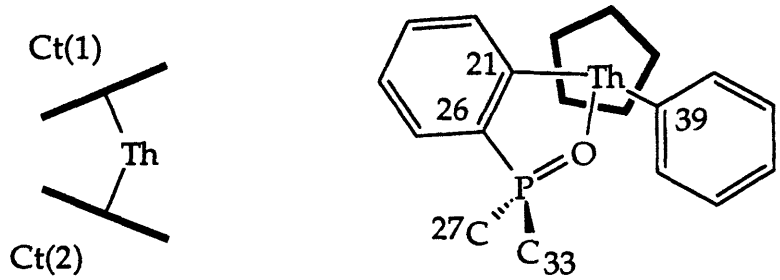

Bond Lengths (Å)

Th	Ct(1)	2.573	P	C(33)	1.781(21)
Th	Ct(2)	2.583	C(21)	C(22)	1.354(23)
Th	O	2.421(12)	C(21)	C(26)	1.439(26)
Th	C(21)	2.634(17)	C(22)	C(23)	1.420(28)
Th	C(39)	2.591(18)	C(23)	C(24)	1.407(31)
P	O	1.526(14)	C(24)	C(25)	1.387(26)
P	C(26)	1.784(17)	C(25)	C(26)	1.419(28)
P	C(27)	1.820(22)			

Bond Angles (deg)

Ct(1)	Th	Ct(2)	135.5	C(26)	P	C(33)	111.1(9)
O	Th	C(39)	72.5(6)	C(27)	P	C(33)	105.1(9)
O	Th	C(21)	68.6(5)	Th	C(39)	C(40)	119.9(16)
C(21)	Th	C(39)	140.8(6)	Th	C(39)	C(44)	126.6(13)
Th	O	P	126.4(6)	P	C(26)	C(21)	113.9(13)
O	P	C(26)	108.4(8)	P	C(26)	C(25)	121.4(15)
O	P	C(27)	108.0(9)	Th	C(21)	C(26)	120.0(11)
O	P	C(33)	111.9(9)	Th	C(21)	C(22)	125.1(13)
C(26)	P	C(27)	112.3(9)				

Figure 9. ORTEP Plot of $Cp^*_2Th(Ph)(o\text{-}C_6H_4P(O)Ph_2)$ (4): Molecule B

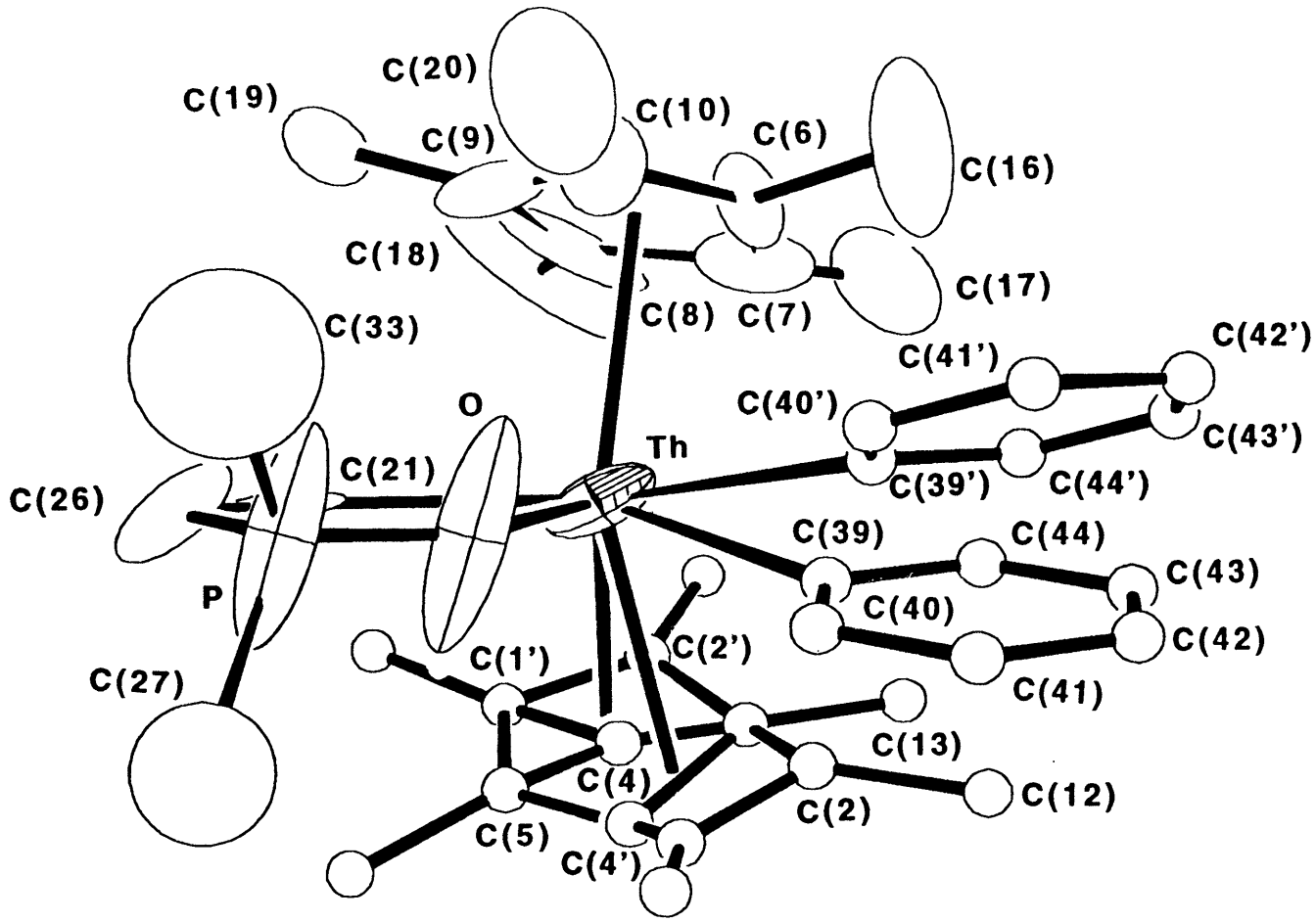

nature of the bonding in the aromatic rings is unexceptional. The thorium-oxygen and phosphorus-oxygen bonding interactions are 2.421(12) Å and 1.526(14) Å, respectively, which are comparable to previously determined Th-O (2.30-2.53 Å) and P=O (1.33-1.54 Å) bonds.[96-98] Intramolecular phosphoryl coordination occurs in **4**, resulting in deformation of the Th-O-P angle (126.4(6)), without however compromising the thorium-oxygen interaction to a significant extent. Aside from **5** (*vide infra*), only three other examples of structurally characterized *o*-phenylphosoyl complexes have been prepared.[94,95] In *trans*-[RhBrCl{(*o*-BrC_6H_4)PPh_2}{*o*-C_6H_4)P(O)Ph_2}] the rhodium-oxygen-phosphorus chelate interaction is approximately linear (Rh-O-P = 175.1(9)°; O-Rh-C = 78.4(8)°), whereas its *cis*-isomer (Rh-O-P = 94.9(3)°; O-Rh-C = 85.6(3)°) and the tin complex Me_2(Cl)Sn(*o*-C_6H_4P(O)Ph_2) (118.7(5)°; O-Sn-C = 78.2(2)°) reflect geometries more similar to that observed in **4**.

The Importance of Donor Atom Stabilization in 2, 3 and 4. In the absence of significant donor atom **2** and **4** may be considered as benzyne precursors in their own right, since the monodentate complexes are simply derivatives of $Cp^*_2ThPh_2$, i.e. $Cp^*_2ThPh(Ar)$ (Figure 10: **2-η¹**: Ar = 2-(4-NMe_2)C_5H_3N);

Figure 10

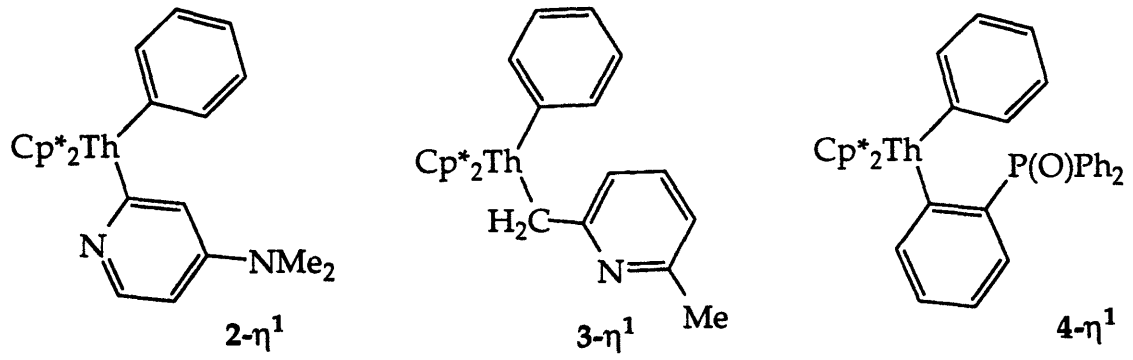

4-η¹: Ar = *o*-C_6H_4P(O)Ph_2). Similarly, **3-η¹** might also be expected to react similarly, since this structure closely resembles alkyl-aryl complexes which also serve as benzyne precursors in related actinide[11,33,53] and group 4[17,26] systems. Furthermore, benzyl-aryl zirconocene derivatives have also been found to generate benzyne intermediates following upon elimination of toluene.[99] Thus if the Th-E (**2**, **3**: E = N; **4**: E = O) coordinative interaction is either weak or labile, all three species might be expected to be extremely thermally unstable, which is not seen to be the case. There is no evidence to

suggest that with prolonged periods of thermolysis any of these species decompose with the elimination of benzene and/or alkane/arene to form respective benzyne derivatives (e.g. **4**: Scheme 7). Decomposition is, however, observed in all cases with extended periods of thermolysis (100 °C, ≈ 18 h).

Scheme 7

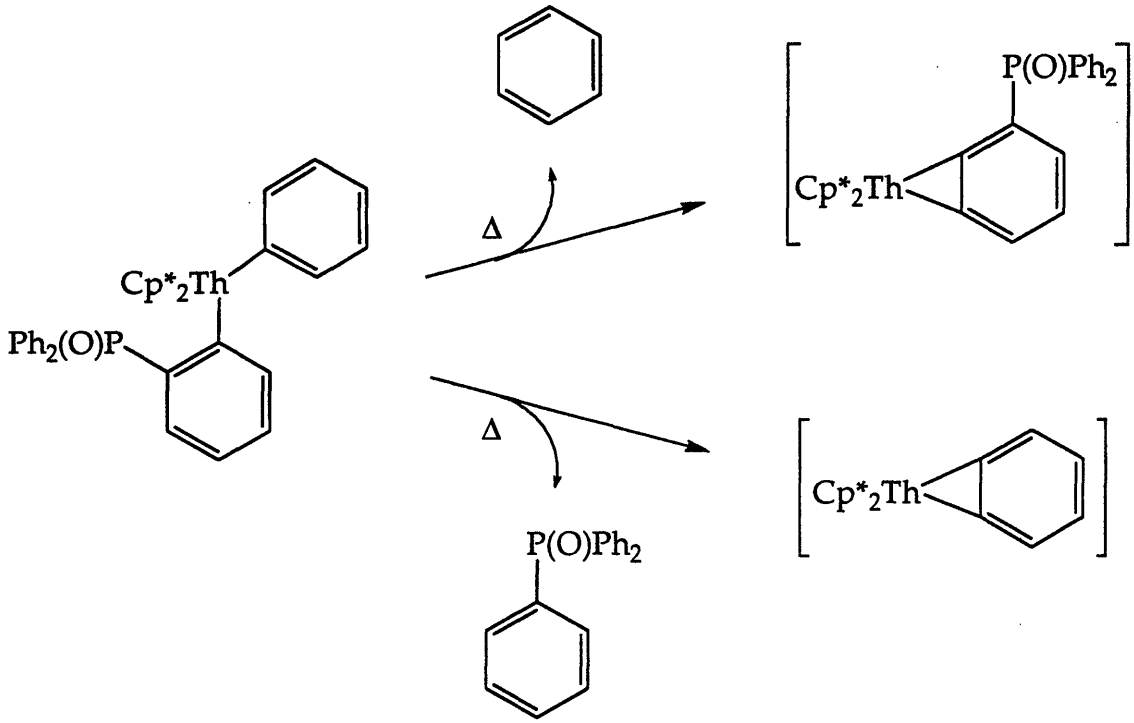

In a system in which the phenylphosphonoyl ligand is monodentate (**4**-η^1), **4** would be expected to be extremely thermally unstable since this structure is effectively that of an *ortho*-substituted diaryl species. To date, the only known examples of *ortho*-substituted diaryl metallocene complexes are the zirconocene systems $Cp_2Zr(Ar)(Ar')$ (Ar, Ar' = Ph, *o*-MeC_6H_4, *m*-MeC_6H_4, *p*-MeC_6H_4) reported by Erker.[1] All of these group 4 species readily undergo facile C-H activation, resulting in the generation of the respective benzyne complexes, under mild thermolysis conditions. Unlike **4**, the zirconium complexes do not possess an element capable of introducing additional intramolecular stabilization to the sterically demanding diaryl species.

More recently, studies on related group 4 systems have demonstrated that bulky, more highly substituted actinide precursors undergo C-H activation far more readily than unsubstituted counterparts.[17,26,33,53,100]

Equally, the bulk of the *ortho*-tolyl substituent in $Cp^*_2Th(Me)(o\text{-}MeC_6H_4)$ facilitates generation of a benzyne intermediate, with extrusion of methane, at lower temperatures than for $Cp^*_2ThPh_2$.[52, 53] In acccordance with this result, exploratory NMR experiments reveal that the parent methyl-phenyl complex $Cp^*_2Th(Me)(Ph)$ demonstrates considerable thermal stability, seemingly due to the absence of the 'steric driving force', responsible for C-H activation in bulkier systems.[17,26,33,100] Furthermore, the introduction of a heteroatom at the *ortho*-position of $Cp^*_2Th(Me)(o\text{-}MeOC_6H_4)$ almost entirely inhibits the typical decomposition pathways experienced by related species, and this species instead demonstrates considerable thermal stability.[33]

The procedure for the preparation of **2**, **3** and **4** alone demonstrates the remarkable thermal stability of these complexes, indicating that the thorium-nitrogen/oxygen interactions, once formed, are not labile. It is therefore apparent that the thermal stability of such complexes depends not only on the level of steric congestion about the metal center, but that it is drastically altered by additional electronic stabilization of the metal center. Similarly, π-donating substituents have been shown to suppress the rates of hydrogenolysis in closely related actinide alkyl species.[41,42]

Overview of the Pathway of C-H Activation of Lewis bases by $Cp^*_2Th(C_6H_4)$. It is apparent from the results of this study that there are only very few requirements to observe, in order to effect clean regioselective activation of Lewis basic substrates. The major barrier to activation of aromatic or benzylic substrates at least, is the presence of unfavorable steric constraints, which either prevent precoordination or access to the requisite transition state for activation. Hydrogen abstraction occurs equally well at positions α, β and γ to the donor atom. Reactive Lewis bases simply have to "fit the Bill" (Clinton) in the sense that the basic site (Scheme 8: B) is positioned proximally to an active hydrogen atom (Scheme 8: H_A), so as to direct the metalation and offer coordinative stabilization to the metal center in the product. The absence of a navigating donor atom does not inhibit hydrogen abstraction from taking place, but rather allows for activation at multiple sites (including solvent). Furthermore, since the trapping effect of intramolecular stabilization is not available the products may themselves be thermally unstable, and subject to additional C-H activation processes, ultimately resulting in a complicated mixture of products. This effect is clearly exemplified by the thermolysis of

Scheme 8

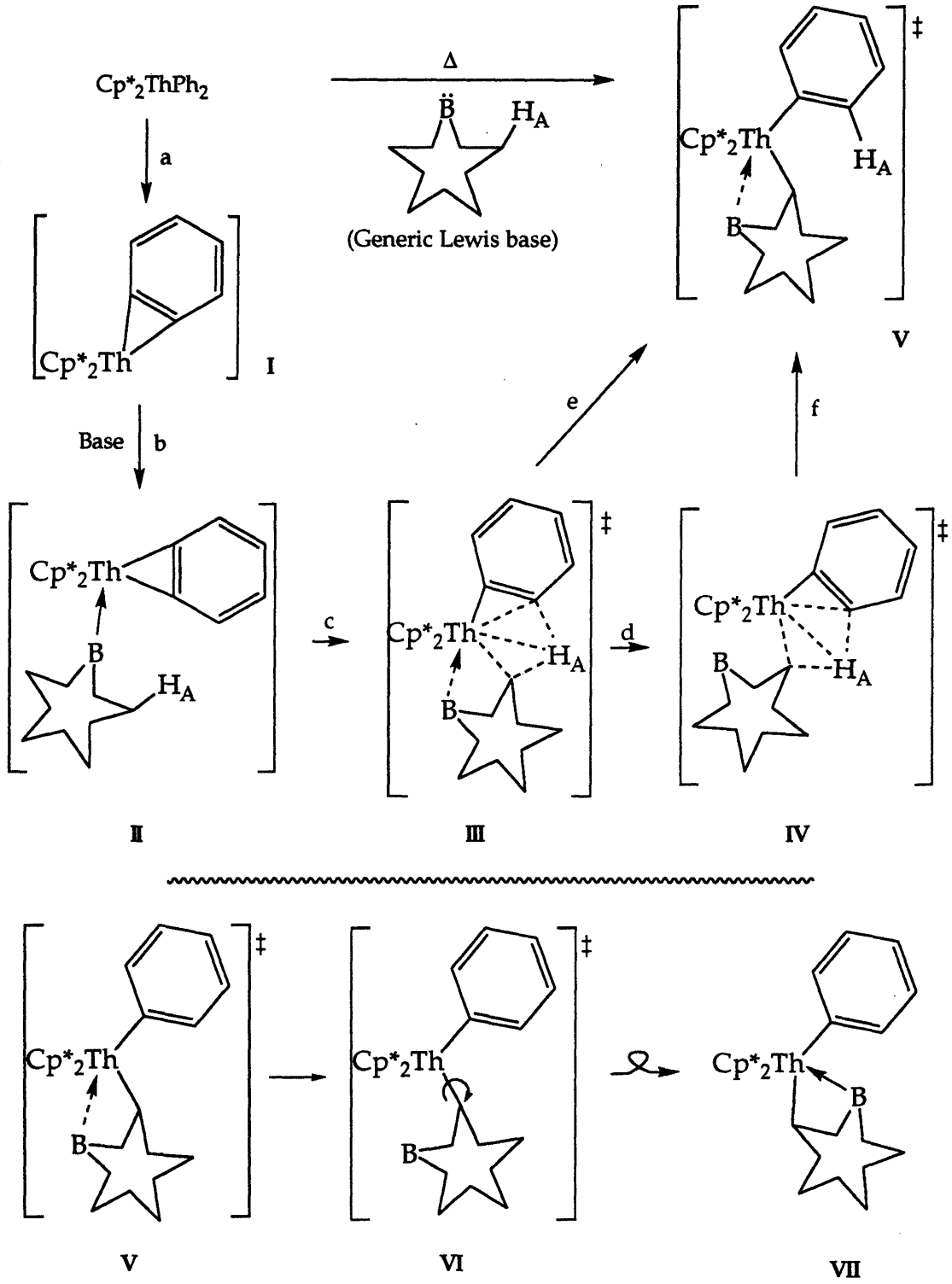
Cp*2ThPh2
a
Δ
B
HA
(Generic Lewis base)
Cp*2Th
I
Base
b
Cp*2Th
B
HA
II
c
Cp*2Th
HA
B
III
d
Cp*2Th
B
HA
IV
e
f
Cp*2Th
B
HA
V
Cp*2Th
B
V
Cp*2Th
B
VI
Cp*2Th
B
VII

Cp_2ZrPh_2 in the presence of toluene, ultimately yielding a variety of diaryl and alkyl-ayl species $Cp_2Zr(Ar)(Ar')$ (Ar, Ar' = Ph, CH_2Ph, *o*-MeC_6H_4, *m*-MeC_6H_4, *p*-MeC_6H_4).[1] In the absence of precoordination, it is possible to imagine that ligands such as pyridine may also be activated in α, β and γ-positions generating the respective phenyl-pyridyl complexes. However, without coordinative stabilization, β and γ-derivatives may be considered as thermally unstable as the benzyne precursor ultimately decomposing to the benzyne or other reactive intermediates. The failure of the C-H activation products **2-4**, or the metallacycle **1**, however, to incorporate deuterium from benzene-d_6 to any significant extent suggests that the observed complexes result from rapid irreversible coordination of the substrate.

All of the observed C-H activation processes reflect identical activation pathways. Precoordination of the Lewis base rapidly follows the initial generation of the thorium benzyne intermediate $Cp^*_2Th(C_6H_4)$ (Scheme 8: a). A kinetic study of the preparation of **2** reveals that the steps following formation of the transient benzyne moiety (Scheme 8: b, e or d, f) are not involved in determining the rate of the reaction as a whole, indicating that both the ligand coordination and activation are extremely fast with respect to the rate of benzyne formation. In each case to date, it remains unclear as to exactly to what degree the donor atom dissociates in order to effect formation of the agostic interaction. The ease of rotation about the thorium-carbon axis (Scheme 8: **VI**), observed in **3** and **4** at least, implies that donor atom coordination in intermediate species is extremely labile, likely due to overwhelming steric constraints (Scheme 8: **III** and **V**). The ultimate stability of the rearrangement products (Scheme 8: **VII**) suggests that this is indeed the case. Electronic structure determinations on group 4 acyl species have implied that dissociation, rotation and association are viable processes (Scheme 8: **V-VII**). Exactly as is proposed to be the case for **3**, **4** and **5** (*vide infra*), the kinetically formed reaction products of the acyl syntheses from metallocene alkyls and carbon monoxide are not the observed species. Rearrangement via σ-bonded monodentate species is calculated to be facile upon consideration of the accessible orbitals.[101,102]

Reaction of $Cp^*_2Th(C_6H_4)$ with Trimethyl Phosphate. Preparation of $Cp^*_2Th(OMe)(o\text{-}C_6H_4P(O)(OMe)_2$ (5). The connectivity of the methyl hydrogens in trimethylphosphate means that the typically observed C-H activation of this ligand by the thorium benzyne intermediate could conceivably result in the formation of a five-membered chelate complex similar to that formed from the reaction with triphenylphosphine oxide, i.e. an analog of **4** (eq 10), as a result of aliphatic hydrogen abstraction from a

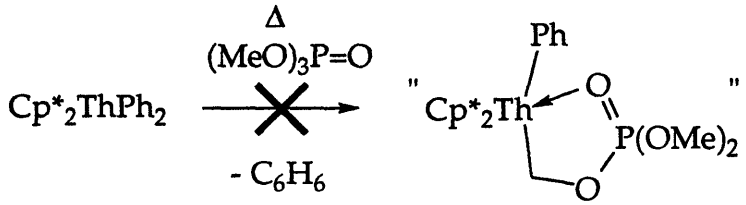

(10)

phosphate methyl group. However, a different activation process results in the preparation of a product which bears a much greater resemblance to the structure **4** (eq 11). Trimethylphosphate proves to be a particularly

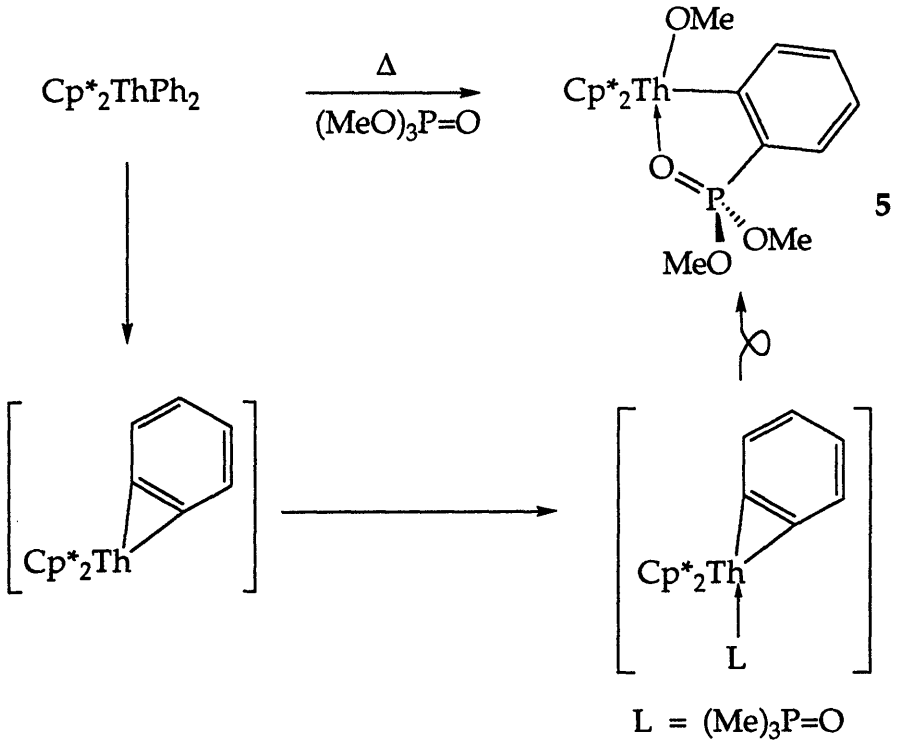

(11)

interesting substrate, since it remains one of few examples studied herein, which inhibit C-H activation, while still undergoing an alternate well-defined reaction with the benzyne intermediate.

Activation of the methyl hydrogen groups might however be expected to occur in a kinetically controlled system, since in the substrate, the phosphorus-oxygen bond (P-O ≈ 97 kcal/mole)[103] is at least as strong as the methoxy carbon-hydrogen interaction (94 ± 2 kcal/mole for *H*-(CH_2OH)).[104] The C-H bond disruption enthalpy in trimethylphosphate may actually be significantly lower than that in localized methoxy groups due to the potential for resonance stabilization throughout the phosphoryl moiety (e.g. *H*-(CH(OH)CH=CH_2) = 81.6 ± 1.8 kcal/mole).[103,104] Furthermore, carbon-hydrogen bond cleavage is certainly reasonable since aromatic C-H bond activation is observed to occur in the formation of **4** (H-(C_6H_5) = 110.9 ± 2 kcal/mole).[104]

Generation of the observed product $Cp^*_2Th(OMe)(o\text{-}C_6H_4P(O)(OMe)_2)$ (**5**) necessitates phosphorus-oxygen bond cleavage, however, a reaction not often observed in transition metal systems.[18,105] The preparation of **5** by this thermolytic route proceeds extremely cleanly, from which colorless crystals of the product are readily obtained (yield: 59%). The absence of a C-H activation derived product, and the formation of **5** is clearly evidenced by the low-field singlet resonance (δ 4.24, 3H) observed for the thorium bound methoxy groups, whereas the remaining phosphorus bound methoxy protons remain typically upfield (δ 3.18, d, J_{PH} = 10.9Hz, 6H). Furthermore, the presence of four distinct aromatic protons, and phosphorus coupling (J_{CP}) throughout the aromatic carbon atoms are consistent with a structure in which the former benzyne fragment is manifested as an *ortho*-phenylene moiety in the product. The move to lower-field due to coordination of the phosphoryl oxygen to the actinide center is clearly illustrated from a comparison of the ^{31}P NMR chemical shifts of **5** (δ 40.8), $(MeO)_3P{=}O$ (δ (-2.4) to 2.5), and $PhP(OMe)_2$ (δ 21.4). Solution NMR data for **5** is consistent with a single species in solution, which suggests either facile rotation of the *ortho*-phenylene moiety about the thorium-carbon bond, or the presence of a single geometric isomer of **5**.

From the starting materials employed it is evident that the reaction proceeds via the proposed benzyne intermediate, followed by intramolecular rearrangement to the observed product. The regiospecific activation processes implicated in the preparation of **2**, **3** and **4** are all believed to be mediated by precoordination of the metal center. However, the situation in the generation of **5** is potentially different. Though the mode of reactivity is extremely selective for the observed phosphorus-oxygen cleavage reaction,

and phosphoryl oxygen coordination is present in the product, this interaction is not necessarily reflected in the transition state geometry. Furthermore, the absence of a phosphoryl oxygen does not preclude the activation of phosphine substrates in a related titanium benzyne system. Aanalogous reactivity to that observed in the preparation of **5** has been demonstrated through the reaction of the Lewis base stabilized titanocene benzyne adduct $Cp_2Ti(o\text{-}MeOC_6H_3)(PMe_3)$ and trimethylphosphite, resulting in the formation of the disubstituted aromatic complex $Cp_2Ti(OMe)(o\text{-}MeO(6\text{-}P(OMe)_2C_6H_3)$ (eq 12).[18] NMR experiments suggest that an analog of this

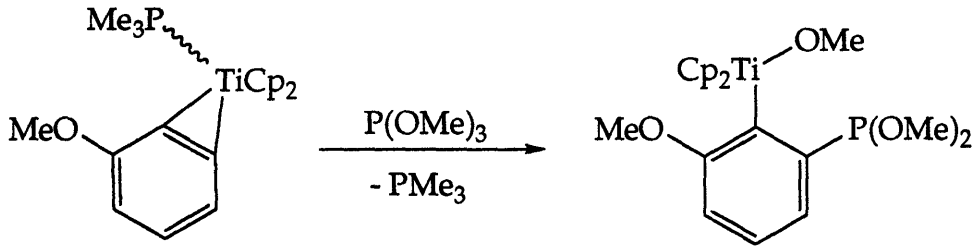

(12)

Campora *et al*, **1983**

titanium species is also formed from the reaction between the thorium benzyne moiety and trimethylphosphite. Products of this type are considered to be the result of thermodynamically controlled processes, with the formation of the metal alkoxide bond serving as the primary driving force of reactions. Tetravalent thorium is among the most oxophilic of all metal centers, with the thorium-oxygen bond having been estimated at 124 ± 4 kcal/mole.[50]

Although the oxygen chelate is observed to be an important feature in the solid state structure of **5**, the nature of ligand precoordination is somewhat less obvious, since multiple donor sites exist in trimethylphosphate. The generation of the related titanium species seemingly indicates that the presence of a phosphoryl oxygen is not essential in order to effect cleavage of the phosphorus-oxygen bond.[18] In the titanocene complex at least, however, since coordination of the phosphine is both sterically and electronically favorable this may serve to trigger the activation process.[18] However, it is clear that any such coordinative interaction does not persist throughout the transition state, since adducts of this type of first row metal centers are electronically saturated and devoid of vacant orbitals. Electronic saturation is not, however, a concern in the

actinide species since the potential for *f*-orbital participation ensures the availability of low-lying vacant orbitals.

A consideration of the geometrical constraints of viable transition state geometries for the formation of **5** is more of an indicator for the existence of phosphoryl precoordination. Sufficient low-lying orbitals on thorium are hydbridized in such a way that coordination of both phosphoryl and methoxy oxygen atoms may coordinate the metal center prior to ligand activation. It is not, however, possible to construct a realistic transition state in which the phosphoryl oxygen remains coordinated whilst cleavage occurs by a concerted σ-bond metathesis process, i.e. the methoxy-phosphorus bond cannot lie in the plane of the benzyne moiety, in the required orientation, with the phosphoryl oxygen tethered to the metal center (Schemes 9 and 10). This observation suggests that either the phosphoryl oxygen is not involved in the mechanism or that the generation of **5** proceeds via a multi-step heterolytic pathway.

Scheme 9

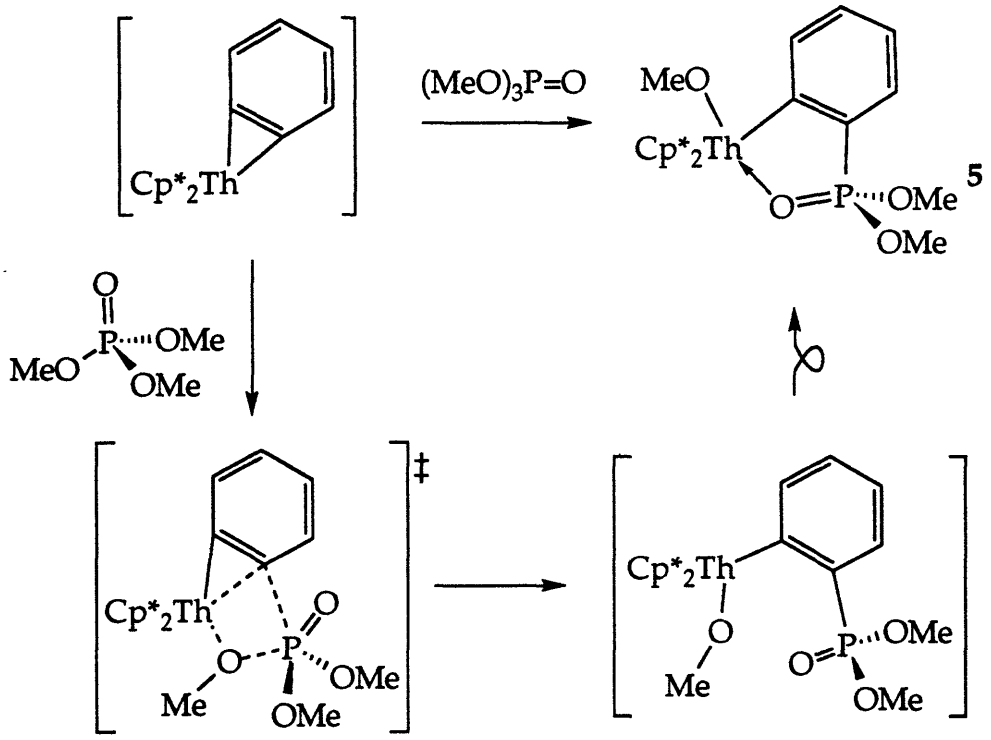

Scheme 10

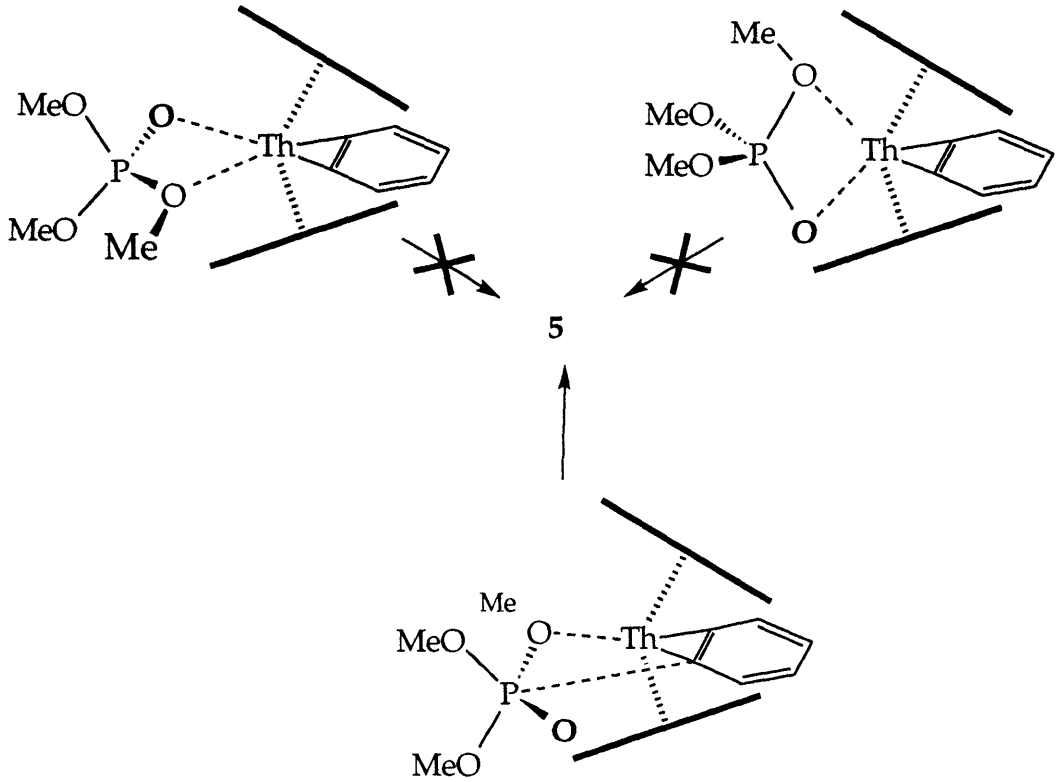

Solid State Structure of 5. The X-ray crystal structure of **5** clearly illustrates the nature of metallacyclic fragment of this phosphoryl complex (Figures 11-13; Appendices 3.13, 3.23-3.25). The five-membered ring is defined by the former benzyne moiety, the metal center and chelating phosphoryl group. Although sterically feasible, neither of the *ortho*-substituents in the related titanocene derivative are believed to coordinate the metal center.[18] Coordination of the three non-Cp* atoms bonded to thorium places both oxygen atoms in the outer coordination sites, with the aryl substituent centermost. The observed structure differs from that of **4**, in which the lone oxygen takes up the inner coordination site. Although the result of an entirely different ligand activation mechanism to **2-4**, the observed product is equally believed to be the thermodynamic product, resulting from rearrangement of the immediate activation product. A consideration of the transition state geometries illustrates that rotation about the thorium-aryl bond is necesssary in order to generate the observed product, from the initally generated species.

Figure 11. ORTEP Plot and Space-filling Diagram of $Cp^*_2Th(OMe)(o\text{-}C_6H_4P(O)(OMe)_2)$ (5)

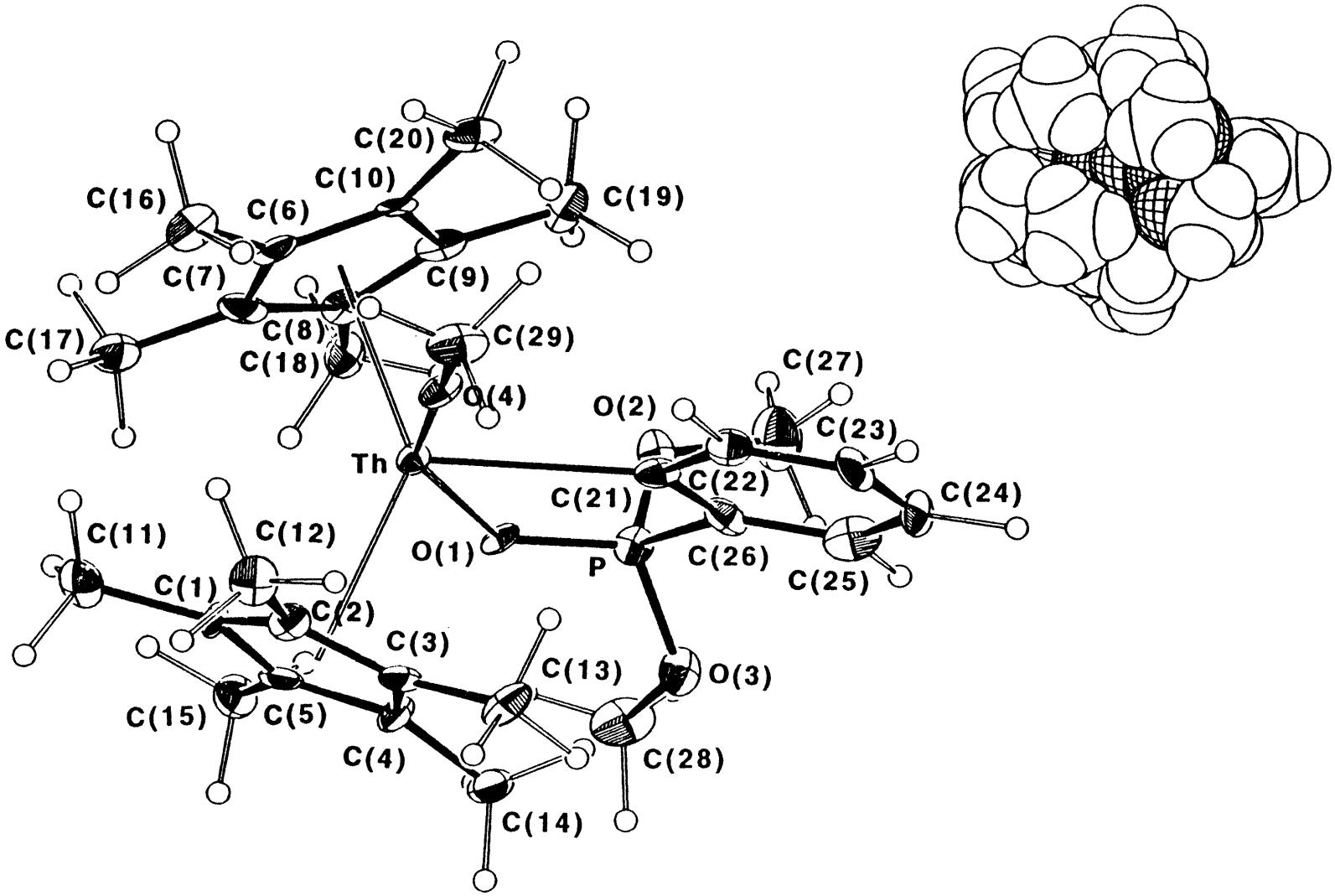

Figure 12. ORTEP Plot of $Cp^*_2Th(OMe)(o\text{-}C_6H_4P(O)(OMe)_2)$ (5)

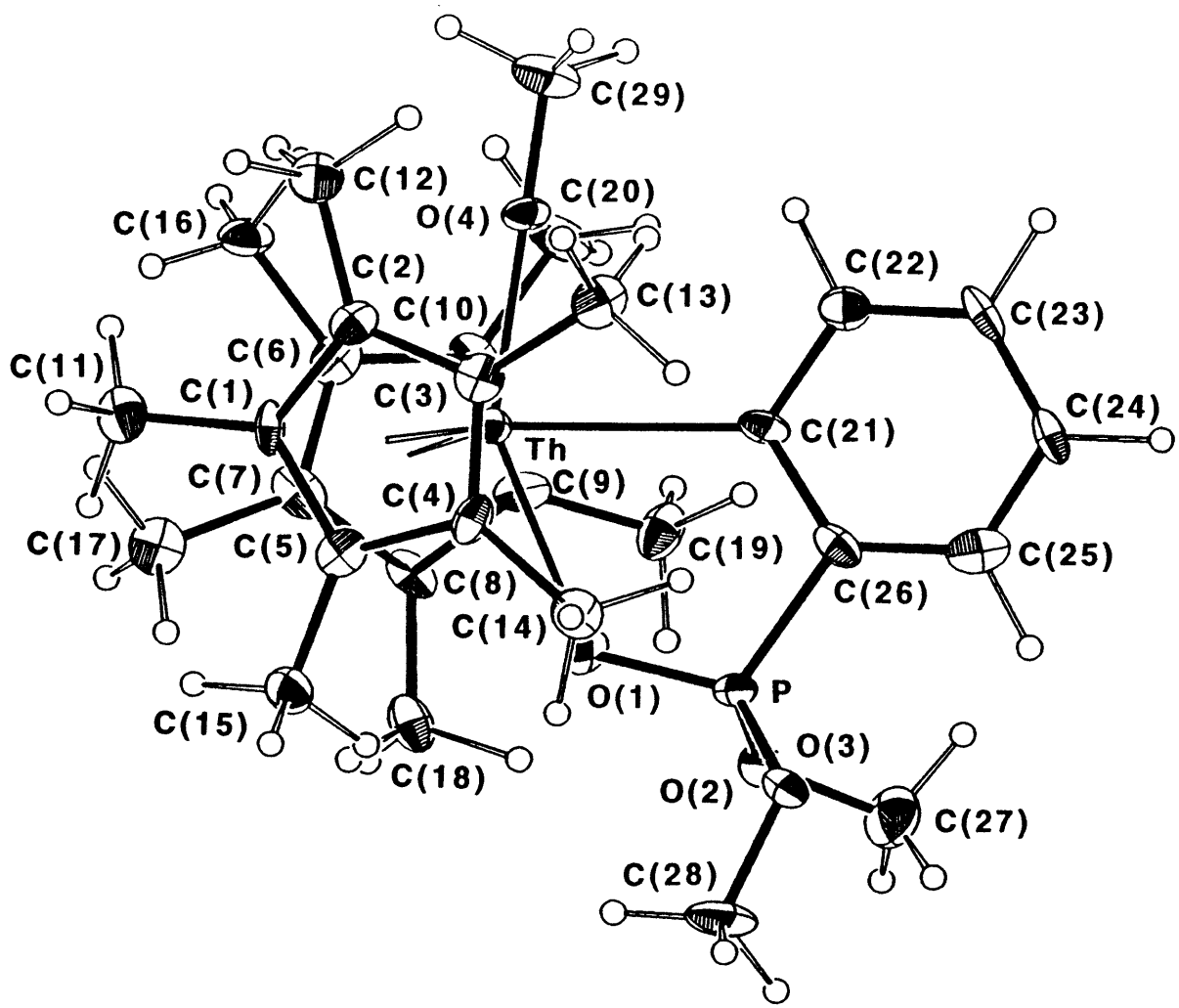

Figure 13. Selected Bond Distances and Angles for $Cp^*_2Th(OMe)(o\text{-}C_6H_4P(O)(OMe)_2)$ (5)

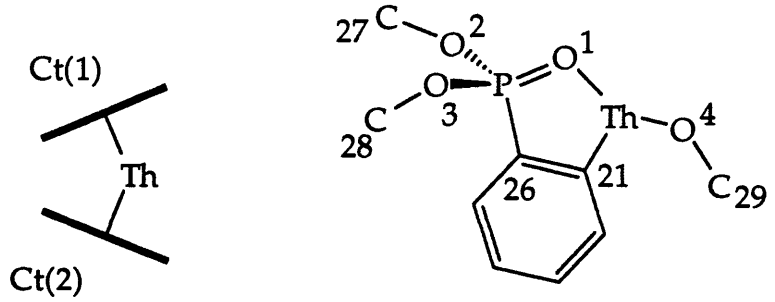

Bond Lengths (Å)

Th	Ct(1)	2.579	P	O(3)	1.583(8)
Th	Ct(2)	2.578	P	C(26)	1.771(11)
Th	O(1)	2.456(8)	O(2)	C(27)	1.448(16)
Th	O(4)	2.138(7)	O(3)	C(28)	1.455(15)
Th	C(21)	2.644(12)	O(4)	C(29)	1.388(14)
P	O(1)	1.494(8)	C(21)	C(26)	1.394(16)
P	O(2)	1.558(9)			

Bond Angles (deg)

Ct(1)	Th	Ct(2)	136.33	O(3)	P	C(26)	104.7(5)
O(1)	Th	O(4)	149.7(3)	Th	O(1)	P	126.6(5)
O(1)	Th	C(21)	67.5(3)	P	O(2)	C(27)	122.4(9)
O(4)	Th	C(21)	82.2(3)	P	O(3)	C(28)	118.6(8)
O(1)	P	O(2)	107.3(5)	Th	O(4)	C(29)	179.5(8)
O(1)	P	O(3)	115.9(5)	Th	C(21)	C(22)	123.2(8)
O(1)	P	C(26)	109.3(5)	Th	C(21)	C(26)	121.7(8)
O(2)	P	O(3)	106.2(4)	P	C(26)	C(21)	113.6(9)
O(2)	P	C(26)	113.6(5)	P	C(26)	C(25)	122.8(9)

The bidentate phenylphosphoryl moiety of **5** adopts two of the available coordination sites bisecting the metallocene wedge. Distances and angles between the centroids and metal center reflect the bulk of the $Cp^*_2ThX_2(L)$ system (Th-Cp = 2.578, 2.579 Å; Cp(1)-Th-Cp(2) = 136.33°) (cf. **1**, **3**, **4**; *vide infra*). As expected, the donor interaction between the phosphoryl oxygen and metal center (2.456(8) Å) is considerably longer than the conventional alkoxide linkage (e.g.Th-O(1) = 2.138(7) Å). The thorium-oxygen distance is at the short end relative to those observed in previously reported thorium alkoxide systems (Th-O(terminal) (range) = 2.141(11)-2.204(6) Å).[106-108] Nonetheless, the bond distance of this donor interaction is significantly strong to influence the orientation of phenylphosphoryl moiety and is comparable in length to typical Th-C distances (e.g. Th-C(21) = 2.644(12) Å; Th-C(range) = 2.4-2.6 Å).[40,49,54,55] Additionally, the thorium-oxygen interaction is also considered to be stable with respect to dissociation under less than rigorous thermal activation.

The thorium-methoxide interaction is approximately linear (Th-O-C = 179.5(8)°), which is typical for short lanthanide, actinide and early *d*-series single bonds to oxygen[109] (Th-O-C (terminal) (range) = 159.6(6)-176.2(11)°).[107,108] The nature of this phenomenomon is uncertain, having been discussed both in terms of steric effects[110] and $d\pi$-$p\pi$ bonding[111-114] among *d*-block complexes. Here, however, it appears as if the steric demands of the ancillary ligand set of **5** are likely not responsible for the extreme bond deformation. Furthermore, although not confirmed for monoalkoxide systems such as **5**, it is known that the metallocene frameworks $Cp_2Th(OR)_2$ and $Cp_3Th(OR)$ both have *d* and *f* orbitals with the appropriate symmetry available for π-bonding.[115-117] The oxophilicity of the actinide metal center is almost certainly a contributiong factor to the strength of the thorium-oxygen bond.[118]

Comparison of the Solid State Structures of 4 and 5. Notwithstanding the orientation of the phenylphosphoryl moiety and the difference in ancillary σ-bonded ligands, the nature of the five-membered chelate ring in **4** and **5** is almost identical (Figure 14). The only noticeable distinction between the two structures is the small discrepancy in the thorium-phosphoryl interaction which exemplifies the possible influences of the different steric and electronic phenomena in effect in these two systems.

Figure 14

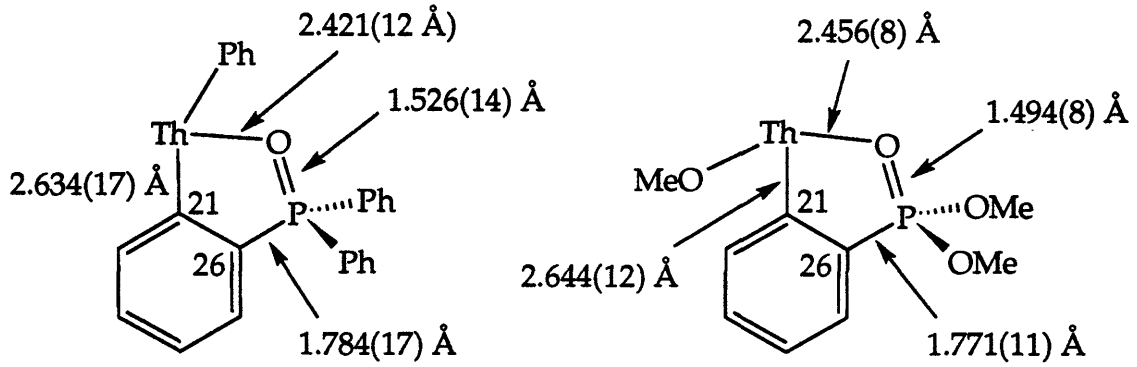

C(21)-C(26) = 1.439(26) Å **4**

Th-Ct(1) = 2.573 Å
Th-Ct(2) = 2.583 Å

∠ Ct(1)-Th-Ct(2) = 135.5°
∠ O-Th-C(21) = 68.6(5)°
∠ Th-O-P = 126.4(6)°
∠ O-P-C(26) = 108.4(8)°
∠ Th-C(21)-C(26) = 120.0(11)°
∠ P-C(26)-C(21) = 113.9(13)°

C(21)-C(26) = 1.394(16) Å **5**

Th-Ct(1) = 2.579 Å
Th-Ct(2) = 2.578 Å

∠ Ct(1)-Th-Ct(2) = 136.33°
∠ O(1)-Th-C(21) = 67.5(3)°
∠ Th-O(1)-P = 126.6(5)°
∠ O(1)-P-C(26) = 109.3(5)°
∠ Th-C(21)-C(26) = 121.7(8)°
∠ P-C(26)-C(21) = 113.6(9)°

The proposed mechanism of formation of **4** traverses intermediates which demonstrate considerable steric congestion at, or about, the metal center (cf. Scheme 6: **A1/B1, B2**). However, the crystal structure of the ultimate product shows that the bulk of the ancillary ligand set does not translate into significant distortion of the five-membered chelate ring. Aside from the position of the coordination of the aryl and oxygen substituents in **4** and **5**, the solid state molecular structures of the common fragment of these two complexes exhibits near identical geometries (Figure 14). In each case the coordination site adopted by the chelating oxygen atom is not believed to be a result of crystal packing phenomena or of a labile coordinative interaction. Rather, the observed relationships are believed to form both in order to alleviate destabilizing steric and/or coulombic interactions and maximize the interaction between the metal center and phosphoryl oxygen.

The difference in electronic contributions between the thorium-phenyl and -methoxy substituents in **4** and **5** may play a part in determining the placement of the phosphoryl oxygen in the coordination sphere. Unless π-donation from the methoxy oxygen to the actinide metal center is an

important factor, however, the contribution of these σ-bonded ligands to the bonding in the repective complexes is essentially identical. However, the linear nature of the Th-O(4)-C(29) angle in **5** (179.5(8)°) suggests that there may indeed be overlap overlap between π-symmetry *f*-orbitals on the actinide and lone pairs on oxygen. The complicated nature of *d-f* hydridization in the bis(cyclopentadienyl) framework is such that the symmetry of the metal based LUMO is influenced by the π-accepting tendencies of the ancillary ligand set of the metallocene fragment $[Cp^*_2Th(R)]^+$ (R = Ph (**4**), OMe (**5**)).[119,120] As a result, the σ-bonded ligand may ultimately prove responsible for determining the way in which the organic moiety interacts with the metal center (Scheme 9). The HOMOs of the differentially substituted phenylphosphoryl fragments of **4** and **5** are otherwise considered to be isolobal, since conjugation does not

Scheme 9

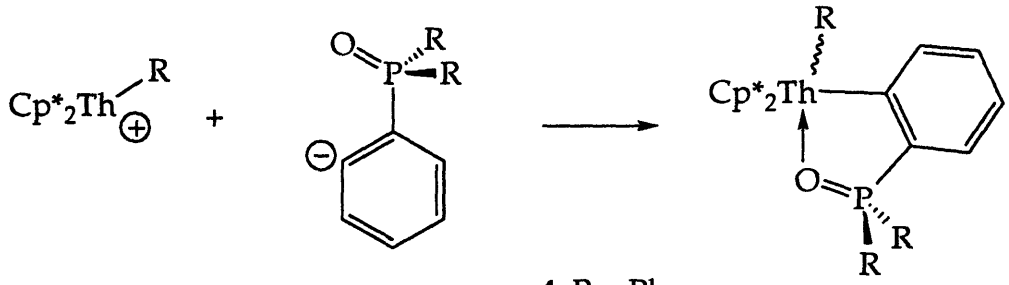

4: R = Ph
5: R = OMe

extend beyond the phenyl anion in either case. From steric arguments alone, it would appear that the preferred orientation of the phosphoryl moiety of both complexes would be the geometry adopted by **5**, since the ancillary ligand framework is considerably less sterically demanding than that of **4** (i.e. $P(OMe)_2$, OMe *vs* PPh_2, Ph). The bond lengths and angles extracted from the crystal structure of **4** do not show evidence of significant strain due to the steric constraints imposed by the bulky aryl framework, however. Sterics factors aside, a consideration of destabilizing coulombic repulsions in **5** demonstrates the converse, in that the 'donor inside' geometry may be disfavored due to the close proximity of the electronegative oxygen bearing functionalities.

Reactivity of $Cp^*_2Th(C_6H_4)$ with Other Differentially Functionalized Lewis Bases. Table 5 contains a summary of the reactivity of the thorium benzyne intermediate $Cp^*_2Th(C_6H_4)$ with a variety of Lewis bases. Typical experiments were conducted on a small scale in benzene-d_6 with the loss fo starting materials and product monitored by ^1H NMR, in the presence of an internal standard. In some cases, the molecular structures of products are only tentatively assigned. Where necessary, the assignments of new reaction products are those suggested from the ^1H NMR spectrum, and by further spectroscopic or comparative analysis.

Table 5. Observed Reaction Products from the Thermolysis of $Cp^*_2ThPh_2$ in the Presence of Differentially Substituted Lewis Bases

Substrate	Reactive Site[a]	Proposed Product [b]	Assignment Method
Phosphines			
PMe_3	N/R	$Cp^*_2Th(C_6D_5)_2$	*c*
PPh_3	N/R	$Cp^*_2Th(C_6D_5)_2$	*c,d*
$P(OMe)_3$	P-O	'$Cp^*_2Th(OMe)(o\text{-}C_6H_4P(OMe)_2)$'	*e*
Phosphine Oxides			
$Ph_3P{=}O$	C-H_{Ar}	$Cp^*_2Th(Ph)(o\text{-}C_6H_4P(O)Ph_2)$ (**4**)	*f*
$Me_3P{=}O$	C-H_{Ar}	*g*	*g*
$(n\text{-Oct})_3P{=}O$	C-H_{Ar}	*g*	*g*
$(c\text{-}C_6H_{11})_3P{=}O$	C-H_{Ar}	*g*	*g*
$(MeO)_3P{=}O$	P-O	$Cp^*_2Th(OMe)(o\text{-}C_6H_4P(O)(OMe)_2)$ (**5**)	*f*
$(EtO)_3P{=}O$	P-O	'$Cp^*_2Th(OEt)(o\text{-}C_6H_4P(O)(OEt)_2)$'	*e*
$(PhO)_3P{=}O$	P-O	'$Cp^*_2Th(OPh)(o\text{-}C_6H_4P(O)(OPh)_2)$'	*e*
$(Me_3SiO)_3P{=}O$	P-O, C-H_{Al}	*h*	*h*

[a] Predicted site of cleavage of Lewis base: aromatic carbon-hydrogen (C-H_{Ar}), benzylic carbon-hydrogen (C-H_{Bz}), aliphatic carbon-hydrogen (C-H_{Al}), nitrogen-hydrogen (N-H), carbon-oxygen (C-O), phosphorus-oxygen (P-O). The absence of a Lewis base derived product is designated as 'no reaction' (N/R).

Table 5 continued

Substrate	Reactive Site[a]	Proposed Product [b]	Assignment Method
Pyridines with α-Hydrogen Atoms			
4-$(Me_2N)C_5H_4N$	C-H_{Ar}	$Cp^*_2Th(Ph)((4\text{-}NMe_2)C_5H_3N)$ (**2**)	*f*
C_5H_5N	C-H_{Ar}	$Cp^*_2Th(Ph)(C_5H_4N)$	*e*
2-MeC_6H_3N	C-H_{Ar}	$Cp^*_2Th(Ph)((6\text{-}Me)C_5H_3N)$	*i*
Pyridines without α-Hydrogen Atoms			
2, 6-$Me_2C_6H_3N$	C-H_{Bz}	$Cp^*_2Th(Ph)(2\text{-}CH_2\text{-}6\text{-}MeC_5H_3N)$ (**3**)	*f*
2, 6-$Et_2C_6H_3N$	N/R	$Cp^*_2Th(C_6D_5)_2$	*c*
2, 6-*i*$Pr_2C_6H_3N$	N/R	$Cp^*_2Th(C_6D_5)_2$	*c*
2, 6-$^t Bu_2$-4-Me-C_6H_3N	N/R	$Cp^*_2Th(C_6D_5)_2$	*c*
2, 6-(*p*-tolyl)$_2C_6H_3N$	N/R	$Cp^*_2Th(C_6D_5)_2$	*c*
Piperidines			
$C_5H_{10}NH$	N-H	$Cp^*_2Th(Ph)(NC_5H_{10})$	*i*
2-MeC_5H_9NH	N-H	$Cp^*_2Th(Ph)(NC_5H_9Me)$	*e*
2, 6-$Me_2C_5H_8NH$	N-H	$Cp^*_2Th(Ph)(NC_5H_8Me_2)$	*e*
2, 2′, 6, 6′-$Me_4C_5H_6NH$	N/R	$Cp^*_2Th(C_6D_5)_2$	*c*
Aliphatic Amines			
NEt_3	N/R	$Cp^*_2Th(C_6D_5)_2$	*c*
NMe_3	N/R	$Cp^*_2Th(C_6D_5)_2$	*c*
$CH(CH_2CH_2)_3N$	N/R	$Cp^*_2Th(C_6D_5)_2$	*c*
$Me_2NCH_2CH_2NMe_2$	N/R	$Cp^*_2Th(C_6D_5)_2$	*c*

[b] Proposed product assignments after thermolysis of $Cp^*_2Th(C_6H_5)_2$, in benzene-d_6, after thermolysis (≈ 100°C, ≥ 1 h ($t_{1/2}$ ≈ 9 min) or 60-70 °C, > 18 h ($t_{1/2}$ ≈ 5 h)), in the presence of at least one equivalent of substrate and an internal standard (hexamethylbenzene) where necessary.

[c] ^1H NMR spectrum of thermolysis product revealed presence of deuterated diphenyl complex, $Cp^*_2Th(C_6D_5)_2$ and unreacted, non-coordinated Lewis base.

Table 5 continued

Substrate	Reactive Site[a]	Proposed Product[b]	Assignment Method
Aliphatic Ethers			
THF (C_4H_8O)	C-O, C-H_{Al}	*h*	*h*
Me_2O	C-H_{Al}	$Cp^*_2Th(Ph)(CH_2OMe)$	*i*
	C-O	$Cp^*_2Th(Ph)(OMe)$	*j,k*
Et_2O	N/R	$Cp^*_2Th(C_6D_5)_2$	*c*
MeO*n*-Pr	C-H_{Al}	$Cp^*_2Th(Ph)(CH_2O$*n*-Pr)	*e*
$MeOCH_2CH_2OMe$	C-O	$Cp^*_2Th(Ph)(OMe)$	*j,k*
	C-O	$[Cp^*_2Th(OMe)]_2O$	*l*
Aromatic Hydrocarbons (Control Substrates)			
Benzene	C-H_{Ar}	$Cp^*_2Th(C_6H_5)_2$	*m*
Benzene-d_6	C-H_{Ar}	$Cp^*_2Th(C_6D_5)_2$	*m*
C_6Me_6	N/R	$Cp^*_2Th(C_6D_5)_2$	*c*

[d] A minor product is clearly observed to form, and is tentatively assigned as the product of aromatic C-H activation of the phosphine, most likely isomeric species resulting from activation at the unhindered positions of the phosphine.

[e] ^1H NMR illustrates loss of diphenyl resonances ($Cp^*_2Th(C_6R_5)_2$ R = H, D) and those of the incorporated Lewis base, and new product signals; structural assignment suggested by the observed product resonances and by a qualitative comparison with data for a structural analog.

[f] Fully characterized reaction product; see experimental section.

[g] ^1H NMR spectra revealed the existence of a reaction between the phosphine oxide, with a loss of all starting material resonances. The nature of the substrate suggests ligand C-H activation, although the identities of the products have yet to be established.

[h] The reaction of the benzyne intermediate with the substrate effects the formation of innumerable products, indecipherable by ^1H NMR.

[i] Structural assignment based upon solution state NMR (^1H and $^{13}C\{^1H\}$) spectra of isolated product.

[j] Product assignment based on investigation by ^1H NMR and comparison with the spectrum of an independently prepared sample of $Cp^*_2Th(Ph)(OMe)$.

[k] The reaction between $Cp^*_2Th(OMe)_2$[122] and one equivalent phenylmagnesium bromide of gave rise to the formation of a product with a ^1H NMR spectrum consistent with that expected for the phenyl-methoxy complex $Cp^*_2Th(Ph)(OMe)$.

[l] A single crystal X-ray crystallographic analysis of a sample of the reaction product recrystallized from hexane demonstrated the existence of the oxobridged dimer $[Cp^*_2Th(OMe)]_2O$. However, standard solution characterization techniques have not been performed on this complex, and hence it is not known whether this complex is generated reproducibly from the activation of dimethoxyethane or whether its formation is a facet of adventitious moisture in the recrystallization attempt.

[m] from reference[11].

Summary

The transient thorium benzyne complex $Cp^*_2Th(C_6H_4)$ demonstrates considerable reactivity when generated by the thermal decomposition of $Cp^*_2ThPh_2$ in the presence of selected Lewis bases. Although analogous group 4 benzyne systems have been stabilized and isolated as Lewis base adducts,[18,24] it has so far not proven possible to utilize a similar strategy for the preparation of the first stable alkyne complex of an actinide. Instead, the interaction of the benzyne moiety with specific differentially substituted neutral ligands results in a variety of novel regioselective ligand activation processes. Structural evidence suggests that coordination of the donor atom to the metal center serves both to direct the activation process and increase product stability. Examples of aromatic (e.g. DMAP (to **2**), $Ph_3P{=}O$ (to **4**)) and benzylic (e.g. 2, 6-lutidine (to **3**) C-H activation are facile with this system, resulting in regeneration of a single thorium-bound phenyl substituent and a 'deprotonated' bidentate Lewis base moiety.

In certain instances, established C-H activation processes may be curtailed by the introduction of bulky substituents (e.g. 2, 5-$R_2NC_5H_3$: R > Me). Furthermore, although C-H activation appears viable, a rare example of transition metal mediated phosphorus-oxygen bond cleavage occurs when trimethyl phosphate is employed as the substrate. The formation of a strong thorium-methoxy bond is the apparent driving force behind the generation of **5**.

Experimental

General Procedures. All manipulations were conducted under an atmosphere of purified helium in a Vacuum Atmospheres Co. drybox. Nuclear Magnetic Resonance (NMR) spectra were recorded on IBM (Bruker) AF-250MHz and WM-300MHz spectrometers, at room temperature, unless otherwise stated. NMR chemical shifts were determined in benzene-d_6 or tetrahydrofuran-d_8, and are internally referenced to the solvent (C_6D_6: ^1H, δ 7.15, ^{13}C: δ 128.0; THF-d_8: ^1H, δ 3.58), or externally to 85% phosphoric acid (^{31}P: δ 0.0). Infrared (IR) spectra were recorded as nujol mulls on KBr plates, using a Bio-Rad FTS-40 spectrometer. Elemental analyses were performed both in the laboratory, using a Perkin-Elmer 2400 CHN analyzer, and by Galbraith Laboratories, Inc., Knoxville, TN. Solvents were dried over either sodium/benzophenone ketyl (hexane, toluene) or calcium hydride (benzene), under an atmosphere of nitrogen or argon, respectively. Tetrahydrofuran-d_8 and benzene-d_6 were vacuum transferred from sodium-potassium alloy (NaK) and calcium hydride, respectively. $Cp^*_2ThCl_2$[11] and $Cp^*_2ThPh_2$[52,53] were prepared according to previously reported procedures. All other reagents were purchased from commercial sources and used as received.

Representative procedure for the thermolysis of $Cp^*_2ThPh_2$ in the presence of a Lewis base or Other Substrate: Preparation of $Cp^*_2Th(Ph)(o\text{-}C_6H_4P(O)Ph_2)$ (4). A solution of $Cp^*_2ThPh_2$ (308 mg, 0.47 mmol), and triphenylphosphine oxide (132 mg, 0.47 mmol) in toluene (6 mL) was sealed in a Schlenk flask, under helium. The reaction vessel was immersed in an oil bath and heated at 100°C for 5 h. After allowing the reaction mixture to cool the solvent was removed *in vacuo*. The residue was extracted with hot hexane (3 x 5-10 mL), and filtered. The filtrate was concentrated under reduced pressure, with heating, before being allowed to gradually cool to room temperature. The desired product, complex **4**, subsequently precipitated from the hexane solution as colorless crystals. Yield: 241 mg (60%). ^1H NMR (250MHz, C_6D_6) δ 1.82 (s, 30H), 6.96 (m, 7H), 7.12 (m, 1H), 7.33 (t, J = 7.0Hz, 1H), 7.51 (m, 2H), 7.67 (t, J = 7.3Hz, 2H), 7.79 (m, 4H), 8.22 (d, J = 7.0Hz, 1H), 8.28 (m, 1H). ^{13}C NMR (62.9MHz, C_6D_6) δ 12.6 (s), 123.4 (s), 124.7(d, J_{CP} = 14Hz), 124.8 (s), 126.5 (s), 128.6 (d, J_{CP} = 3Hz), 128.8 (d, J_{CP} = 12Hz), 129.9 (d, J_{CP} = 24Hz), 132.0 (d, J_{CP} = 10Hz), 132.5 (d, J_{CP} = 3Hz), 133.5 (d, J_{CP} = 102Hz), 136.6 (d, J_{CP} = 118Hz), 139.1

(s), 140.7 (d, J_{CP} = 25Hz), 218.3 (d, J_{CP} = 6Hz), 230.5 (d, J_{CP} = 42Hz). ^{31}P NMR (101.3MHz, C_6D_6) δ 58.4. IR 1125 (sh), 1121 (s), 1083 (m), 1060 (s), 998 (w).

Preparation of $Cp^*_2Th(C_6H_4C(C_2H_5)=C(C_2H_5))$ (1). Reagents: $Cp^*_2Th(C_6H_5)_2$ (302 mg, 0.46 mmol) and 3-hexyne (108 mg, 1.31 mmol). Yield: 210 mg (69%) as yellow crystals; recrystallized from hexane, at -40°C. ^{1}H NMR (250MHz, C_6D_6) δ 1.08 (t, J = 7.5Hz, 3H), 1.29 (t, J = 7.5Hz, 3H), 1.85 (s, 30H), 2.60 (q, J = 7.6Hz, 2H), 2.67 (q, J = 7.5Hz, 2H), 7.18- d 7.31 (m, 3H), 7.62 (d, J = 7.5Hz, 1H). ^{13}C NMR (62.9MHz, C_6D_6) δ 11.4, 11.8, 14.3, 22.8, 25.4, 122.7, 123.9, 124.3, 127.5, 133.3, 147.0, 152.9, 215.3, 235.2.

Preparation of $Cp^*_2Th(Ph)((4\text{-}Me_2N)C_5H_3N)$ (2). Reagents: $Cp^*_2Th(C_6H_5)_2$ (305 mg, 0.46 mmol) and 4-dimethylaminopyridine (57 mg, 0.47 mmol). Yield: 147 mg (45%) as colorless crystals; recrystallized from hexane at -40 °C. ^{1}H NMR (250 MHz, C_6D_6) δ 1.91 (s, 30H), 2.35 (s, 6H), 6.13 (dd, J_1 = 2.7Hz, J_2 = 6.3Hz, 1H), 7.20 (d, J = 2.0Hz, 1H), 7.32 (t, J = 7.3Hz, 1H), 7.62 (t, J = 7.5Hz, 2H), 8.10 (d, J = 6.5Hz, 2H), 8.45 (dd, J_1 = 0.7Hz, J_2= 3.0Hz, 1H). ^{13}C NMR (62.9MHz, C_6D_6) δ 11.5, 38.7, 108.9, 110.3, 122.1, 125.8, 127.0, 138.9, 142.7, 154.5, 215.0, 231.3. Anal. Calcd for $C_{33}H_{44}N_2Th$: C, 56.56; H, 6.33; N, 4.00. Found: C, 55.66; H, 6.26; N, 3.96.

Preparation of $Cp^*_2Th(Ph)(2\text{-}CH_2\text{-}6\text{-}MeC_5H_3N)$ (3). Reagents: $Cp^*_2Th(C_6H_5)_2$ (298 mg, 0.45 mmol), 2,6-lutidine (157 mg, 1.47 mmol). Yield: 217 mg (70%) as pale yellow crystals, after recrystallization from hexane at -40 °C. ^{1}H NMR (250MHz, THF-d_8, 245 K) δ 1.78 (s, 3H), 1.91 (s, 30H), 2.11 (s, 2H), 6.06 (d, J = 6.2Hz, 1H), 6.48 (d, J = 7.1Hz, 1H), 6.84 (m, 3H), 7.27 (m, 1H), 7.33 (t, J = 7.6Hz, 1H), 7.70 (d, J = 7.6Hz, 1H). ^{13}C NMR (62.9MHz, C_6D_6) δ 12.1 (q, J_{CH} = 126Hz), 25.3 (q, J_{CH} = 126Hz), 59.7 (t, J_{CH} = 133Hz), 113.5 (d, J = 170Hz), 118.9 (d, J = 167Hz), 123.1 (s), 125.7 (d, J = 157Hz), 126.9 (d, J = 156Hz), 137.6 (d, J = 154Hz), 138.0 (d, J = 158Hz), 159.9 (s), 163.9 (s), 213.0.

Preparation of $Cp^*_2Th(OMe)(o\text{-}C_6H_4P(O)(OMe)_2)$ (5). Reagents: $Cp^*_2Th(C_6H_5)_2$ (301 mg, 0.46 mmol) and trimethyl phosphate (72 mg, 0.51 mmol). Yield: 195 mg (59%) as colorless crystals; recrystalized from toluene. ^{1}H NMR (250 MHz, C_6D_6) δ 2.10 (s, 30H), 3.18 (d, J_P = 10.9Hz, 6H), 4.24 (s, 3H), 7.01 (m, 1H), 7.27 (m, 1H), 7.43 (m, 1H), 8.32 (d, J_P = 7.2Hz, 1H). ^{13}C {^{1}H} NMR (62.9MHz, C_6D_6) δ 11.4 (s), 52.2 (dq, J_P = 6.9Hz, J_H = 147.8Hz), 56.6 (q, J_H =

137.8Hz), 121.5 (s), 125.3 (d, J_P = 15.8Hz), 129.2 (d, J_P = 20.8Hz), 131.0 (d, J_P = 4.8Hz), 133.6 (d, J_P = 195.7Hz), 141.1 (ddd, J_P = 32.3Hz, $J_H{}^1$ = 6.5Hz, $J_H{}^2$ = 160.0Hz), 216.0 (d, J_P = 49.3Hz). ^{31}P NMR (101.3MHz, C_6D_6) δ 40.8. IR 1466 (s), 1462 (s), 1452 (s), 1377 (s), 1365 (sh), 1179 (m), 1155 (w), 1131 (m), 1140 (s), 1082 (w), 1050 (m), 1029 (m). Anal. Calcd for $C_{29}H_{43}O_4PTh$: C, 48.47; H, 6.03. Found: C, 47.81; H, 5.37.

Determination of Kinetic Activation Parameters for the Formation of 2 from $Cp^*_2Th(C_6H_5)$. Representative Procedure. The rate of thermal decomposition of $Cp^*_2Th(C_6H_5)_2$, and concomitant formation of **3** were monitored as a function of time and temperature, by ^{1}H NMR spectroscopy. Reaction rates were measured by changes in the integrals of Cp* ring methyl resonances of both the starting material and product (δ 1.77 and δ 1.91, respectively). Throughout the course of the reactions, the aggregate total spectral integrals for the starting material and product remained constant, within experimenatal error, demonstrating near quantitative conversion. Concentrations of reagents in the reaction mixture were determined by a comparison of spectral integrals with the ^{1}H NMR spectral resonances of a known amount of internal standard (hexamethylbenzene δ 2.12). Representative sample solutions were composed of $Cp^*_2Th(C_6H_5)_2$ (10 mg, 0.015 mmol), 4-dimethylaminopyridine (2 mg, 0.016 mmol, ≈ 1 equiv), and hexamethylbenzene (3 g, 0.024mmol) in benzene-d_6 (500 µl). Solutions were sealed under an atmosphere of helium in NMR tubes fitted with J. Young valves. Immediately after preparing the reaction solutions all sample tubes were stored at 0 °C until immediately prior to insertion into the preheated probe. Thermolyses were performed in the NMR probe itself with the use of a computer controlled variable temperature unit. Temperatures in the probe were determined by calibration against an ethylene glycol NMR thermometer.[122] Spectra were recorded immediately upon inputting the sample tube into the probe, and then after allowing the temperatures to equilibrate at timed intervals for a total of eighty minutes. Each spectrum was composed of the signal averaging of a total of eight scans, each separated by a five second pulse delay. A total of two kinetic runs was monitored for each different experiment in order to ensure consistency in the observed data. In order to determine the reaction activation parameters, experiments were

performed at three different temperatures (temperature range: 72-90 °C) (Experiments A1, A2, B1, B2, C1 and C2; Appendices 3.1-3.7).

Under otherwise identical conditions, a data set was collected for the observed reaction when carried out in the presence of an excess of DMAP (≈ 6 equiv) (Experiments D1 and D2; Appendices 3.8 and 3.9)..
Observed reaction rates were unchanged at the higher concentration of ligand, demonstrating the independence of the rate determining step on the concentration of DMAP.

Observed rate constants (k), the activation energy (E_a) and enthalpy of activation ($\Delta H^{\ddagger}$) were derived from kinetic, Arrhenius and Eyring plots respectively (Appendices 3.10 and 3.11). The gradient of each plot was determined from a linear regression least squares line fit to the data set. Values for the entropy ($\Delta S^{\ddagger}$) and free energy ($\Delta G^{\ddagger}$) of activation were subsequently calculated from $\Delta H^{\ddagger}$. Confidence limits were determined at the 95% confidence level from estimated standard deviations.[123] Activation parameters were further computed at 25 °C ($\Delta G^{\ddagger}$) and 70 °C (k and $\Delta S^{\ddagger}$) by extrapolation, for the purpose of comparison with related literature experiments.[47]

References

(1) Erker, G. *J. Organomet. Chem.* **1977**, *134*, 189-202.

(2) Erker, G.; Kropp, K. *J. Am. Chem. Soc.* **1979**, *101*, 3659-3660.

(3) Erker, G.; Kropp, K. *J. Organomet. Chem.* **1980**, *194*, 45-60.

(4) Kropp, K.; Erker, G. *Organometallics* **1982**, *1*, 1246-1247.

(5) Erker, G. *Acc. Chem. Res.* **1984**, *17*, 103-109.

(6) Erker, G.; Czisch, P.; Mynott, R.; Tsay, Y.-H.; Krüger, C. *Organometallics* **1985**, *4*, 1310-1312.

(7) Erker, G.; Mühlenbernd, T.; Benn, R.; Ruflinskà, A.; Tainturier, G.; Gautheron, B. *Organometallics* **1986**, *5*, 1023-1028.

(8) Erker, G.; Sonsna, F.; Zwettler, R.; Krüger, C. *Organometallics* **1989**, *8*, 450-454.

(9) Erker, G.; Dorf, U.; Lecht, R.; Ashby, M. T.; Aulbach, M.; Schlund, R.; Krüger, C.; Mynott, R. *Organometallics* **1989**, *8*, 2037-2044.

(10) McLain, S., J; Schrock, R. R.; Sharp, P. R.; Churchill, M. R.; Youngs, W. J. *J. Am. Chem. Soc.* **1979**, *99*, 263-265.

(11) Fagan, P. J.; Manriquez, J. M.; Maatta, E. A.; Seyam, A. M.; Marks, T. J. *J. Am. Chem. Soc.* **1981**, *103*, 6650-6667.

(12) Tung, H.-S.; Brubaker, C. H. *Inorg. Chim. Acta* **1981**, *52*, 197-204.

(13) Negishi, E.; Takahashi, T. *Aldrichimica Acta* **1985**, *18*, 31-47.

(14) Negishi, E.; Takahashi, T. *Synthesis* **1988**, 1-19.

(15) Buchwald, S. L.; Nielsen, R. N. *J. Am. Chem. Soc.* **1988**, *110*, 3171-3175.

(16) Negishi, E. *Chem. Scr.* **1989**, *29*, 457-468.

(17) Broene, R. D.; Buchwald, S. L. *Science (Washington, D. C.)* **1993**, *261*, 1696-1701.

(18) Campora, J.; Buchwald, S. L. *Organometallics* **1993**, *12*, 4182-4187.

(19) Bulls, A. R.; Schaefer, W. P.; Serfas, M.; Bercaw, J. E. *Organometallics* **1987**, *6*, 1219-1226.

(20) Bennett, M. A.; Schwemlein, H. P. *Angew. Chem. Int. Ed. Engl.* **1989**, *28*, 1296-1320.

(21) Van Wagenen, B. C.; Livinghouse, T. *Tetrahedron Lett.* **1989**, *30*, 3495-3498.

(22) Takagi, K.; Rousset, C. J.; Negishi, E. *J. Am. Chem. Soc.* **1991**, *113*, 1440-1442.

(23) Cockcroft, J. K.; Gibson, V. C.; Howard, J. A. K.; Poole, A. D.; Siemling, U. *J. Chem. Soc., Chem. Commun.* **1992**, 1668-1669.

(24) Buchwald, S. L.; Watson, B. T.; Huffman, J. C. *J. Am. Chem. Soc.* **1986**, *108*, 7411-7413.

(25) Buchwald, S. L.; Lucas, E. A.; Dewan, J. C. *J. Am. Chem. Soc.* **1987**, *109*, 4396-4397.

(26) Buchwald, S. L.; Nielsen, R. N. *Chem. Rev.* **1988**, *88*, 1047-1058.

(27) Hsu, D. P.; Lucas, E. A.; Buchwald, S. L. *Tetrahedron Lett.Tett. Lett.* **1990**, *31*, 5563-5566.

(28) Cockcroft, J. K.; Gibson, V. C.; Howard, J. A. K.; Poole, A. D.; Siemling, U. *J. Chem. Soc., Chem. Commun.* 1668-1669.

(29) Fisher, R. A.; Buchwald, S. L. *Organometallics* **1990**, *9*, 871-873.

(30) Buchwald, S. L.; Lucas, E. A.; Davis, W. M. *J. Am. Chem. Soc.* **1989**, *111*, 397-398.

(31) Buchwald, S. L.; Lum, R. T.; Dewan, J. C. *J. Am. Chem. Soc.* **1986**, *108*, 7441-7442.

(32) Buchwald, S. L.; Kreutzer, K. A.; Fisher, R. A. *J. Am. Chem. Soc.* **1990**, *112*, 4600-4601.

(33) See Chapter Two.

(34) Secaur, C. A.; Day, V. W.; Ernst, R. D.; Kennelly, W. J.; Marks, T. J. *J. Am. Chem. Soc.* **1976**, *98*, 3713-3715.

(35) Tilley, T. D.; Andersen, R. A.; Spencer, B.; Ruben, H.; Zalkin, A.; Templeton, D. H. *Inorg. Chem.* **1980**, *19*, 2999-3003.

(36) Evans, W. J.; Deming, T. J.; Ziller, J. W. *Organometallics* **1989**, *8*, 1581-1583.

(37) Evans, W. J.; Shreeve, J. L.; Ziller, J. W. *Organometallics* **1994**, *13*, 731-733.

(38) See Chapter Four.

(39) *Fundamental and Technological Aspects of Organo-f-Element Chemistry*; Marks, T. J.; Fragalà, I. L., Ed.; Reidel: Dordrecht, Holland, 1984, pp 49-76.

(40) Bruno, J. W.; Smith, G. M.; Marks, T. J.; Fair, C. K.; Schultz, A. J.; Williams, J. M. *J. Am. Chem. Soc.* **1986**, *108*, 40-56.

(41) Marks, T. J. *Inorg. Chim. Acta* **1987**, *140*, 1-2.

(42) Fendrick, C. M.; Marks, T. J. *J. Am. Chem. Soc.* **1986**, *108*, 425-437.

(43) Arney, D. S. J.; Burns, C. J.; Smith, D. C. *J. Am. Chem. Soc.* **1992**, *114*, 10068-10069.

(44) Hall, S. W.; Huffman, J. C.; Miller, M. M.; Avens, L. R.; Burns, C. J.; Arney, D. S. J.; England, A. F.; Sattelberger, A. P. *Organometallics* **1993**, *12*, 752-758.

(45) Arney, D. S. J.; Burns, C. J. *J. Am. Chem. Soc.* **1993**, *115*, 9840-9841.

(46) Shannon, R. D. *Acta Crystallogr., Sect A: Cryst. Phys., Diffr., Theor. Gen. Crystallogr.* **1976**, *A32*, 751-767.

(47) Schock, L. E.; Brock, C. P.; Marks, T. J. *Organometallics* **1987**, *6*, 232-241.

(48) Fendrick, C. M.; Marks, T. J. *J. Am. Chem. Soc.* **1984**, *106*, 2214-2216.

(49) Bruno, J. W.; Marks, T. J.; Day, V. W. *J. Am. Chem. Soc.* **1982**, *104*, 7357-7356.

(50) Bruno, J. W.; Marks, T. J.; Morss, L. R. *J. Am. Chem. Soc.* **1983**, *105*, 6824-6832.

(51) Mintz, E. A.; Moloy, K. G.; Marks, T. J.; Day, V. W. *J. Am. Chem. Soc.* **1982**, *104*, 4692-4695.

(52) England, A. F.; Burns, C. J.; Buchwald, S. L. *Organometallics* **1994**, *13*, 3491-3496.

(53) See Chapter One.

(54) Lin, Z.; Le Marechal, J.-F.; Sabat, M.; Marks, T. J. *J. Am. Chem. Soc.* **1987**, *109*, 4127-4129.

(55) Yang, X.; Stern, C. L.; Marks, T., J. *J. Am. Chem. Soc.* **1991**, *113*, 3623-3625.

(56) England, A. F.; Buchwald, S. L. Unpublished results; the formation of the DMAP adduct of the zirconocene stabilized benzyne complex $Cp_2Zr(3,6\text{-}Br_2C_6H_2)$(DMAP) from the thermolysis of $Cp_2Zr(3,5\text{-}Br_2C_6H_3)$ in the presence of the pyridine ligand is suggested by NMR.

(57) Klei, E.; Teuben, J. H. *J. Organomet. Chem.* **1981**, *214*, 53-64.

(58) Watson, P. L. *J. Chem. Soc., Chem. Commun.* **1983**, 276-277.

(59) den Haan, K. H.; Wielstra, Y.; Teuben, J. H. *Organometallics* **1987**, *6*, 2053-2060.

(60) Arnold, J.; Woo, H.-G.; Tilley, T. D.; Rheingold, A. L.; Geib, S. J. *Organometallics* **1988**, *7*, 2045.

(61) Thompson, M. E.; Baxter, S. M.; Bulls, A. R.; Burger, B. J.; Nolan, M. C.; Santarsiero, B. D.; Schaefer, W. P.; Bercaw, J. E. *J. Am. Chem. Soc.* **1987**, *109*, 203-219.

(62) Jordan, R. F.; Guram, A. S. *Organometallics* **1990**, *9*, 2116-2123.

(63) Jordan, R. F.; Taylor, D. F.; Baenziger, N. C. *Organometallics* **1990**, *9*, 1546-1547.

(64) Deelman, B.-J.; Stevels, W. M.; Teuben, J. H.; Lakin, M. T.; Spek, A. L. *Organometallics* **1994**, *13*, 3881-3891.

(65) Evans, W. J.; Meadows, J. H.; Hunter, W. E.; Atwood, J. L. *J. Am. Chem. Soc.* **1984**, *106*, 1291-1300.

(66) Jordan, R. F.; LaPointe, R. E.; Bradley, P. K.; Baenziger, N. C. *Organometallics* **1989**, *8*, 2892-2903.

(67) Jordan, R. F.; Bradley, P. K.; LaPointe, R. E.; Taylor, D. F. *New. J. Chem.* **1990**, *14*, 505-511.

(68) See Chapter Three.

(69) Dormond, A.; Elbouadilli, A. A.; Moïse, C. *J. Chem. Soc., Chem. Commun.* **1984**, 749-751.

(70) Marks, T. J.; Day, V. W. In *Fundamental and Technological Aspects of Organo-f-Element Chemistry*; Marks, T. J.; Fragalà, I. L., Ed.; Reidel: Dordrecht, Holland, 1984; Vol. 155, 115-157 and references therein.

(71) Fagan, P. J.; Manriquez, J. M.; Marks, T. J.; Vollmer, S. H.; Day, C. S.; Day, V. W. *J. Am. Chem. Soc.* **1981**, *103*, 2206-2220.

(72) Schock, L. E.; Brock, C. P.; Marks, T. J. *Organometallics* **1987**, *6*, 232-241 and references therein.

(73) Boekel, C. P.; Teuben, J. H.; de Liefde Meijer, H. J. *J. Organomet. Chem.* **1975**, *102*, 161-165.

(74) Waters, J. A.; Vickroy, V. V.; Mortimer, G. A. *J. Organomet. Chem.* **1971**, 33, 41-52.

(75) McDade, C.; Green, J. C.; Bercaw, J. E. *Organometallics* **1982**, *1*, 1629-1634.

(76) Kasahara, A. *Bull. Chem. Soc., Japan* **1968**, *41*, 1272-

(77) Hartwell, G. E.; Lawrence, R. V.; Smas, M. J. *J. Chem. Soc., Chem. Commun.* **1970**, 912.

(78) Foot, R. J.; Heaton, B. T. *J. Chem. Soc., Chem. Commun.* **1973**, 838-839.

(79) Nonoyama, M. *J. Organomet. Chem.* **1974**, *74*, 115-120.

(80) Bruce, M. I.; Goodall, B. L.; I, M. *Aust. J. Chem.* **1975**, *28*, 1259-1264.

(81) Beshouri, S. M.; Fanwick, P. E.; Rothwell, I. P.; Huffman, J. C. *Organometallics* **1987**, *6*, 2498-2502.

(82) Beshouri, S. M.; Fanwick, P. E.; Rothwell, I. P.; Huffman, J. C. *Organometallics* **1987**, *6*, 891-893.

(83) Beshouri, S. M.; Chebi, D. E.; Fanwick, P. E.; Rothwell, I. P. *Organometallics* **1990**, *9*, 2375-2385.

(84) Guram, A. S.; Swenson, D. C.; Jordan, R. F. *J. Am. Chem. Soc.* **1992**, *114*, 8991-8996.

(85) Silverstein, R. M.; Baxter, G. C.; Morill, T. C. *Spectrophotometric Identification of Organic Compounds*; Wiley: New York, NY, 1979, 273.

(86) Henderson, M. J.; Papasergio, R. I.; Raston, C. L.; White, A. H.; Lappert, M. F. *J. Chem. Soc., Chem. Commun.* **1986**, 672-674.

(87) Bailey, S. I.; Colgan, D.; Engelhardt, L. M.; Leung, W.-P.; Papasergio, R. I.; Raston, C. L.; White, A. H. *J. Chem. Soc., Dalton Trans.* **1986**, 603-613.

(88) Canty, A. J.; Minchin, N. J.; Engelhardt, L. M.; Skelton, B. W.; White, A. H. *Aust. J. Chem.* **1988**, *41*, 651-665.

(89) Jordan, R. F.; Guram, A. S. *Organometallics* **1990**, *9*, 2116-2123.

(90) Guram, A. S.; Jordan, R. F.; Taylor, D. F. *J. Am. Chem. Soc.* **1991**, *108*, 1833-1835.

(91) Mark, V.; Dungan, C. H.; Crutchfield, M. M.; Van Wazer, J. R. In *Topics in Phosphorus Chemistry, Volume 5: P^{31} Nuclear Magnetic Resonance*; M. Grayson and E. J. Griffith, Ed.; Wiley: New York, N. Y., 1967; 227-457.

(92) *Comprehensive Organometallic Chemistry II*; Abel, E. W.; Stone, G. A.; Wilkinson, G., Ed.; Pergamon: New York, NY, 1994.

(93) Schaub, B.; Jenny, T.; Schlosser, M. *Tetrahedron Lett.* **1984**, *25*, 4097-4100.

(94) Solans, X.; Font-Altaba, M.; Aguilo, M.; Miravitlles, C.; Besteiro, J. C.; Lahuerta, P. *Acta Crystallogr., Sect. C* **1985**, *41*, 841-844.

(95) Hartung, H.; Petrick, D.; Schmoll, C.; Weichmann, H. Z. *Anorg. Allg. Chem.* **1987**, *550*, 140-148.

(96) Malik, K. M. A.; Jeffery, J. W. *Acta. Cryst.* **1973**, *B29*, 2687-26982.

(97) Leipoldt, J. G.; Wessels, G. F. S.; Bok, L. D. C. *J. Inorg. Nucl. Chem.* **1975**, *37*, 2487-2490.

(98) Alcock, N. W.; Esperås; Bagnall, K. W.; Hsian-Yun, W. *J. Chem. Soc., Dalton Trans.* **1978**, 638-646.

(99) Tsai, J.-C.; England, A. F.; Buchwald, S. L. Unpublished results.

(100) Buchwald, S. L.; King, S. M. *J. Am. Chem. Soc.* **1991**, *113*, 259-265.

(101) Tatsumi, K.; Nakamura, A.; Hofmann, P.; Stauffert, P.; Hoffman, R. *J. Am. Chem. Soc.* **1985**, *107*, 4440-4451.

(102) Hofmann, P.; Stauffert, P.; Tatsumi, K.; Nakamura, A.; Hoffman, R. *Organometallics* **1985**, *4*, 404-406.

(103) Emsley, J.; Hall, D. *The Chemistry of Phosphorus: Environmental, Organic, Inorganic, Biochemical and Spectroscopic Aspects*; Harper and Row: London, 1976, 306-349.

(104) McMillen, D. F.; Golden, D. M. In *Annual Review of Physical Chemistry*; B. S. Rabinovitch, J. M. Schurr and H. L. Strauss, Ed.; Annual Reviews: Palo Alto, CA, 1982; Vol. 33; 493-532.

(105) Collum, D. B.; Depue, R. T.; Klang, J. A. *Organometallics* **1986**, *5*, 1015-1018 and references therein.

(106) Clark, D. L.; Huffman, J. C.; Watkin, J. G. *J. Chem. Soc., Chem. Commun.* **1992**, 266-268.

(107) Clark, D. L.; Watkin, J. G. *Inorg. Chem.* **1993**, *32*, 1766-1772.

(108) Barnhart, D. M.; Clark, D. L.; Gordon, J. C.; Huffman, J. C.; Watkin, J. G. *Inorg. Chem.* **1994**, *33*, 3939-3944.

(109) Evans, W. J.; Hanusa, T. P.; Levan, K. R. *Inorg. Chim. Acta.* **1985**, *110*, 191-195 and references therein.

(110) Babian, E. A.; Hrncir, D. C.; Bott, S. G.; Atwood, J. L. *Inorg. Chem.* **1986**, *25*, 4818-4821.

(111) Chisholm, M. H.; Clark, D. L. *Comments Inorg. Chem.* **1987**, *6*, 23-40.

(112) Chisholm, M. H. *Polyhedron* **1983**, *2*, 681-722.

(113) Sigel, G. A.; Decker, D.; Olmstead, M. M.; Power, P. P. *Inorg. Chem.* **1987**, *26*, 1773-1780.

(114) Coffindaffer, T. W.; Steffy, B. D.; Rothwell, I. P.; Folting, K.; Huffman, J. C.; Streib, W. E. *J. Am. Chem. Soc.* **1989**, *111*, 4742-4749.

(115) Hessler, J. P.; Carnall, W. T. In *Lanthanide and Actinide Chemistry and Spectroscopy*; N. M. Edelstein, Ed.; American Chemical Society: Washington, D. C., 1980.

(116) Ionova, G. V.; Pershina, V. G.; Spitsyn, V. I. *Dokl. Akad. Nauk. SSSR* **1982**, *263*, 130.

(117) Bursten, B. E.; Rhodes, L. R.; Strittmatter, R. J. *J. Less-Common Met.* **1989**, *149*, 207.

(118) Cotton, S. *Lanthanides and Actinides*; Oxford University: New York, NY, 1991.

(119) Tatsumi, K.; Nakamura, A.; Hofmann, P.; Stauffert, P.; Hoffman, R. *J. Am. Chem. Soc.* **1985**, *107*, 4440-4451 and references therein.

(120) Sonnenberger, D. C.; Morss, L. R.; Marks, T. J. *Organometallics* **1985**, *4*, 352-355.

(121) Duttera, M. R.; Day, V. W.; Marks, T. J. *J. Am. Chem. Soc.* **1984**, *106*, 2907-2912.

(122) Van Geet *Anal. Chem.* **1968**, *40*, 2227-2229.

(123) Hecht, H. G. *Mathematics In Chemistry: An introduction to Modern Methods*; Prentice-Hall: Englewood Cliffs, NJ, 1990, 267-273.

CHAPTER FOUR

The Cerium(IV)-Nitrogen Bond: Studies into the Synthesis of Simple Amide Complexes of Cerium(IV)

Introduction

It is ironic to think that a synthetic organic chemist likely has far greater knowledge of the chemistry of cerium(IV) than an inorganic colleague. Cerium(IV) reagents have long since been employed as oxidants in effecting a wide variety of organic transformations.[1,2] Conversely, prior to the late 1980s, the number of well characterized cerium(IV) complexes did not extend past a handful of known species.[3-7] Though in many other areas, interest in the molecular chemistry of the 4*f*-elements has undergone an explosive growth over the last twenty years,[8] the chemistry of cerium(IV) has for the most part been overlooked.

The reactivity of cerium(IV) has not been developed much beyond the use of ceric ammonium nitrate ($(NH_4)_2[Ce(NO_3)_6]$, CAN) and related salts as a one electron oxidants. As a result, the full potential of the tetravalent lanthanide as a reagent in organic synthesis has yet to be realized, since such reagents typically suffer from low solubility in organic solvents, poor selectivity in reactions, and the limitation of a relatively inflexible, untunable ligand environment. Several recent reports have appeared regarding the use of neutral cerium(IV) species as oxidants,[9,10] as well as systems which employ this lanthanide catalytically.[2,11-15] There have, however, been few attempts extended towards the development of a better overall understanding of the nature of the tetravalent lanthanide in an effort to alleviate the problems associated with cerate reagents, and design a more general oxidation system.

There are, however, distinct reasons why the tetravalent cerium has mostly been overlooked until this point. Much of the recent expansion of the chemistry of the lanthanides has been directed toward applications of organometallic systems in organic synthesis[15-20] and catalysis.[15,21-24] Furthermore, where the literature abounds with examples of divalent and trivalent rare earth alkyl derivatives,[25,26] the preparation of a stable cerium(IV)-alkyl remains a challenge of immense proportions. This is in stark contrast to the extensive body of knowledge surrounding the tetravalent organometallic chemistry of group 4 and early actinide (Th, U) elements.

Understanding the problematic nature of high oxidation state cerium chemistry begins with an examination of the reduction potentials for the lanthanide series (Table 1). Although tetravalent fluorides and/or oxides of praseodymium (Pr), neodymium (Nd), terbium (Tb) and dysprosium (Dy) are

Table 1. Aqueous Reduction Potentials (Volts) of the Lanthanides[a]

Ln	EC of Ln^0	$Ln^{3+} + 3e^- \rightarrow Ln$	$Ln^{3+} + e^- \rightarrow Ln^{2+}$	$Ln^{4+} + e^- \rightarrow Ln^{3+}$
La	$[Xe]5d^1 6s^2$	-2.37	(-3.1)[c]	-
Ce	$4f^1 5d^1 6s^2$	-2.34	(-3.2)[c]	1.61[b]/1.7
Pr	$4f^3 6s^2$	-2.35	(-2.7)[c]	2.86[b]/(3.4)[c]
Nd	$4f^4 6s^2$	-2.32	-2.6[d]	(4.6)[c]
Pm	$4f^5 6s^2$	-2.29	(-2.6)[c]	(4.9)[c]
Sm	$4f^6 6s^2$	-2.30	-1.55	(5.2)[c]
Eu	$4f^7 6s^2$	-1.99	-0.34	(6.4)[c]
Gd	$4f^7 5d^1 6s^2$	-2.29	(-3.9)[c]	(7.9)[c]
Tb	$4f^9 6s^2$	-2.30[c]	(-3.7)[c]	(3.3)[c]
Dy	$4f^{10} 6s^2$	-2.29	-2.5[d]	(5.0)[c]
Ho	$4f^{11} 6s^2$	-2.33	(-2.9)[c]	(6.2)[c]
Er	$4f^{12} 6s^2$	-2.31	(-3.1)[c]	(6.1)[c]
Tm	$4f^{13} 6s^2$	-2.31	-2.3[d]	(6.1)[c]
Yb	$4f^{14} 6s^2$	-2.22	-1.05	(7.1)[c]
Lu	$4f^{14} 5d^1 6s^2$	-2.30	-	(8.5)[c]

[a] from ref[8]
[b] from ref[27]
[c] values in parentheses are calculated potentials
[d] determined in tetrahydrofuran

also known, of the five, only cerium(IV) demonstates any level of stability in coordination compounds. Nonetheless, the reduction potential reflects the strongly oxidizing nature of the cerium(IV) metal center. Since the potential for the oxidation of water is lower than that for the cerium(IV)/cerium(III) couple it is only the kinetic control of the process that allows acidic solutions of the cerium(IV) ion to be metastable (E^0 (Ce^{IV}/Ce^{III}): 1.44 V (1M H_2SO_4), 1.6 V (1M HNO_3), 1.7 V (1M $HClO_4$); E^0 ($2H_2O \rightarrow O_2 + 4H^+ + 4e^-$) = -1.23 V).[8,28] The reduction potentials of only a very small group of metal ions approaches or exceeds the value demonstrated by cerium(IV), and does not include the tetravalent group 4 and early actinide (An = Th, U; An ≠ Am, Bk) homologues, which are considerably less active with respect to redox chemistry (Table 2).

The stability of high oxidation state cerium relative to other lanthanides ultimately derives from the noble gas electron configuration of

Table 2. Reduction Potentials of Cerium(IV), Strongly Oxidizing Metal Centers and Tetravalent Homologues[27]

Pr^{4+}	+	e^-	→	Pr^{3+}	=	+2.86V
Am^{4+}	+	e^-	→	Am^{3+}	=	+2.18V
Ag^{2+}	+	e^-	→	Ag^{+}	=	+1.98V
Co^{3+}	+	e^-	→	Co^{2+}	=	+1.81V
Au^{+}	+	e^-	→	Au	=	+1.69V
Ce^{4+}	+	e^-	→	Ce^{3+}	=	+1.61/1.7[a]V
Bk^{4+}	+	e^-	→	Bk^{3+}	=	+1.6V
Au^{3+}	+	$3e^-$	→	Au	=	+1.50V
Tl^{3+}	+	$2e^-$	→	Tl^{2+}	=	+1.25V
Ce^{4+}	+	e^-	→	Ce^{3+}	=	+1.61/1.7[a]V
$(TiO)^{2+}$	+	e^-	→	Ti^{3+}	=	+0.01V
U^{4+}	+	e^-	→	U^{3+}	=	-0.61V
Zr^{4+}	+	$4e^-$	→	Zr	=	-1.53V
Hf^{4+}	+	$4e^-$	→	Hf	=	-1.7V
Th^{4+}	+	$4e^-$	→	Th	=	-1.90V

[a] *from* ref[8]

the tetrapositive ion. It is therefore not immediately apparent why such an electropositive metal center has such a tendency to adopt an f^1 configuration. However, unlike the *d*-transition series and the early actinide elements, the minimal radial extent of the 4*f* valence orbital is such that preferred lanthanide oxidation states are determined more by the balance between successive ionization potentials and the electronegativity of the ligand environment, rather than simply the stability of specific electron configurations (Table 3). Although in general, trivalent lanthanide ions result, it is the additional stabilization due to the closed shell configuration of cerium(IV) which promotes the high oxidation state. A similar pattern evolves in the reverse sense for the stable divalent oxidation states among the lanthanides samarium (Sm), europium (Eu) and ytterbium (Yb).[8,18,19] The somewhat precarious balance is however readily offset by the introduction of electron rich ligands into the coordination sphere, typically resulting in facile redox chemistry, reduction of the metal center and substrate

oxidation. Hence, a cerium(IV) metal center supported in a framework of σ-bonded alkyls or amide derivatives is seemingly an extremely reactive combination. Although presenting a considerable synthetic challenge, such reactivity may also potentially be the source of further utility of cerium(IV) species, providing of course that it can both be harnessed, and subsequently controlled. Although the facile oxidation of a variety of organic substrates by CAN and other reagents seemingly demonstrates the incompatibility of such systems, it remains to be seen as to whether stable cerium(IV) alkyls and amides may be prepared.

Table 3. Ionization Potentials of the Lanthanides[29]

Ln	I_1	I_2	I_3	I_4
La	538.1	1067	1850	4819
Ce	527.4	1047	1949	3547
Pr	523.1	1018	2086	3761
Nd	529.6	1035	2130	3899
Pm	523.9	1052	2150	3970
Sm	543.3	1068	2260	3990
Eu	546.7	1085	2404	4110
Gd	592.5	1167	1990	4250
Tb	564.6	1112	2114	3839
Dy	571.9	1126	2200	4501
Ho	580.7	1139	2204	4150
Er	588.7	1151	2194	4115
Tm	596.7	1163	2285	4119
Yb	603.4	1176	2415	4220
Lu	523.5	1340	2022	4360

From an examination of early efforts into the preparation of cerium(IV) organometallic species alone, it appears as if all of the expected difficulties associated with this chemistry are unfounded. A series of reports have appeared regarding the synthesis of complexes of the type $(Cp)_3Ce(X)$ (Cp = η^5-C_5H_5) and $(\eta^5\text{-}C_9H_7)_2Ce(X)_2$ (X = H, BH_4, Cl, N_3, CN, NCO, NCS, NO_2, OR, CO_2R, SR, NH_2, alkyl, aryl)[30-37] as well as tetrakis(cyclopentadienyl)-cerium(IV),[30] but these results have been hotly disputed (Scheme 1 (i)).[7,38-42]

The synthesis of Cp_4Ce, specifically, has since been refuted, with the major reaction product identified as the reduced tris(cyclopentadienyl) species Cp_3Ce (Scheme 1 (ii)),[42] whilst other results have so far proven irreproducible.[7,38-42]

Scheme 1

$$(pyH)_2[CeCl_6] + 4NaCp \not\longrightarrow Cp_4Ce + 4NaCl + 2(pyH)Cl \qquad \text{(i)}$$

$$2(pyH)_2[CeCl_6] + 12NaCp \longrightarrow Cp_3Ce + 12NaCl + 4py + (Cp)_2 + 4C_5H_6 \qquad \text{(ii)}$$

After an initial report (Scheme 2 (i)),[7] the first confirmed synthesis (Scheme 2 (ii)), of an organocerium(IV) species was that for cerocene, $Ce(COT)_2$ (COT = η^8-C_8H_8) which unlike "Cp_4Ce",[30] actually does demonstrate amazing stability towards water.[41]

Scheme 2

$$Ce(O^iPr)_4(^iPrOH) + 5AlEt_3 \xrightarrow[\substack{C_8H_8\ \text{(Solvent)} \\ -\,C_2H_6,\ -\,4C_2H_5^{\bullet}}]{\Delta} \begin{matrix} Ce(COT)_2 \\ + \\ 5AlEt_2(O^iPr) \end{matrix} \qquad \text{(i)}$$

$$K^+[Ce(C_8H_8)_2]^- \xrightarrow[O_2\ \text{or}\ NOBF_4]{[O]} Ce(COT)_2 \qquad \text{(ii)}$$

The hydrolytic stability of cerocene is certainly not common amongst organolanthanide systems,[38,43] and thus, in many respects, the bis(cyclooctatetraene) framework might be considered a both a perfect steric and electronic partner for the stabilization of tetravalent cerium. Although an extremely basic ligand the bulk of the COT rings serves to coordinatively saturate the metal center, while resonance stabilization due to the aromatic dianions disfavor single electron transfer.[44] Furthermore, recent calculations on the ring-metal interaction of cerocene has demonstrated that the participation of higher energy metal *d* orbitals in the bonding of this system is at least as important as that of the valence *f* orbitals.[6] The increased radial extent of the 5*d* orbitals relative to the valence 4*f* orbitals thus imparts a considerable degree of covalency to the cerium-COT interaction, in turn further stabilizing

the high oxidation state metal center.[41] Similar observations have also been made for the actinide analogs thorocene, $Th(COT))_2$, and uranocene, $U(COT))_2$,[45,46] although here, the differences between low lying *6d* and *5f* orbitals is far from that exxperienced in the lanthanides.[8]

Even after the preparation and characterization of cerocene it nonetheless remained questionable as to what extent other organic frameworks might be able to stabilize cerium(IV) derivatives. The synthesis of $Cp_3Ce(O^iPr)$ had been reported, albeit in only 4% yield from the metathesis reaction between cerium(IV) tetraisopropoxide and magnesium bis(cyclopentadienide) (Scheme 3 (i)).[7] This species was only demonstrated to

Scheme 3

$$Ce(O^iPr_4)(^iPrOH) + 2MgCp_2 \longrightarrow \underset{4\%}{Cp_3Ce(O^iPr)} + 2Mg(O^iPr)_2 + CpH \quad \text{(i)}$$

$$Ce(O^iPr_4) + 2R_3SnCp \xrightarrow{\Delta} Cp_3Ce(O^iPr) + 3R_3Sn(O^iPr) \quad \text{(ii)}$$

R = Me; 69%
R = *n*-Bu; 20%

be a major reaction product after the development a route utilizing tin transfer agents.[47] A variety of differentially substituted cerocene derivatives have since been prepared,[48,49] although only two other cerium(IV) cyclopentadienyl containing species ($Cp_2Ce(O^tBu)_2$ and $Cp_3Ce(O^tBu)$), have been reported, synthesized from their respective alkoxide nitrate precursors (Scheme 4).[50]

Scheme 4

$$(^tBuO)_2Ce(NO_3)_2(THF)_2 + 2NaCp \xrightarrow[-2THF]{} Cp_2Ce(O^tBu)_2 + 2NaNO_3 \quad \text{(i)}$$

$$(^tBuO)Ce(NO_3)_3(THF)_2 + 3NaCp \xrightarrow[-2THF]{} Cp_3Ce(O^tBu) + 3NaNO_3 \quad \text{(ii)}$$

The preparation of stable mono(cyclopentadienyl) derivatives has, however, yet to be reported. Attempts to extend metathetical procedures to the preparation of more electron rich pentamethylcyclopentadienyl analogs were

found to result only in reduction of the the metal center.[50] Results to date suggest that it is the presence of an alkoxide ancillary ligand framework that enables stabilization of seemingly incompatible Ce^{IV}-Cp interactions in the plain-ring systems. In addition, although pentamethyl-cyclopentadienyl (η^5-C_5Me_5, Cp*) anion is also known to reduce europium(III) (E^0(Eu(III)/Eu(II) = -0.35 ± 0.03 V), a recent report of the preparation of the dimeric species $[(Cp^*Eu(O^tBu)(\mu\text{-}O^tBu)]_2$, the first example of a stable Eu^{III}-Cp* complex demonstrates the ability of the *tertiary*-butoxide ligand to promote stability in high oxidation state lanthanide complexes.[51] The *tertiary*-butoxide substituent offers not only bulk to aid steric saturation, but also the strong interaction between the lanthanide and electronegative oxygen which together serve to stabilize the high oxidation state metal center.

It is the absence of suitable routes to alkoxide precursors that has hampered efforts to further study differentially substituted cerium(IV) species. Numerous examples of homoleptic cerium(IV) alkoxides ($Ce(OR)_4$ (R = Me,[52] O^iPr,[53] O^tBu,[54] *n*-Octyl;[52] $Ce(OSiR_3)_4$ (R = Me,[55] Et,[55,56] Ph)[55-57] have appeared in the literature. In addition, a variety of stable isopropoxy aminoalkoxy derivatives ($Ce(O^iPr)_{4-n}(OR)_n$: OR = $CH_2CH_2NEt_2$, n = 1-4;[58] OR = $OCH_2CH_2N(Me)CH_2CH_2NMe_2$, n = 1;[59] $Ce(O^iPr)_{4-2n}(OR)_n$: OR = $(CH_2CH_2)NH/Et$, n = 0.5, 1, 2;[58] $Ce(O^iPr)_{4-3n}(OR)_n$: OR = $(CH_2CH_2)N$, n = 1),[58] and precursor complexes of the type $(RO)_{4-n}Ce(X)_n$ (X = exchangeable ligand, e.g. halide, nitrate; n = 1-3) were not known until recently, however. [54] The synthesis of such aminoalkoxide and siloxide derivatives has been achieved by protonolysis of cerium(IV) tetraisopropoxide, which along with other tetralkoxides is prepared directly from the 'CeX_4' precursor CAN. The use of this commercially available cerate species as a precursor for the preparation of neutral cerium(IV) complexes has itself only been established in the last ten years.[52] Previously, the laborious synthesis of dipyridinium hexachlorocerate was required in order to effect similar transformations.[3-5]. The major breakthrough with regard to the preparation of novel cerium(IV) complexes came with the synthesis of the readily prepared *tertiary*-butoxide nitrate derivatives $(^tBuO)_nCe(NO_3)_{4-n}(L)_2$ (n = 1, 2: L = THF, ^tBuOH; n = 3: L = THF) from the deprotonation/transmetallation process between CAN and sodium *tertiary*-butoxide (eq 1). So far, however, the generality of this reaction scheme has only been demonstrated in the case of the *tertiary*-butoxide ligand.[54]

$$(NH_4)_2[Ce(NO_3)_6] + nNaO^tBu \xrightarrow[\text{Solvent = L}]{} (^tBuO)_nCe(NO_3)_{4-n}(L)_2 + 2NH_3 + (n-2)^tBuOH + nNaNO_3 \quad (1)$$

n = 1, 2: L = THF, ^{t}BuOH; n = 3: L = THF

Needless to say, alternative routes exist for the preparation of cerium(IV) complexes. Oxidative pathways, starting with anionic cerium(III) precursors, have previously been employed for the synthesis of cerocene derivatives,[41,45,46,48,49] and metalloporphyrin and -phthalocyanine species.[60-63] Both anodic and chemical oxidation have been utilized to effect such transformations. Although it has clearly been demonstrated that oxidation of the trivalent metal center can be achieved in a variety of different ligand environments, utilizing established oxidants, the problem with the use of oxidative pathways in the preparation of simple organocerium(IV) species, or amides is that the ability to access the product does not ensure product stability. While the intrinsic bulk and aromaticity of the bis(cyclooctatetraene) and porphyrin and/or phthalocyanine sandwich complexes serve as stable templates in supporting the high oxidation state lanthanide, simple organocerium(IV) species and amide derivatives are expected to be highly reactive species. Since the exact nature of the reactivity of such species has yet to be determined, oxidative routes embody too many unknown variables to allow for a systematic study of the foundations required for stabilizing cerium(IV)-carbon and cerium(IV)-nitrogen interactions.

There has been less effort directed toward the preparation of tetravalent amide of cerium(IV) derivatives than analogous organometallic systems. To date, the only reported examples of species containing anionic metal-nitrogen interactions are the porphyrin and phthalocyanine derivatives, which do not represent discrete cerium(IV)-nitrogen σ-bonded systems. Likewise, a variety of nitrogen donor interactions have been observed, both for neutral amine[59] and imine[64,65] ligands. Not only are cerium(IV) amide derivatives of interest in their own right, but in many respects the preparation of a cerium(IV)-nitrogen bond is a logical progression *en route* to a separate goal of preparing stable σ-alkyl species.

In this present study, the underlying interest in the preparation of cerium(IV) amide species over an extension of the known alkoxide or cyclopentadienyl chemistry lies in the additional valence site open to the pnictogen, which together with the move from a trivalent to a tetravalent lanthanide system, opens up entirely new possibilities in the area of terminal lanthanide imido species, i.e. Ce^{IV}=NR. Imido functionalities have proven to be extremely effective in stabilizing high oxidation state metal centers throughout the *d*-transition series.[66,67] Although advances in the chemistry of group 4 imide chemistry have only occurred in the last few years,[68-79] numerous examples of M=N bonded species have been isolated and characterized for the elements of groups 5 to 8. More recently, the preparation of the first imides of uranium(VI),[80,81] have demonstrated that such ligands are also capable of stabilizing high oxidation state actinide centers. However in the absence of an extremely bulky ligand environment, such as the biscyclopentadienyl framework, the ability to achieve steric saturation in the trigonal lanthanide imide becomes an important concern. Isolation of such a potentially reactive species may ultimately neccessitate additional intra- or intermolecular donor stabilization, however, as is observed to be the case in related group 4 systems.[69-79]

Investigations into the preparation of the first imide complex of a lanthanide have so far been precluded by the lack of availablility of suitable amide, or other, precursor complexes. Thus, in the interests of making inroads into the synthesis of molecular high-valent lanthanide complexes stabilized by metal-ligand multiple bonds this study centers around efforts to prepare the first cerium(IV) amide complexes. By analogy with known *d*-series chemistry, routes to the desired imide may be envisioned starting from both mono- and bisamide complexes. In theory, at least, perhaps the most direct route to an imide involves the formation of a transient monoamide as an intermediate in a one-pot protonolysis and elimination sequence (Scheme 5: (a)). This strategy has been employed successfully in the desilylation of silylamines in the preparation of a variety of *d*-series complexes.[66] Similar reaction chemistry may conceivably be induced from stable, isolated or *in situ* generated monoamide species (b).[72,78] In the past, C-H activation chemistry has demonstrated considerable utility in the preparation of group 4 imide complexes.[68,69,73-75] This route must be ruled out for the synthesis of

Scheme 5

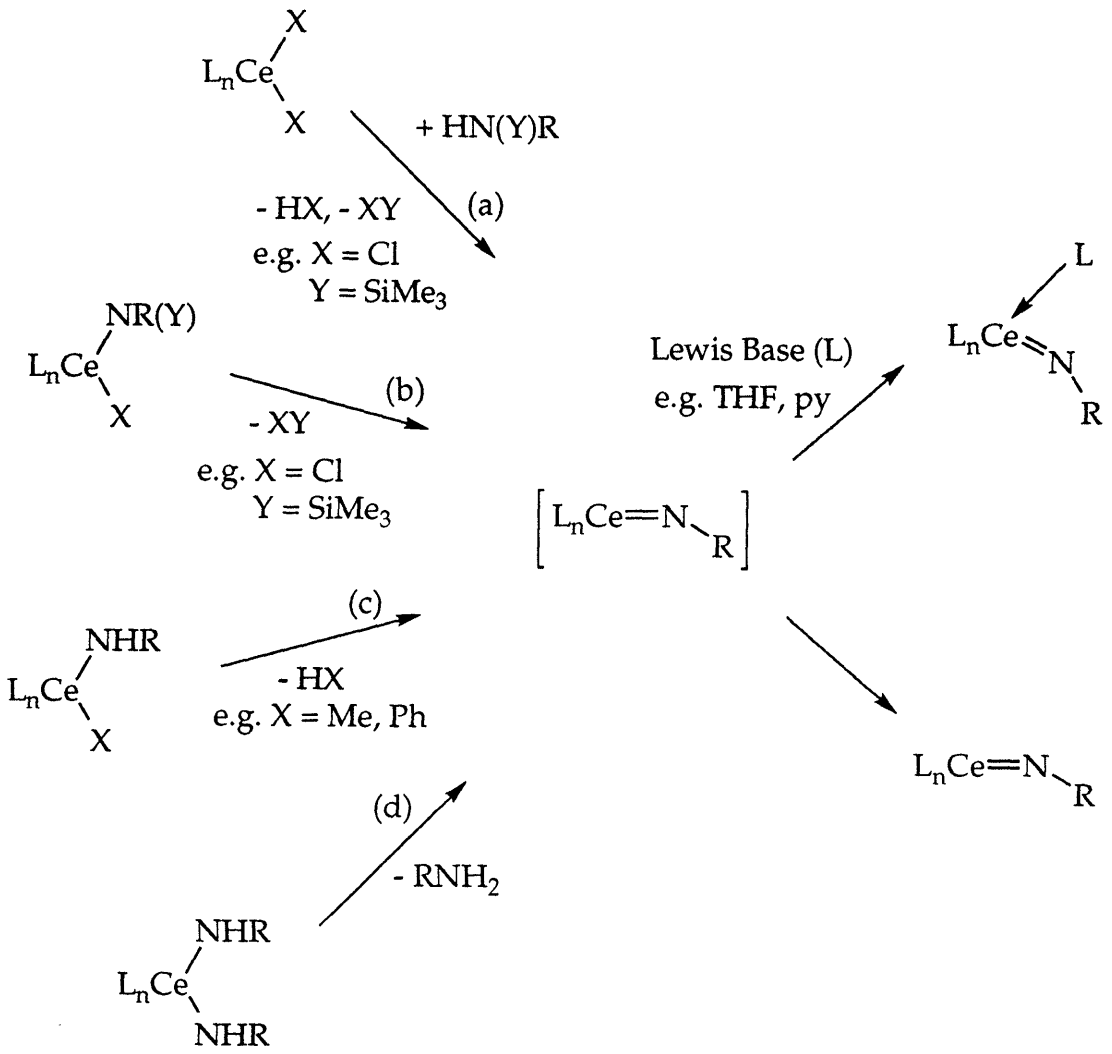

cerium(IV) analogs (c), however, since the requisite precursors are not yet realistic synthetic targets. The other avenue of σ-bond metathesis, α-hydrogen abstraction and amine elimination (d), would appear to offer greater potential both in the sense that the reaction chemistry is well precedented[71,79], and that bisamide species represent the closest nitrogen derived species to established alkoxide and cyclopentadienyl cerium(IV) derivatives. Attempts so far to utilize this strategy for the preparation of analogous uranium species have so far proven unsuccessful.[82]

Results and Discussion

The Reaction of CAN with Lithium Amides. Early efforts to develop novel cerium(IV)-amido chemistry have attempted to exploit strategies analogous to those previously used in cerium(IV) alkoxide systems.[54] The preparation of a series of cerium(IV) alkoxide nitrate species was achieved from the reaction between the cerate salt $(NH_4)_2[Ce(NO_3)_6]$ (CAN) and sodium *tertiary*-butoxide (eq 2).[54] In THF, the addition of two equivalents of alkoxide to CAN

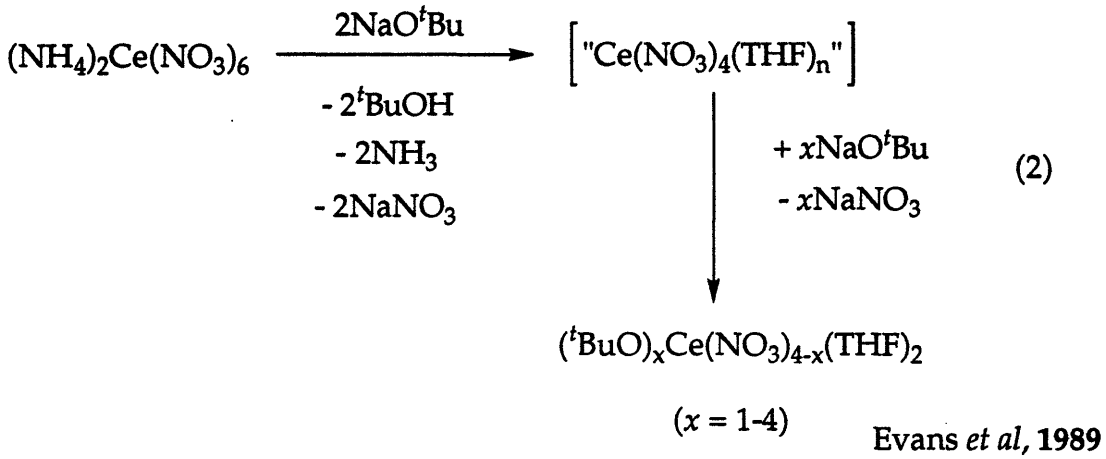

serves to 'deprotonate' the cerate salt, resulting in the formation of a neutral 'CeX_4' equivalent. The product of this reaction has tentatively been assigned the structure "$Ce(NO_3)_4(THF)_x$" ($x \geq 1$) based on stoichiometry and reactivity considerations. However, this species has not been isolated, and no structural evidence has been provided to support this formulation. The possibility that this reactive species exists as a higher order *tertiary*-butoxide substituted ammonium cerate derivative (e.g. "$(NH_4)_xCe(O^tBu)_x(NO_3)_4(THF)_y$" ($x, y \geq 1$)) has not been not ruled out.[54] Successive equivalents of sodium *tertiary*-butoxide effect metathesis of the inner sphere nitrate ligands. This methodology represents the only route so far uncovered into the chemistry of neutral cerium(IV) species containing less than four exchangeable ligands, i.e $Ce(O^tBu)_x(NO_3)_{4-x}(THF)_2$ ($x = 1$-3), and has so far only been demonstrated to be viable in all cases for the *tertiary*-butoxide system.

All of the efforts so far extended to the deprotonation and nitrate metathesis of CAN with nitrogen bases have resulted only in rapid decomposition of the complex, with reduction of the metal center and the formation of an unidentifiable mixture of organic products (eq 3). Almost

$$(NH_4)_2Ce(NO_3)_6 \xrightarrow[\substack{R^1, R^2 = H, SiMe_3 \\ \text{alkyl, aryl}}]{\substack{\geq 1 \text{ equiv } LiNR^1R^2 \\ THF}} \xrightarrow{[H]} Ce^{III} \qquad (3)$$

identical results were reported in analogous reactions between CAN and sodium cyclopentadienide.[83] Typically, lithium amides have been employed in reactions of this type, although significant differences in reactivity have not been observed with sodium analogs. Potassium amides have not been employed in this present study.

Previous studies into the reactions of amines with cerium(IV) oxidants demonstrate that redox processes are facile, although product identification has so far proven to be a barrier to extending the synthetic applications of this chemistry. That rapid decomposition of the cerium(IV) precursor is observed in the presence of as little as one equivalent of amide reagent also provides support for a mechanism in which association of the anion occurs prior to deprotonation of the ammonium counterions of CAN, rather than direct deprotonation (cf. "$(NH_4)_xCe(O^tBu)_x(NO_3)_4(THF)_y$": eq 1). A combination of the fundamental differences in both the steric demands and reducing nature of the amide and alkoxide ligands explains the changes in reactivity observed.[84,85] As might be expected for the extremely electropositive, oxophilic lanthanides in general, and tetravalent cerium more so, alkoxide ligands provide the most favorable ligand set outside of oxo, hydroxy and halide coordination environments.[8]

Several different strategies have been successfully employed in the preparation of a wide range of stable cerium(IV) alkoxide derivatives.[52-59] In certain cases, additional intra-[58,59,64,65] or intermolecular[52,54-57] donor atom coordination is required. A comparative study of known alkoxide complexes reveals that the flexibility of the high oxidation state metal center is such that it can be maintained in a range of different steric and electronic environments, provided that a '$Ce(OR)_4$' core remains intact. The substitution of amide ligands into the coordination sphere proves detrimental to product stability due to the incompatibility of the strongly oxidizing metal center with the reducing amide ligand. Not only are primary amides the most basic, and therefore the most reducing substrates, but these

derivatives also potentially offer additional decomposition pathways over dialkyl substituted amide analogs, since the residual nitrogen-bound proton is susceptible to activation.[86] Furthermore, since the nitrate ligands of CAN are known to serve as an electron source in the reduction of the high oxidation state lanthanide (e.g. Scheme 7), it also realistic to expect that the amide-nitrate transmetalation process initiates the observed redox chemistry, as opposed to decomposition resulting from the formation of unstable cerium(IV)-amide species.

Cerium(IV) mediated one-electron oxidation of neutral organic substrates typically proceeds by way of the initial formation of a radical cation (a), which subsequently decomposes generating free radical and cationic fragments (b), giving rise to reactivity typical of radicals (c and d) and/or electrophiles (e) (Scheme 6).[87] Furthermore, the reduction of cerium(IV) is

Scheme 6

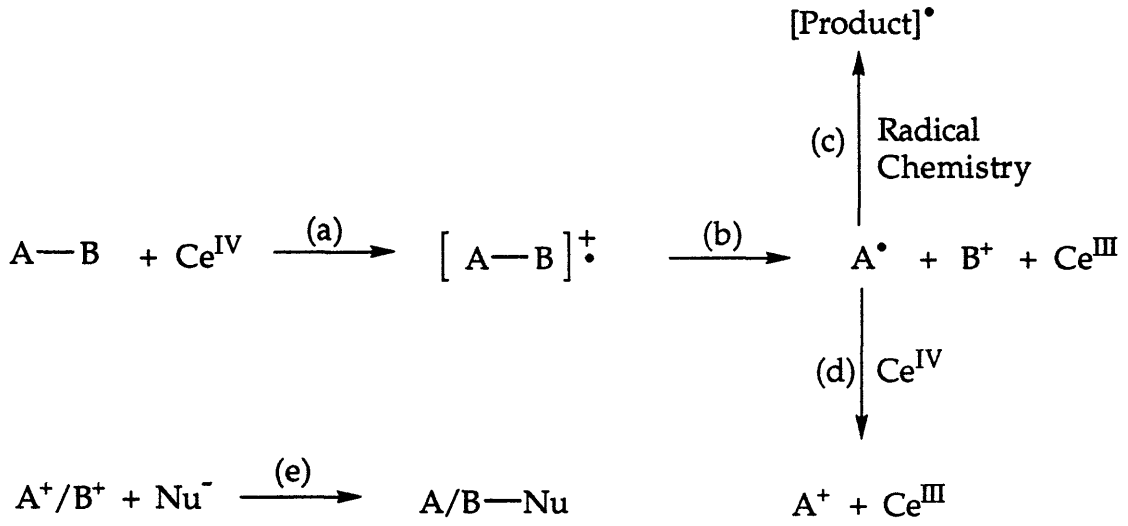

Kagan, **1984**

considered to proceed via one of three general electron transfer pathways.[2] Two of the possible routes utilize ancillary ligands or counterions in initiating redox chemistry, e.g. nitrates in CAN (Scheme 7). Rapid reduction of the metal center may be effected either by a direct outer sphere electron transfer (e.g. Scheme 7: (i)) or by inner sphere ligand transfer processes (ii). In addition, electron transfer may be the ultimate result of a multi-step process (iii). The utility of cerium(IV) oxidation processes arises from the subsequent

Scheme 7

$$R^{\bullet} + Ce^{IV} \longrightarrow R^{+} + Ce^{III} \qquad \text{(i)}$$

$$R^{\bullet} + ONO_2Ce^{IV} \longrightarrow RONO_2 + Ce^{III} \qquad \text{(ii)}$$

$$\left.\begin{array}{l} R^{\bullet} + ONO_2^{-} \longrightarrow RONO_2^{\bullet -} \\ RONO_2^{\bullet -} + Ce^{IV} \longrightarrow RONO_2 + Ce^{III} \end{array}\right. \qquad \text{(iii)}$$

Ho, **1986**

reaction pathways available to free radicals generated under such conditions, including C-H or C-C bond scission, hydrogen atom transfer, radical coupling reactions, or any number of related modes of reactivity (e.g. Scheme 8: (i) pinacol oxidation; (ii) decarboxylation of α-hydoxy carboxylic acids).[2,15]

Scheme 8

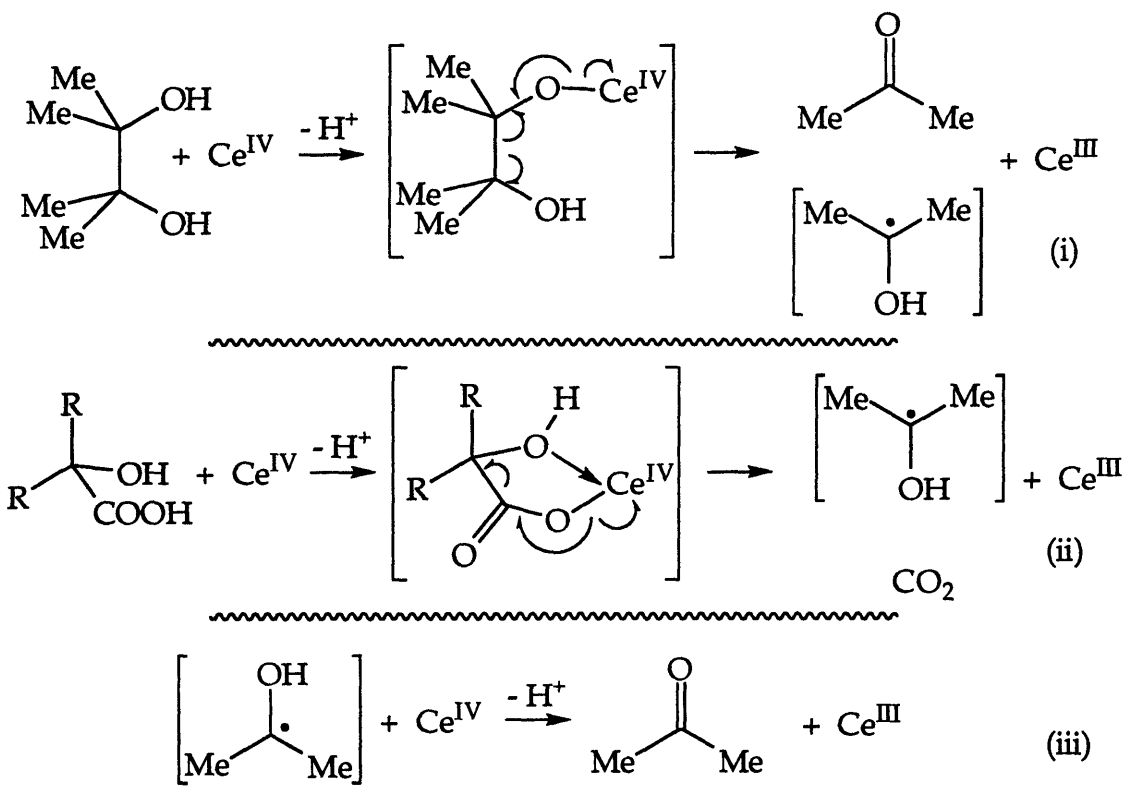

(i), (ii) and (iii): Ho, **1986**

From the available kinetic and mechanistic data, the existence of discrete cerium-bound intermediates has been proposed,[86] although, to date, no such complexes have been isolated or structurally characterized. Similar modes of reactivity are observed between cerium(IV) salts and amine substrates.[86] Although there have been no reported studies on the reactivity of anionic nitrogen based ligands, neutral amine substrates are known to undergo C-N bond cleavage, *N*-nitration and dimerization. In certain instances, the oxidation of aniline derivatives to quinones has been achieved.[86]

Although it is conceivable that cerium(IV) amide nitrate complexes could be prepared via a metathesis route from a 'CeX_4' precursor, these results demonstrate that the ill-defined tetranitrate "$Ce(NO_3)_4(THF)_x$" does not appear to be a suitable starting material. Several well-defined analogs, however, have been prepared and structurally characterized,[10,88-92] which may potentially serve as viable alternative precursors in this chemistry.

The Choice of an Ancillary Framework to Support Cerium(IV)-Nitrogen Bonded Species. In many respects it is possible to simply extrapolate from the chemistry of the tetravalent group 4 elements to that of the early actinides. Where the brunt of the studies of reactivity in group 4 systems has been conducted on metallocene centered frameworks of the type Cp_2M (M = Ti, Zr, Hf),[93] the permethylated analogs Cp^*_2An (An = Th, U) have formed the backbone to synthetic actinide chemistry.[25] Although in its trivalent state cerium fits the pattern of reactivity expected for a trivalent lanthanide,[8,16,26,39,94,95] the reactivity of the lone tetravalent lanthanide bears little resemblance to group 4 or actinide congeners. In addition, where the alkyl chemistry of lanthanide metallocenes is an increasingly important area of research,[18,19,22-24] outside of COT derivatives there are but three known cerium(IV) metallocene complexes,[7,47,50] and as yet no examples of cerium(IV) σ-bonded species. These observations, together with the apparent requirements for the formation of stable, isolable complexes of the type CeX_2Y_2 (e.g., X = ^{t}BuO, Y = NO_3), demonstrate a significant challenge for the preparation of stable cerium(IV) amide complexes with metallocene, or other ancillary ligand sets.

The group 4 metallocene and actinide complexes Cp'_2MCl_2 (M = Ti, Zr; Cp' = Cp; M = Th, U; Cp' = Cp*) are readily available, reactive precursors commonly used in the preparation of variously functionalized complexes. In

contrast, the closest relative to any of these species in cerium(IV) chemistry is the di-*tertiary*-butoxide derivative $Cp_2Ce(O^tBu)_2$.[50] The tris(cyclopentadienyl) analog $Cp_3Ce(O^tBu)$ has also been prepared and structurally characterized.[50] Studies of the reactions between $Cp_2Ce(O^tBu)_2$ and alkali metal amides, however, demonstrate that this is not a suitable precursor for the preparation of amide substituted metallocene derivatives (eq 4). ^1H NMR

$$Cp_2Ce(O^tBu)_2 \xrightarrow[\substack{C_6D_6 \\ RT, > 48\ h}]{\text{excess } LiN(TMS)_2} \underset{\mathbf{1}}{(^tBuO)_2Ce(N(TMS)_2)_2} \qquad (4)$$

spectroscopy indicates initial formation of several products which ultimately give rise to a single major species identified as the bisalkoxide bisamide derivative $(^tBuO)_2Ce(N(TMS)_2)_2$ (**1**), the initial synthesis of which will be discussed later. This investigation into the reactivity of the cerium metallocene was actually conducted after the isolation and characterization of the first cerium(IV) amide complex, $(^tBuO)_2Ce(N(TMS)_2)_2$ (**1**), allowing for identification of the primary reaction product and an understanding of the underlying processes involved. The outcome of this reaction is unsurprising given the oxophilicity of the lanthanide center, demonstrating that the π-bonded cyclopentadienyl rings are considerably more labile than the *tertiary*-butoxide group. Nothwithstanding, the cerium-oxygen linkage does prove labile in a related system. In pentane, at room temperature, the reaction between the tetra-*tertiary*-butoxide $Ce(O^tBu)_4(THF)_2$ and an excess of lithium hexamethyldisilazide shows conversion of approximtely 50% of the material to the bisalkoxide bisamide complex **1**, the only detectable amide-bearing species in the reaction mixture, as evidenced by ^1H NMR (eq 5). This reaction

$$Ce(O^tBu)_4(THF)_2 \xrightarrow[\substack{C_6D_6 \\ RT, > 2\ h}]{4\text{ eq } LiN(TMS)_2} \underset{\mathbf{1}}{(^tBuO)_2Ce(N(TMS)_2)_2} \qquad (5)$$

alone clearly exemplifies the fact that alkoxide-amide exchange is readily achievable, although it does not answer all of the pertinent questions regarding this process. Further exchange may be precluded as a result of the steric demands of the bis(trimethylsilyl)amide and *tertiary*-butoxide ligands which may conceivably prevent the formation of the extremely sterically

encumbered species (^{t}BuO)Ce(N(TMS)$_2$)$_3$. Numerous other examples of tris(hexamethyldisilazide) complexes have, however, been prepared and structurally characterized, including the recently neutral titanium(IV) species Ti(N(TMS)$_2$)$_3$(X) (X = F, Cl, Me).[96-98] The substantial difference between the ionic radii of tetravalent cerium and titanium certainly suggests that the cerium alkoxide tris(amide) be expected to be a reasonable target. The failure of the cerium(IV) trialkoxide amide to form is believed to simply be the result of steric crowding in the bisalkoxide bisamide not permitting the requisite interaction between the incoming nucleophile and the metal center. The additional bulk due to the *tertiary*-butoxide ligands in **1** is likely the determining factor in this respect, whereas the smaller metal center of the difluoride Ti(N(TMS)$_2$)$_2$(F)$_2$ remains accessible. Furthermore, the absence of ligand redistribution processes in (^{t}BuO)$_2$Ce(N(TMS)$_2$)$_2$ (**1**) is more an indication of the stability of the bisalkoxide bisamide nucleus, rather than the instability of the triamide complex. Such a phenomenon is exemplified in the related species Cp$_2$Ce(O^{t}Bu)$_2$ and Cp$_3$Ce(O^{t}Bu) which are known not to interconvert.[50] Though the bulk of the bis(trimethylsilyl)amide ligand may inhibit a further study of the factors contributing to the cerium-oxygen bond cleavage process, it is likely extremely important to the thermodynamic stability of (^{t}BuO)$_2$Ce(N(TMS)$_2$)$_2$ (*vide infra*).

The presence of a single alkoxide in the coordination sphere is known to offer considerable thermodynamic stability to high oxidation state metal centers in seemingly destabilizing ligand environments.[50,51] However, it is apparent from a comparison of this and previous investigations into systems incorporating alkoxide, nitrate and cyclopentadienyl ligands that such reactions generate a high proportion of the bisalkoxide species, presumably by way of facile redistribution processes.[50] For the purpose of the present study, with the need for the flexibility offered by two accessible valence sites and the apparent structural stability offered by the bis-*tertiary*-butoxide framework, the bisalkoxide bisnitrate complex (^{t}BuO)$_2$Ce(NO$_3$)$_2$(THF)$_2$ was deemed the best choice for a precursor in an investigation into the amide chemistry of cerium(IV).

Studies Toward the Preparation and Characterization of Cerium(IV) Bisamide Complexes. Primary Amides. All of the efforts so far directed towards the preparation of cerium(IV) complexes of primary amides have resulted in rapid decomposition of the starting materials and reduction of the metal center (eq 6). Following the successful preparation of first simple cerium(IV) bisamide complex, $(^tBuO)_2Ce(N(TMS)_2)_2$ (**1**), it remains unclear as to whether

$$(^tBuO)_2Ce(NO_3)_2(THF)_2 \xrightarrow[R = \text{alkyl, aryl}]{\geq 1\text{ eq LiNHR}} \xrightarrow{[H]} Ce^{III} \qquad (6)$$

the instability of complexes of the type $(^tBuO)_2Ce(NHR)_2$ derives from the presence of the residual amide proton, or is simply due to the reducing nature of such extremely nucleophilic substrates.[84]

As earlier work with cyclopentadienyl species has demonstrated,[50] cerium(IV) complexes are prone to facile ligand redistribution processes, a typical mode of reactivity observed among the lanthanides.[8] Studies into other cerium(IV) amide systems further emphasizes the possibility that redistribution of either $(^tBuO)_2Ce(NHR)_2$, or its immediate precursor $(^tBuO)_2Ce(NO_3)(NHR)$ may be responsible for the subsequent redox chemistry observed (*vide infra*).

Dialkyl and Diaryl Amides. Similarly to the studies with primary amides, reduction of the cerium(IV) metal center has so far hampered all attempts to incorporate dialkyl or diaryl amides in the cerium(IV) coordination sphere. Although the presence of the residual *N*-proton in primary amides may

$$(^tBuO)_2Ce(NO_3)_2(THF)_2 \xrightarrow[R^1, R^2 = \text{alkyl, aryl}]{\geq 1\text{ eq LiNR}^1R^2} \xrightarrow{[H]} Ce^{III} \qquad (7)$$

provide additional pathways for decomposition of such complexes,[86] it is clear that this is not the primary cause of redox chemistry. Rather, a combination of the reducing nature of simple alkyl and aryl amides, and the ease with which these species form free radicals is believed to be responsible for the observed reduction pathways.[99]

Silicon Stabilized Amides. In order to prepare stable lanthanide species it is important to both employ bulk to fill-up the coordination sphere of the metal center and prohibit access to incoming species. However, it is evident that the reducing nature of the specific amide ligands plays an important role in stabilization of the complexes of cerium(IV). This phenomenom has been clearly exemplified in studies with differentially substituted cyclopentadienyl ligands. Although the biscyclopentadienyl complexes $Cp_2Ce(O^tBu)_2$ and $Cp_3Ce(O^tBu)$ are perfectly stable, isolable species, attempts to prepare the pentamethylcyclopentadienyl analogs of these complexes simply resulted in reduction of the high oxidation state metal center and the formation of organic oxidation products.[50] Given the oxidizing nature of the tetravalent lanthanide it is perhaps not surprising that the strongly reducing permethylated cyclopentadienyl framework should have this effect.

The above are also foremost considerations in the preparation of cerium(IV) amide derivatives, since it is clear that the tetravalent lanthanide is unstable both in the presence of extremely basic substrates, or those with a ready tendency to undergo facile oxidation. These apparent barriers to stability are alleviated somewhat with the use of considerably less basic silicon substituted amide ligands,[84,100,101] which have enabled the preparation of a range of differentially substituted cerium(IV) amide species.

Hexamethyldisilazide. Preparation of $(^tBuO)_2Ce(N(TMS)_2)_2$ (1). Unlike the almost colorless mixtures of reduction products generated from the reactions of alkyl or aryl amides with $(^tBuO)_2Ce(NO_3)_2(THF)_2$ in hydrocarbon solvents, the addition of two equivalents of lithium hexamethylsilazide ($LiN(TMS)_2$ (TMS = trimethylsilyl)) to this precursor complex results in the instantaneous formation of a deep red suspension (eq 8). This reaction proceeds equally well

$$(^tBuO)_2Ce(NO_3)_2(THF)_2 \xrightarrow[\text{Hexane, RT, 5 min}]{2LiN(TMS)_2} \underset{\mathbf{1}}{(^tBuO)_2Ce(N(TMS)_2)_2} \quad (8)$$

$$- 2LiNO_3, -2THF$$

with the equivalent sodium amide, however, the lithium reagent is more employed because of its increased solubility in hydrocarbon solvents and its ease of preparation. No further changes in the product mixture are observed

with extended reaction times, and after removing by-product salts the desired bisalkoxide bisamide complex $(^tBuO)_2Ce(N(TMS)_2)_2$ (**1**) may be obtained as an orange-red solid in near quantitative yield (≥ 90% isolated yield; ≈ 95% pure by ^1H NMR). This reaction proceeds without the formation of significant quantities of side-products. Analytically pure **1** may be obtained with recrystallization from a highly concentrated pentane solution upon cooling to -40 °C. Red crystals suitable for X-ray crystallographic analysis were grown upon cooling a concentrated solution of the bisamide in hexamethyldisiloxane (TMS_2O), to -40 °C. The bis(amide) complex is extremely air sensitive, decomposing after just a few seconds in air to a pale yellow residue. As expected, the diamagnetic NMR spectra of **1** are extremely simple, since the complex demonstrates a high degree of symmetry both in solution and the solid state. Coordination of the amide ligands to the metal center does not dramatically effect the chemical shift of the *tertiary*-butoxide methyl protons from that observed in the precursor or the related biscyclopentadienyl analog (^1H, C_6D_6 $(^tBuO)_2Ce(N(TMS)_2)_2$ (**1**) δ 1.34, $(^tBuO)_2Ce(NO_3)_2(THF)_2$ δ 1.2, $Cp_2Ce(O^tBu)_2$ δ 1.26). The presence of a cerium(IV) amide is clearly evidenced by the down-field shift of the amide trimethylsilyl resonances following transmetallation (^1H, C_6D_6 $(^tBuO)_2Ce(N(TMS)_2)_2$ (**1**); δ 0.43, $LiN(TMS)_2$ δ 0.21).

The addition of a clear excess of the bis(trimethylsilyl)amide (≥ 4 equiv) to the alkoxide nitrate precursor, produces **1** and unreacted $LiN(TMS)_2(THF)_x$ and is an indication of the stability of the bisalkoxide bisamide complex (eq 9). There is no evidence to support formation of the tris- or

$$(^tBuO)_2Ce(NO_3)_2(THF)_2 \xrightarrow[\text{Hexane,}]{\geq 4LiN(TMS)_2} \begin{array}{c}(^tBuO)_2Ce(N(TMS)_2)_2\\ + \\ LiN(TMS)_2(THF)_x\end{array} \qquad (9)$$

tetrakisamide analogs of **1**. This is, however, contrary to the known chemistry of the *tertiary*-butoxide systems. The addition of successive equivalents of sodium *tertiary*-butoxide to any of the known alkoxide nitrate complexes results in the formation of higher order, sometimes polynuclear cerate derivatives (Scheme 9).

Scheme 9

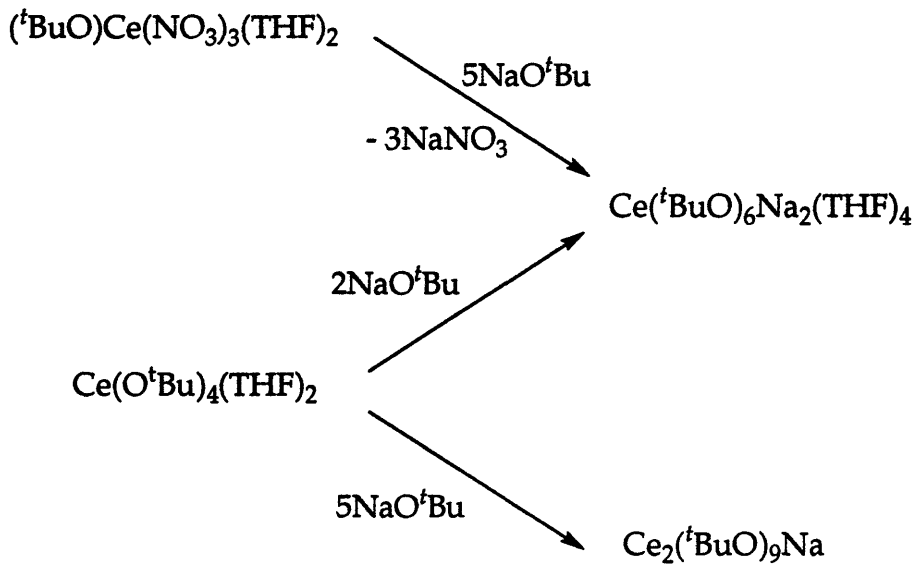

Evans, **1989**

Crystallographic analysis of $Ce_2(O^tBu)_9Na$ {$Ce_2(O^tBu)_4(\mu\text{-}O^tBu)_3(\mu_3\text{-}O^tBu)_2Na$} and $Ce(O^tBu)_6Na_2(DME)_2$ {$Ce(O^tBu)_2(\mu\text{-}O^tBu)_2(\mu_3\text{-}O^tBu)_2Na(DME)_2$} (DME = 1, 2-dimethoxyethane) reveals that multiply bridging alkoxides ligands are required in order to sustain the integrity of these complexes.[54] Although bulky primary silylamide ligands (e.g. μ-$NHSiR_3$ (R = Et, Ph) in $[Me_2AlN(H)SiR_3]_2$)[102] are known to form bridging ligands, it remains questionable as to whether the bis(trimethylsilyl)amide ligand is able to accommodate such moieties in a complex in which the amide to cerium ratio is greater than two to one.

Solid State Structure of (^{t}BuO)$_2$Ce(N(TMS)$_2$)$_2$ (1). The crystal structure of **1** reflects the preferred coordination mode of the bulky bis(trimethylsilyl)amide moiety (Figures 1-2; Appendices 4.1, 4.3-4.5). In the solid state, (^{t}BuO)$_2$Ce(N(TMS)$_2$)$_2$ adopts a pseudo-tetrahedral geometry, in which the pairs of alkoxide and amide ligands are related by a plane of symmetry running through the metal center. Hexamethyldisilazide is known to be very effective ligand in stabilizing metal centers in low coordination environments. The complex demonstrates no tendency to obtain additional stabilization form agostic interactions, as is observed tobe the case in the trivalent bis(trimethylsilyl)amide derivative $Cp^*_2YN(TMS)_2$.[103]

Figure 1. ORTEP Plot and Space-filling Diagram of $(^{t}BuO)_2Ce(N(TMS)_2)_2$ (1)

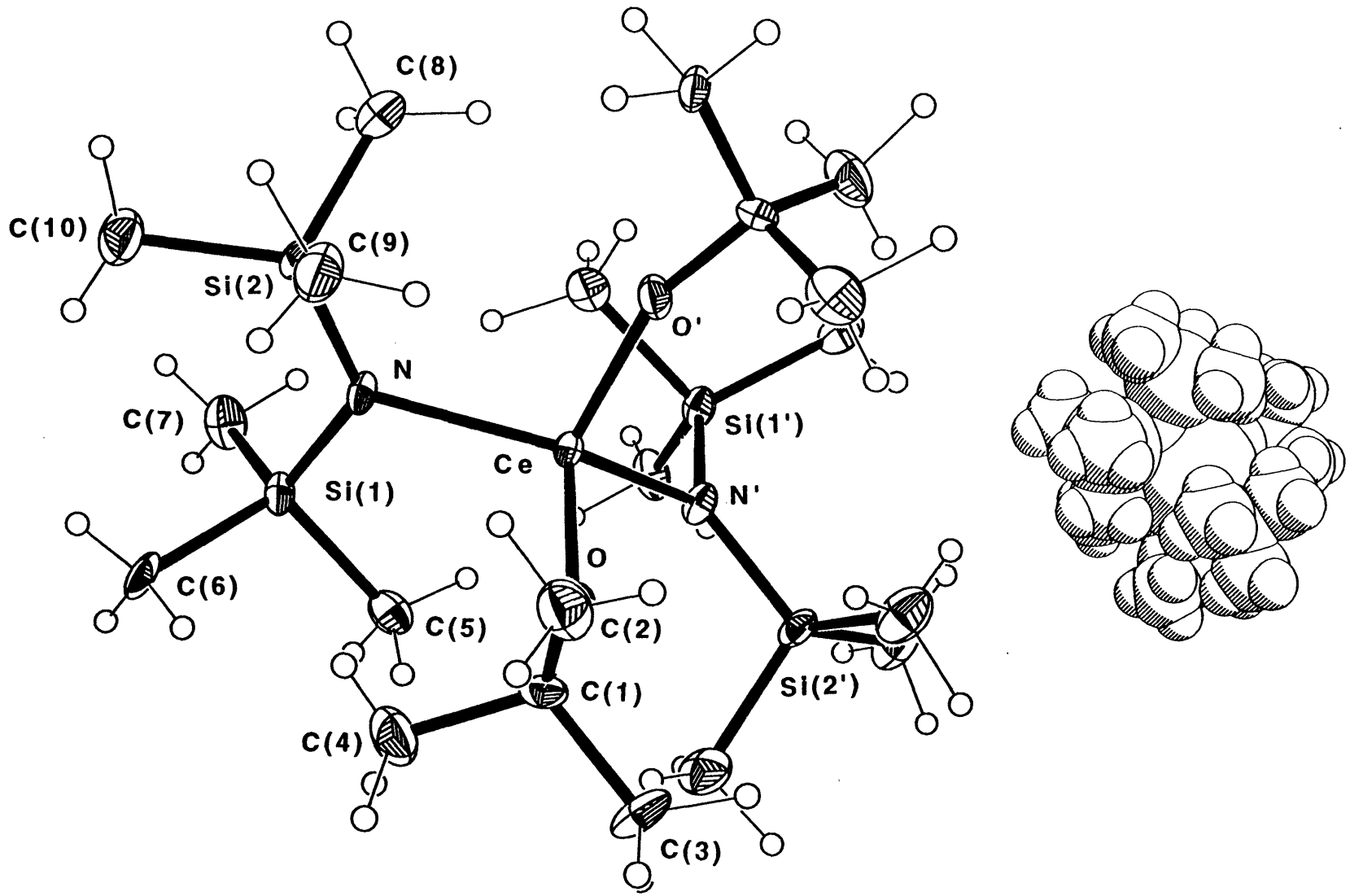

Figure 2. Selected Bond Distances and Angles for $(^tBuO)_2Ce(N(TMS)_2)_2$ (1)

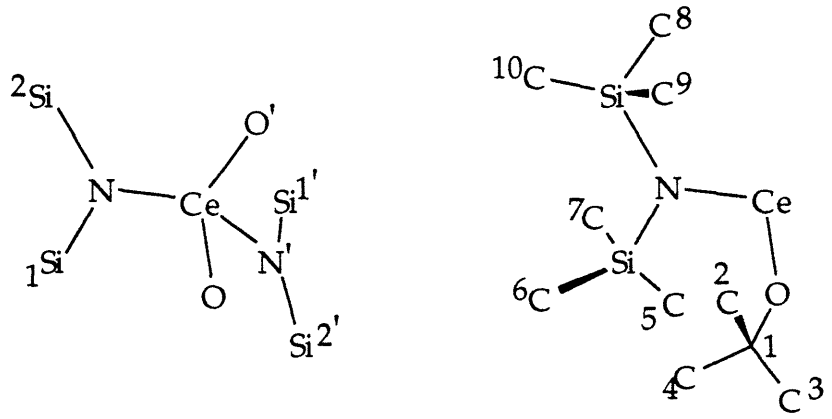

Bond Lengths (Å)

Ce	N	2.260(7)	Si(1)	C(6)	1.868(10)
Ce	N'	2.260(7)	Si(1)	C(7)	1.852(10)
Ce	O	2.052(6)	Si(2)	C(8)	1.866(11)
Ce	O'	2.052(6)	Si(2)	C(9)	1.871(11)
N	Si(1)	1.708(7)	Si(2)	C(10)	1.867(11)
N	Si(2)	1.744(7)	C(1)	C(2)	1.503(14)
O	C(1)	1.431(11)	C(1)	C(3)	1.517(13)
Si(1)	C(5)	1.874(11)	C(1)	C(4)	1.517(14)

Bond Angles (deg)

N	Ce	N'	128.1(4)	N	Si(1)	C(5)	106.0(4)
N	Ce	O	106.4(2)	N	Si(1)	C(6)	115.5(4)
N	Ce	O'	104.5(2)	N	Si(1)	C(7)	112.7(4)
O	Ce	O'	105.3(3)	C(5)	Si(1)	C(6)	106.8(5)
Ce	N	Si(1)	114.3(3)	C(5)	Si(1)	C(7)	107.1(5)
Ce	N	Si(2)	120.0(4)	C(6)	Si(1)	C(7)	108.3(5)
Si(1)	N	Si(2)	125.3(4)	N	Si(2)	C(8)	109.7(4)
Ce	O	C(1)	159.9(5)	N	Si(2)	C(9)	109.5(4)

The amide linkages in **1** represent the shortest Ce^{IV}-N interactions observed to date (Ce-N = 2.26(7) Å), which is as expected, since the bialkoxide bisamide derivative represents the first example of a simple cerium(IV) amide. The only prior examples of complexes containing cerium(IV)-nitrogen bonding have been those of dianionic phthalocyanine and/or porphyrin ligands, and neutral Lewis bases. The bulk and aromaticity of such macrocylicic sandwich complexes leads to significantly longer Ce-N interactions (2.41-2.79 Å),[60-63] whereas neutral amine[59] and imine[64,65] donor interactions are typically expected to be weaker than that of an amide interaction (2.56-2.79 Å). The Ce-O bond lengths in the terminal *tertiary*-butoxide ligands of **1** are unexceptional at 2.052(6) Å.[50,54,57,59] The majority of similar systems also accommodate solvent molecules into the coordination sphere.[52,54-59,64,65] The stability of the unsolvated bisamide complex $(^{t}BuO)_2Ce(N(TMS)_2)_2$, however, indicates coordinative saturation, and hence stability, on the part of the lanthanide center. Although not linear, the lanthanide-oxygen-carbon bond angles are typically highly obtuse (Ce-O-C(1) 159.9(5)°).[50,54] Notwithstanding the bulk of the ligand environment, the nitrogen atoms are held planar as is expected in silicon stabilized amide complexes.[101] The effects of the trimethylsilyl substituted amide groups are seen in the geometry of the four ligands about the metal center, which is distorted away from tetrahedral. The N-Ce-O and O-Ce-O bond angles remain approximately tetrahedral (104.5(2)-106.4(2)°), while the N-Ce-N angle is deformed significantly (128.1(4)°) (Figure 3).

Figure 3

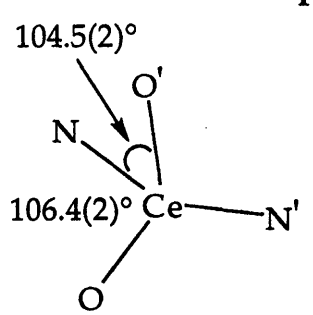

∠ N-Ce-N' = 128.1(4)°
∠ O-Ce-O' = 105.3(3)°

***N*-(Trimethylsilyl) Anilides.** It has been determined that stable tetravalent cerium amide complexes may also be prepared from judiciously substituted derivatives of *N*-(trimethylsilyl) aniline. The trimethyl substitutent serves both to increase the bulk and decrease the basicity of the ligand environment ultimately serving to reduce the likelihood of redox chemistry

The reaction between two equivalents of the *N*-trimethylsilylated amide $LiN(TMS)C_6H_5$ and the cerium(IV) precursor $(^tBuO)_2Ce(NO_3)_2(THF)_2$ yields a complex tentatively identified as the bisamide species $(^tBuO)_2Ce(N(TMS)C_6H_5)_2$ (eq 10). It is clear from the ^1H NMR spectrum that

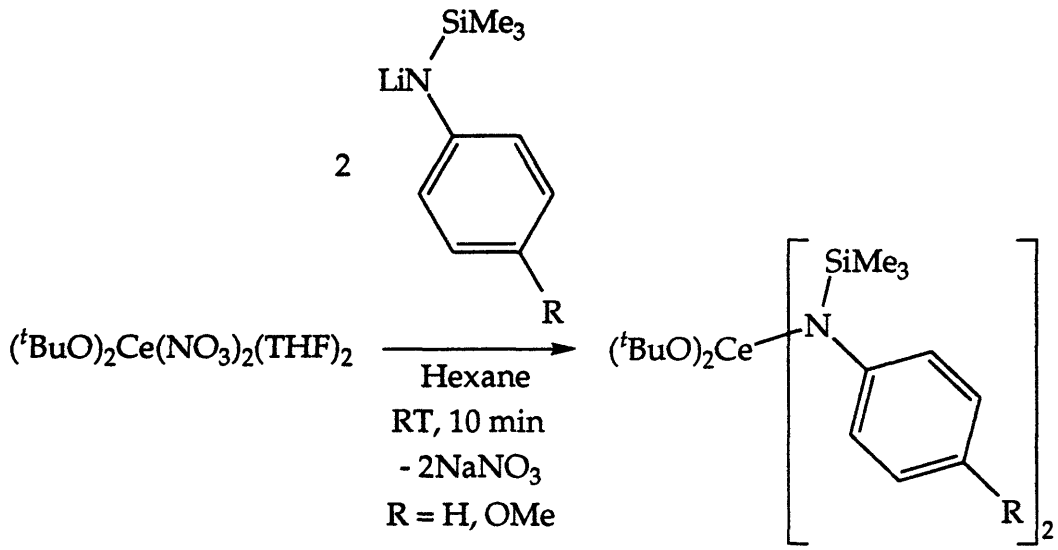

(10)

this complex is the major product, but that significant quantities of as yet unidentified impurities are also present in the reaction mixture. In line with the chemistry of the 2, 6-diisopropylaniline analog (cf. **3** (*vide infra*)), it is not unreasonable to expect that one such impurity is the trialkoxide amide $(^tBuO)_3Ce(N(TMS)Ph)$. The low yield of conversion and the high solubility of the product has so far precluded the isolation and further characterization of this species. An attempt has been made to prepare of a more crystalline analog of this complex, but isolation and characterization of the *para*-anisidine (*para*-anisidine = 4-methoxyaniline) derivative $(^tBuO)_2Ce(N(TMS)(p\text{-}MeOC_6H_4)_2$ has proven equally problematical (eq 10).

***N*-(Trimethylsilyl)-*ortho*-Anisidine. Preparation of $(^tBuO)_2Ce(N(TMS)(o\text{-}MeOC_6H_4))_2$ (2).** Whereas the inclusion of the methoxy substituent of *para*-anisidine does not offer considerable improvement over the use of the parent

anilide in attempts to synthesize isolable bisamide derivatives, the use of the *ortho*-anisidine isomer not only leads to the clean preparation of a readily isolated bisamide species, but the methoxy oxygen atoms also coordinate the metal center. As per the preparation of **1**, the reaction between two equivalents of the lithium anilide derivative LiN(TMS)(*o*-$MeOC_6H_4$) and the cerium(IV) source $(^tBuO)_2Ce(NO_3)_2(THF)_2$ in pentane results in the immediate formation of a dark purple suspension, containing the bisamide complex $(^tBuO)_2Ce(N(TMS)(o\text{-}MeOC_6H_4))_2$ (**2**) (eq 11). After only a few minutes, the reaction is observed to undergo no further change. The desired

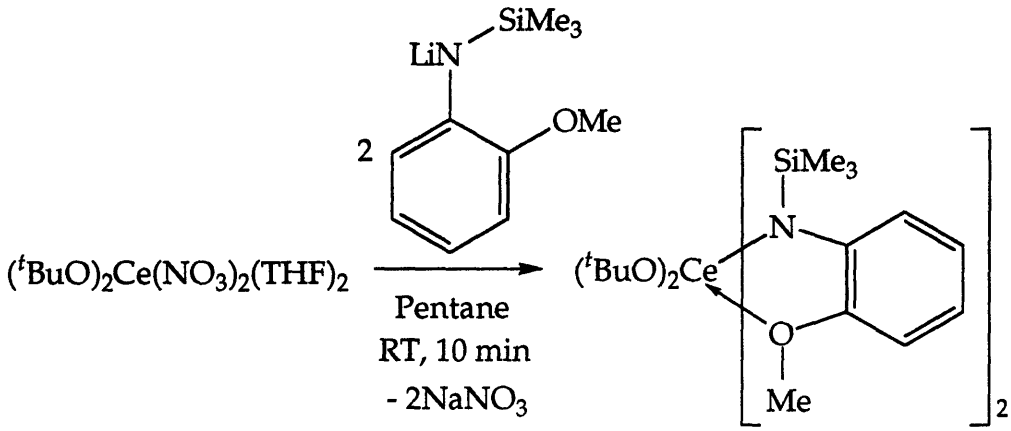

(11)

2

product is isolated as a dark solid. Pure crystalline purple **2** may be obtained in moderate yield (31%) by recrystallization of the isolated solid from a hot concentrated solution in TMS_2O. As is the case for **1**, the presence of a cerium(IV)-nitrogen bond is clearly indicated in the ^1H NMR spectrum by the low-field chemical shift of the trimethylsilyl protons (δ 0.63; **1** δ 0.43). Again, the singlet resonance of the bis-*tertiary*-butoxide framework does not prove useful for the purposes of structural elucidation. Likewise, from simple solution spectra alone it is not possible to determine if the *ortho*-anisidine moieties adopt a monodentate coordination mode, or whether the ligands also chelate by way of a methoxy oxygen donor interaction.

Though mass balance from starting materials to products is high (≈ 93%), the ^1H NMR spectrum of the crude product reveals that conversion to the bisamide **2** occurs only to the extent of 65-70%. The presence of additional low-field trimethylsilyl resonances in the ^1H NMR spectrum of the product mixture seemingly indicates the presence of redistribution products; such

processes have been observed to be facile amongst transiently stable monoamide nitrate intermediates (*vide infra*). Conversely, as in the synthesis of **1**, there is no evidence to suggest formation of a significant quantity of the triamide species (^{t}BuO)Ce(N(TMS)(*o*-MeOC$_6$H$_4$)$_3$ (cf. **3**). The observed low-percentage conversion to **2** appears to be a general concern for the preparation of aniline-derived cerium(IV) species, whereas the synthetic route to **1** is extremely clean, generating the bis(trimethylsilyl)amide as the sole reaction product, in high yield.

Solid State Structure of (^{t}BuO)$_2$Ce(N(TMS)(*o*-MeOC$_6$H$_4$))$_2$ (2). Methoxy-cerium donor interactions prove to be a prominent feature of the solid state structure of **2** (Figures 4 and 5; Appendices 4.1, 4.6-4.8). X-ray crystallographical analysis of the complex shows the presence of a distorted octahedral environment about the metal center as a result of cerium-methoxy chelation (Figure 3). Given the oxophilicity of cerium(IV) it is highly

Figure 3

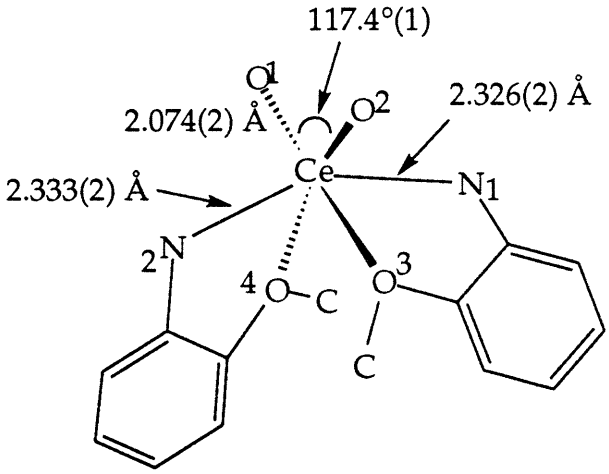

Ce-O(2) = 2.073(2) Å

Ce-O(3) = 2.567(2) Å
Ce-O(4) = 2.564(2) Å

∠ N(1-Ce-N(2) = 135.9°(1)

∠ N(1)-Ce-O(3) = 65.7°(1)
∠ N(2)-Ce-O(4) = 65.4°(1)

unlikely that the methoxy groups chelate chelate in the solid state but not in solution. As expected for the hexacoordinate metal center, the cerium-nitrogen bond lengths (Ce-N(ave) = 2.330(2) Å), are somewhat longer than for tetracoordinate **1** (Ce-N = 2.26(7) Å), though there is no obvious effect on the cerium-alkoxide bond lengths.

Figure 4. ORTEP Plot of $(^{t}BuO)_2Ce(N(TMS)(o\text{-}MeOC_6H_4))_2$ (2)

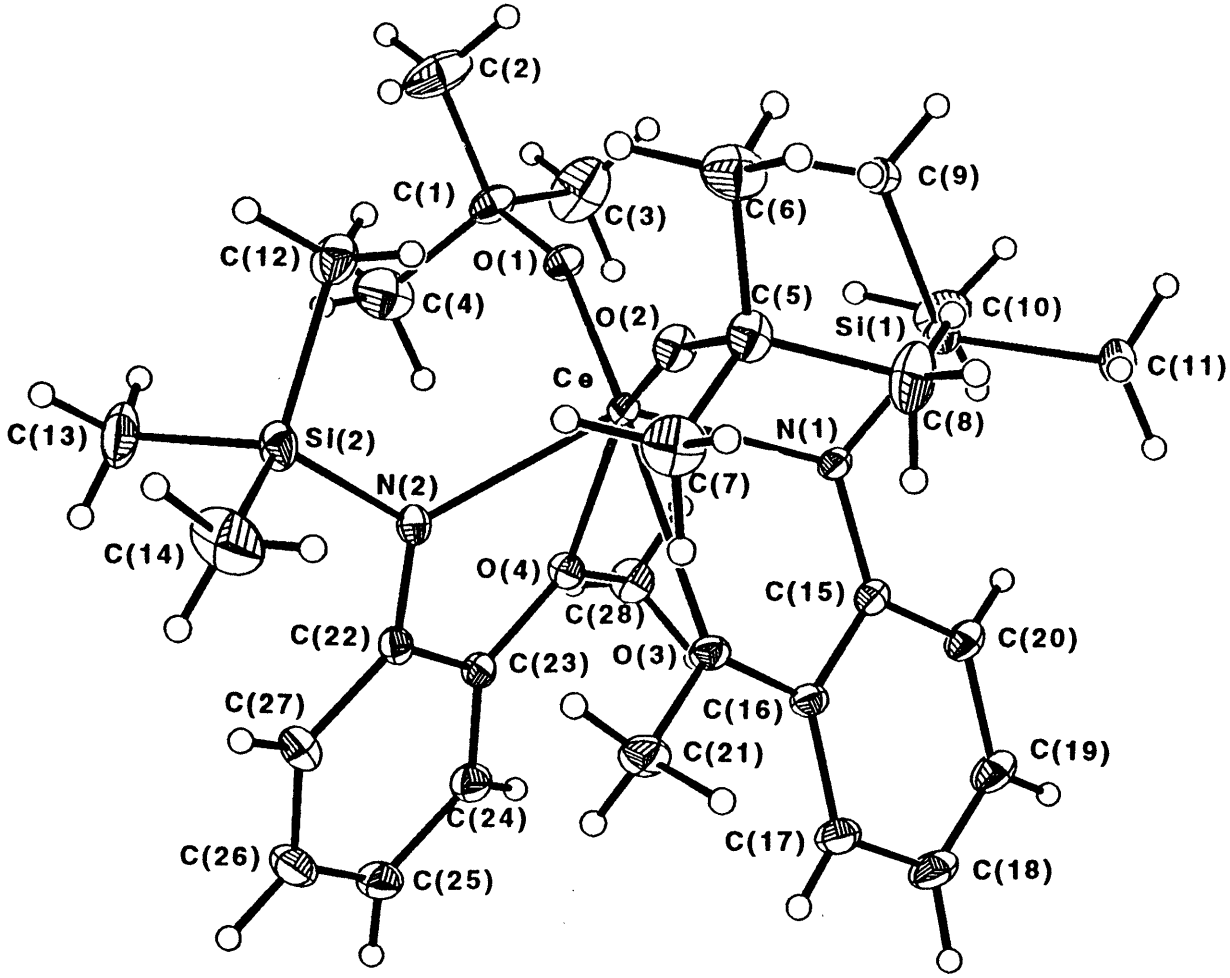

Figure 5. Selected Bond Distances and Angles for (^{t}BuO)$_2$Ce(N(TMS)(*o*-MeOC$_6$H$_4$))$_2$ (2)

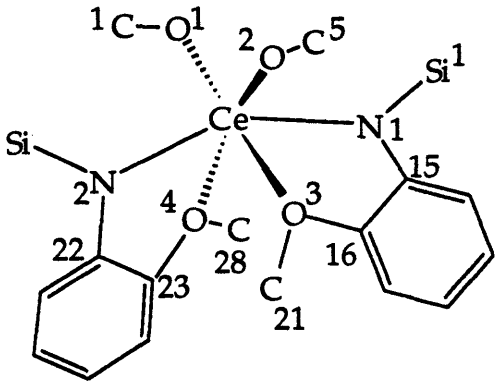

Bond Lengths (Å)					
			Ce	N(1)	2.326(2)
			Ce	N(2)	2.333(2)
			Ce	O(1)	2.074(2)
			Ce	O(2)	2.073(2)
			Ce	O(3)	2.567(2)
			Ce	O(4)	2.564(2)
N(1)	Si(1)	1.736(2)	O(2)	C(5)	1.430(3)
N(2)	Si(2)	1.737(3)	O(3)	C(16)	1.396(4)
N(1)	C(15)	1.394(3)	O(3)	C(21)	1.439(3)
N(2)	C(22)	1.383(3)	O(4)	C(23)	1.385(2)
O(1)	C(1)	1.429(3)	O(4)	C(28)	1.440(3)

Bond Angles							
N(1)	Ce	N(2)	135.9(1)	Ce	N(1)	Si(1)	118.8(1)
N(1)	Ce	O(1)	102.1(1)	Ce	N(1)	C(15)	120.0(1)
N(1)	Ce	O(2)	101.1(1)	Si(1)	N(1)	C(15)	121.1(2)
N(1)	Ce	O(3)	65.7(1)	Ce	N(2)	Si(2)	118.1(1)
N(1)	Ce	O(4)	78.3(1)	Ce	N(2)	C(22)	119.7(2)
N(2)	Ce	O(1)	99.7(1)	Si(2)	N(2)	C(22)	122.2(1)
N(2)	Ce	O(2)	102.1(1)	Ce	O(1)	C(1)	159.1(1)
N(2)	Ce	O(3)	79.0(1)	Ce	O(2)	C(5)	161.9(2)
N(2)	Ce	O(4)	65.4(1)	Ce	O(3)	C(16)	114.4(1)
O(1)	Ce	O(2)	117.4(1)	Ce	O(3)	C(21)	127.1(2)
O(1)	Ce	O(3)	155.9(1)	C(16)	O(3)	C(21)	117.2(2)
O(1)	Ce	O(4)	86.3(1)	Ce	O(4)	C(28)	127.0(1)
O(2)	Ce	O(3)	86.1(1)	Ce	O(4)	C(23)	114.4(1)
O(2)	Ce	O(4)	155.5(1)	C(23)	O(4)	C(28)	117.2(2)
O(3)	Ce	O(4)	71.1(1)				

Although the stabilizing influence of a second trimethylsilyl group is absent, the planarity of the amide nitrogen atoms is preserved by incorporation into the five-membered chelate ring. The cerium(IV) akoxide bonding interactions (Ce-O(ave) = 2.074 Å) in this hexacoordinate species are slightly longer than those observed in **1** (Ce-O(ave) = 2.052(6) Å), with the angles about the *tertiary*-butoxide oxygen atom almost identical (Ce-O-C(ave): **2**, 160.5(2)°; **1**, 159.9(5)). The 'wedge' of the alkoxide ligand framework differs considerably between the two structures, however, actually proving to be more obtuse in the octahedral species (O-Ce-O: **2**, 117.4(1)°; **1**, 105.3(3)°). This is contrary to that which would be expected for the more congested metal center. The combined observations of the respective cerium-oxygen bond lengths and this 'wedge' angle clearly indicates that although the metal center is subject to a greater degree of coordinative saturation in the anisidine derivative, the bis(hexamethyldisilazide) ligand set proves more sterically encumbering. The physical inability of **1** to react with additional equivalents of amide reagents or to undergo redistribution processes is therefore believed to be responsible for the increased stability over **2** and other smaller bis(anilide) analogs. Bonding distances of the cerium-oxygen coordinative interactions are comparable (Ce-O(ave) = 2.566(2) Å) to those determined in related six-coordinate cerium(IV) species.[54,57] These coordinative distances are surprisingly[104] slightly longer than the cerium-THF interactions observed in the trivalent cerium species $Ce(OSiPh_3)_3(THF)_3$,[56] presumably owing to differences in both the steric demands of the ligand set and the basicities of the donor oxygen atoms. Both the amide-amide and alkoxide-alkoxide angles (N(1)-Ce-N(1) = 135.9(1)°; O(1)-Ce-O(2) = 117.4(1)°) observed in $(^tBuO)_2Ce(N(TMS)(o\text{-}MeOC_6H_4))_2$ (**2**) are more obtuse than those than of $(^tBuO)_2Ce(N(TMS)_2)_2$ (**1**) (N-Ce-N = 128.1(4)°; O-Ce-O = 105.3(3)°). Conversely, the distance between the *tertiary*-butoxide oxygen atoms might be expected to decrease as the coordination number of the metal center increases, which is contrary to that which is observed upon moving from **1** to **2**. This phenomenom may be simply be a result of the bulk of the ligand set of **1**, although tying-back of the silyl group by chelation of the silyl-aryl ligands in **2** certainly serves to reduce intramolecular repulsions (TMS-OMe, TMS-O^{t}Bu) and open-up the coordination sphere in the proximity of the alkoxides.

***N*-(Trimethylsilyl)-2, 6-Diisopropylanilide.** Reactions with the bulky *N*-trimethylsilyl-2, 6-diisopropylanilide (TMSDIPA) ligand affords considerably different products to those which have been observed to form with other anilide derivatives. This is not to say that the reaction pathways of the TMSDIPA ligands are fundamentally different than those of smaller amide moieties, but rather that this sterically demanding ligand injects a degree of stability which allows for the isolation of species which are apparently otherwise subject to decomposition. The majority of the chemistry of this particular system has been studied in attempts to prepare stable cerium(IV) monoamide species of the type $(^tBuO)_2Ce(NR_2)(X)$ ($X = NO_3$, OSO_2CF_3). However, it is clear from efforts made so far to prepare a bis(alkoxide) bis(amide) complex of the TMSDIPA ligand that the desired product is not the major species formed under the conditions employed. Instead, the primary reaction product is observed to be the rearrangement product $(^tBuO)_3Ce(N(TMS)(2, 6\text{-}^iPr_2C_6H_3))$ (**3**). There are indications that other stable cerium(IV) amide species are produced in the reaction mixture in low yield and although complexity of the product mixture precludes positive identification, it is not unreasonable to expect that one of the products is the sterically encumbered bisalkoxide bisamide derivative $(^tBuO)_2Ce(2, 6\text{-}^iPr_2NC_6H_3)_2$. The existence of other cerium(IV) bonded amide species is demonstrated in the ^1H NMR spectrum by the presence of low-field trimethylsilyl resonances (^1H, C_6D_6 δ 0.41, 0.40, 0.32).

***N*-(Trimethylsilyl)-2-Methoxyethylamide.** In contast with earlier studies on primary and dialkyl amines, judiciously substituted aliphatic amines also appear to be viable substrates for the preparation of cerium(IV) amide complexes. The product of the reaction between the cerium precursor and two equivalents of the lithium silyl-alkyl amide $LiN(TMS)CH_2CH_2OMe$ in hexane yields several products, the major species of which is believed to be the bisamide derivative $(^tBuO)_2Ce(N(TMS)CH_2CH_2OMe)_2$ (eq 12). In the ^1H NMR spectrum, clear singlet resonances are observed which correspond to the trimethylsilyl (^1H, C_6D_6 δ 0.36, 18H), *tertiary*-butoxide (δ 1.42, 18H) and methoxy (δ 3.35, 6H) methyl groups, with integral ratios as expected for the bisamide complex. Identification of the corresponding methylene resonances is less obvious in the spectrum of the impure product.

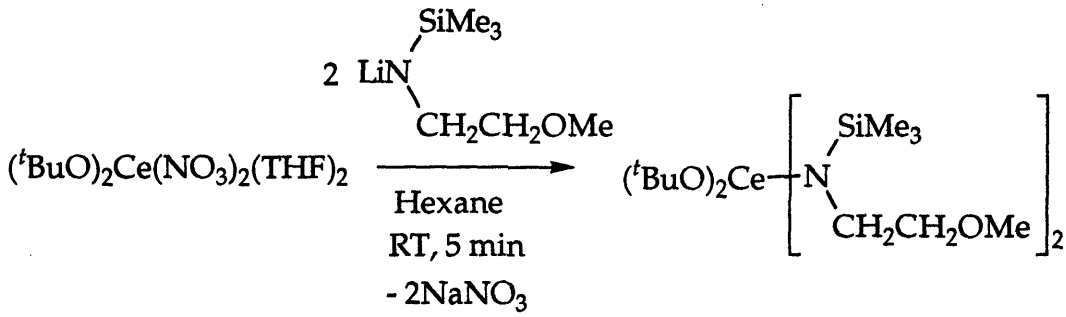

(12)

From a comparison of the integral due to the *tertiary*-butoxide containing products it is clear that the complex comprises at most half of the material generated during the course of the reaction. Paramagnetic cerium(III) species also account for a significant quantity of the products. Furthermore, the major product identified as the bisamide undergoes complete decomposition, to an unidentifiable product mixture, after extended periods (≈ 48 h, RT) without isolation from the reaction mixture. This observation would seem to indicate that either the complex is a kinetic product, or that the *N*-trimethylsilylated methoxyethylamide ligands offers only limited stabilization with respect to redox chemistry and/or ligand redistribution processes (*vide infra*). The absence of multiplet signals for the ethanolamine derived methylene resonances seemingly confirms this, since a rigid chelate species might be expected to exhibit a diastereotopic ethylene moieties. Thus, the amide ligands are either bonded to the metal center in a monodentate fashion, or the methoxy donor interaction is fluctional on the NMR timescale. Either eventuality, however, is a likely cause of decomposition. Nonetheless, the generation of an observable cerium(IV) alkylamide complex, whatever the exact molecular structure, is somewhat of an accomplishment, given the facile nature with which redox chemistry occurs in other alkyl amine systems. The decreased reducing tendency of *N*-silylated amides relative to dialkyl or diaryl analogs is most certainly the primary contributing factor in stabilizing high oxidation state species. However, the importance of chelation of the pendant ether cannot be disregarded and especially since intramolecular coordination of the considerably less basic anisole derivative plays such an important role in determining product stability in **2** (Figure 6) (*vide supra*).

Figure 6

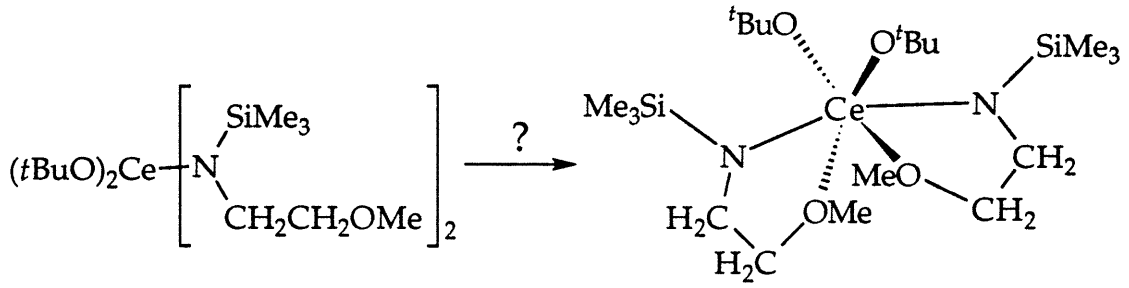

The Preparation and Characterization of Cerium(IV) Monoamide Complexes. The Reaction of $(^tBuO)_2Ce(NO_3)_2(THF)_2$ with Lithium Amides LiN(TMS)R (R ≠ 2, 6-^{i}Pr$_2$C$_6$H$_3$). All efforts so far directed towards the synthesis of monoamide analogs of known bisalkoxide bisamide complexes have resulted in decomposition of the cerium(IV) precursor and reduction of the metal center (eq 13). This is somewhat surprising given that monamide nitrate complexes of the type $(^tBuO)_2Ce(N(TMS)R)(NO_3)$ (R = *o*-MeOC$_6$H$_4$, TMS) are obvious intermediates *en route* to the formation of stable bisamide species.

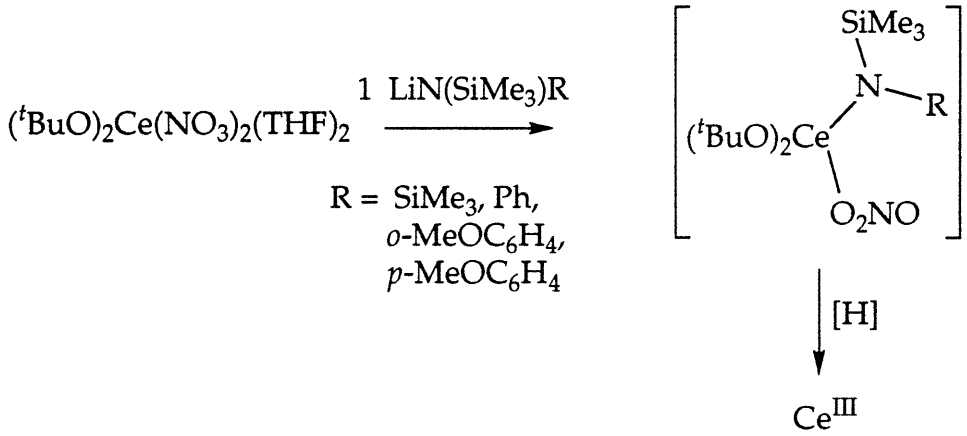

(13)

There are three major arguments which may be employed to explain the observed decomposition processes: (i) intrinsic stability: ligand redistribution reactions and intramolecular chemistry; (ii) ligand incompatibility; (iii) additional Lewis base stabilization. The ionic nature of the bonding in lanthanide complexes is such that ligand redistribution processes are extremely facile.[8] Redistribution induced decomposition pathways appear to be a major contributing factor behind the reactivity patterns observed for systems involving the TMSDIPA ligand (*vide infra*) (e.g., eq 13). As is hoped, as one of the goals of this study, it is not

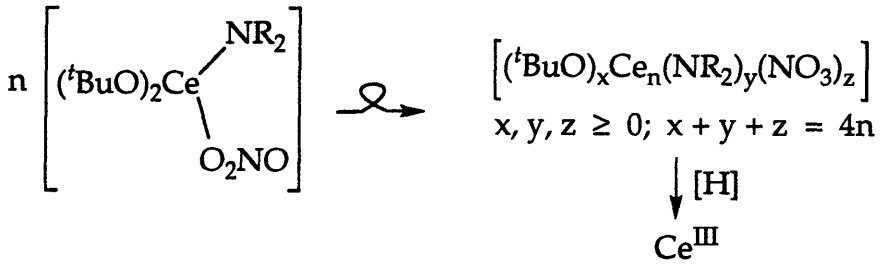

(13)

inconceivable that complexes of this type react in an intramolecular fashion to desilylate the amide nitrogen with concomitant elimination of the residual nitrate equivalent (e.g., eq 14). Similar strategies have been employed

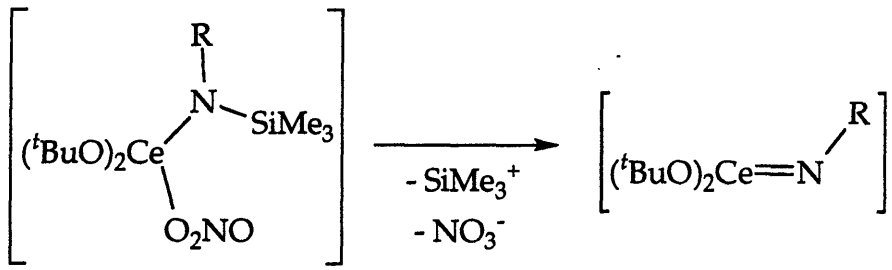

(14)

effectively in the preparation of group 4 imide derivatives.[72,78] Though monoamide intermediates with silylated substrates are considered to be at least transiently stable, lifetimes of analogous primary, dialkyl and diaryl amide derived species are fleeting at best. Since there is no indication that the high oxidation state cerium center is at all stable in the presence of highly reducing ligands, it is seemingly much more likely that the redox chemistry of these systems derives from an immediate interaction with the cerium(IV) the precursor complex (e.g., eq 15).

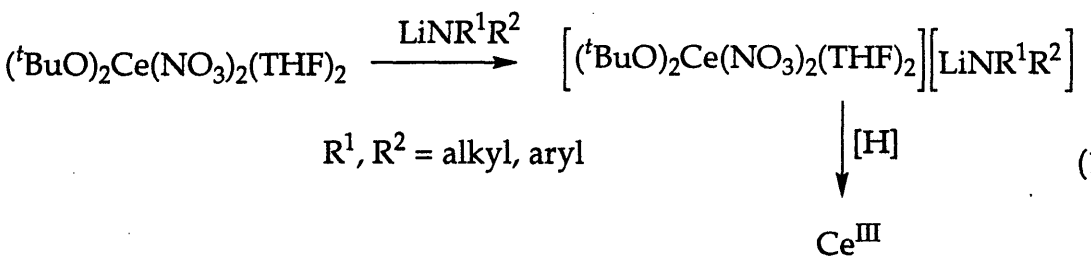

(15)

Recent advances in the synthesis of isolable Lewis base adducts of transition metal complexes of high energy organic substrates serve to illustrate that extremely reactive species can be stabilized and sequestered in the presence of a satisfactory donor ligand.[69-79,105-109] Equally, stabilization of transient cerium(IV) monoamide derivatives may ultimately necessitiate the

incorporation of further intra- or intermolecular donor interactions in order to provide additional electronic stabilization and/or steric saturation (e.g. eq 16).

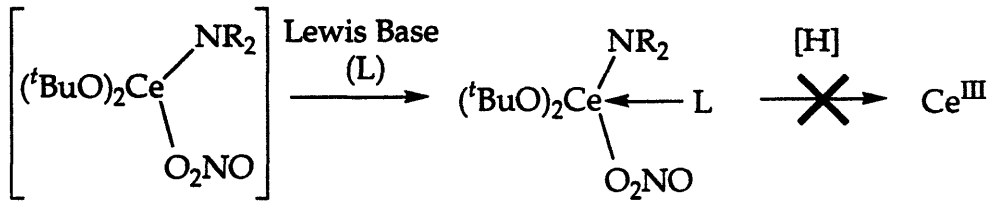

(16)

The Reaction of $(^tBuO)_2Ce(NO_3)_2(THF)_2$ with LiN(TMS)(2, 6-$^iPr_2C_6H_3$). Preparation of $(^tBuO)_3Ce$(2, 6-$^iPr_2C_6H_3$). To date, *N*-trimethylsilyl-2, 6-diisopropylaniline (TMSDIPA) is the only amine derivative studied which yields identifiable cerium(IV) species from the reaction between equimolar quantities of the cerium and amide precursors. However, the reaction chemistry of the bis-*tertiary*-butoxide cerium(IV) backbone in conjunction with the bulky anilide derivative is not as straight forward as to yield the desired monoamide species $(^tBuO)_2Ce(N(TMS)(2, 6\text{-}^iPr_2C_6H_3))(NO_3)$. Likewise, where less bulky anilides readily generate bisamide complexes, it is not clear that this is the case here. Whereas the bulk of the TMSDIPA ligand appears to preclude formation of a bisamide as the major product, this anilide offers stability to monoamide derived redistribution products, which are not observed with other amide ligands so far studied.

The trialkoxide amide $(^tBuO)_3Ce(N(TMS)(2, 6\text{-}^iPr_2C_6H_3)$ (**3**) is the major species formed from the reaction between equimolar quantities of $(^tBuO)_2Ce(NO_3)_2(THF)_2$ and LiN(TMS)(2,6-$^iPr_2C_6H_3$) (eq 17). This first

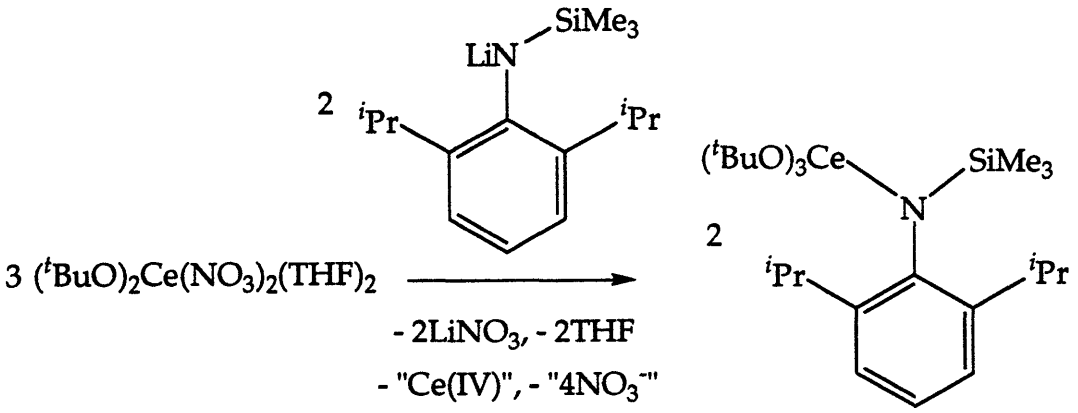

(17)

example of a cerium(IV) monoamide derivative has been characterized in both solution and the solid state. However, the preparation of **3** via such a

redistribution process is not an efficient procedure. Though NMR studies reveal that conversion to the trisalkoxide species from the bisalkoxide precursor is highly reproducible, the monoamide is generated in low yield, and in the presence of difficult to remove side-/by-products. The ease with which **3** is isolated varies considerably depending on the exact conditions employed. The reaction stoichiometry alone determines that two-thirds conversion of the cerium precursor to the observed product is the most that can be expected. Experimentally, however, the degree of conversion is considerably less than the maximum; significant impurities (≈ 50%) due to both diamagnetic and paramagnetic species are present in the ^1H NMR spectrum of the crude product, including several other silane derived resonances. The low percentage conversion to **3** and the equal solubilities of the accompanying impurities have severely hampered efforts to establish a routine procedure for the preparation and isolation of this complex by such a redistribution pathway. Pure crystalline **3** has been obtained allowing for solution state characterization of the complex; crystals of **3** suitable for X-ray crystallographic analysis were prepared in an analogous procedure from a bisalkoxide bistriflate precursor complex. Although the preparation of this trialkoxide amide may be achieved by redistribution routes from the bisalkoxide precursor, it is clear that a clean, efficent synthesis of this complex is surely best accomplished by direct metathesis between a cerium(IV) trialkoxide precursor, e.g $(^tBuO)_3Ce(NO_3)(THF)_2$[54] and an alkali metal amide. The proviso here of course is that the repective reaction intermediates in this case are not themselves subject to decomposition via ligand redistribution processes. The use of trialkoxide precursor complexes is certainly beneficial in a study of differentially substituted tri-*tertiary*-butoxide amide complexes, although this strategy likely provides little insight into the chemistry of desired $(^tBuO)_2Ce(NR_2)(X)$ species. It remains to be seen as to whether other trialkoxide monoamide derivatives such as $(^tBuO)_3CeN(TMS)_2$ and $(^tBuO)_3CeN(TMS)(o\text{-}MeOC_6H_4)$ are subject to redistribution to bisalkoxide bisamide species. The related metallocene derivatives $Cp_2Ce(O^tBu)_2$ and $Cp_3Ce(O^tBu)$ are, however, known to be stable with respect to redistribution.[50]

The diamagnetic solution state NMR spectra (^1H, ^{13}C) of the monoamide **3** (1H, C_6D_6, δ 0.42 (s, 9H, $SiMe_3$), δ 1.24 (s, 27H, $(^tBuO)_3$) are comparable to those of the bisamide derivatives $(^tBuO)_2Ce(N(TMS)_2)_2$ (**1**) and

$(^tBuO)_2Ce(N(TMS)(o\text{-}MeOC_6H_4))_2$ (**2**). Interconversion of the isopropyl groups of the bulky amide is observed to be slow on the NMR timescale (^1H, C_6D_6 δ 1.22 (δ, J = 6.9 Hz, 6H), δ 1.49 (δ, J = 7.2 Hz, 6H)) demonstrating the existence of hindered rotation about the methine-arene axis.

Solid State Structure of $(^tBuO)_3Ce(N(TMS)(2,6\text{-}^iPr_2C_6H_3)$ (3). The impact of steric crowding of the metal center by the TMSDIPA ligand is further evident in the solid state structure of **3** (Figures 7-9; Appendices 4.2, 4.9-4.11). A prominent feature in the crystal structure of the trialkoxide amide is the angle between respective pairs of *tertiary*-butoxide oxygen atoms and the metal center. Here, the O-Ce-O angles average 106.5(4)°, which is extremely close to the value determined in the bis(hexamethyldisilazide) complex **1** (105.3(3)°), and significantly less than that observed in **2** (117.4(1)°). It is fair enough that the two tetrahedral species adopt a similar geometry about the metal center, however, it might be expected that the difference between the CeO_2N_2 and CeO_3N cores of these two species also be reflected crystallographically. Though there is no distinct difference between the cerium-alkoxide bond distances in **1**, **2** or **3** (Ce-O(range) 2.052(6)-2.070(10) Å), the angles about the *tertiary*-butoxide oxygen atoms (Ce-O-C(ave) = 168.8(9)°) are considerably more obtuse in the trialkoxide than the respective angles in either of the bisalkoxide complexes (Ce-O-C(ave): **1**, 159.9(5)°; **2**, 160.5(2)°). In *d*-series and actinide systems, oxygen to metal π-overlap is a likely cause of the short M-O bond distances and the linearity of the angles about the alkoxide oxygen.[110-114] The involvement of π-donation among lanthanide systems is questionable, however, due to the extensive shielding of the 4*f*- valence orbitals.[8] Furthermore, although the observed M-O distances and M-O-C angles are consistent with π-interactions, such phenomena may equally well be attributed to the oxophilicity and steric demands in lanthanide metal centers.[115] It has been postulated that in the presence of both oxygen and nitrogen based ligands, that the nitrogen center dominates π-bonding and therefore reduces the level of π-overlap from the oxygen.[116] The linearity of the Ce-O^{t}Bu angles of **3** with respect to **1** and **2** could therefore be considered to be the result of the incorporation of the *tertiary*-butoxide ligands into the less electron rich CeO_3N core. The structural similarity between **1** and **3** further extends to the cerium-nitrogen bond distances (Ce-N(ave): **1**, 2.260(7) Å; **3**, 2.250(12) Å) which are, as expected, shorter than those observed in

hexacoordinate **2** (Ce-N(ave) = 2.33(2) Å). Neither the nitrogen-silicon bonding interactions, nor the planarity of the nitrogen atoms are affected by differences in the ligand environments of **1**, **2** and **3**.

Figure 7. Selected Bond Distances and Angles for (^{t}BuO)$_3$Ce(N(TMS)(2, 6-^{i}Pr$_2$C$_6$H$_3$) (3)

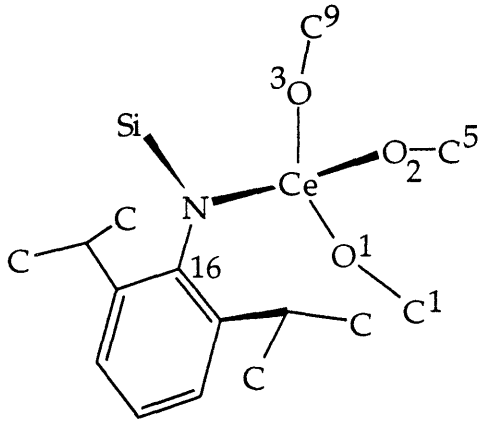

Bond Lengths (Å)

Ce	N	2.250(12)
Ce	O(1)	2.070(10)
Ce	O(2)	2.058(10)
Ce	O(3)	2.060(9)
N	Si	1.731(13)
N	C(16)	1.387(18)
O(1)	C(1)	1.392(17)
O(2)	C(5)	1.396(17)
O(3)	C(9)	1.434(16)

Bond Angles (deg)

N	Ce	O(1)	119.1(4)	Ce	N	Si	125.8(7)
N	Ce	O(2)	110.7(4)	Ce	N	C(16)	105.8(9)
N	Ce	O(3)	107.1(4)	Si	N	C(16)	129.2(10)
O(1)	Ce	O(2)	105.9(4)	Ce	O(1)	C(1)	176.7(8)
O(1)	Ce	O(3)	106.0(4)	Ce	O(2)	C(5)	163.2(10)
O(2)	Ce	O(3)	107.6(4)	Ce	O(3)	C(9)	166.6(8)

Figure 8. ORTEP Plot of $(^{t}BuO)_3Ce(N(TMS)(2, 6\text{-}^{i}Pr_2C_6H_3)$ (3)

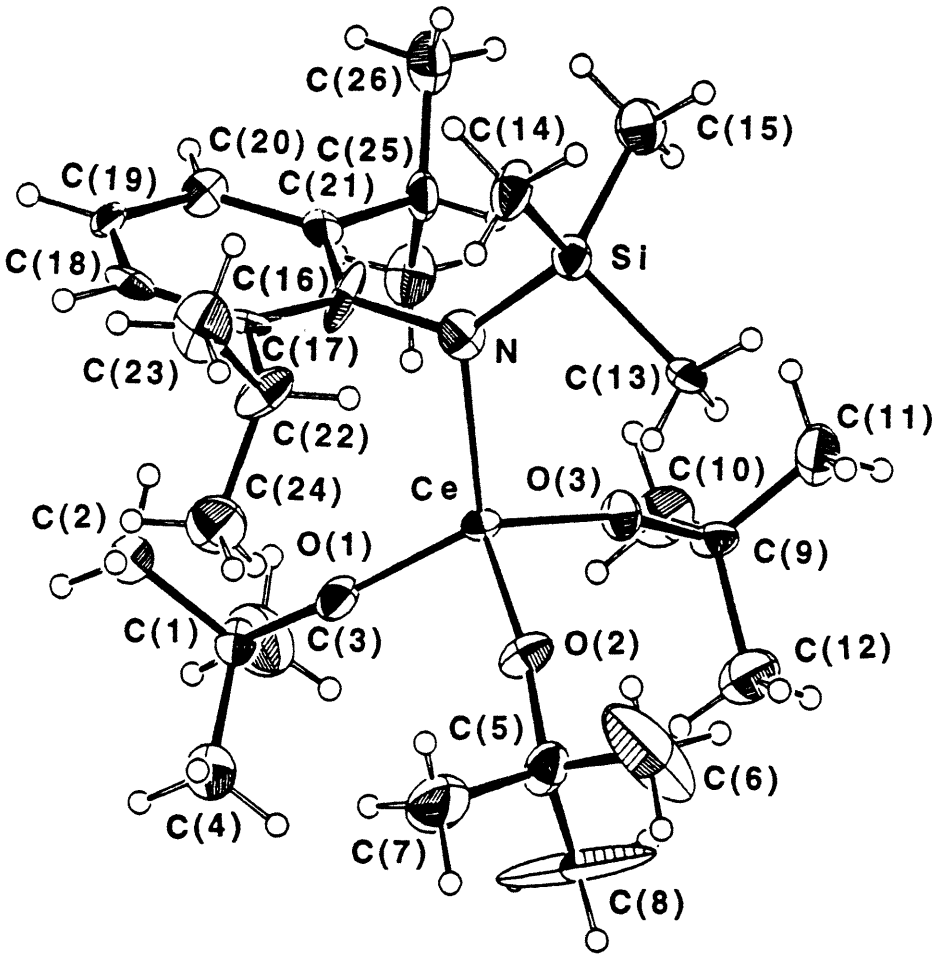

Figure 9. ORTEP Plot of $(^{t}BuO)_3Ce(N(TMS)(2, 6\text{-}^{i}Pr_2C_6H_3)$ (3)

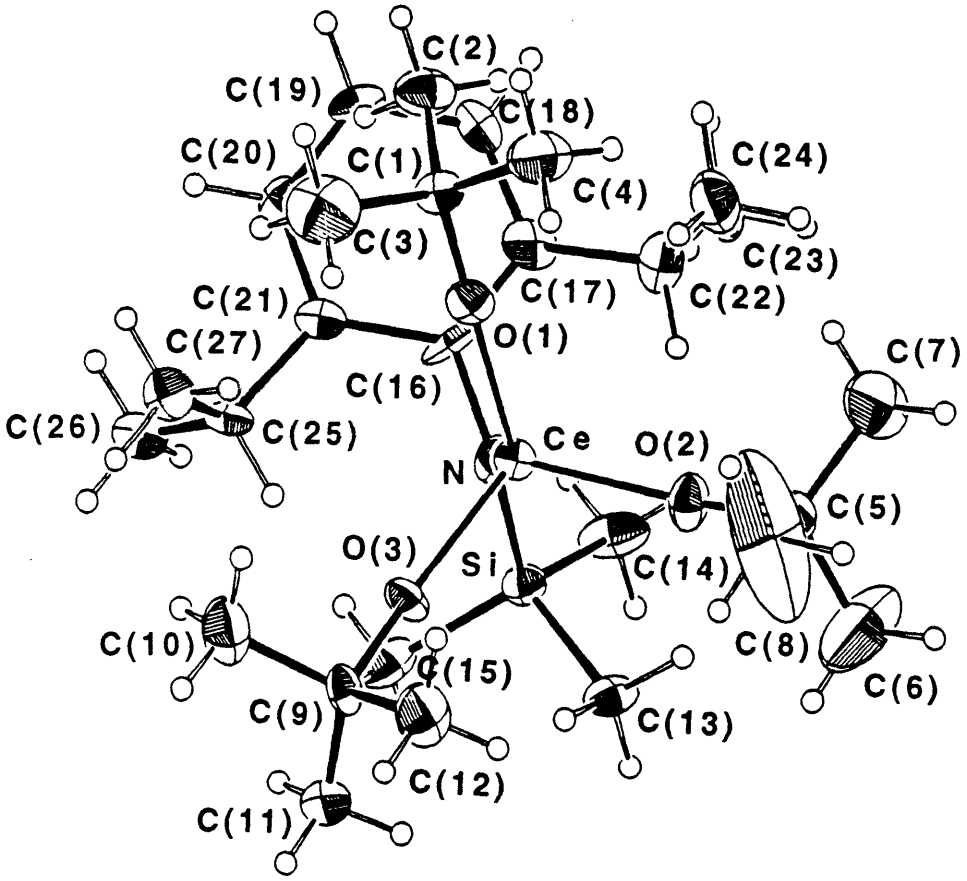

Transiently stable cerium(IV) nitrate species have previously been implicated in efforts directed towards the preparation of metallocene complexes of the high oxidation state lanthanide.[50] The synthesis of the biscyclopentadienyl bisalkoxide derivative $Cp_2Ce(O^tBu)_2$ has been achieved in high yield by the metathetical exchange between the cerium(IV) precursor $(^tBuO)_2Ce(NO_3)_2(THF)_2$ and sodium cyclopentadienide (eq 18).

$$(^tBuO)_2Ce(NO_3)_2(THF)_2 \xrightarrow[\text{THF, RT, 30 sec}]{2NaCp} Cp_2Ce(O^tBu)_2 \qquad (18)$$

$$- 2NaNO_3, -2THF$$

Evans *et al*, **1989**

Though there are no reports of the successful preparation of mono(Cp) cerium(IV) complexes, several different strategies have been employed with varying degrees of success to prepare the triscyclopentadienyl alkoxide analogs $Cp_3Ce(OR)$ (R = ^iPr,[7,47] ^tBu)[50]. When applied to the synthesis of $Cp_3Ce(O^tBu)$, the nitrate-cyclopentadienyl metathesis between the requisite alkoxide nitrate precursor $(^tBuO)Ce(NO_3)_3(THF)_2$ and sodium cyclopentadienide is reported to yield the desired product, along with significant quantities of the bis(cyclopentadienyl) derivative $Cp_2Ce(O^tBu)_2$ and other products (eq 19).[50] Since these metallocene derivatives are known to be stable with respect to

$$(^tBuO)Ce(NO_3)_3(THF)_2 \xrightarrow[\text{THF, RT, 30 sec}]{3NaCp} \begin{array}{c} Cp_3Ce(O^tBu) \\ + \\ Cp_2Ce(O^tBu)_2 \\ + \\ \text{other products} \end{array} \qquad (19)$$

Evans *et al*, **1989**

ligand redistribution processes, the formation of biscyclopentadienyl bis-*tertiary*-butoxide is postulated to occur following ligand redistribution processes in intermediates of the type $Cp_xCe(O^tBu)_y(NO_3)_z$ (x, y, z = 1 or 2; x + y + z = 4) (eq 21). Even though successive transmetallation steps to generate $Cp_3Ce(O^tBu)$ are fast, intermolecular ligand exchange processes allow for the build-up of a considerable quantity of species other than the desired product.[50]

Identical phenomena can be envisioned to take place in the formation of **3** from $(^tBuO)_2Ce(NO_3)_2(THF)_2$ and LiN(TMS)(2, 6-^{i}Pr$_2$C$_6$H$_3$) (e.g. Scheme 10: $LiNR_2$ = LiN(TMS)(2, 6-^{i}Pr$_2$C$_6$H$_3$).

Scheme 10

$$(^tBuO)_2Ce(NO_3)_2(THF)_2 \xrightarrow[-\,LiNO_3]{LiNR_2} \text{"}(^tBuO)_2Ce(NR_2)(NO_3)\text{"} \quad \text{(i)}$$

$$\begin{array}{c}\text{"}(^tBuO)_2Ce(NR_2)(NO_3)\text{"} \\ + \\ (^tBuO)_2Ce(NO_3)_2(THF)_2\end{array} \xrightarrow[\begin{array}{c}-\,Ce^{IV},\,-^tBuO^-,\\ -\,3NO_3^-,\,-\,2THF\end{array}]{} (^tBuO)_3Ce(NR_2) \quad \text{(ii)}$$

$$2\ \text{"}(^tBuO)_2Ce(NR_2)(NO_3)\text{"} \xrightarrow[\begin{array}{c}-\,Ce^{IV},\,-^tBuO^-,\\ -\,NR_2^-,\,-\,3NO_3^-\end{array}]{} (^tBuO)_3Ce(NR_2) \quad \text{(iii)}$$

$$2\ (^tBuO)_2Ce(NR_2)_2 \xrightarrow[\begin{array}{c}-\,Ce^{IV},\,-^tBuO^-,\\ -\,3(NR_2^-)\end{array}]{} (^tBuO)_3Ce(NR_2) \quad \text{(iv)}$$

In the systems under study here, the effect of amide functionalities on the metal center bears a much closer relationship to that of previously examined cyclopentadienyl species, in that the complexes $(^tBuO)_2Ce(E)(NO_3)$ (E = NR_2, Cp) are subject to rapid redistribution processes, whereas the range of *tertiary*-butoxide nitrate species $(^tBuO)_nCe(NO_3)_{4-n}$ (n = 1-3) are all readily isolated. However, before drawing too many conclusions on the nature of the amide and Cp reactivity from the observed redistribution processes, it is important to ascertain the extent to which the chemistry of such 'alkoxide' nitrate[54] complexes may be extended with ligands other than *tertiary*-butoxide.

Solid State Structure of $Ce_3(O^tBu)_{10}(NO_3)$ (4). A single additional redistribution product has so far been isolated. In an effort to isolate the product of a reaction between $(^tBuO)_2Ce(NO_3)_2(THF)_2$ and LiTMSDIPA, i.e. **3**, by recrystallization of the crude reaction product from hexane, a crystalline yellow-brown material were precipitated, after several months at -40 °C (eq 21). This product has subsequently been characterized by X-ray

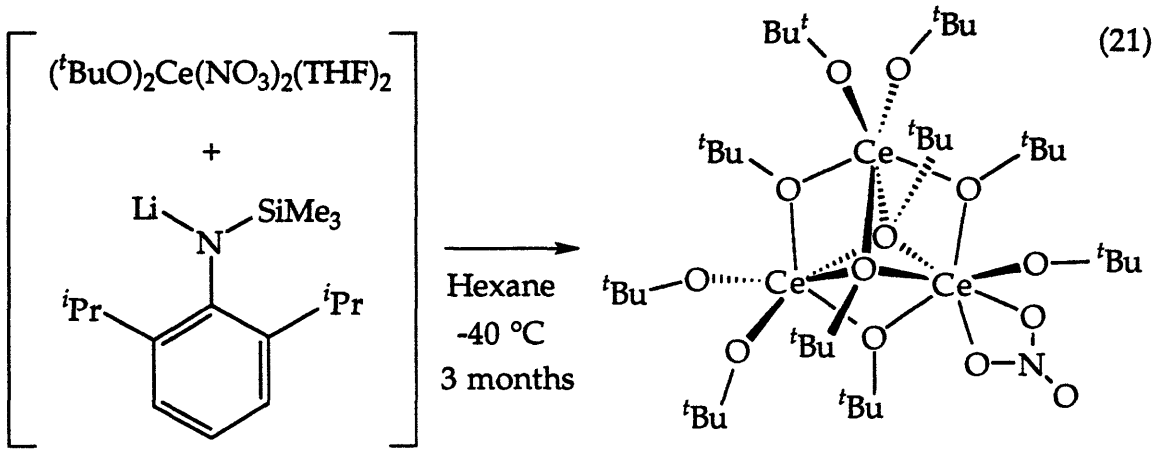

4

crystallography and determined to be the tricerium decaalkoxide nitrate cluster $Ce_3(O^tBu)_{10}(NO_3)$(pentane) (**4**) (Figures 10-12; Appendices 4.2, 4.12-4.14). Rhombohedral crystals of **4** were separated from an amorphous pale yellow matrix composing the remaining fraction of the precipitate. The ^1H NMR spectrum of the precipitate reveals the presence of resonances due to several different diamagnetic and paramagnetic species. Although it is true to say that a single crystal X-ray study is not necessarily representative of the bulk sample there are several interesting features regarding the synthesis and structure of this species. The first point of note is the presence a nitrate ligand in the coordiantion sphere which indicates that although this species possesses a high alkoxide to cerium ratio (10:3) it does not appear to be a decomposition product of the trialkoxide amide **3** or related species. Rather, **4** is seemingly the ultimate thermodynamic product of redistribution pathways in which higher order mono and dinuclear alkoxide nitrate species serve as intermediates.[50] This observation goes some way to accounting for the low degree of conversion observed in the preparation of **3**. Since the fully oxidized tricerium decaalkoxide oxide $Ce_3(O^tBu)_{10}O$ cluster has previously been prepared from alkoxide precursors,[54] the existence of the partially

Figure 10. Selected Bond Distances and Angles for $Ce_3(O^tBu)_{10}(NO_3)$(Pentane) (4)

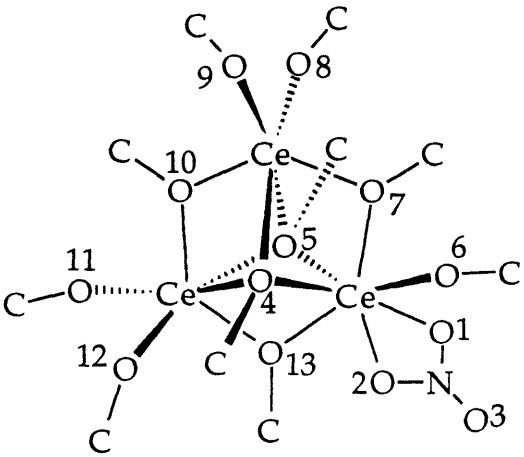

Bond Lengths (Å)

Ce(1)	O(1,2)	2.580(4), 2.582(4)
Ce(1)	O(6)	2.134(3)
Ce	O(7,10,13)	2.263(3)-2.516(3)
Ce(2,3)	O(8,9,11,12)	2.066(3)-2.080(3)
N	O(1)	1.274(6)
N	O(2)	1.238(5)
N	O(3)	1.223(6)
C	O(4)	1.448(6)
C	O(5)	1.469(6)
C	O(6)	1.417(6)
C	O(7,10,13)	1.443(6)
C	O(8,9,11,12)	1.442(6)-1.454(6)

Bond Angles (deg)

O(1)	Ce(1)	O(2)	49.15(12)
O(1,2)	Ce(1)	O(6)	87.34(13)-91.22(12)
O(4)	Ce	O(5)	61.17(10)-64.13(10)
O(4,5)	Ce	O(7,10,13)	68.71(10)-75.58(11)
O(7,13)	Ce(2,3)	O(10)	140.22(12)-140.33(11)
O(7)	Ce(1)	O(13)	131.90(10)
O(8,11)	Ce(2,3)	O(9,12)	97.64(13)-97.82(14)
O(1)	N	O(2)	117.4(4)
O(1,2)	N	O(3)	120.4(5)-122.1(5)
Ce(1)	O(1,2)	N	95.9(3)-96.8(3)
Ce	O(4,5)	Ce	93.85(10)-96.09(11)
Ce	O(4,5)	C	115.67(26)-124.21(27)
Ce(1)	O(6)	C	169.5(3)
Ce	O(7,10,13)	Ce	102.19(12)-102.88(12)
Ce	O(7,10,13)	C	126.34(28)-131.4(3)
Ce(2,3)	O(8,9,11,12)	C	168-3(3)-172.2(3)

Figure 11. ORTEP Plot of $Ce_3(O^tBu)_{10}(NO_3)$(Pentane) (4). Pentane molecule removed for clarity

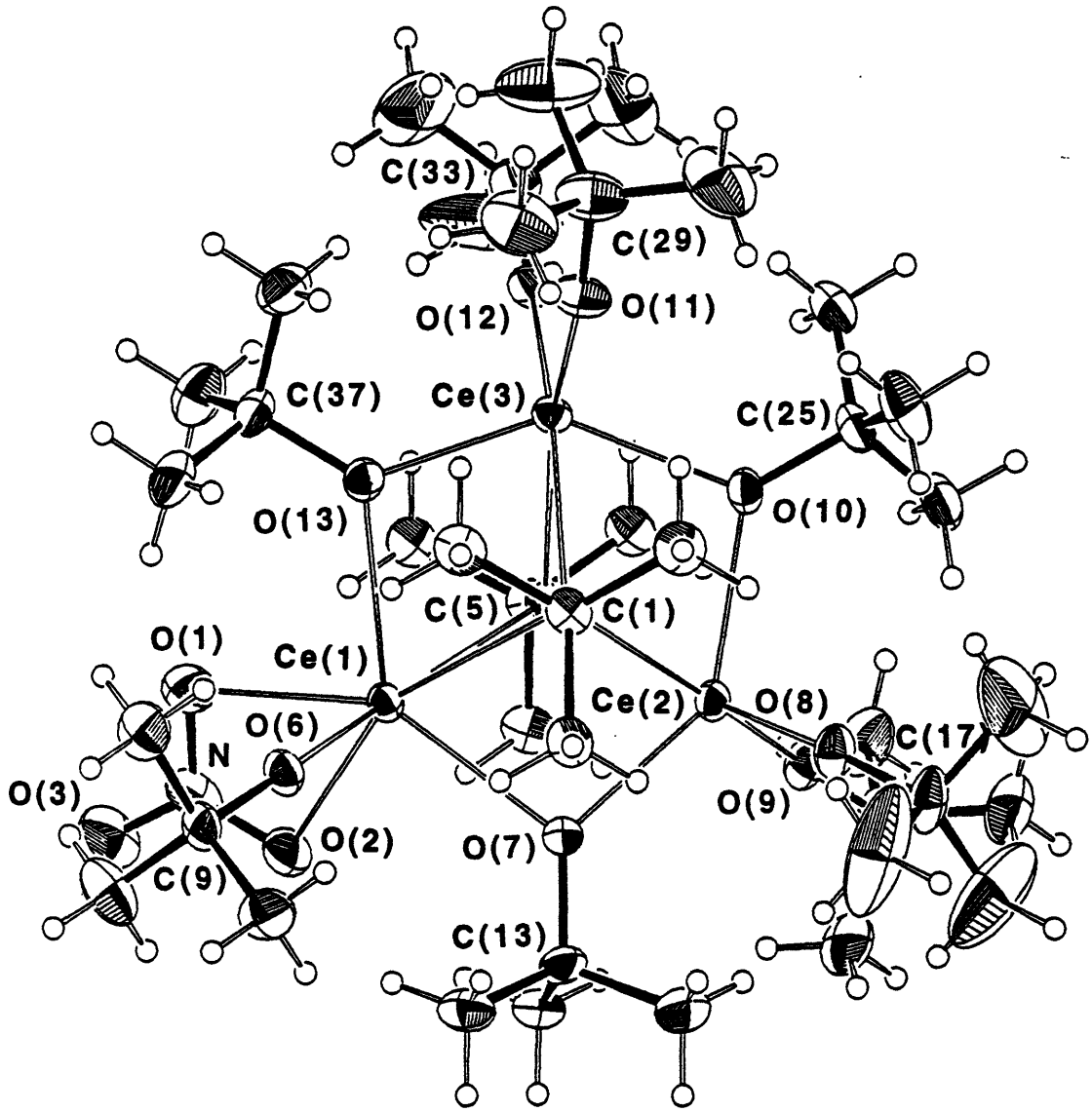

Figure 12. ORTEP Plot of $Ce_3(O^tBu)_{10}(NO_3)$(Pentane) (4). Pentane molecule removed for clarity

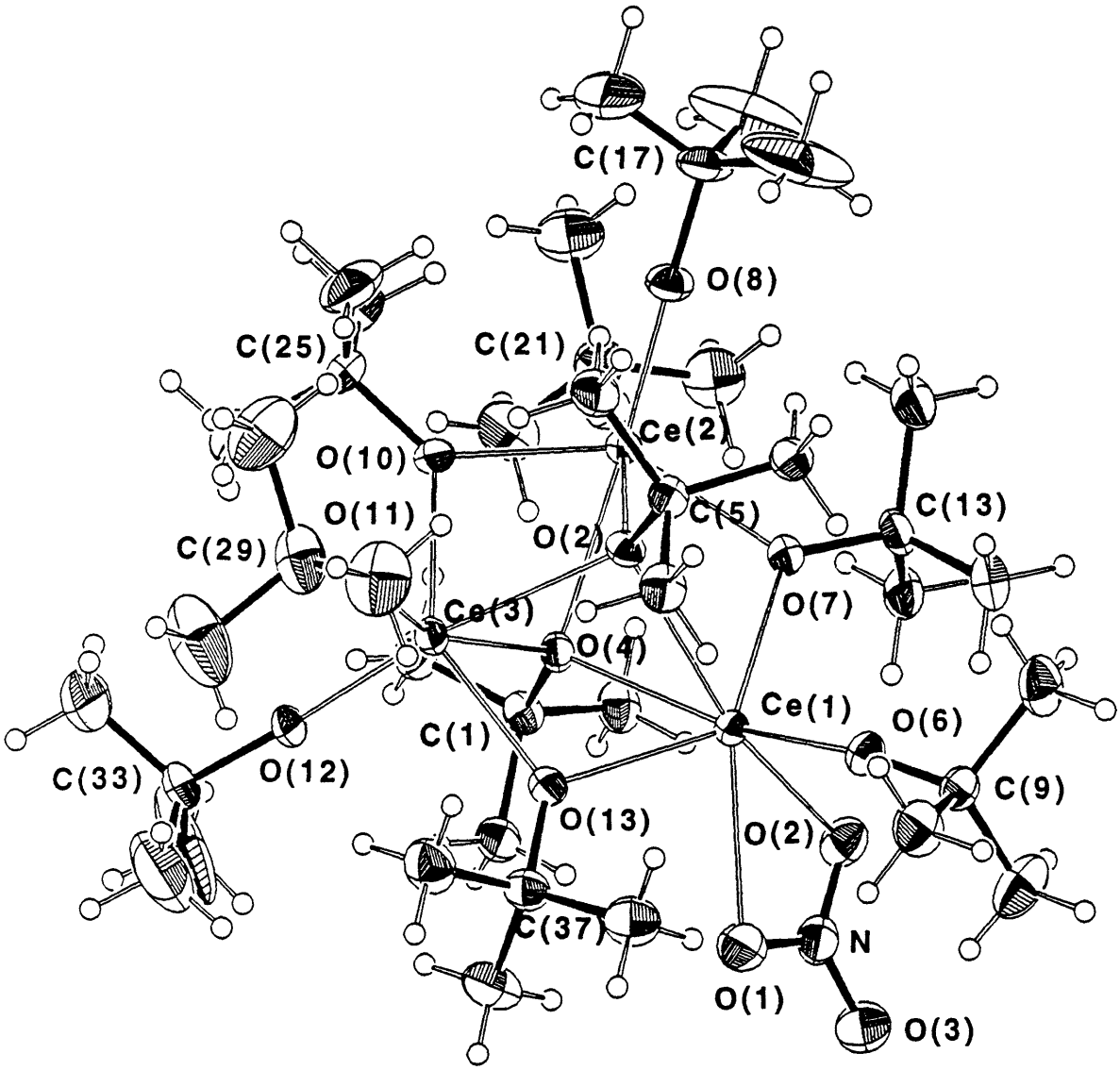

reduced core of **4** is perhaps an indication of involvement of the amide on the course of the reaction. Like **4**, the formation of $Ce_3(O^tBu)_{10}O$ is observed to be the final resting place of certain cerium(IV) tertiary-butoxide redistribution processes. It has been reported that slow conversion of either $Ce(O^tBu)_4(THF)_2$ or $Ce_2(O^tBu)_9Na$ gives rise to the formation of the trimetallic cluster, in quantitative yield (eq 22).[54] Attempts to reproduce the transformation from the tetraalkoxide to the oxobridged product have,

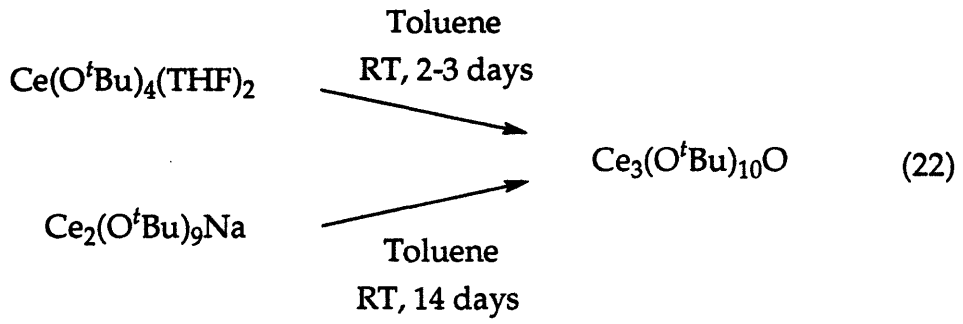

(22)

Evans *et al*, **1989**

however, not always resulted in the same degree of conversion. It has further been suggested that for the preparation of the analogous uranium derivative $U_3(O^tBu)_{10}O$ the addition of water is actually necessary in order to effect clean conversion to the oxo complexes.[117] Although stored under seemingly rigorously dry, oxygen-free conditions, it is conceivable that with time adventitious moisture participates in the formation of **4**. If this is indeed the case, then it is certainly surprising that no oxide moiety is present in the ultimate product and that a one electron reduction of the tricerium nucleus is observed to occur. Cerium(III) intermediates may also be involved in redistribution processes with tetravalent species to effect formation of the observed core.

The geometries of **4** and the complexes $M_3(O^tBu)_{10}(O)$ (M = Ce, U) are similar. The structures of these cerium and uranium oxo species have been determined by solution state NMR[54] and X-ray crystallography,[118,119] respectively. The only noteable discrepancy between the structures is that the oxo moiety of the alkoxide oxide complexes serves to cap the triangular core, whereas the nitrate of **4** is terminally disposed. Although in related *d*-transition metal systems, there is evidence to support the existence of metal-metal bonds in similarly constructed complexes,[120,121] the interatom distances (> 3.5 Å) in both the uranium oxide[118,119] and **4** give no indication of similar

interactions. Although this eventuality is stated as being somewhat surprising for the actinide species,[118,119,122-124] metal-metal bonding is certainly not expected to occur in the tricerium complex, both due to the absence of available valence electrons in the $(Ce^{III})(Ce^{IV})_2$ system and as a result of the strong shielding of the $4f$ orbitals by the $5s^25p^6$ electrons which effectively renders lanthanide-lanthanide bonding an impossibility.[122] Furthermore, the angles about the μ_2-bridging alkoxide oxygen atoms are far from acute (Ce-O-C(range) = 102.19(°12)-102.88(12)°), with the Ce_3O_3 core adopting a distorted hexagonal geometry. Since steric crowding about the unique NO_3/O^tBu metal center is not a factor relative to the other cerium ions, it is clear that the majority of the electron density is centered here. This is further reflected by the elongated bond distance of the unique terminal *tertiary*-butoxide (Ce(1)-O(6) = 2.134(3) Å) with respect to the other terminally bonded alkoxides (Ce(2,3)-O(8,9,11,12)(range) = 2.066(3) Å-2.080(3) Å), and by a comparison with analogous interactions in other cerium(IV) *tertiary*-butoxide[50,54] and cerium(III) alkoxide complexes (Ce^{III}-O ≈ 2.14-2.23 Å.[56,94,95] Significant differences are not, however, observed in the angles about the respective oxygen atoms (Ce-O(6)-C = 169.5(3)°; Ce-O(8, 9, 11, 12)-C(range) = 168-3(3)-172.2(3)°), presumably due to the considerable steric congestion about the pseudo-octahedral sub-units forcing the bonds angles closer to linear than might otherwise be expected. A comparison of the ^tBuO-Ce-O^tBu angles of **4** (O(8,11)-Ce(2,3)-O(9,12) = 97.64(13)°, 97.82(14)°) with the respective values in **1-3** reveals that this is indeed observed to the case (O-Ce-O: **1**, 105.3(3)°; **2**, 117.4(1)°; **3**, 106.5(4)°). Cerium-nitrate bond distances (Ce-O(1,2)(ave) = 2.581(4) Å) do not accurately reflect the oxidation state of the metal center, however, but rather vary considerably depending on the specific nature of the ligand environment (e.g. Ce-O: $(^tBuO)_2Ce(NO_3)(^tBuOH)_2$, 2.515(6)-2.593 Å(5);[54] $Ce(NO_3)_3(DME)$, 2.529(2)-2.606 Å(2)).[125,83] The fact that the bond distances of both oxygen atoms of this bidentate ligand are relatively long simply exemplifies the bulk of the system as a whole. The distances and angles about the nitrate moiety are typical.[125]

Alternatives to the Cerium(IV) Bisalkoxide Bisnitrate Precursor $(^tBuO)_2Ce(NO_3)_2(THF)_2$. The protonation of two of the *tertiary*-butoxide ligands of the tetraalkoxide $Ce(O^tBu)_4(THF)_2$ by ammonium triflate (triflate = trifluoromethanesulfonate, OSO_2CF_3) leads to the formation of a product with solution NMR spectra corresponding to the solvated bisalkoxide bistriflate species $(^tBuO)_2Ce(OSO_2CF_3)_2$ (eq 23).

$$\begin{array}{c}Ce(O^tBu)_4(THF)_2\\ \text{and/or}\\ Ce_3(O^tBu)_{10}(O)\end{array} \xrightarrow[\substack{-2\,NH_3,\,-2\,^tBuOH\\ RT,\,2\,h}]{\substack{2\ NH_4OSO_2CF_3\\ THF}} (^tBuO)_2Ce(OSO_2CF_3)(THF)_2 \qquad (23)$$

Preliminary experiments indicate that the ammonium protonolysis chemistry is more general, and may ultimately be useful in the preparation of bisalkoxide bishalide species. Complexes of the type '$(RO)_2CeCl_2$' are established synthetic intermediates in the chemistry of tetravalent ions,[71,76,126,127] although not yet for cerium, where such species potentially offer considerable benefits over nitrate bearing precursors in efforts to prepare novel cerium(IV) species. Unlike flouride derivatives,[8] chloride ligands are likely to be reactive in transmetallation procedures while remaining far less prone to participate in redox processes than nitrate analogs. This methodology has already demonstrated promise since the bistriflate complex effects formation of the trialkoxide amide **3** from LiTMSDIPA as effectively as the bisnitrate precursor (cf. eq 18) and the preparation of $(^tBuO)_2Ce(N(TMS)_2)_2$ (**1**) from the analogous dichloride precursor and lithium hexamethyldisilazide proceeds in good yield.

Organocerium(IV). The Reactivity of $(^tBuO)_2Ce(N(TMS)_2)_2$ (1) with Acidic Hydrocarbons. Though the preparation of the first σ-bonded alkyl of cerium(IV) remains a major synthetic challenge, the chemistry of cerium(IV) π-complexes has previously been probed with the preparation of the metallocene complexes $Cp_2Ce(O^tBu)_2$[50] and $Cp_3Ce(OR)$ (R = ^iPr,[7,47] ^tBu),[50] and several differentially substituted cerocene derivatives (cerocene = $Ce(COT)_2$ (COT = cyclooctatetraene)).[7,41,48,49] An analog of $Cp_2Ce(O^tBu)_2$, the bis(trimethylsilylated) metallocene complex $(TMSCp)_2Ce(O^tBu)_2$ (**5**) (TMSCp = η^5-$C_5H_4SiMe_3$) is readily prepared from **1** by way of the thermally induced deprotonation of trimethylsilylcyclopentadiene (eq 24). The bisamide

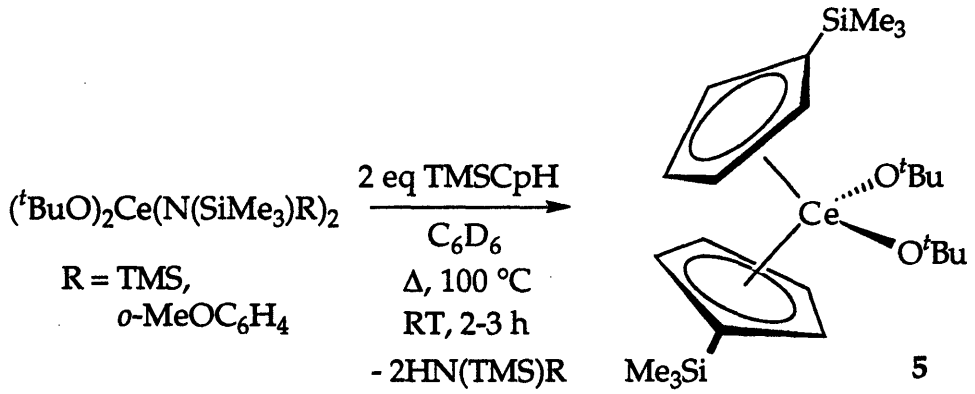

(24)

complex is stable in the presence of the diene for extended periods (≥ 18 h) at room temperature. Similar thermolysis conditions have also been employed to prepare this metallocene product from the *ortho*-anisidine derived bisamide $(^tBuO)_2Ce(N(TMS)(o\text{-}MeOC_6H_4))_2$ (**2**). Under the thermolysis conditions employed, silicon-carbon bond cleavage is not observed to occur.[47] Assignment of the product from the ^1H NMR is straight forward due to the resemblance to the spectrum of the plain-ring derivative (^1H, C_6D_6 $(TMSCp)_2Ce(O^tBu)_2$ δ 0.47 (s, 18H), 1.32 (s, 18H), 6.24 (t, J = 2.4Hz, 4H), 6.64 (t, J = 2.6Hz, 4H); $Cp_2Ce(O^tBu)_2$ δ 1.26 (s, 18H), 6.14 (s, 10H)). As per the preparation of $Cp_2Ce(O^tBu)_2$, the synthesis of this complex may also be achieved metathetically, from the interaction between $(^tBuO)_2Ce(NO_3)_2(THF)_2$ and lithium trimethylsilylcyclopentadienide (eq 25).

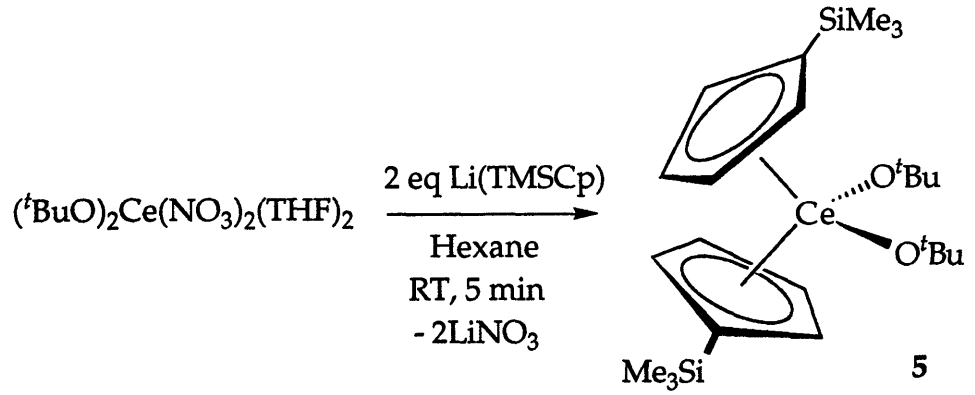

(25)

Thermolysis of **1** in the presence of an excess of the organic substrate does not result in the formation of the sterically crowded triscyclopentadienyl analog $(TMSCp)_3Ce(O^tBu)$, whereas the primary product of the reaction with a single equivalent of TMSCpH remains the bicyclopentadienyl species. Neither redistribution nor cerium-oxygen cleavage processes appear to result

in the formation of a tris(Cp) species, although in the presence of sub-stoichiometric quantities of the organic substrate, the existence of small impurities may perhaps be explained by the existence of monocyclo-pentadienyl intermediates of the type "(TMSCp)Ce(O^tBu)$_2$(N(TMS)$_2$)".

To this point, all efforts to prepare stable, isolable cerium(IV) metallocene amide derivatives from alkoxide precursors have proved futile. Cerium-oxygen bond cleavage processes have, however, been successfully employed in the synthesis of $Cp_3Ce(O^iPr)$[47] and $Ce(COT)_2$[7] (Scheme 11). Attempts to prepare $Cp_3Ce(O^iPr)$ from $Ce(O^iPr)_4$ and magnesium or thallium cyclopentadienide derivatives yielded extensive redox chemistry.[7,47]

Scheme 11

$$Ce(O^iPr)_4 \xrightarrow[\text{Toluene}\ \Delta,\ 65\ ^\circ C]{3R_3SnCp} Cp_3Ce(O^iPr) + 3R_3Sn(O^iPr) \qquad \text{(i)}$$

Gulino *et al*, **1988**

$$Ce(O^iPr)_4(^iPrOH) + 5AlEt_3 \xrightarrow[C_8H_8\ \text{(Solvent)}\ 140\ ^\circ C,\ 2\ h\ -C_2H_6,\ -4C_2H_5^\bullet]{\Delta} Ce(COT)_2 + 5AlEt_2(O^iPr) \qquad \text{(ii)}$$

Greco *et al*, **1976**

Previous effots to prepare the pentamethylcyclopentadienyl derivatives $Cp^*_2Ce(O^tBu)$ and $Cp^*_3Ce(O^tBu)$ by an analogous procedure to that used for the preparation of the respective plain-ring complexes (Scheme 12: (i)) resulted only in redox chemistry (ii).[50] A similar pattern of reactivity is observed in attempts to prepare the same bis(pentamethylcyclopentadienyl) analog a deprotonation route. The preparation of $(TMSCp)_2Ce(O^tBu)$ from **1** and TMSCpH is facile, however the analogous reaction with pentamethycyclopentadiene (Cp*H) yields only paramagnetic species. In related systems, though the pentamethylcyclopentadienide anion is known to effect reduction of the trivalent europium species,[128] the preparation of the dimeric complex $[Cp^*Eu(O^tBu)(\mu\text{-}O^tBu)]_2$, composing these apparently incompatible entities, has recently been achieved by a judicious choice of both the reaction pathway and ancillary ligand set.[51]

Scheme 12

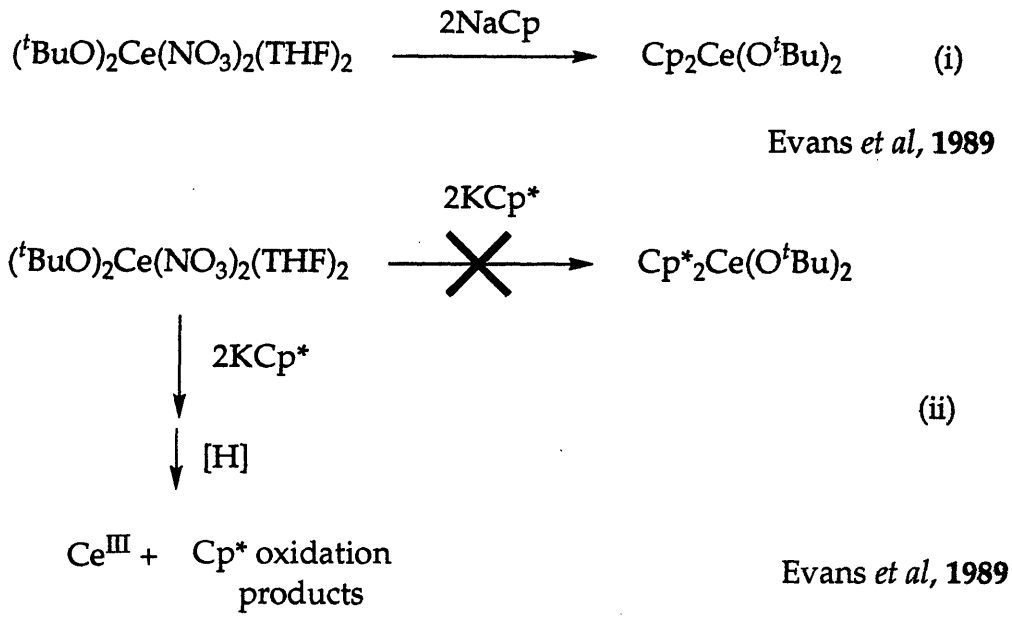

The preparation of this first example of trivalent europium pentamethylcyclopentadienide demonstrates that apparent metal-ligand incompatibilities can be overcome in certain instances. However, the sum of the experimental evidence to date, and the Ce(IV)/Ce(III) reduction potential infers that a stable cerium(IV)-Cp* interaction may be impossible to stabilize whatever the ancillary ligand framework. This negative result and successes in the preparation of the plain-ring and trimethylsilylated species $(C_5H_4R)_2Ce(O^tBu)_2$ (R = H, TMS) provide insight into prerequisites for the advancement of the chemistry of π-complexes tetravalent cerium. The bisCp* ancillary ligand set is perhaps the most widely employed framework in the organometallic chemistry of the *f*-transition series.[25,129] The recent explosion in catalytic organolanthanide chemistry is only one of the major reasons for the body of work on this ligand system.[21-24] The permethylated metallocene framework is typically exploited in *f*-element systems for its bulk, since unsubstituted cyclopentadienyl ligands generally employed in *d*-series metallocene complexes are subject to redistribution processes in larger lanthanide and actinide metal centers.[25,129] Furthermore, the bis(Cp*) backbone is considerably more electron rich than the unsubstituted framework. This often serves as a desireable feature in the *d*-block, trivalent lanthanide, or actinide systems, although not in the chemistry of cerium(IV). Trimethylsilyl substituted cyclopentadiene ligands appear to offer a viable

alternative for the future development of cerium(IV) metallocene systems. Substitution of the cyclopentadienyl rings in an $(RCp)_2Ce^{2+}$ framework potentially allows for tunability of both the steric and electronic environment surrounding the metal center. A satisfactory degree of coordinative saturation is essential for stability in complexes of this high oxidation state lanthanide, and the capacity of silicon to stabilize proximal carbanions only serves to decrease the likelihood of ligand reduced redox chemistry.[101,130]

A recent report states that the preparation of a series of trimethylsilylated substituted cerium bis(cyclooctatetraene) derivatives, including two tetravalent complexes.[49] The stability of $Ce(\eta^8\text{-}TMS_2C_8H_6)_2$ and $Ce(\eta^8\text{-}TMS_3C_8H_5)_2$ is expected, however, since cerocene itself has been known for some time. There is certainly considerable benefit to be gained by reducing the capacity for radical formation in Cp-ligands. though this is not an important concern in the chemistry of the aromatic COT dianion $C_8H_8^{2-}$.[44] Although all novel cerium(IV) species are of interest at this stage, given the extremely small knowledge base at present, future applications of organocerium(IV) chemistry are likely not centered around COT derivatives since not only does the aromatic ligand set establish a thermodynamic sink for the single electron oxidant,[6] but complexes of this type are also devoid of reactive valence sites.

Summary

For the first time, tetravalent cerium has been stabilized in a coordination environment containing simple amide ligands. Only reduction of the metal center is observed in the presence of primary, dialkyl or diaryl substrates, however, judiciously substituted trimethylsilyamides stabilize the high oxidation state metal center in the presence of a bis-*tertiary*-butoxide framework. The bisamide complexes $(^tBuO)_2Ce(N(TMS)_2)_2$ (**1**) and $(^tBuO)_2Ce(N(TMS)(o\text{-}MeOC_6H_4))_2$ (**2**) have been prepared and structurally characterized by direct metathetical routes from the reaction between the cerium(IV) precursor $(^tBuO)_2Ce(NO_3)_2(THF)_2$ and the requisite lithium amide salts (2 equiv). Conversely, the trialkoxide amide complex $(^tBuO)_3Ce(N(TMS)(2, 6\text{-}^iPr_2C_6H_3))$ (**3**) is the major species generated as a result of redistribution processes initiated by the bulky amide $LiN(TMS)(2, 6\text{-}^iPr_2C_6H_3)$ ($\geq$ 1 equiv). Although isolable bisamide species have been prepared, efforts so far to prepare synthetically appealing amide nitrate complexes have so far proven unsuccessful owing to rapid redistribution and/or reduction processes.

In reactivity studies, the bis(trimethylsilyl)amide complex **1** readily deprotonates trimethylsilylcyclopentadiene tupon thermolysis to selectively give rise to formation of the metallocene bisalkoxide $(TMSCp)_2Ce(O^tBu)_2$.

Experimental

General Procedures. All manipulations were conducted under an atmosphere of purified argon in a Vacuum Atmospheres Co. drybox. Nuclear Magnetic Resonance (NMR) spectra were recorded on a Bruker AC-250 MHz, Varian XL-300 or UN-300 spectrometers. NMR chemical shifts were determined in benzene-d_6 , and are internally referenced to the solvent (^{1}H, δ 7.15; ^{13}C, δ 128.0). Elemental analyses were performed by Oneida Research Services, Inc., Whitesboro, New York. Solvents were distilled (hexane, pentane and THF) or vacuum transferred (benzene-d_6 and hexamethyldisiloxane) after drying over sodium/benzophenone ketyl under nitrogen/argon. The complexes $(^tBuO)_2Ce(NO_3)_2(THF)_2$[54], $Ce(O^tBu)_4(THF)_2$[54] and $Cp_2Ce(O^tBu)_2$[50] were prepared according to published procedures. Lithium hexamethyldisilazide ($LiN(TMS)_2$) and lithium trimethylsilylclopentadienide (LiTMSCp) were prepared from hexamethyldisilazane and trimethylsilylcyclopentadiene, respectively, in hexane or pentane, by deprotonation with a limiting quantity of solution of *n*-butyllithium in hexane. All other lithium amides were prepared, at room temperature in hexane or pentane, in an otherwise similar procedure employed to that reported for related *N*-trimethylsilylamide reagents.[109] All other starting materials were purchased from commercial sources and used as received.

Representative Procedure for the Reaction of CAN with Alkali Amides. The addition of a colorless solution of $NaN(TMS)_2$ (67 mg, 0.37 mmol), in THF (9 mL) to an amber solution of $(NH_4)_2Ce(NO_3)_6$ (CAN) (102 mg, 0.19 mmol) in THF (9 mL) gave rise to immediate formation of a mustard yellow suspension. The ^{1}H NMR spectrum of the evaporated residue, extracted into benzene-d_6, revealed the presence of resonances due to hexamethyldisilazane (δ 0.09) and THF (δ 1.77, 3.57) as well as a broad downfield singlet (δ 7.96, width at half height ≈ 25Hz), presumably due to reduced cerium ammonium species. In THF-d_8, the ammonium protons of CAN are observed as a nitrogen split triplet resonance (δ 7.00, J_{NH} = 51.6 Hz).

Reactions of $(^tBuO)_2Ce(NO_3)_2(THF)_2$ Resulting in Amide Induced Redox Chemistry. In the presence of two equivalents of primary, dialkyl or diaryl lithium amide reagents, or a single equivalent of any amide other the

trimethylsilylated anilide derivative LiN(TMS)(2, 6-$^{i}Pr_2C_6H_3$) so far examined, facile decomposition of cerium(IV) precursor complex $(^{t}BuO)_2Ce(NO_3)_2(THF)_2$ is observed to take place. Experimentally, the addition of colorless solutions or suspensions of the respective amide reagent to a yellow-orange solution/suspension of the cerium precursor typically effects an immediate, brief darkening of the reaction mixture (cf. **1-3**; cf. CAN/NaCp).[83] However, any such intense coloration of the reaction mixture rapidly subsides, ultimately resulting in the formation of a pale lustrous/translucent yellow-orange suspension containing a pale precipitate. After extended periods, the supernatant is observed to become almost colorless.

Preparation of $(^{t}BuO)_2Ce(N(TMS)_2)_2$ (1). A colorless solution of $LiN(TMS)_2$ (2.41 g, 14.4 mmol), in pentane (25 mL), was added to a yellow suspension of $(^{t}BuO)_2Ce(NO_3)_2(THF)_2$ (4.00 g, 7.21 mmol), also in pentane (75 mL), at room temperature. Addition of the amide to the cerium complex was carried out as quickly as possible, with vigorous stirring, in an attempt to reduce the lifetime of unstable intermediates. The reaction mixture was immediately observed to change to a dark red-brown color with concomitant precipitation of the metathesis by-product, lithium nitrate. Further stirring was allowed for a total of 10 min, prior to removal of the solvent *in vacuo*, resulting in precipitation of a red-orange solid. Pentane (50 mL) was added to the solid residue, and the insoluble salts were removed by filtration through a Celite-topped glass frit. The solvent was subsequently evaporated from the filtrate, yielding the desired product as a red-orange powder, after drying *in vacuo*. Yield: 4.09 g (93%, ≈ 95% pure by ^{1}H NMR). Analytically pure **1** was obtained upon recrystallization from a concentrated solution in pentane, at -40 °C. Suitable crystals for an X-ray structural determination of **1** were obtained from a concentrated solution in hexamethyldisiloxane, at -40 °C. ^{1}H NMR (300 MHz, C_6D_6) δ 0.43 (s, 36H, $SiMe_3$), 1.34 (s, 18H, ^{t}BuO). ^{13}C NMR (75.0 MHz, C_6D_6) δ 4.5, 33.5, 85.0. Anal. Calcd for $C_{20}H_{54}CeN_2O_2Si_4$: C, 39.57; H, 8.97; N, 4.61. Found: C, 38.49; H, 8.61; N, 4.25.

Reaction of $Cp_2Ce(O^{t}Bu)_2$ with $LiN(TMS)_2$. A dark brown solution containing $Cp_2Ce(O^{t}Bu)_2$ (18 mg, 0.043 mmol), $LiN(TMS)_2$ (25 mg, 0.15 mmol) and hexamethylbenzene as an internal standard (7 mg, 0.043 mmol) was

prepared in benzene-d_6 (1.2 mL), and sealed in a J. Young capped NMR tube. After 30 min at room temperature, the starting reagents remained the only discernable species in solution by ^{1}H NMR. After a total of 18 h at room temperature, numerous different unidentifiable species were observed to have formed (range of observed resonances: TMS δ 0.00-0.43; ^{t}BuO δ 1.25-1.58; Cp δ 5.60-6.31). After greater than 48 h the reaction mixture is observed to be contain significantly fewer observable species, in which $(^t\text{BuO})_2\text{Ce}(\text{N}(\text{TMS})_2)_2$ (**1**) now comprises approximately 60% of the $^t\text{BuO}/\text{N}(\text{TMS})_2$ resonances. No considerable loss of material is observed during the course of the reaction (range of observed resonances: TMS δ 0.09-0.49; ^{t}BuO δ 1.26-1.58; Cp δ 5.60-6.31).

Cerium-Oxygen Bond Cleavage. Reaction of $\text{Ce}(\text{O}^t\text{Bu})_4(\text{THF})_2$ with $\text{LiN}(\text{TMS})_2$. The combination of a solutions of $\text{Ce}(\text{O}^t\text{Bu})_4(\text{THF})_2$ (20 mg, 0.035 mmol) (pale yellow) and $\text{LiN}(\text{TMS})_2$ (33 mg, 0.20 mmol) (colorless) both in benzene-d_6 (500 μL each) resulted in the immediate formation of golden yellow solution. After sealing in a J. Young capped NMR tube, the ^{1}H NMR spectrum of the mixture was recorded, demonstrating that considerable decomposition of the tetraalkoxide to a variety of different inidentified species had occurred. The reaction mixture was kept at room temperature for 2 h, and subjected to sonication by submersion in a water filled ultrasonic cleaning bath for a period of 15 min. After sonication, the now orange solution, still proved to contain numerous species, although the presence of a significant quantity (≈ 10%) of $(^t\text{BuO})_2\text{Ce}(\text{N}(\text{TMS})_2)_2$ (**1**) was readily identifiable by ^{1}H NMR as the only discernable cerium(IV) amide species. The majority (≈ 95%) of other resonances due to TMS groups are accounted for by the presence of hexamethyldisilazane and unreacted $\text{LiN}(\text{TMS})_2$.

Preparation of $(^t\text{AmO})_2\text{Ce}(\text{NO}_3)_2(\text{THF})_2$ ($^t\text{AmO} = \text{OC}(\text{CH}_3)_2(\text{CH}_2\text{CH}_3)$). This alternative cerium(IV) precursor was prepared according to the literature procedure employed for the synthesis of $(^t\text{BuO})_2\text{Ce}(\text{NO}_3)_2(\text{THF})_2$, in similar yield.[54] The reaction chemistry of this complex is identical to that of the previously prepared *tertiary*-butoxide analog, and hence has been utilized in exploratory studies in order to exploit the *tertiary*-amyl group as a spectroscopic handle. ^{1}H NMR (250 MHz, C_6D_6) δ 0.95 (t, J = 7.2Hz, 6H, $\text{Et}(\text{CH}_3)$), 1.24 (s, 12H, CMe_2), 1.28 (s, 8H, THF), 1.47 (q, J = 7.3Hz, 4H, $\text{Et}(\text{CH}_2)$),

3.76 (s, 8H, THF) (*cf.* $(^tBuO)_2Ce(NO_3)_2(THF)_2$ δ 1.25 (s, 18H, ^tBu), 1.30 (s, 8H, THF), 3.79 (s, 8H, THF)).

Preparation of $(^tAmO)_2Ce(N(TMS)(4\text{-}C_6H_4R))_2$ (R = H, OMe). Under otherwise identical reaction conditions to those employed for the synthesis of **2**, the addition of two equivalents of the lithium anilide reagents $LiN(TMS)(4\text{-}C_6H_4R)$ (R = H, OMe) to a solution/suspension of $(^tAmO)_2Ce(NO_3)_2(THF)_2$ results in the formation of dark brown reaction suspensions, one of the major components of which is proposed to be the respective bisalkoxide bisamide complexes $(^tAmO)_2Ce(N(TMS)(4\text{-}C_6H_4R))_2$ (R = H, OMe). In each case, ^1H NMR spectra of the crude reaction mixtures clearly show the presence of several different diamagnetic species, making positive identification of the amide derivatives extremely difficult. Furthermore, since in each of the major product is generated in only 30-35% yield (determined by integration of total TMS resonances) isolation, and subsequent characterization, of individual species from these reaction mixtures has so far proven impossible. Tentative structural assignments are therefore based on comparative observations of ^1H NMR spectral data for the key resonances, e.g for $(^tAmO)_2Ce(N(TMS)(4\text{-}C_6H_5))_2$: ^1H, C_6D_6 δ 0.31 (s, 18H, 2 x $SiMe_3$), δ 1.19 (s, 12H, 2 x CMe_2).

Preparation of $(^tBuO)_2Ce(N(TMS)(o\text{-}MeOC_6H_4))_2$ (2). To a vigorously stirred suspension of $LiN(TMS)(o\text{-}MeOC_6H_4)$ (643 mg, 3.19 mmol) in hexane (25 mL) was added a suspension of $(^tBuO)_2Ce(NO_3)_2(THF)_2$ (886 mg, 1.60 mmol) in hexane (35 mL), at room temperature. The initial yellow color of the cerium complex rapidly gave way to the the formation of a purple suspension. After completion of the addition the reaction mixture was allowed to stir for a further 10 min before the solvent was removed *in vacuo*. The resultant solid was extracted into pentane (30 mL) and the solution was filtered. Removal of the solvent from the filtrate yielded the desired product as an impure purple solid (1004 mg). Analytically pure **2** may be obtained in the form of X-ray quality purple crystals upon allowing a hot concentrated solution of the complex in TMS_2O to gradually cool to room temperature. Yield of first crop: 330 mg (31%). The high solubility of **2** in all common solvents has so far precluded the isolation of the pure product in significantly greater yields. Somewhat improved yields may, however, be obtained with further

concentration and cooling of the supernatant to -40 °C. ^{1}H NMR (300 MHz, C_6D_6) δ 0.63 (s, 18H, $SiMe_3$), 1.35 (s, 18H, ^{t}BuO), 3.39 (s, 6H, OMe), 6.18 (dd, J^1 = 1.4Hz, J^2 = 8.1Hz, 2H), 6.47 (m, 4H), 6.96 (dt, J^1 = 1.4Hz, J^2 = 7.7Hz, 2H). ^{13}C NMR (75.0 MHz, C_6D_6) δ 2.1, 33.8, 57.3, 83.8, 109.9, 117.7, 118.3, 122.2, 145.5, 152.0. Anal. Calcd for $C_{28}H_{50}CeN_2O_4Si_2$: C, 49.82; H, 7.47; N, 4.15. Found: C, 49.60; H, 7.69; N, 3.69.

Attempted Preparation of (^{t}BuO)$_2$Ce(N(TMS)(2, 6-^{i}Pr$_2$C$_6$H$_3$))$_2$. To a vigorously stirred suspension of (^{t}BuO)$_2$Ce(NO$_3$)$_2$(THF)$_2$ (35 mg, 0.63 mmol), in hexane (3 mL) at room temperature was added a suspension of LiN(TMS)(2, 6-^{i}Pr$_2$C$_6$H$_3$) (32 mg, 0.12 mmol) in hexane (3 mL) resulting in immediate formation of a red-brown suspension. After an additional 10 min an aliquot of the reaction mixture was filtered away from insoluble salts and taken to dryness under reduced pressure. The subsequent solid residue was further dissolved into benzene-d$_6$ and the ^{1}H NMR spectrum of the product recorded. A comparison of the ^{1}H NMR spectrum with that formed from a similar reaction with a single equivalent of lithium amide reagent reveals that the major product is the same in both cases, i.e. **3**, in similar yield. The presence of resonances of smaller intensity which are seemingly due to cerium(IV) bonded amide derivatives ($SiMe_3$: δ 0.41, 0.40, 0.32) indicates that the desired bisamide may actually be present as a minor product, however, innumerable overlapping *tertiary*-butoxide and isopropyl resonances does not allow for confirmation of this observation. Approximately 35% of the total observable amide species remains unreacted as THF solvated LiN(TMS)(2, 6-^{i}Pr$_2$C$_6$H$_3$)(THF)$_x$ species.

Preparation of (^{t}BuO)$_2$Ce(N(TMS)CH$_2$CH$_2$OMe)$_2$. Preliminary ^{1}H NMR scale experiments suggests that the major product of the reaction between the (^{t}BuO)$_2$Ce(NO$_3$)$_2$(THF)$_2$ and LiN(TMS)(CH$_2$CH$_2$OMe) (2 equiv), in hexane, at room temperature is the bisalkoxide bisamide derivative (^{t}BuO)$_2$Ce(N(TMS)CH$_2$CH$_2$OMe)$_2$. The addition of a solution of LiN(TMS)(CH$_2$CH$_2$OMe) (19 mg, 0.124 mmol) in hexane (1-2 mL) to a suspension of (^{t}BuO)$_2$Ce(NO$_3$)$_2$(THF)$_2$ (35 mg, 0.063 mmol) in hexane (1-2 mL) results in immediate formation of a dark brown suspension. After a few minutes (5-10 min) at room temperature an aliquot of the reaction mixture was filtered, and the solvent removed *in vacuo* to yield a dark brown solid

product. The crude product mixture was subsequently extracted into benzene-d_6, for the purpose of spectroscopic analysis. The ^1H NMR spectrum of the benzene soluble species reveals the existence of a major species, composing approximately 30-40% of the resonances due to obervable *tertiary*-butoxide resonances, or 60% of the total trimethylsilyl signals. ^1H NMR (300 MHz, C_6D_6) δ 0.36 (s, 18H, $SiMe_3$), 1.42 (s, 18H, ^tBuO), 3.35 (s, 6H, OMe). The impurity of the reaction mixture prevents clear cut identification of the methylene resonances. After extended periods (48 h) at room temperature the product mixture is observed to change considerably, however, resulting in the formation of a pale colored suspension similar to that observed in reactions resulting only in reduction products. ^1H NMR spectroscopy reveals the loss of all of the previously observed resonances due to the major and other species, and the formation of innumerable organic species.

Preparation of ($^tBuO)_3Ce(N(TMS)(2, 6\text{-}^iPr_2C_6H_3)$ (3). This species is observed to be the major species formed from attempts to prepare bisalkoxide amide species of the type ($^tBuO)_3Ce(N(TMS)(2, 6\text{-}^iPr_2C_6H_3)(X)$ (X = NO_3, OSO_2CF_3). As a result the synthesis of this complex may be achieved from either nitrate or triflate precursors although isolation and purification in both cases has so far proven extremely problematic. Although this species has subsequently been fully characterized the low-percentage conversion, reaction impurities and extreme solubility of the ultimate product have combined to hamper efforts to gain a realistic estimate for the yield of the product when prepared by either of the following representative procedures. Isolated yields to date have been of the order of approximately 10%. ^1H NMR (300 MHz, C_6D_6) δ 0.42 (s, 9H, $SiMe_3$), 1.22 (d, J = 6.9Hz, 6H, $^iPr(Me)$), 1.24 (s, 27H, ^tBuO), 1.49 (d, J = 7.2Hz, 6H, $^iPr(Me)$), 3.46 (heptet, J = 6.8Hz, 2H, $^iPr(CH)$), 6.99 (t, J = 7.8Hz, 1H), 7.29 (d, J = 7.8Hz, 2H). ^{13}C NMR (75 MHz, C_6D_6) δ 2.4, 25.1, 26.9, 27.2, 33.5, 82.3, 124.8, 125.8, 144.0. Signals for only three of the four distinct aromatic carbon atoms are detected in the ^{13}C NMR spectrum in benzene-d_6 at room temperature, presumably as a result of the coincidence of the chemical shift with the large intensity triplet due to residual solvent. Anal. Calcd for $C_{27}H_{53}CeNOSi$: C, 53.34; H, 8.79; N, 2.30. Found: C, 53.79; H, 8.97; N, 2.23.

Preparation of 3 from a Cerium(IV) Nitrate Precursor. To a vigorously stirred yellow suspension of ($^tBuO)_2Ce(NO_3)_2(THF)_2$ (3.26 g, 5.88 mmol) in pentane

(60 mL) was added a colorless suspension of LiN(TMS)(2, 6-$^{i}Pr_2C_6H_3$) (1.50 g, 5.87 mmol), also in pentane. Addition of the lithium amide reagent to the cerium(IV) species effected an instantaneous change in the reaction mixture to a red-brown colored suspension. After an additional five minute period no further changes were observed to occur and the reaction mixture was filtered away from insoluble salts. At this stage, an examination of the ^{1}H NMR spectrum of an aliquot of the crude product reveals the presence of the trialkoxide amide ($^{t}BuO)_3Ce(N(TMS)(2, 6\text{-}^{i}Pr_2C_6H_3))$ as the major species (≈ 50%), together with a variety of other unidentified diamagnetic and paramagnetic impurities. The solvent was evaporated from the blood red filtrate *in vacuo*, ultimately yielding a sticky solid after a period of greater than 1 h under reduced pressure. Pentane was added, and evaporated, in an effort to remove residual THF, without apparent changes in the appearance of the product. The resultant solid was dissolved into a minimum volume of pentane and again filtered to remove persistent metastable salts. Finally, concentration of the filtrate and cooling to -40 °C (sometimes) results in the precipitation of a crystalline solid. Depending on the specific conditions employed recrystallization in this manner sometimes yields analytically pure crystalline material, while other instances result only in the precipitation of am impure microcrystalline solid.

Preparation of 3 from a Cerium(IV) Triflate Precursor. The addition of a colorless pentane (20 mL) suspension of LiN(TMS)(2, 6-$^{i}Pr_2C_6H_3$) (528 mg, 2.06 mmol) to a rapidly stirring yellow suspension of ($^{t}BuO)_2Ce(OSO_2CF_3)_2(THF)_2$ (1.50 g, 2.06 mmol), in pentane (20 mL) results in the immediate formation of a dark red solution. After a short period without further changes (≈ 2 min) the solvent was removed *in vacuo* to yield an orange-brown powder. Dissolution of the solid in a minimum volume of solvent revealed the presence of insoluble salts which were removed by filtration through a Celite-topped glass frit. At this point, an examination of the ^{1}H NMR of the crude product shows the presence of the trialkoxide amide **3** as the major species, although present in only 30-50% yield, as determined by a comparison of spectral integrals due to the *tertiary*-butoxide signals. Howevrt, trimethysilyl and isopropyl resonances demonstrate that **3** is the only observable cerium(IV) amide present in the reaction mixture. Other than the low degree of conversion observed to take place in this system, the

major barrier to isolation of the product in pure form is seemingly the presence of metastable lithium triflate species, "$Li_x(OSO_2CF_3)_y(THF)_z$", which continue to precipitate gradually throughout the course of all recrystallization efforts. Suitable crystals of the extremely hydrocarbon soluble amide species were ultimately obtained for X-ray crystallographic analysis by slow evaporation of a pentane solution.

Preparation of $Ce(O^tBu)_4(THF)_2/Ce_3(O^tBu)_{10}O$. An attempt to utilize the literature procedure[54] for a large-scale (37 mmol) preparation of the tetra-*tertiary*-butoxide complex $Ce(O^tBu)_4(THF)_2$ was not found to reproducibly yield the desired product as the sole, analytically pure product. Rather, by ^1H NMR, the composition of the yellow product was determined to be a mixture of $Ce(O^tBu)_4(THF)_2$ and the known trimetallic species $Ce_3(O^tBu)_{10}O$ (ratio ≈ 1.3:1). The decaalkoxide oxide cluster complex has previously been determined to be the ultimate thermodynamically stable "$Ce_x(O^tBu)_{4x}$" species, known to be generated by slow decomposition of $Ce(O^tBu)_4(THF)_2$ over a period of days at room temperature.[54] Repeated attempts to remove the decalkoxide impurity by recrystallization from mixtures of THF and hexane simply resulted in further decomposition to $Ce_3(O^tBu)_{10}O$, ultimately resulting in a majority of the trimetallic species.

Subsequently, since gaining a pure sample of $Ce(O^tBu)_4(THF)_2$ was deemed unrealistic, a further effort was made to convert all of the material to the stable cluster, prior to undertaking further reactivity studies. Although the reported procedure for this process (toluene, RT, 2-3 days)[54] is proposed to be quantitative, herein, conversion was, however, only observed to take place to the extent of a total of three quarters that expected, even after a significant extension (> 7 days) of the reaction time employed in the original prodecure. It has been suggested that the incorporation of moisture into the reaction mixture of such a ligand redistribution process facillitates conversion to the trimetallic species $U_3(O^tBu)_{10}O$.[117] A similar phenomenom has yet to be proven in the preparation of this lanthanide analog, however.

Ultimately, in the absence of pure $Ce(O^tBu)_4(THF)_2$, the otherwise pure mixture of two "$Ce_x(O^tBu)_{4x}$" species (76.6% $Ce(O^tBu)_4(THF)_2$ and 23.4% $Ce_3(O^tBu)_{10}O$, as determined by ^1H NMR) was employed in protonolysis studies, and in the preparation of the cerium(IV) bisalkoxide bistriflate complex $(^tBuO)_2Ce(OSO_2CF_3)_2(THF)_2$.

Preparation of $(^tBuO)_2Ce(OSO_2CF_3)_2(THF)_2$. A suspension of ammonium triflate (3.43 g, 20.5 mmol), in THF (20 mL), was added to a rapidly stirring yellow THF solution (75 mL) containing a mixture of $Ce(O^tBu)_4(THF)_2$ (5.37 g, 9.31 mmol) and $Ce_3(O^tBu)_{10}O$ (1.64 g, 1.40 mmol). The reaction mixture was observed to lighten in color slightly upon dissolution of the ammonium salt. In accordance with precedented protonolysis reactions of this type,[54] the reaction was allowed to continue for a further 2 h at room temperature prior to removal of the solvent *in vacuo*. Subsequently, the yellow residue was extracted into hexane (≈ 50 mL) and filtered. Evaporation of the solvent resulted in precipitation of a yellow solid which was subsequently recrystallized from THF with cooling to -40 °C. Yield of yellow prisms: 618 mg (9%, if pure $(^tBuO)_2Ce(OSO_2CF_3)_2(THF)_2$). The ^1H and ^{13}C NMR spectra of the crystalline product are consistent with formation of the bisalkoxide disolvate $(^tBuO)_2Ce(OSO_2CF_3)_2(THF)_2$ although a single elemental analysis result is somewhat closer to that expected for the tetrasolvate $(^tBuO)_2Ce(OSO_2CF_3)_2(THF)_4$. Though the subsequent reactivity (i.e., preparation of **3**) of this species potentially suggests a trialkoxide triflate precursor, this is not evidenced by either NMR or analytical data. ^1H NMR (300 MHz, C_6D_6) δ 1.43 (s, 18H, ^tBuO), 1.47 (s, 8H, THF), 3.70 (s, 8H, THF). ^{13}C NMR (75 MHz) δ 25.5 (THF), 33.3 (^tBuO, $C(CH_3)_3$), 69.9 (THF), 84.5 (^tBuO, CMe_3); the proximity of the fluorine nuclei to the carbon atom effects splitting of the trifluoromethyl group to a quartet such that signal intensity precludes detection in a routine ^{13}C NMR experiment. Anal. Calcd for the disolvate $C_{18}H_{34}CeF_6O_{10}S_2$: C, 29.67; H, 4.70; for the tetrasolvate $C_{26}H_{50}CeF_6O_{10}S_2$: C, 35.77; H, 5.77. Found: C, 35.29; H, 6.11.

Preparation of $(^tBuO)_2Ce(Cl)_2(THF)_{\approx 2}$. Solid ammonium chloride (301 mg, 0.93 mmol) was added to a pale lemon yellow solution containing a mixture of $Ce(O^tBu)_4(THF)_2$ (115 mg, 0.20 mmol) and $Ce_3(O^tBu)_{10}(O)$ (186 mg, 0.16 mmol) in THF (20 mL). With rapid stirring, the ammonium salt was observed to slowly dissolve into the reaction mixture. The susequent solution was further allowed to stir at room temperature for 3 h. After such time an aliquot was removed from the golden yellow solution and taken to dryness *in vacuo*. The ^1H NMR spectrum of the orange solution in benzene-d_6 exhibits only two signals, presumably due to the coincidental chemical shifts of the *tertiary*-butoxide resonance and upfield THF resonances.

Notwithstanding, the spectrum is consistent with a tentative assignment for the product as the solvated bisalkoxide dichloride species "$(^tBuO)_2Ce(Cl)_2(THF)_{\approx 2}$". ^1H NMR (300 MHz, C_6D_6) δ 1.49 (s, 26H, ^tBuO and THF), 3.87 (s, 8H, THF). Furthermore, an attempt to prepare the bisamide **1**, by an analogous procedure to that employed with the nitrate precursor $(^tBuO)_2Ce(NO_3)_2(THF)_2$ resulted in conversion to the desired product in approximately 74% yield, as determined by a comparison of the integrals for *tertiary*-butoxide containing species. There are no distinct diamagnetic species in solution other than the bisalkoxide bisamide product, solvated lithium hexamethylsilazide, coordinated THF, and hexamethyldisilazane.

Preparation of $Ce_3(O^tBu)_{10}(NO_3)$ (4). In an attempt to isolate a pure sample of **3** from a $(^tBuO)_2Ce(NO_3)_2(THF)_2/LiN(TMS)(2, 6\text{-}^iPr_2C_6H_3)$ product mixture by recrystallization from pentane, the crude product mixture was stored as a concentrated solution in the refrigerator of the laboratory glove-box. After several months at -40 °C, the recrystallization attempt was observed to yield a significant quantity of two distinct solid phases. Large yellow-brown rhombohedral crystals were observed to be dispersed in an approximately equal amount of an amorphous pale yellow matrix of paramagnetic decomposition products. An X-ray crystal structure determination of the crystalline product identified the product as the trimetallic alkoxide nitrate cluster $Ce_3(O^tBu)_5(\mu\text{-}O^tBu)_3(\mu_3\text{-}O^tBu)_2(NO_3)$(pentane) (**4**).

Thermolysis of $(^tBuO)_2Ce(N(TMS)_2)_2$ in the Presence of Trimethylsilylcyclopentadiene. Preparation of $(TMSCp)_2Ce(O^tBu)_2$ (5). A solution of $(^tBuO)_2Ce(N(TMS)_2)_2$ (**1**) (28 mg, 0.046 mmol), trimethylsilylcyclopentadiene (15 μL, 0.091 mmol), and hexamethylbenzene as the internal standard (2 mg, 0.012 mmol) was prepared in benzene-d_6 and sealed in a J. Young valve-capped NMR tube. The ^1H NMR spectrum of the solution was as expected for the components, with no reaction, or intermolecular interactions observed simply on mixing. The composition remained unchanged even after extended periods (≈ 18 h) at room temperature. At elevated temperatures (70-100 °C), however, the red amide containing solution is observed to change colour to a dark brown solution. On further thermolysis (100 °C, 18 h) each of the resonances in the ^1H NMR spectrum of the starting cerium(IV) bisamide complex were observed to give

rise to signals corresponding to a single new species along with liberation of hexamethyldisilazane (^1H, C_6D_6 δ 0.09). The new resonance due to *tertiary*-butoxide ligands in the product accounts for approximately half (53%) of that of the precursor complex, with the free amine formed in comparable yield (58%). Furthermore, the resonances due to trimethylsilyl methyl protons in the rapidly equilibrating isomers of the cyclopentadiene substrate[131,132] are observed to merge to a single signal in the product. From the reagents and reaction stoichiometry employed, the ^1H NMR spectrum of the product and a comparison with the related metallocene complex $Cp_2Ce(O^tBu)_2$ the product has been assigned the structure $(TMSCp)_2Ce(O^tBu)_2$. In addition, this structure has been confirmed from an independent synthesis by the metathesis reaction between $(^tBuO)_2Ce(NO_3)_2(THF)_2$ and lithium trimethylsilylcyclopentadienide. ^1H NMR (300 MHz, C_6D_6) δ 0.47(s, 18H, $SiMe_3$), 1.32 (s, 18H, ^tBuO), 6.24 (t, J = 2.4Hz, 4H, Cp(CH)), 6.64 (t, J = 2.6Hz, 4H, Cp(CH)).

Reaction of $(^tBuO)_2Ce(NO_3)_2(THF)_2$ with Li(TMSCp). To a rapidly stirring suspension of $(^tBuO)_2Ce(NO_3)_2(THF)_2$ (59 mg, 0.11 mmol), in pentane (5 mL) was added a suspension of Li(TMCp) (30 mg, 0.21 mmol), also in pentane (10 mL). Combination of reagents resulted in the immediate formation of a brown suspension from the yellow colored cerium(IV) precursor. After 5 min at room temperature, the product mixture was filtered away from insoluble salts and the solvent was removed from the brown filtrate under reduced pressure. The resultant solid was subsequently extracted with benzene-d_6. The ^1H NMR spectrum of the crude product revealed the presence of a major species constituting approximately 58% of each of the total integral due to *tertiary*-butoxide and trimethylsilyl protons, with the respective chemical shift data corresponding to that of the $(^tBuO)_2Ce(N(TMS)_2)_2$/TMSCp derived product. ^1H NMR (300 MHz, C_6D_6) δ 0.47(s, 18H, $SiMe_3$), 1.32 (s, 18H, ^tBuO), 6.25 (t, J = 2.4Hz, 4H, Cp(CH)), 6.65 (t, J = 2.6Hz, 4H, Cp(CH)).

Thermolysis of $(^tBuO)_2Ce(N(TMS)_2)_2$ (1) in the Presence of Pentamethylcyclopentadiene. As per the reaction with trimethylsilyl-cyclopentadiene, a solution of **1** (21 mg, 0.035 mmol), C_5Me_5H (0.16 mmol), and the intermal standard C_6Me_6 (0.03 mmol) was thermolysed (≈ 100-110 °C)

in a J. Young capped NMR tube. After only 2 h, a significant quantity of free hexamethyldisilazane was evident in the reaction mixture, along with residual **1**, however, no resonances due to new η^5-C_5Me_5 species were evident. Further thermolysis resulted only in the formation of the free amine, no Cp*-resonances, and the absence of observable signals due to *tertiary*-butoxide ligands, presumably as a result of reduction of the metal center. After several hours, a distinct, as yet unidentified broad singlet is observed at low-field (δ 6.87, width at half height $\approx$ 20Hz).

References

(1) Molander, G. A. *Chem. Rev.* **1992**, *92*, 29-68.

(2) Ho, T. L. In *Organic Syntheses by Oxidation with Metal Compounds*; W. J. Mijs and C. R. H. De Jonge, Ed.; Plenum: New York, NY, 1986; pp 569-631.

(3) Bradley, D. C.; Chatterjee, A. K.; Wardlaw, W. J. *J. Chem. Soc.* **1956**, 2260-2264.

(4) Bradley, D. C.; Chatterjee, A. K.; Wardlaw, W. J. *J. Chem. Soc.* **1956**, 3469-3472.

(5) Bradley, D. C.; Chatterjee, A. K.; Wardlaw, W. J. *J. Chem. Soc.* **1957**, 2600-2604.

(6) Streitwieser, A. J.; Kinsley, S. A. In *Fundamental and Technological Aspects of Organo-f-Element Chemistry*; T. J. Marks and Fragalà, Ed.; Reidel: Dordrecht, Holland, 1984; 77-114.

(7) Greco, A.; Cesca, S.; Bertolini, G. *J. Organomet. Chem.* **1976**, *113*, 321-330.

(8) Cotton, S. *Lanthanides and Actinides*; Oxford University: New York, NY, 1991.

(9) Kurz, M. E.; Ngoviwatchi, P. *J. Org. Chem.* **1981**, *46*, 4672-4676.

(10) Imamoto, T.; Koide, Y.; Hiyama, S. *Chem. Lett.* **1990**, 1445-1446.

(11) Ho, T.-L. *Synthesis* **1978**, 936.

(12) Hatanaka, Y.; Imamoto, T.; Yokoyama, M. *Tett. Lett.* **1983**, *24*, 2399-2400.

(13) Skarzewski, J. *Polyhedron* **1984**, *40*, 4997-5000.

(14) Kanemoto, S.; Tomioka, H.; Oshima, K.; Nozaki, H. *Bull. Chem. Soc. Jpn.* **1986**, *58*, 105-108.

(15) Molander, G. A. *Chem. Rev.* **1992**, *92*, 29-68 and references therein.

(16) Heeres, H. J.; Nijhoff, J.; Teuben, J. H.; Rogers, R. D. *Organometallics* **1993**, *12*, 2609-2617.

(17) Evans, W. J.; Keyer, R. A.; Ziller, J. W. *Organometallics* **1993**, *12*, 2618-2633.

(18) Evans, W. J.; Gummersheimer, T. S.; Boyle, T. J.; Ziller, J. W. *Organometallics* **1994**, *13*, 1281-1284.

(19) Evans, W. J.; Rabe, G. W.; Ziller, J. W. *Organometallics* **1994**, *13*, 1641-1645.

(20) Forsyth, C. M.; Nolan, S. P.; Stern, C. L.; Marks, T. J.; Rheingold, A. L. *Organometallics* **1993**, *12*, 3618-3623.

(21) Sasai, K.; Suzuki, T.; Itoh, N.; Tanaka, K.; Date, T.; Okamura, K.; Shibasaki, M. *J. Am. Chem. Soc.* **1993**, *115*, 10372-10373.

(22) Li, Y.; Fu, P.-F.; Marks, T. J. *Organometallics* **1994**, *13*, 439-440.

(23) Giardello, M. A.; Conticello, V. P.; Brard, L.; Sabat, M.; Rheingold, A. L.; Stern, C. L.; Marks, T. J. *J. Am. Chem. Soc.* **1994**, *116*, 10212-10240 and references therein.

(24) Giardello, M. A.; Conticello, V. P.; Brard, L.; Gagné, M. R.; Marks, T. J. *J. Am. Chem. Soc.* **1994**, *116*, 10241-10254 and references therein.

(25) *Fundamental and Technological Aspects of Organo-f-Element Chemistry*; Marks, T. J.; Fragalà, I. L., Ed.; Reidel: Dordrecht, Holland, 1984.

(26) Evans, W. J. *Polyhedron* **1987**, *6*, 803-835.

(27) de Bethune, A. J.; Loud, N. A. S. *Standard Aqueous Electrode Potentials and Temperature Coefficients at 25 °C*; C. A. Hampel: Skokie, IL, 1964.

(28) Cotton, F. A.; Wilkinson, G. *Advanced Inorganic Chemistry: A Comprehensive Text. 5th Ed.*; Wiley-Interscience: New York, NY, 1988, 975-976.

(29) Martin, W. C. *J. Phys. Chem. Ref. Data* **1974**, *3*, 771.

(30) Kalsotra, B. L.; Anand, S. P.; Multani, R. K.; Jain, B. D. *J. Organomet. Chem.* **1971**, *28*, 87-89.

(31) Kalsotra, B. L.; Multani, R. K.; Jain, B. D. *Isr. J. Chem.* **1971**, *9*, 569-572.

(32) Kalsotra, B. L.; Multani, R. K.; Jain, B. D. *J. Organomet. Chem.* **1971**, *31*, 67-69.

(33) Kalsotra, B. L.; Multani, R. K.; Jain, B. D. *J. Inorg. Nucl. Chem.* **1972**, *34*, 2679-2680.

(34) Kalsotra, B. L.; Multani, R. K.; Jain, B. D. *Chem. Ind. (London)* **1972**, 339-340.

(35) Kalsotra, B. L.; Multani, R. K.; Jain, B. D. *Inorg. Nucl. Chem.* **1973**, *35*, 311-313.

(36) Kapur, S.; Multani, R. K. *J. Organomet. Chem.* **1973**, *63*, 301-303.

(37) Kapur, S.; Kalsotra, B. L.; Multani, R. K. *J. Inorg. Nucl. Chem.* **1973**, *35*, 1689-1691.

(38) Schumann, H. In *Organometallics of the f-Elements*; T. J. Marks and R. D. Fischer, Ed.; Reidel: Dordrecht, Holland, 1979; 81-112.

(39) Schumann, H. *Angew. Chem. Int. Ed. Engl.* **1984**, *23*, 474-493.

(40) Jacob, K.; Glanz, M.; Tittes, K.; Thiele, K. H. *Z. Anorg. Allg. Chem.* **1988**, *556*, 170-178.

(41) Streitwieser, A., Jr; Kinsley, S. A.; Rigsbee, J. A.; Fragalà, I. L.; Ciliberto, E.; Rösch, N. *J. Am. Chem. Soc.* **1985**, *107*, 7786-7788.

(42) Deacon, G. B.; Tuong, T. D.; Vince, D. G. *Polyhedron* **1983**, *2*, 969-970.

(43) Marks, T. J. *Progr. Inorg. Chem.* **1978**, *24*, 51.

(44) Carey, F. A.; Sundberg, R. J. *Advanced Organic Chemistry, 3d Ed: Part A. Structure and Mechanisms*; Plenum: New York, NY, 1990, 513-518.

(45) Rösch, N.; Streitwieser, A., Jr. *J. Organomet. Chem.* **1978**, *145*, 195-200.

(46) Rösch, N.; Streitwieser, A., Jr. *J. Am. Chem. Soc.* **1983**, *105*, 7237-7240.

(47) Gulino, A.; Casarin, M.; Conticello, V. P.; Gaudiello, J. G.; Mauermann, H.; Fragala, I.; Marks, T. J. *Organometallics* **1988**, *7*, 2360-2364.

(48) Boussie, T. R.; Eisenberg, D. C.; Rigsbee, J.; Streitwieser, A.; Zalkin, A. *Organometallics* **1991**, *10*, 1922-1928.

(49) Kilimann, U.; Herbst-Irmer, R.; Stalke, D.; Edelmann, F. T. *Angew. Chem. Int. Ed. Engl.* **1994**, *33*, 1618-1621.

(50) Evans, W. J.; Deming, T. J.; Ziller, J. W. *Organometallics* **1989**, *8*, 1581-1583.

(51) Evans, W. J.; Shreeve, J. L.; Ziller, J. W. *Organometallics* **1994**, *13*, 731-733.

(52) Gradeff, P. S.; Schreiber, F. G.; Brooks, K. C.; Sievers, R. E. *Inorg. Chem.* **1985**, *24*, 1110-1111.

(53) Gradeff, P. S.; Schreiber, F. G.; Mauermann, H. *J. Less-Common Met.* **1986**, *126*, 335-338.

(54) Evans, W. J.; Deming, T. J.; Olofson, J. M.; Ziller, J. W. *Inorg. Chem.* **1989**, *28*, 4027-4034.

(55) Gradeff, P. S.; Yunlu, K. *J. Less-Common Met.* **1989**, *149*, 81-85.

(56) Gradeff, P. S.; Yunlu, K.; Deming, T. J.; Olofson, J. M.; Doedens, R. J.; Evans, W. J. *Inorg. Chem.* **1990**, *29*, 420-424.

(57) Gradeff, P. S.; Yunlu, K.; Gleizes, A.; Galy, J. *Polyhedron* **1989**, *8*, 1001-1005.

(58) Gradeff, P. S.; Mauermann, H.; Schreiber, F. G. *J. Less-Common Met.* **1989**, *149*, 87-94.

(59) Hubert-Pfalzgraf, L. G.; El Khokh, N.; Daran, J.-C. *Polyhedron* **1992**, *11*, 59-63.

(60) Buchler, J. W.; De Cian, A.; Fischer, J.; Kihn-Botulinski, M.; Paulus, H.; Weiss, R. *J. Am. Chem. Soc.* **1986**, *108*, 3652-3659.

(61) Buchler, J. W.; De Cian, A.; Fischer, J.; Hammerschmitt, P.; Löffler, J.; Scharbert, B.; Weiss, R. *Chem. Ber.* **1989**, *122*, 2219-2228.

(62) Lachkar, M.; De Cian, A.; Fischer, J.; Weiss, R. *New. J. Chem.* **1988**, *12*, 729-731.

(63) Haghighi, M. S.; Teske, C. L.; Homborg, H. *Z. Anorg. Allg. Chem.* **1992**, *608*, 73-80.

(64) Timmons, J. H.; Martin, J. W. L.; Martell, A. E.; Rudolf, P.; Clearfield, A.; Arner, J. H.; Loeb, S. J.; Willis, C. J. *Inorg. Chem.* **1980**, *19*, 3553-3557.

(65) Terzis, A.; Mentzafos, D.; Tajmir-Riahi, H. A. *Inorg. Chim. Acta* **1984**, *84*, 187-193.

(66) Nugent, W. A.; Mayer, J. M. *Metal-Ligand Multiple Bonding*; John Wiley and Sons: New York, NY, 1988.

(67) Hessen, B.; Buijink, J.-K.; Meetsma, A.; Teuben, J. H.; Helgesson, G.; Håkansson, M.; Jagner, S. *Organometallics* **1993**, *12*, 2268-2276.

(68) Cummins, C. C.; Baxter, S., M; Wolczanski, P. T. *J. Am. Chem. Soc.* **1988**, *110*, 8731-8733.

(69) Walsh, P. J.; Hollander, F. J.; Bergman, R. G. *J. Am. Chem. Soc.* **1988**, *110*, 8729-8731.

(70) Doxsee, K. M.; Farahi, J. B. *J. Chem. Soc., Chem. Commun.* **1990**, 1452-1454.

(71) Hill, J. E.; Profilet, R. D.; Fanwick, P. E.; Rothwell, I. P. *Angew. Chem. Int. Ed. Engl.* **1990**, *29*, 664-665.

(72) Roesky, H. W.; Voelker, H.; Witt, M.; Noltemeyer, M. *Angew. Chem. Int. Ed. Engl.* **1990**, *29*, 669-670.

(73) Cummins, C. C.; Schaller, C. P.; Van Duyne, G. D.; Wolczanski, P. T.; Chan, A. W. E.; Hoffman, R. *J. Am. Chem. Soc.* **1991**, *113*, 2985-2994.

(74) Cummins, C. C.; Van Duyne, G. D.; Schaller, C. P.; Wolczanski, P. T. *Organometallics* **1991**, *10*, 164-170.

(75) Walsh, P. J.; Carney, M. J.; Bergman, R. G. *J. Am. Chem. Soc.* **1991**, *113*, 6343-6345.

(76) Hill, J. E.; Fanwick, P. E.; Rothwell, I. P. *Inorg. Chem.* **1991**, *30*, 1143-1144.

(77) Duchateau, R.; Williams, A. J.; Gambarotta, S.; Chiang, M. Y. *Inorg, Chem.* **1991**, *30*, 4863-4866.

(78) Arney, D. J.; Bruck, M. A.; Huber, S. R.; Wigley, D. E. *Inorg. Chem.* **1992**, *31*, 3749-3755.

(79) Winter, C. H.; Sheridan, P. H.; Lewkebandara, T. S.; Heeg, M. J.; Proscia, J. W. *J. Am. Chem. Soc.* **1992**, *114*, 1095-1097.

(80) Arney, D. S. J.; Burns, C. J.; Smith, D. C. *J. Am. Chem. Soc.* **1992**, *114*, 10068-10069.

(81) Arney, D. S. J.; Burns, C. J. *J. Am. Chem. Soc.* **1993**, *115*, 9840-9841.

(82) Smith, D. C.; Burns, C. J.; Arney, D. S. J. Unpublished work.

(83) Gradeff, P. S.; Yunlu, K.; Deming, T. J.; Olofson, J. M.; Ziller, J. W.; Evans, W. J. *Inorg. Chem.* **1989**, *28*, 2600-2604 and references therein.

(84) Lappert, M. F.; Power, P. P.; Sanger, A. R.; Srivastava, R. C. *Metal and Metalloid Amides*; Ellis-Horwood: Chichester, 1980.

(85) Bradley, D. C.; Mehrotra, R. C.; Gaur, D. P. *Metal Alkoxides*; Academic: London, 1978.

(86) Ho, T. L. In *Organic Syntheses by Oxidation with Metal Compounds*; W. J. Mijs and C. R. H. De Jonge, Ed.; Plenum: New York, NY, 1986; 569-631 and references therein.

(87) Kagan, H. B. In *Fundamental and Technological Aspects of Organo-f-Element Chemistry*; T. J. Marks and Fragalà, Ed.; Reidel: Dordrecht, Holland, 1984; 49-76.

(88) Lin, J.; Hey-Hawkins, E.; von Schnering, H. G. *Z. Naturforsch* **1990**, *45a*, 1241-1247.

(89) Mazhar-Ul-Haque; Caughlan, C. N.; Hart, F. A.; Van Nice, R. *Inorg. Chem.* **1971**, *10*, 115-122.

(90) Brezina, F. *Coll. Czech. Chem. Commun.* **1971**, *36*, 2889-2894.

(91) Barry, J.; Du Preez, J. G. H.; Els, E.; Rowher, H. E.; Wright, P. J. *Inorg. Chim. Acta* **1981**, *53*, L17-L18.

(92) Du Preez, J. G. H.; Rowher, H. E.; De Wet, J. F.; Caira, M. R. *Inorg. Chim. Acta* **1978**, *26*, L59-L60.

(93) *Comprehensive Organometallic Chemistry II*; Abel, E. W.; Stone, G. A.; Wilkinson, G., Ed.; Pergamon: New York, NY, 1994.

(94) Evans, W. J.; Golden, R. E.; Ziller, J. W. *Inorg. Chem.* **1991**, *30*, 4963-4968.

(95) Stecher, H. A.; Sen, A.; Rheingold, A. L. *1988* **1988**, *27*, 1130-1133.

(96) Airoldi, C.; Bradley, D. C.; Chudzynska, H.; Hursthouse, M. B.; Malik, K. M. A.; Raithby, P. R. *J. Chem. Soc., Dalton Trans.* **1980**, 2010-2015.

(97) Bradley, D. C.; Chudzynska, H.; Backer-Dirks, J. D.; Hursthouse, M. B.; Ibrahim, A. A.; Motevalli, M.; Sullivan, A. C. *Polyhedron* **1990**, *9*, 1423-1427.

(98) Laurent, F.; Cyr-Athis, O.; Legros, J.-P.; Choukroun, R.; Valade, L. *New. J. Chem.* **1994**, *18*, 575-580.

(99) Roberts, J. R.; Ingold, K. U. *J. Am. Chem. Soc.* **1973**, *95*, 3228-3235.

(100) In *Comprehensive Organometallic Chemistry*; G. Wilkinson, F. G. A. Stone and E. W. Abel, Ed.; Pergamon: New York, NY, 1982; Vol. 2; 120-130.

(101) Bartlett, R. A.; Power, P. P. *J. Am. Chem. Soc.* **1987**, *109*, 6509-6510.

(102) Choquette, D. M.; Timm, M. J.; Hobbs, J. L.; Rahim, M. M.; Ahmed, K. J.; Planalp, R. P. *Organometallics* **1992**, *11*, 529-534.

(103) Teuben, J. H. In *Fundamental and Technological Aspects of Organo-f-Element Chemistry*; T. J. Marks and Fragalà, Ed.; Reidel: Dordrecht, Holland, 1984; 195-227.

(104) Shannon, R. D. *Acta Crystallogr., Sect A: Cryst. Phys., Diffr., Theor. Gen Crystallogr.* **1976**, *A32*, 751-767.

(105) Bennett, M. A. *Pure. Appl. Chem.* **1989**, *61*, 1695-1700.

(106) Bennett, M. A.; Schwemlein, H. P. *Angew. Chem. Int. Ed. Engl.* **1989**, *28*, 1296-1320.

(107) Buchwald, S. L.; Watson, B. T. *J. Am. Chem. Soc.* **1986**, *108*, 7411-7413.

(108) Buchwald, S. L.; Lucas, E. A.; Dewan, J. C. *J. Am. Chem. Soc.* **1987**, *109*, 4396-4397.

(109) Buchwald, S. L.; Watson, B. T.; Wannamaker, M. W.; Dewan, J. C. *J. Chem. Soc., Chem. Commun.* **1989**, *111*, 4486-4494.

(110) Chisholm, M. H. *Polyhedron* **1983**, *2*, 681-721.

(111) Sonnenberger, D. C.; Morss, L. R.; Marks, T. J. *Organometallics* **1985**, *4*, 352-355.

(112) Chisholm, M. H.; Clark, D. L. *Comments Inorg. Chem.* **1987**, *6*, 23-40.

(113) Sigel, G. A.; Decker, D.; Olmstead, M. M.; Power, P. P. *Inorg. Chem.* **1987**, *26*, 1773-1780.

(114) Clark, D. L.; Watkin, J. G. *Inorg. Chem.* **1993**, *32*, 1766-1772.

(115) Evans, W. J.; Grate, J. W.; Bloom, I.; Hunter, W. E.; Atwood, J. L. *J. Am. Chem. Soc.* **1985**, *107*, 405-409.

(116) Miskowski, V.; Gray, H. B.; Poon, C. K.; Ballhausen, C. J. *Mol. Phys.* **1974**, *28*, 747-757.

(117) Van der Sluys, W. G.; Sattelberger, A. P. *Polyhedron* **1990**, *9*, 1843-1848.

(118) Cotton, F. A.; Marler, D. O.; Schwotzer, W. *Inorg. Chim. Acta* **1984**, *85*, L31-L32.
(119) Cotton, F. A.; Marler, D. O.; Schwotzer, W. *Inorg. Chim. Acta* **1984**, *95*, 207-209.
(120) Chisholm, M. H.; Folting, K.; Huffman, J. C.; Kirkpatrick, C. C. *J. Am. Chem. Soc.* **1981**, *103*, 5967-5968.
(121) Chisholm, M. H.; Folting, K.; Huffman, J. C.; Kober, E. M. *Inorg. Chem.* **1985**, *24*, 241-245.
(122) Edelstein, N. M. *Organometallics of the f-Elements;* Reidel: Dordrecht, Holland, 1979.
(123) Veal, B. W.; Lam, D. J. In *ACS Symposium Series No. 131;* N. M. Edelstein, Ed.; Washington, D.C., 1980; 427-441.
(124) Denning, R. G.; Norris, J. O. W. In *ACS Symposium Series No. 131;* N. M. Edelstein, Ed.; Washington, D.C., 1980; 313-330.
(125) Gradeff, P. S.; Yunlu, K.; Deming, T. J.; Olofson, J. M.; Ziller, J. W.; Evans, W. J. *Inorg. Chem.* **1989**, *28*, 2600-2604.
(126) Beshouri, S. M.; Fanwick, P. E.; Rothwell, I. P.; Huffman, J. C. *Organometallics* **1987**, *6*, 891-893.
(127) Beshouri, S. M.; Fanwick, P. E.; Rothwell, I. P.; Huffman, J. C. *Organometallics* **1987**, *6*, 2498-2502.
(128) Tilley, T. D.; Andersen, R. A.; Spencer, B.; Ruben, H.; Zalkin, A.; Templeton, D. H. *Inorg. Chem.* **1980**, *19*, 2999-3003.
(129) *Organometallic Chemistry of the f-Block Elements;* Marks, T. J.; Fischer, R. D., Ed.; Reidel: Dordrecht, Holland, 1979.
(130) Colvin, E. W. *Silicon in Organic Synthesis (Butterworths Monographs in Chemistry and Chemical Engineering);* Butterworths: London, 1981, 4-14.
(131) Ashe, A. J. *J. Am. Chem. Soc.* **1970**, *92*, 1233-1235.
(132) Schulman, E. M. *J. Am. Chem. Soc.* **1983**, *105*, 3988-3991.

APPENDIX TO CHAPTER TWO

Appendix 2.1. ^1H NMR NOE of $Cp_2Zr(Me)(o\text{-}MeOC_6H_4)$ (1) (Zr-Me Irradiated)

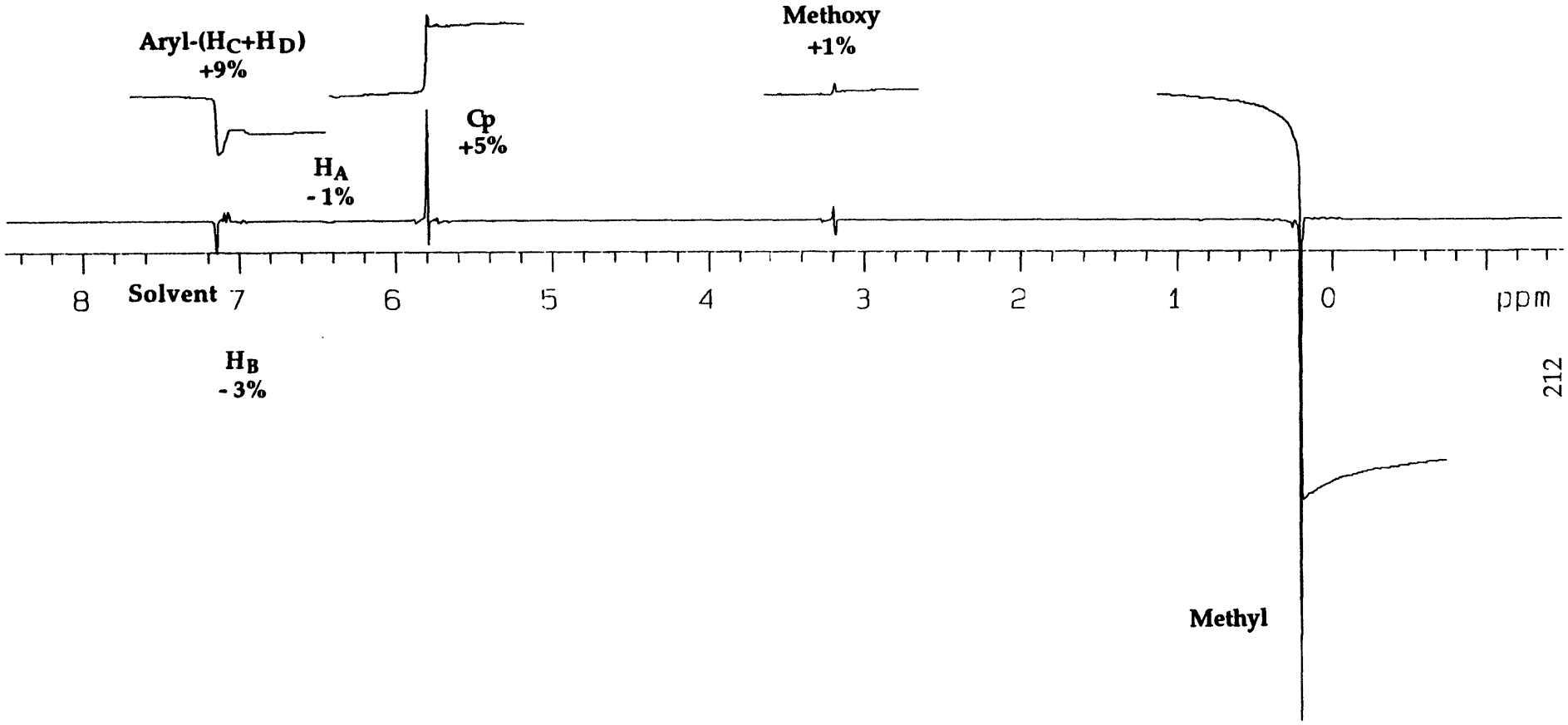

Appendix 2.2. ^1H NMR NOE of $Cp_2Zr(Me)(o\text{-}MeOC_6H_4)$ (1) (Methoxy Irradiated)

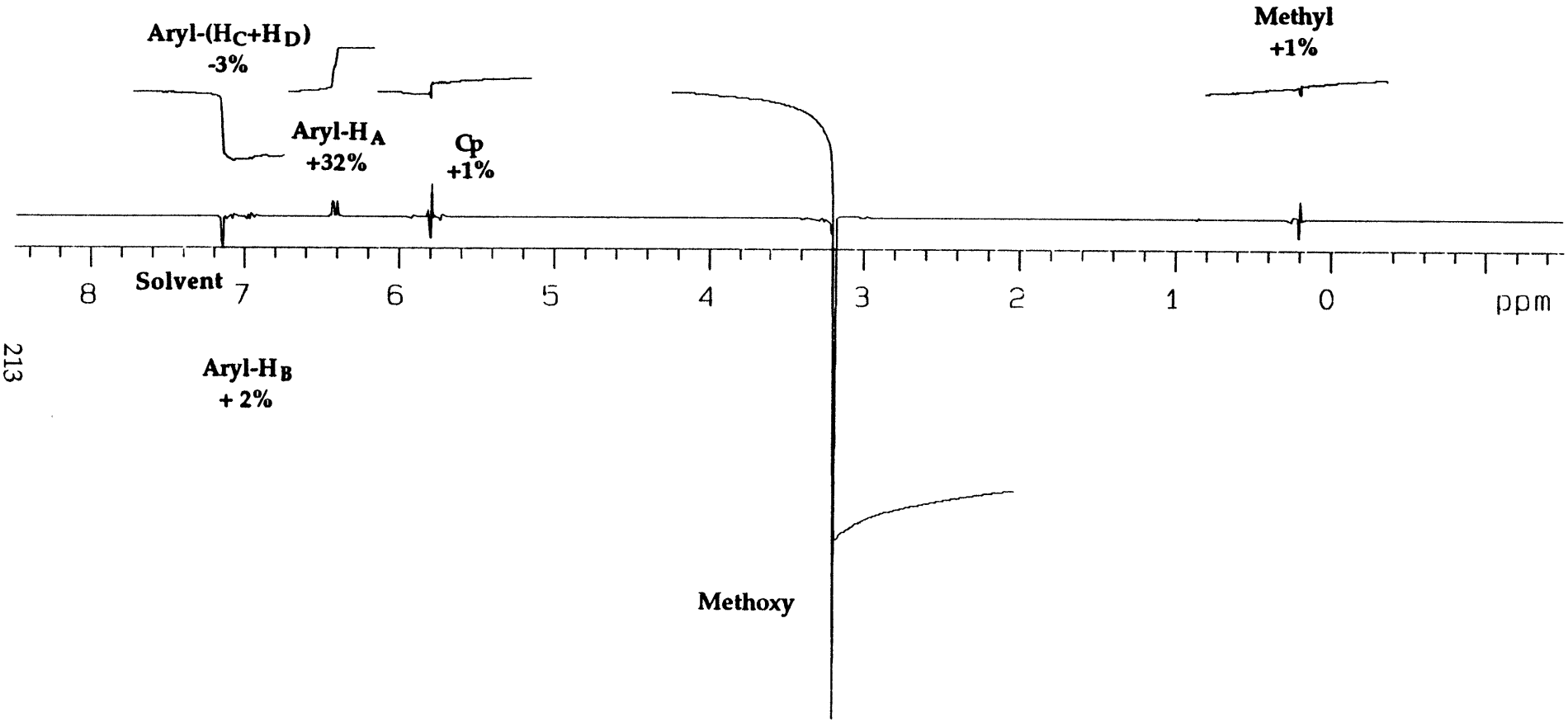

Appendix 2.3. ^1H NMR NOE of $Cp_2Zr(Me)(o\text{-}MeOC_6H_4)$ (1) (Aryl-H_A Irradiated)

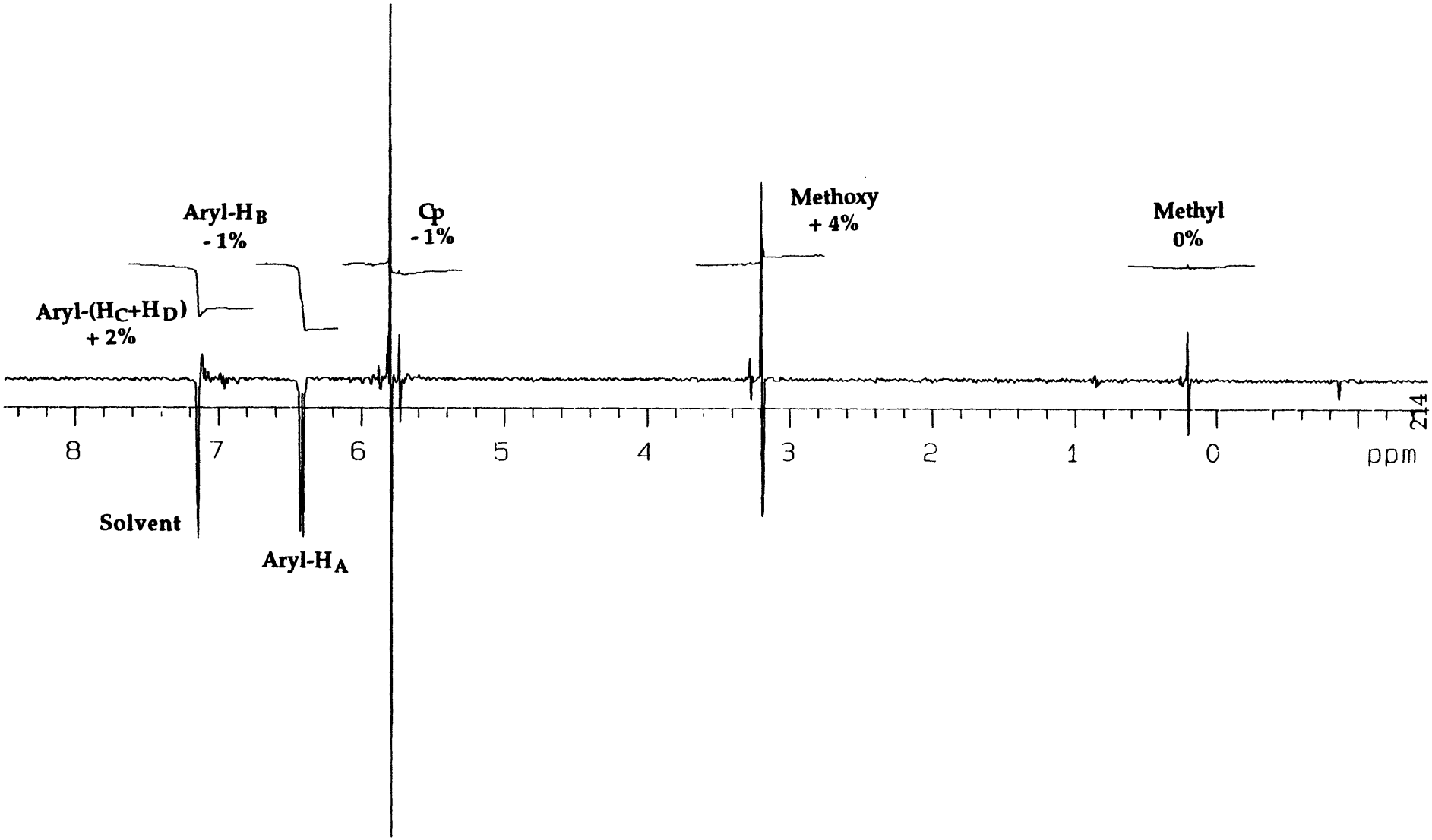

Appendix 2.4. ^1H NMR NOE of $Cp_2Zr(Me)(o\text{-}MeOC_6H_4)$ (1) (Aryl-H_B Irradiated)

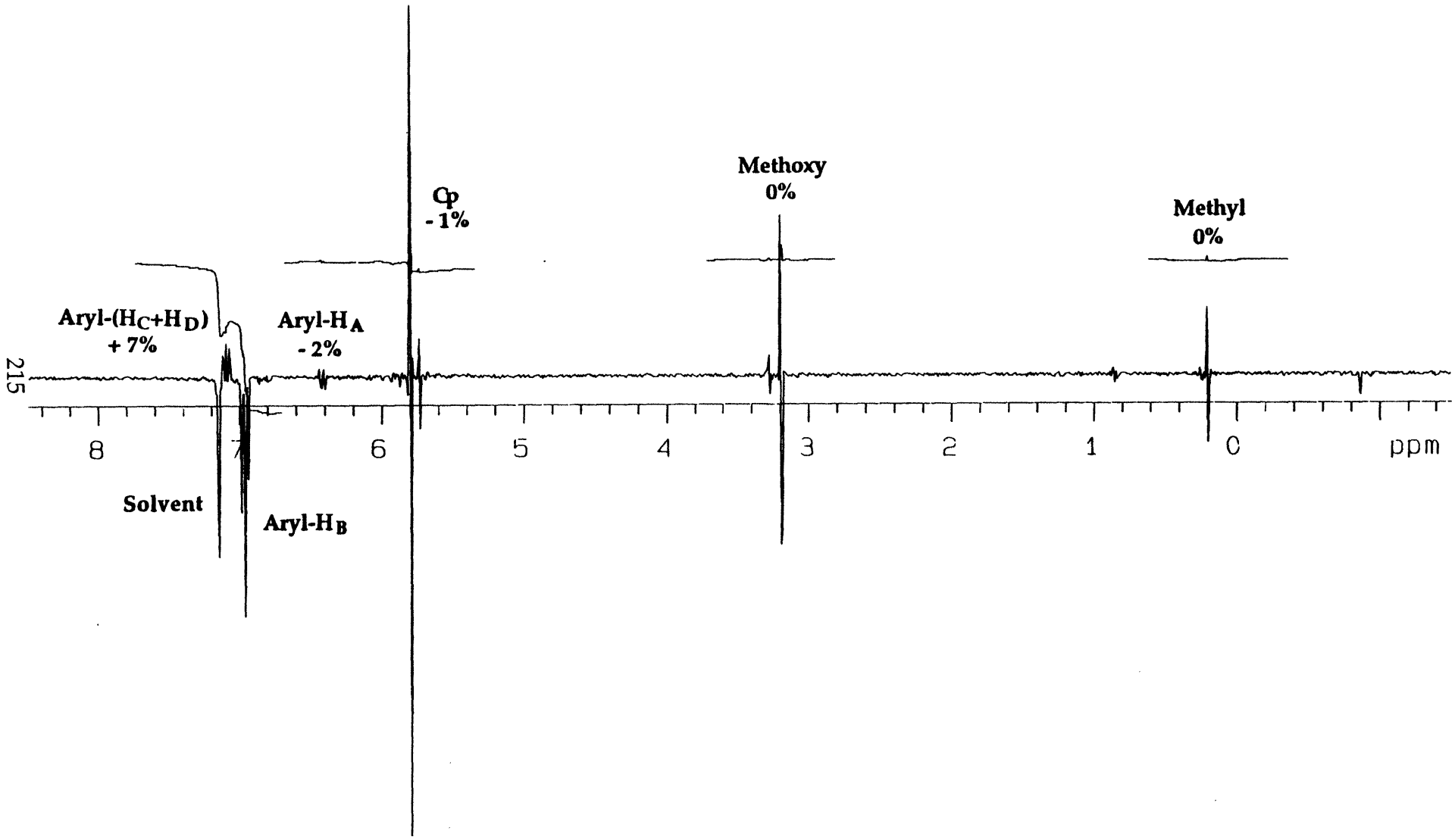

Appendix 2.5. ^1H NMR NOE of $Cp_2Zr(Me)(o\text{-}MeOC_6H_4)$ (1) (Aryl-(H_C+H_D) Irradiated)

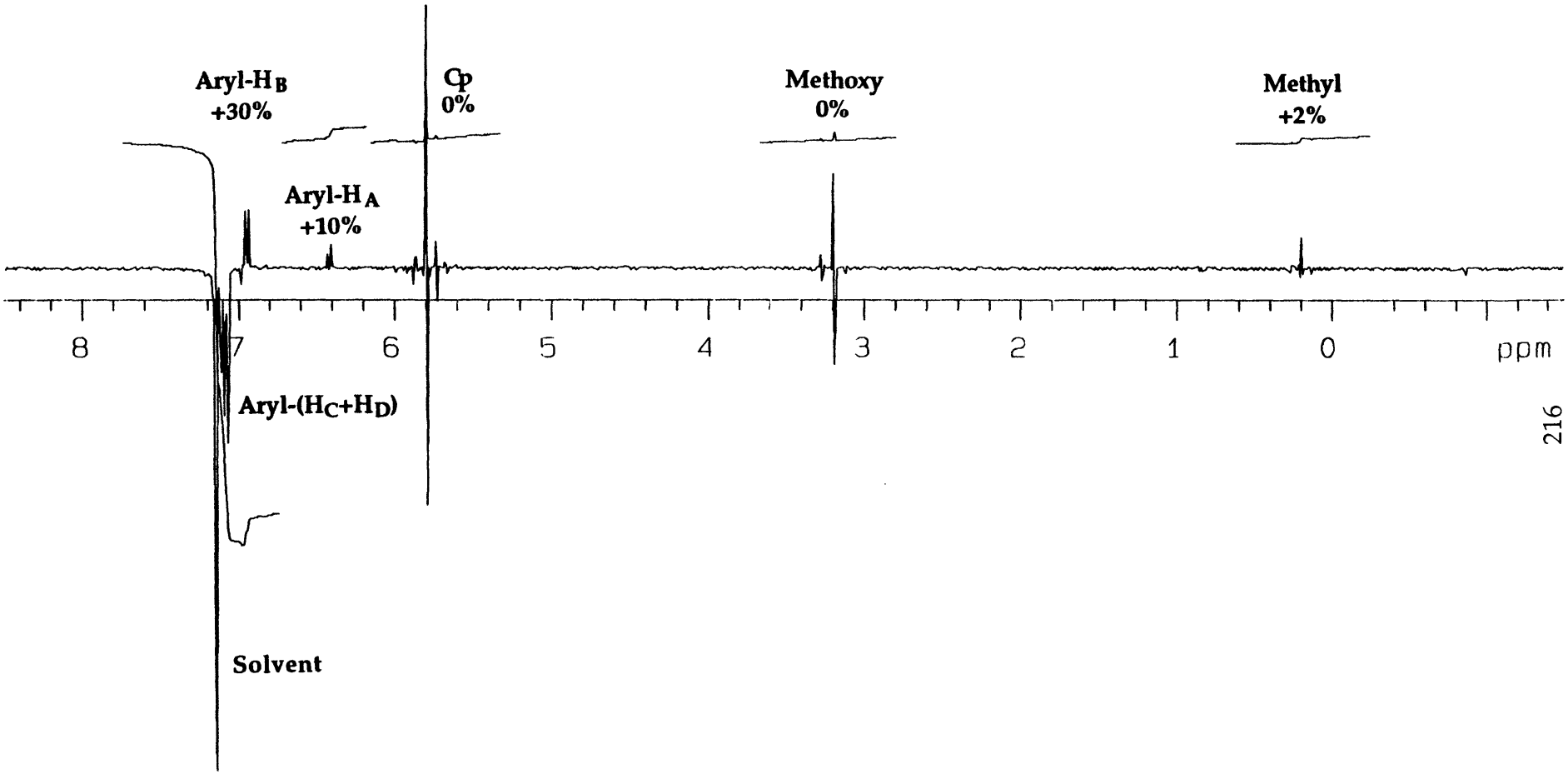

Appendix 2.6. ^1H NMR NOE of $Cp^*_2Th(Me)(o\text{-}MeOC_6H_4)$ (2) (Th-Me Irradiated) (Chris Schnabel, LANL)

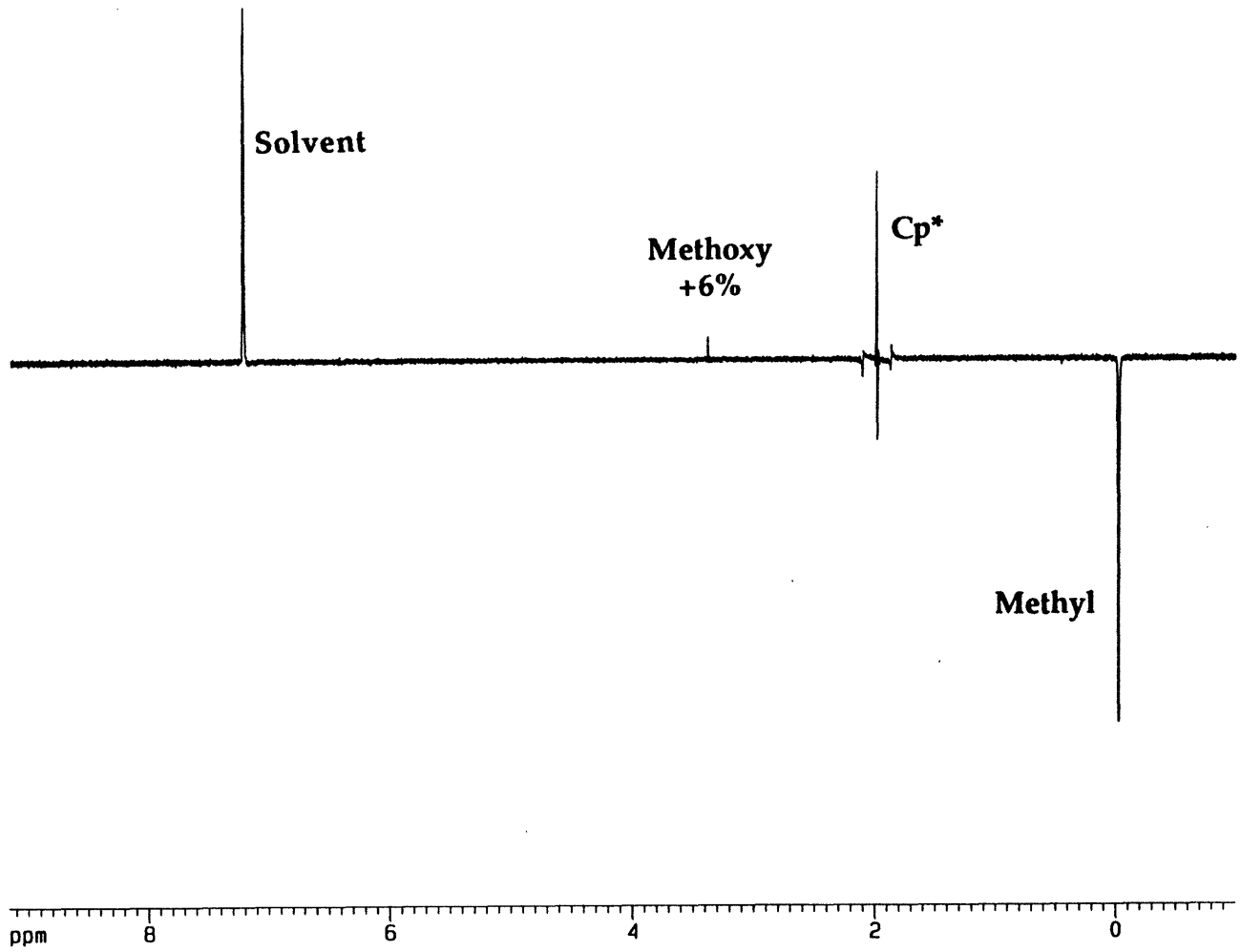

Appendix 2.7. ^1H NMR NOE of $Cp^*_2Th(Me)(o\text{-}MeOC_6H_4)$ (2) (Methoxy Irradiated) (Chris Schnabel, LANL)

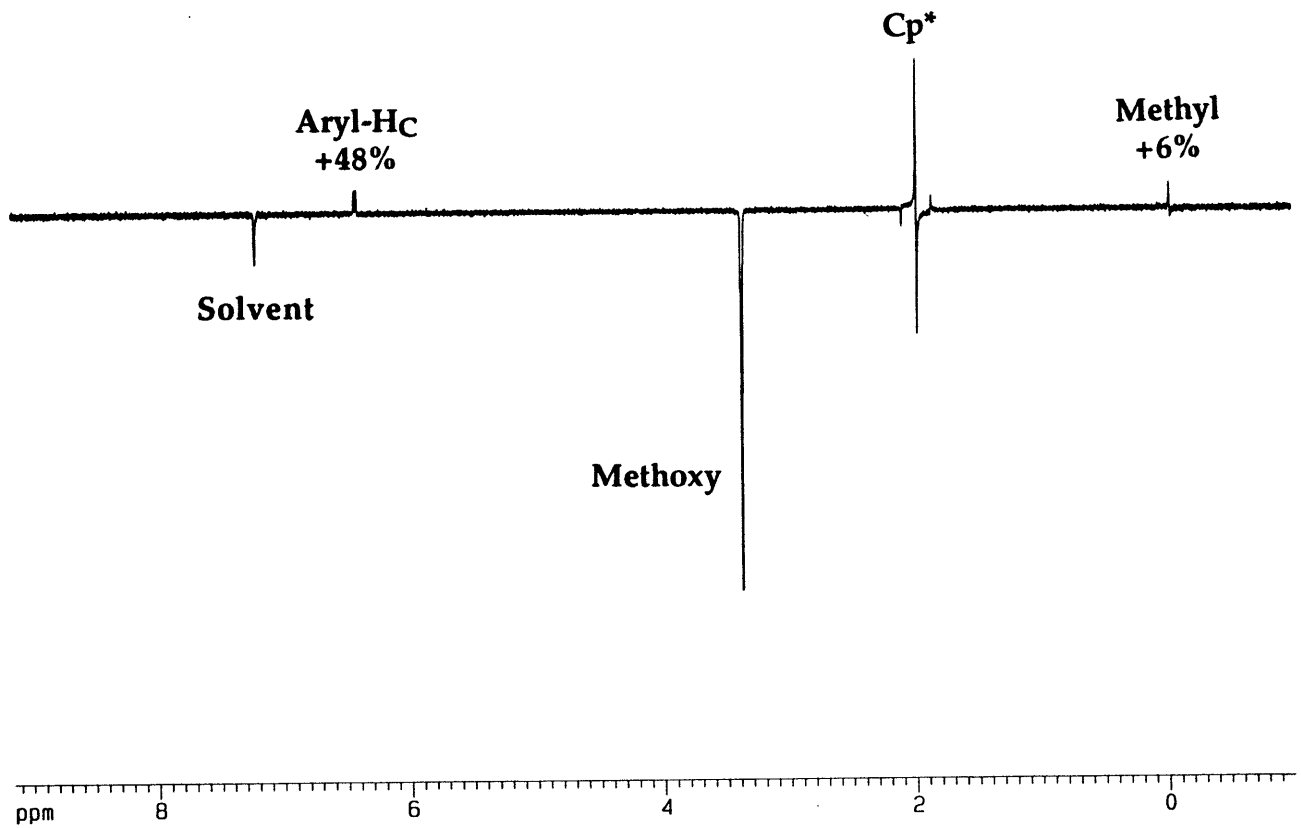

Appendix 2.8. Crystal Data Collection and Refinement Parameters for $Cp_2Zr(Me)(o\text{-}MeOC_6H_4)$ (1) and $Cp^*_2Th(Me)(o\text{-}MeOC_6H_4)$ (2)

compound	1	2
chemical formula	$C_{18}H_{20}OZr$	$C_{28}H_{40}OTh$
color, habit	colorless prisms	colorless prisms
crystal size (mm)	0.25 x 0.27 x 0.30	0.25 x 0.25 x 0.25
crystal system	orthorhombic	orthorhombic
space group	*P*cab	*P*mnb
a (Å)	14.406 (2)	14.383 (3)
b (Å)	15.798 (2)	20.331 (4)
c (Å)	13.543 (1)	8.639 (2)
α (deg)	90	90
β (deg)	90	90
γ (deg)	90	90
V (Å^3)	3082.11	2526.19
Z	8	4
density (calcd) (g/cm^3)	1.481	1.642
μ (cm^{-1})	6.94	45.308
temerature (K)	99	104
radiation	Mo Kα	Mo Kα
wavelength (Å)	0.71069	0.71069
monochromator	HOG crystal	HOG crystal
diffractometer	Picker	Picker
2Θ range (deg)	6-45	6-45
index ranges	$0 \le h \le 15$,	$0 \le h \le 15$,
	$0 \le k \le 16$,	$0 \le k \le 21$,
	$0 \le l \le 14$	$0 \le l \le 9$
no. rflns measured	2273	1945
no. indep. rflns	2016	1721
R_{int} (%)	1.8	0.0
R_w (%)	2.61	3.83
R (%)	2.61	3.95
solution	direct methods	direct methods

Appendix 2.9 Fractional Coordinates and Isotropic Thermal Parameters for $Cp_2Zr(Me)(o\text{-}MeOC_6H_4)$ (1)

atom	x	y	z	$B_{iso}/Å^2 \times 10^4$
Zr	0.88661(2)	0.0238(2)	0.27552(3)	14
O	0.6978(2)	0.1540(2)	0.3111(3)	37
C(1)	0.8493(3)	0.1383(2)	0.3715(3)	18
C(2)	0.9181(3)	0.1674(3)	0.4352(3)	28
C(3)	0.9045(4)	0.2338(3)	0.5012(3)	35
C(4)	0.8191(4)	0.2720(3)	0.5052(3)	33
C(5)	0.7492(3)	0.2465(3)	0.4427(3)	26
C(6)	0.7652(3)	0.1816(2)	0.3772(3)	22
C(7)	0.6127(4)	0.1996(4)	0.3073(7)	65
C(8)	1.0365(3)	0.0071(3)	0.3306(4)	29
C(9)	0.8824(3)	-0.1154(3)	0.3679(3)	22
C(10)	0.8419(3)	-0.1291(2)	0.2760(3)	20
C(11)	0.7599(3)	-0.0831(3)	0.2720(4)	22
C(12)	0.7499(3)	-0.0401(2)	0.3615(3)	22
C(13)	0.8264(3)	-0.0594(3)	0.4204(3)	19
C(14)	0.8788(4)	0.0038(3)	0.0927(3)	28
C(15)	0.8193(4)	0.0702(3)	0.1151(3)	31
C(16)	0.8812(7)	0.1373(3)	0.1466(3)	50
C(17)	0.9699(5)	0.1074(5)	0.1462(4)	59
C(18)	0.9692(4)	0.0267(5)	0.1132(4)	48

Appendix 2.10. Bond Distances for $Cp_2Zr(Me)(o\text{-}MeOC_6H_4)$ (1)

atom	atom	distance/Å	atom	atom	distance/Å
Zr	C(1)	2.291(4)	C(2)	C(3)	1.392(6)
Zr	C(8)	2.300(5)	C(3)	C(4)	1.372(7)
Zr	C(10)	2.500(4)	C(1)	C(2)	1.392(6)
Zr	C(9)	2.532(4)	C(5)	C(6)	1.376(6)
Zr	C(11)	2.487(4)	C(4)	C(5)	1.375(6)
Zr	C(12)	2.501(4)	C(9)	C(10)	1.391(6)
Zr	C(13)	2.516(4)	C(9)	C(13)	1.393(6)
Zr	C(14)	2.499(4)	C(10)	C(11)	1.387(6)
Zr	C(15)	2.490(5)	C(11)	C(12)	1.398(6)
Zr	C(16)	2.504(5)	C(12)	C(13)	1.395(6)
Zr	C(17)	2.501(5)	C(14)	C(15)	1.389(7)
Zr	C(18)	2.499(5)	C(14)	C(18)	1.380(7)
O	C(6)	1.390(5)	C(15)	C(16)	1.450(8)
O	C(7)	1.423(6)	C(16)	C(17)	1.363(10)
C(1)	C(6)	1.394(6)	C(17)	C(18)	1.351(9)
Zr	Ct(1)	2.210	Zr	Ct(2)	2.203

Appendix 2.11. Bond Angles for $Cp_2Zr(Me)(o\text{-}MeOC_6H_4)$ (1)

atom	atom	atom	angle/degree
C(1)	Zr	C(9)	113.58(14)
C(1)	Zr	C(10)	134.50(14)
C(1)	Zr	C(11)	112.04(14)
C(1)	Zr	C(12)	82.52(14)
C(1)	Zr	C(13)	83.63(13)
C(1)	Zr	C(14)	130.64(14)
C(1)	Zr	C(15)	99.85(14)
C(1)	Zr	C(16)	79.78(16)
C(1)	Zr	C(17)	95.31(23)
C(1)	Zr	C(18)	126.55(20)
C(8)	Zr	C(1)	97.29(17)
C(8)	Zr	C(9)	76.26(17)
C(8)	Zr	C(10)	97.47(16)
C(8)	Zr	C(11)	128.11(16)
C(8)	Zr	C(12)	122.82(18)
C(8)	Zr	C(13)	90.61(17)
C(8)	Zr	C(14)	110.43(19)
C(8)	Zr	C(15)	133.05(20)
C(8)	Zr	C(16)	109.74(26)
C(8)	Zr	C(17)	80.63(23)
C(8)	Zr	C(18)	80.80(20)
C(9)	Zr	C(10)	32.09(13)
C(9)	Zr	C(11)	53.26(14)
C(9)	Zr	C(12)	53.14(14)
C(9)	Zr	C(13)	32.04(13)
C(9)	Zr	C(14)	112.27(14)
C(9)	Zr	C(15)	132.68(15)
C(1)	Zr	C(9)	113.58(14)
C(9)	Zr	C(16)	165.07(15)
C(9)	Zr	C(17)	144.77(24)
C(9)	Zr	C(18)	117.54(21)
C(10)	Zr	C(11)	32.30(13)

atom	atom	atom	angle/degree
C(10)	Zr	C(12)	53.55(14)
C(10)	Zr	C(13)	53.45(14)
C(10)	Zr	C(14)	82.47(15)
C(10)	Zr	C(15)	100.75(15)
C(10)	Zr	C(16)	133.31(16)
C(10)	Zr	C(17)	129.50(22)
C(10)	Zr	C(18)	98.23(20)
C(11)	Zr	C(12)	32.55(14)
C(11)	Zr	C(13)	53.68(15)
C(11)	Zr	C(14)	82.06(16)
C(11)	Zr	C(15)	84.10(16)
C(11)	Zr	C(16)	116.74(22)
C(11)	Zr	C(17)	134.22(19)
C(11)	Zr	C(18)	110.18(19)
C(12)	Zr	C(13)	32.28(13)
C(12)	Zr	C(14)	112.03(16)
C(12)	Zr	C(15)	102.62(17)
C(12)	Zr	C(16)	126.09(25)
C(12)	Zr	C(17)	156.55(21)
C(12)	Zr	C(18)	142.37(18)
C(13)	Zr	C(14)	133.75(14)
C(13)	Zr	C(15)	134.45(16)
C(13)	Zr	C(16)	155.10(24)
C(13)	Zr	C(17)	170.98(19)
C(13)	Zr	C(18)	149.28(20)
C(14)	Zr	C(15)	32.32(15)
C(14)	Zr	C(16)	53.01(16)
C(14)	Zr	C(17)	52.73(19)
C(14)	Zr	C(18)	32.06(16)
C(15)	Zr	C(16)	33.75(19)
C(15)	Zr	C(17)	54.57(20)
C(15)	Zr	C(18)	54.04(19)

atom	atom	atom	angle/degree
C(16)	Zr	C(17)	31.61(22)
C(16)	Zr	C(18)	52.31(23)
C(17)	Zr	C(18)	31.34(22)
C(6)	O	C(7)	117.8(4)
Zr	C(1)	C(2)	116.5(3)
Zr	C(1)	C(6)	128.5(3)
C(2)	C(1)	C(6)	115.0(4)
C(1)	C(2)	C(3)	123.2(4)
C(2)	C(3)	C(4)	118.9(5)
C(3)	C(4)	C(5)	120.2(4)
C(4)	C(5)	C(6)	119.5(4)
O	C(6)	C(1)	114.7(3)
O	C(6)	C(5)	122.2(4)
C(1)	C(6)	C(5)	123.1(4)
Zr	C(9)	C(10)	72.70(23)
Zr	C(9)	C(13)	73.36(22)
C(10)	C(9)	C(13)	108.2(4)
Zr	C(10)	C(9)	75.21(23)
Zr	C(10)	C(11)	73.35(22)
C(9)	C(10)	C(11)	108.1(4)
Zr	C(11)	C(10)	74.35(22)
Zr	C(11)	C(12)	74.27(23)
Ct(1)	Zr	Ct(2)	132.59

atom	atom	atom	angle/degree
C(10)	C(11)	C(12)	107.9(4)
Zr	C(12)	C(11)	73.18(22)
Zr	C(12)	C(13)	74.44(22)
C(11)	C(12)	C(13)	108.0(4)
Zr	C(13)	C(9)	74.60(22)
Zr	C(13)	C(12)	73.28(23)
C(9)	C(13)	C(12)	107.7(4)
Zr	C(14)	C(15)	73.48(25)
Zr	C(14)	C(18)	74.00(27)
C(15)	C(14)	C(18)	109.9(4)
Zr	C(15)	C(14)	74.20(26)
Zr	C(15)	C(16)	73.66(28)
C(14)	C(15)	C(16)	103.7(4)
Zr	C(16)	C(15)	72.59(26)
Zr	C(16)	C(17)	74.10(3)
C(15)	C(16)	C(17)	108.8(5)
Zr	C(17)	C(16)	74.3(3)
Zr	C(17)	C(18)	74.3(3)
C(16)	C(17)	C(18)	108.7(6)
Zr	C(18)	C(14)	73.94(27)
Zr	C(18)	C(17)	74.4(3)
C(14)	C(18)	C(17)	108.8(6)

Appendix 2.12. Fractional Coordinates and Isotropic Thermal Parameters for $Cp^*_2Th(Me)(o\text{-}MeOC_6H_4)$ (2)

atom	x	y	z	$B_{iso}/Å^2 \times 10^4$
Th	0.2500[a]	0.87457(5)	0.1299(1)	14
O	0.2500[a]	0.7526(7)	0.2303(15)	16
C(1)	0.2500[a]	0.7719(10)	-0.0353(22)	24
C(2)	0.2500[a]	0.7446(11)	-0.1884(26)	21
C(3)	0.2500[a]	0.6775(12)	-0.2174(26)	24
C(4)	0.2500[a]	0.6339(10)	-0.0941(25)	30
C(5)	0.2500[a]	0.6561(10)	0.0599(25)	30
C(6)	0.2500[a]	0.7212(9)	0.0807(20)	20
C(7)	0.2500[a]	0.7117(12)	0.3627(29)	52
C(8)	0.2500[a]	0.8756(12)	0.4298(21)	24
C(9)	0.4160(17)	0.8843(16)	-0.0511(30)	9(5)
C(10)	0.4484(23)	0.8574(16)	0.0889(40)	9(8)
C(11)	0.4445(22)	0.9077(18)	0.2051(39)	14(7)
C(12)	0.4033(20)	0.9657(14)	0.1362(47)	14(5)
C(13)	0.3860(19)	0.9509(18)	-0.0266(37)	13(5)
C(14)	0.0659(30)	0.8632(22)	0.0550(54)	26(10)
C(15)	0.0662(24)	0.8842(21)	0.2099(38)	20(7)
C(16)	0.0977(18)	0.9499(14)	0.2125(36)	8(4)
C(17)	0.1212(17)	0.9687(12)	0.0598(41)	6(4)
C(18)	0.1014(28)	0.9168(27)	-0.0423(45)	35(8)
C(19)	0.4283(19)	0.8540(13)	-0.2145(32)	14(5)
C(20)	0.4881(24)	0.7900(16)	0.1158(47)	38(7)
C(21)	0.4820(28)	0.9070(21)	0.3607(48)	46(8)
C(22)	0.3817(26)	1.0322(20)	0.2127(48)	42(8)
C(23)	0.3619(22)	0.9988(16)	-0.1563(37)	31(6)
C(24)	0.0247(24)	0.8007(17)	0.0032(45)	37(7)
C(25)	0.0269(24)	0.8535(17)	0.3545(41)	34(7)
C(26)	0.1074(20)	0.9974(15)	0.3491(35)	26(6)
C(27)	0.1490(22)	1.0400(16)	0.0040(38)	31(6)
C(28)	0.1175(19)	0.9135(15)	-0.2178(34)	17(5)

[a]Parameters were not varied

Appendix 2.13. Bond Distances for $Cp^*_2Th(Me)(o\text{-}MeOC_6H_4)$ (2)

atom	atom	distance/Å
Th	O	2.627(15)
Th	C(1)	2.529(20)
Th	C(8)	2.591(18)
Th	C(9)	2.861
Th	C(10)	2.897
Th	C(11)	2.949
Th	C(12)	2.880
Th	C(13)	2.839
Th	C(14)	2.736
Th	C(15)	2.740
Th	C(16)	2.766
Th	C(17)	2.731
Th	C(18)	2.742
O	C(6)	1.442(22)
O	C(7)	1.414(26)
C(1)	C(2)	1.434(3)
C(1)	C(6)	1.437(27)
C(2)	C(3)	1.386(3)
C(3)	C(4)	1.386(3)
C(4)	C(5)	1.405(3)
C(5)	C(6)	1.335(3)
C(9)	C(10)	1.407(4)
C(9)	C(13)	1.436(4)
C(9)	C(19)	1.550(4)
C(10)	C(11)	1.435(5)
C(10)	C(20)	1.503(5)
C(11)	C(12)	1.447(5)
C(11)	C(21)	1.459(5)
C(12)	C(13)	1.459(5)
C(12)	C(22)	1.538(5)
C(13)	C(23)	1.525(4)
C(14)	C(15)	1.404(6)
C(14)	C(18)	1.468(6)
C(14)	C(24)	1.471(5)
C(15)	C(16)	1.412(5)
C(15)	C(25)	1.506(5)
C(16)	C(17)	1.414(4)
C(16)	C(26)	1.532(4)
C(17)	C(18)	1.405(6)
C(17)	C(27)	1.579(4)
C(18)	C(28)	1.535(5)
Th	Ct(1)	2.614
Th	Ct(2)	2.463

Appendix 2.14. Bond Angles for $Cp^*_2Th(Me)(o\text{-}MeOC_6H_4)$ (2)

atom	atom	atom	angle/degree
O	Th(1)	C(1)	53.6(6)
O	Th(1)	C(8)	71.2(6)
C(1)	Th(1)	C(8)	124.8(7)
Th(1)	O	C(6)	97.0(10)
Th(1)	O	C(7)	145.3(13)
C(6)	O	C(7)	117.7(16)
Th(1)	C(1)	C(2)	147.1(13)
Th(1)	C(1)	C(6)	101.5(13)
C(2)	C(1)	C(6)	111.4(17)
C(1)	C(2)	C(3)	123.2(20)
C(2)	C(3)	C(4)	119.3(21)
C(3)	C(4)	C(5)	121.5(20)
C(4)	C(5)	C(6)	116.5(19)
O	C(6)	C(1)	107.9(15)
O	C(6)	C(5)	124.0(17)
C(1)	C(6)	C(5)	128.1(18)
C(10)	C(9)	C(13)	109.8(24)
C(10)	C(9)	C(19)	126.1(27)
C(10)	C(9)	C(24)	46.5(19)
C(10)	C(9)	C(28)	177.1(26)
C(13)	C(9)	C(19)	123.0(25)
C(13)	C(9)	C(24)	155.9(23)
C(13)	C(9)	C(28)	72.5(22)
C(19)	C(9)	C(24)	79.8(20)
C(19)	C(9)	C(28)	51.3(16)
C(24)	C(9)	C(28)	131.0(22)
C(9)	C(10)	C(11)	108.1(27)
C(9)	C(10)	C(18)	21.3(16)
C(9)	C(10)	C(24)	87.6(28)
C(11)	C(10)	C(15)	19.5(23)
C(11)	C(10)	C(18)	86.9(25)
C(20)	C(10)	C(24)	40.4(20)
C(10)	C(11)	C(12)	108.0(28)
C(10)	C(11)	C(14)	13.1(23)
C(10)	C(11)	C(25)	93.3(27)
C(12)	C(11)	C(16)	29.0(20)
C(21)	C(11)	C(25)	38.7(19)
C(11)	C(12)	C(13)	107.4(26)
C(11)	C(12)	C(15)	11.6(18)
C(11)	C(12)	C(18)	85.4(25)
C(11)	C(12)	C(26)	85.1(27)
C(13)	C(12)	C(15)	100.9(22)
C(13)	C(12)	C(17)	24.4(28)
C(13)	C(12)	C(18)	22.0(16)
C(22)	C(12)	C(26)	44.7(20)
C(15)	C(12)	C(17)	79.1(22)
C(15)	C(12)	C(26)	89.5(23)
C(18)	C(12)	C(26)	165.0(25)
C(9)	C(13)	C(12)	106.6(24)
C(9)	C(13)	C(27)	177.8(22)
C(9)	C(13)	C(28)	58.7(20)
C(12)	C(13)	C(17)	21.8(23)
C(12)	C(13)	C(27)	73.4(25)
C(23)	C(13)	C(27)	55.4(19)
C(23)	C(18)	C(28)	66.0(19)
C(17)	C(13)	C(28)	121.2(20)
C(18)	C(13)	C(27)	9.7(23)
C(11)	C(21)	C(15)	19.0(18)
C(11)	C(21)	C(16)	32.6(17)
C(11)	C(21)	C(25)	46.3(20)
C(12)	C(22)	C(16)	25.5(15)
C(12)	C(22)	C(17)	23.4(15)

atom	atom	atom	angle/degree
C(12)	C(22)	C(27)	72.9(25)
C(16)	C(22)	C(17)	46.7(17)
C(16)	C(22)	C(26)	58.5(23)
C(16)	C(22)	C(27)	97.1(25)
C(17)	C(26)	C(27)	50.4(17)
C(13)	C(23)	C(17)	23.3(14)
C(13)	C(23)	C(27)	74.0(22)
C(13)	C(23)	C(28)	64.7(21)
C(17)	C(23)	C(27)	50.8(16)
C(17)	C(23)	C(28)	87.7(18)
C(27)	C(23)	C(28)	138.4(24)
C(9)	C(19)	C(28)	67.3(21)
C(9)	C(14)	C(18)	26.6(24)
C(11)	C(14)	C(15)	18.1(19)
C(20)	C(14)	C(24)	35.2(20)
C(10)	C(15)	C(14)	13.9(28)
C(12)	C(15)	C(16)	21.6(15)
C(21)	C(15)	C(25)	42.0(18)
C(11)	C(16)	C(21)	47.8(26)
C(11)	C(16)	C(15)	16.7(25)
C(21)	C(16)	C(22)	123.3(24)
C(21)	C(16)	C(15)	52.4(21)
C(21)	C(16)	C(17)	152.1(24)
C(21)	C(16)	C(26)	80.1(21)
C(22)	C(16)	C(17)	72.2(23)
C(22)	C(16)	C(26)	50.4(19)
C(15)	C(16)	C(17)	108.5(25)
C(12)	C(17)	C(13)	121.8(25)
C(12)	C(17)	C(16)	17.4(28)
C(13)	C(17)	C(18)	24.3(28)
C(22)	C(17)	C(23)	117.4(20)
C(22)	C(17)	C(16)	61.1(21)
C(22)	C(17)	C(27)	65.3(19)

atom	atom	atom	angle/degree
C(23)	C(17)	C(16)	172.9(22)
C(23)	C(17)	C(18)	70.4(28)
C(23)	C(17)	C(27)	52.9(18)
C(16)	C(17)	C(18)	109.5(27)
C(16)	C(17)	C(27)	126.4(27)
C(10)	C(18)	C(12)	79.7(22)
C(10)	C(18)	C(14)	5.9(25)
C(10)	C(18)	C(17)	100.9(27)
C(12)	C(18)	C(17)	22.0(13)
C(9)	C(24)	C(10)	45.9(19)
C(9)	C(24)	C(14)	31.6(19)
C(10)	C(24)	C(14)	14.8(24)
C(11)	C(25)	C(15)	15.7(18)
C(12)	C(26)	C(22)	51.4(21)
C(12)	C(26)	C(16)	19.9(13)
C(22)	C(26)	C(16)	71.1(24)
C(13)	C(27)	C(22)	89.5(21)
C(13)	C(27)	C(23)	50.6(17)
C(13)	C(27)	C(17)	25.8(12)
C(22)	C(27)	C(23)	139.3(26)
C(22)	C(27)	C(17)	64.3(21)
C(23)	C(27)	C(17)	76.3(22)
C(9)	C(28)	C(13)	48.8(16)
C(9)	C(28)	C(23)	97.8(21)
C(9)	C(28)	C(19)	61.4(19)
C(9)	C(28)	C(18)	25.7(18)
C(13)	C(28)	C(23)	49.3(15)
C(13)	C(28)	C(19)	109.6(24)
C(13)	C(28)	C(18)	23.2(19)
C(23)	C(28)	C(19)	154.1(26)
C(23)	C(28)	C(18)	72.4(26)
C(1)	Th	C(8)	124.81
C(1)	Th	O	53.63

atom	atom	atom	angle/degree
C(1)	Th	C(17)	116.96
C(1)	Th	C(14)	78.28
C(1)	Th	C(15)	101.60
C(1)	Th	C(18)	87.27
C(1)	Th	C(16)	127.06
C(1)	Th	C(13)	100.52
C(1)	Th	C(9)	75.45
C(1)	Th	C(12)	122.79
C(1)	Th	C(10)	80.29
C(1)	Th	C(11)	108.23
C(8)	Th	O	71.18
C(8)	Th	C(17)	102.47
C(8)	Th	C(14)	103.71
C(8)	Th	C(15)	75.35
C(8)	Th	C(18)	122.68
C(8)	Th	C(16)	74.79
C(8)	Th	C(13)	118.14
C(8)	Th	C(9)	123.10
C(8)	Th	C(12)	88.62
C(8)	Th	C(10)	97.08
C(8)	Th	C(11)	77.17
O	Th	C(17)	137.26
O	Th	C(14)	89.90
O	Th	C(15)	89.08
O	Th	C(18)	118.33
O	Th	C(16)	115.95
O	Th	C(13)	132.30
O	Th	C(9)	104.24
O	Th	C(12)	126.93
O	Th	C(10)	85.79
O	Th	C(11)	98.21
C(17)	Th	C(14)	49.48
C(17)	Th	C(15)	49.57

atom	atom	atom	angle/degree
C(17)	Th	C(18)	29.74
C(17)	Th	C(16)	29.79
C(17)	Th	C(13)	88.79
C(17)	Th	C(9)	113.34
C(17)	Th	C(12)	94.18
C(17)	Th	C(10)	136.52
C(17)	Th	C(11)	122.14
C(14)	Th	C(15)	29.72
C(14)	Th	C(18)	31.09
C(14)	Th	C(16)	48.81
C(14)	Th	C(13)	126.91
C(14)	Th	C(9)	133.19
C(14)	Th	C(12)	143.12
C(14)	Th	C(10)	156.13
C(14)	Th	C(11)	171.63
C(15)	Th	C(18)	50.37
C(15)	Th	C(16)	29.71
C(15)	Th	C(13)	138.25
C(15)	Th	C(9)	159.76
C(15)	Th	C(12)	133.49
C(15)	Th	C(10)	171.95
C(15)	Th	C(11)	147.49
C(18)	Th	C(16)	49.41
C(18)	Th	C(13)	96.19
C(18)	Th	C(9)	109.40
C(18)	Th	C(12)	113.94
C(18)	Th	C(10)	137.68
C(18)	Th	C(11)	141.93
C(16)	Th	C(13)	111.45
C(16)	Th	C(9)	139.75
C(16)	Th	C(12)	104.19
C(16)	Th	C(10)	151.44
C(16)	Th	C(11)	124.58

atom	atom	atom	angle/degree
C(13)	Th	C(9)	29.18
C(13)	Th	C(12)	29.55
C(13)	Th	C(10)	47.85
C(13)	Th	C(11)	47.68
C(9)	Th	C(12)	47.69
C(9)	Th	C(10)	28.29
C(9)	Th	C(11)	46.62
C(12)	Th	C(10)	47.60
C(12)	Th	C(11)	28.71
C(10)	Th	C(11)	28.39
C(2)	C(1)	C(6)	111.4(17)
C(1)	C(2)	C(3)	123.2(20)
C(2)	C(3)	C(4)	119.3(21)
C(3)	C(4)	C(5)	121.5(20)
C(4)	C(5)	C(6)	116.5(19)
O	C(6)	C(1)	107.9(15)
C(1)	C(6)	C(5)	128.09(18)
O	C(6)	C(5)	124.0(17)
C(1)	C(6)	C(5)	128.1(18)
C(6)	O	C(7)	117.68(16)
C(10)	C(9)	C(13)	109.8(24)
C(10)	C(9)	C(19)	126.1(27)
C(9)	C(10)	C(11)	108.11(27)
C(9)	C(10)	C(20)	127.87
C(11)	C(10)	C(20)	123.86
C(10)	C(11)	C(12)	108.0(28)
C(10)	C(11)	C(21)	93.3(27)
C(12)	C(11)	C(21)	122.86

atom	atom	atom	angle/degree
C(11)	C(12)	C(13)	107.4(26)
C(11)	C(12)	C(22)	128.49
C(13)	C(12)	C(22)	124.15
C(9)	C(13)	C(12)	106.59
C(9)	C(13)	C(23)	124.17
C(12)	C(13)	C(23)	127.96
C(15)	C(14)	C(18)	108.60
C(15)	C(14)	C(24)	123.65
C(18)	C(14)	C(24)	127.31
C(14)	C(15)	C(16)	107.68
C(14)	C(15)	C(25)	131.55
C(16)	C(15)	C(25)	119.95
C(15)	C(16)	C(17)	108.53
C(15)	C(16)	C(26)	129.67
C(17)	C(16)	C(26)	121.79
C(18)	C(17)	C(16)	109.54
C(18)	C(17)	C(27)	123.30
C(16)	C(17)	C(27)	126.39
C(17)	C(18)	C(14)	105.57
C(17)	C(18)	C(28)	128.49
C(14)	C(18)	C(28)	125.86
Ct(2)	Th(1)	C(1)	103.00
Ct(2)	Th(1)	C(8)	96.06
Ct(2)	Th(1)	Ct(1)	138.10
Ct(2)	Th(1)	O	111.28
C(1)	Th(1)	Ct(1)	97.89
C(8)	Th(1)	Ct(1)	101.18
Ct(1)	Th(1)	O	110.39

APPENDIX TO CHAPTER THREE

Appendix 3.1. Kinetic Data for the Thermolysis of $Cp^*_2ThPh_2$ in the presence of DMAP: Legend

time (x) = Length of thermolysis expressed in units of 10^3 s.

SM_{int} = Integral of ^1H NMR spectral resonance due to pentamethylcyclopentadienyl protons of the unreacted starting material, i.e $Cp^*_2Th(C_6R_5)_2$ (R = H, D).

P_{int} = Integral of ^1H NMR spectral resonance due to pentamethylcyclopentadienyl protons of the observed product, i.e **2**

IS_{int} = Integral of ^1H NMR spectral resonance due to pentamethylcyclopentadienyl protons of the internal standard hexamethylbenzene.

$[SM]_t$ = Effective concentration of $Cp^*_2Th(C_6R_5)_2$ (R = H, D) relative to the internal standard, at any given point in time:

$$[SM]_t = \frac{SM_{int}}{IS_{int}}$$

$[SM]_t$ = Effective concentration of **2** relative to the internal standard, at any given point in time:

$$[P]_t = \frac{P_{int}}{IS_{int}}$$

Since conversion from the starting complex to the observed product is seen to be quantitative (to within experimental error), two data points are obtained ($SM \rightarrow y^1; P \rightarrow y^2$) for each time interval:

SM_y (y^1) = Value employed in rate plots reflecting the decrease in concentration of the starting complex as a function of time, expressed in terms of the integral of the peak due to $Cp^*_2Th(C_6R_5)_2$ (R = H, D) ($[SM]_o = [SM]_t$ when t = 0):

$$SM_y = 1000 \ln \left(\frac{[SM]_t}{[SM]_o} \right)$$

P_y (y^1) = Value employed in rate plots reflecting the decrease in concentration of the starting complex as a function of time, expressed in terms of the integral of the peak due to the product ($[SM]_o = [SM]_t$ when t = 0):

$$SM_y = 1000 \ln \left(\frac{[SM]_o - [P]_t}{[SM]_o} \right)$$

Appendix 3.2. Kinetic Data for the Thermolysis of $Cp^*_2ThPh_2$ in the presence of DMAP (≈ 1 equiv) at 345.8 K; First Run: Experiment A1

time (x)	SM_{int}	P_{int}	IS_{int}	$[SM]_t$	$[P]_t$	SM_y (y^1)	P_y (y^2)
0.00	30259.59	340.82	27977.18	1.08	0.01	0.00	0.00
0.60	74526.93	2985.02	71906.96	1.04	0.04	42.64	27.81
1.20	37829.34	2464.99	37403.88	1.01	0.07	67.11	51.54
1.86	36685.28	4670.82	38794.19	0.95	0.12	134.32	106.69
2.40	25661.65	5170.35	29123.95	0.88	0.18	204.99	167.97
3.00	33896.68	7499.58	38265.80	0.89	0.20	199.66	188.59
3.60	58654.29	14911.97	68962.06	0.85	0.22	240.32	211.72
4.26	31970.46	10737.64	39086.11	0.82	0.27	279.38	281.70
4.80	30596.12	11679.38	38868.65	0.79	0.30	317.74	314.15

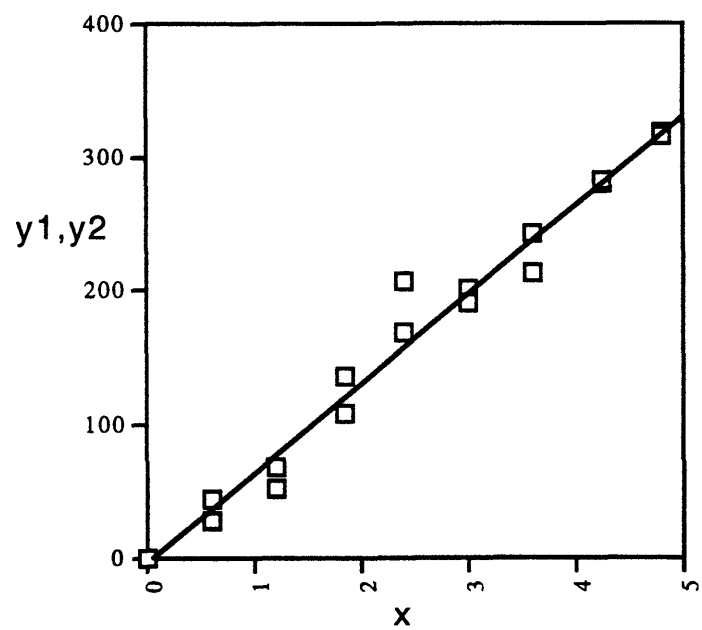

$y = 66.631x - 3.229 \quad r^2 = 0.978$

Gradient = $10^6\, k_{(obs)}$

$k_{(obs)} = 6.66(0.5) \times 10^{-5}\ s^{-1}$; $t_{1/2} = 173.4$ min

Appendix 3.3. Kinetic Data for the Thermolysis of $Cp^*_2ThPh_2$ in the presence of DMAP (≈ 1 equiv) at 345.8 K; Second Run: Experiment A2

time (x)	SM_{int}	P_{int}	IS_{int}	$[SM]_t$	$[P]_t$	SM_y (y^1)	P_y (y^2)
0.00	47348.84	842.28	45363.18	1.04	0.02	0.00	0.00
0.60	54092.05	2357.00	51078.79	1.06	0.05	-14.48	27.27
1.20	42360.08	1590.74	40951.23	1.03	0.04	9.02	19.98
1.80	87962.11	10329.50	90049.48	0.98	0.11	66.29	98.47
2.40	67961.84	7757.82	68955.59	0.99	0.11	57.36	96.10
3.00	76469.60	13156.36	83271.94	0.92	0.16	128.06	146.18
3.30	71427.09	13066.26	80248.04	0.89	0.16	159.29	151.65
3.90	30957.44	6788.66	35622.00	0.87	0.19	183.19	183.66
4.20	26825.00	6186.78	30209.49	0.89	0.20	161.66	200.47
4.92	79143.12	25563.16	93339.98	0.85	0.27	207.83	286.39

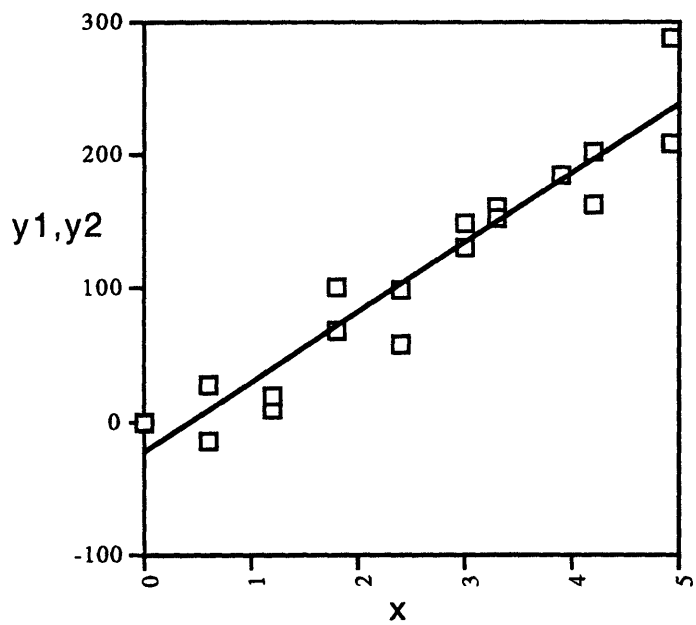

$y = 51.807x - 22.755 \quad r^2 = 0.920$

Gradient = $10^6\, k_{(obs)}$

$k_{(obs)} = 5.18(0.8) \times 10^{-5}\ s^{-1}$; $t_{1/2} = 223.0$ min

Appendix 3.4. Kinetic Data for the Thermolysis of $Cp^*_2ThPh_2$ in the presence of DMAP (≈ 1 equiv) at 351.3 K; First Run: Experiment B1

time (x)	SM_{int}	P_{int}	IS_{int}	$[SM]_t$	$[P]_t$	SM_y (y^1)	P_y (y^2)
0.00	60376.11	194.64	59305.15	1.02	0.00	0.00	0.00
0.60	36683.45	2988.67	40123.31	0.91	0.07	107.53	72.75
1.20	33497.52	5566.92	39504.68	0.85	0.14	182.85	145.76
1.80	30197.58	8221.27	38053.12	0.79	0.22	249.12	235.30
2.40	28103.16	12876.33	40345.72	0.70	0.32	379.50	372.90
3.06	26484.83	15896.20	42051.05	0.63	0.38	480.21	460.90
3.60	23042.45	18522.71	41671.12	0.55	0.44	610.37	570.56
4.20	22324.75	20561.22	41902.07	0.53	0.49	647.54	654.54
4.80	18073.89	20497.97	37940.44	0.48	0.54	759.45	753.25

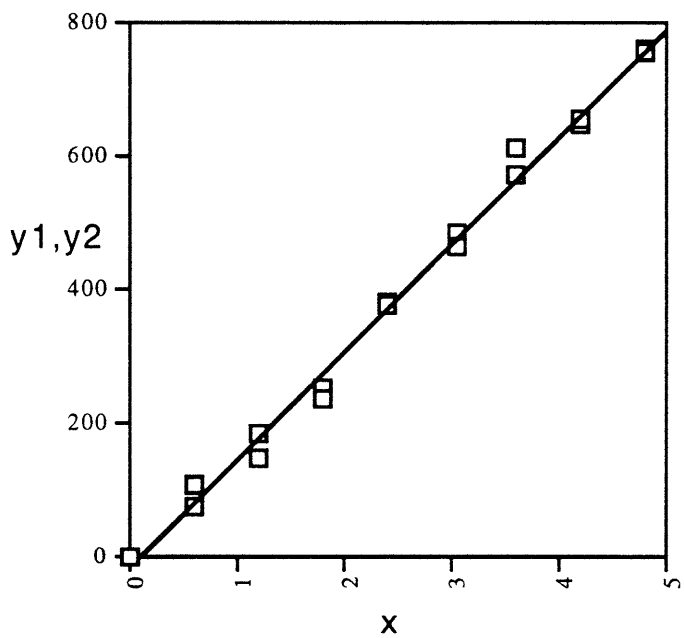

$y = 160.516x - 15.057 \quad r^2 = 0.994$

Gradient = $10^6\, k_{(obs)}$

$k_{(obs)} = 16.13(0.7) \times 10^{-5}\ s^{-1}$; $t_{1/2} = 72.0$ min

Appendix 3.5. Kinetic Data for the Thermolysis of $Cp^*_2ThPh_2$ in the presence of DMAP (≈ 1 equiv) at 351.3 K; Second Run: Experiment B2

time (x)	SM_{int}	P_{int}	IS_{int}	$[SM]_t$	$[P]_t$	SM_y (y^1)	P_y (y^2)
0.00	26106.46	1.55	26159.07	1.00	0.00	0.00	0.00
0.60	25625.70	1805.69	25225.09	1.02	0.07	-17.77	74.37
1.20	24968.44	4222.66	26151.51	0.95	0.16	44.28	176.43
1.80	22470.11	6112.83	25322.71	0.89	0.24	117.50	276.86
2.40	20524.86	8016.21	26417.29	0.78	0.30	250.37	362.43
3.00	20494.04	10947.07	29309.13	0.70	0.37	355.75	468.76
3.60	15966.54	10254.00	25571.02	0.62	0.40	468.95	513.79
4.20	14399.11	11293.37	24759.09	0.58	0.46	540.01	610.68
4.80	13058.83	13417.93	25983.30	0.50	0.52	685.98	728.60

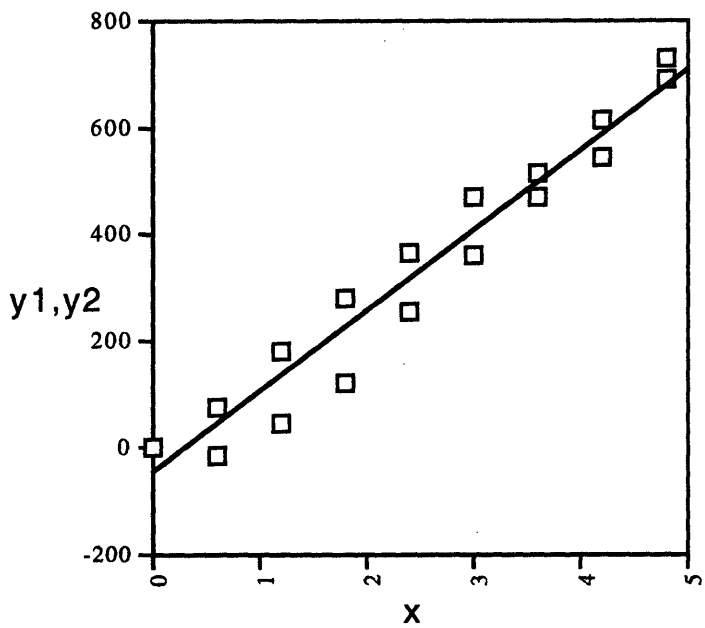

y = 151.316x - 48.882 r2 = 0.950

Gradient = $10^6\, k_{(obs)}$

$k_{(obs)} = 15.05(1.9) \times 10^{-5}\ s^{-1}$; $t_{1/2} = 76.4$ min

Appendix 3.6. Kinetic Data for the Thermolysis of $Cp^*_2ThPh_2$ in the presence of DMAP (≈ 1 equiv) at 362.1 K; First Run: Experiment C1

time (x)	SM_{int}	P_{int}	IS_{int}	$[SM]_t$	$[P]_t$	SM_y (y^1)	P_y (y^2)
0.00	72727.38	443.63	71176.13	1.02	0.01	0.00	0.00
0.60	39580.07	8592.94	52503.24	0.75	0.16	304.11	168.44
1.20	32011.83	17730.53	57343.78	0.56	0.31	604.52	354.28
1.80	24302.62	26156.27	50217.23	0.48	0.52	747.33	706.73
2.40	20987.19	33881.57	54860.95	0.38	0.62	982.45	921.28
3.00	15214.25	40926.32	55522.61	0.27	0.74	1316.12	1271.82
3.60	10739.45	41490.54	51564.00	0.21	0.80	1590.46	1542.60
4.32	9450.06	49907.45	61188.27	0.15	0.82	1889.49	1594.56
4.50	7800.54	47011.32	53323.06	0.15	0.88	1943.74	1980.40

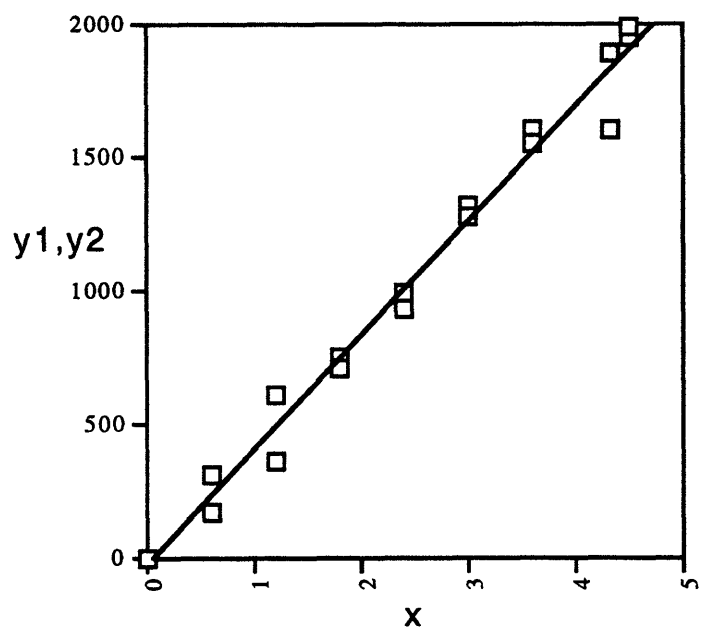

$y = 428.344x - 23.996 \quad r^2 = 0.984$

Gradient = $10^6\, k_{(obs)}$

$k_{(obs)} = 42.83(2.9) \times 10^{-5}\ s^{-1}$; $t_{1/2} = 27.0$ min

Appendix 3.7. Kinetic Data for the Thermolysis of $Cp^*_2ThPh_2$ in the presence of DMAP (≈ 1 equiv) at 362.1 K; Second Run: Experiment C2

time (x)	SM_{int}	P_{int}	IS_{int}	$[SM]_t$	$[P]_t$	SM_y (y^1)	P_y (y^2)
0.00	58246.43	181.68	57169.14	1.02	0.00	0.00	0.00
0.60	36358.40	7045.09	42670.22	0.85	0.17	178.74	173.68
1.20	27551.31	13096.21	42989.02	0.64	0.30	463.56	352.13
1.80	24318.38	25126.65	53752.25	0.45	0.47	811.82	610.86
2.40	31124.28	51443.73	86212.72	0.36	0.60	1037.50	877.97
3.00	11592.50	31542.12	43035.63	0.27	0.73	1330.34	1267.61
3.60	10196.07	35513.26	45457.56	0.22	0.78	1513.45	1452.69
4.20	8410.86	37690.71	45107.94	0.19	0.84	1698.20	1712.30
4.80	5991.67	40623.86	45451.00	0.13	0.89	2044.93	2094.59

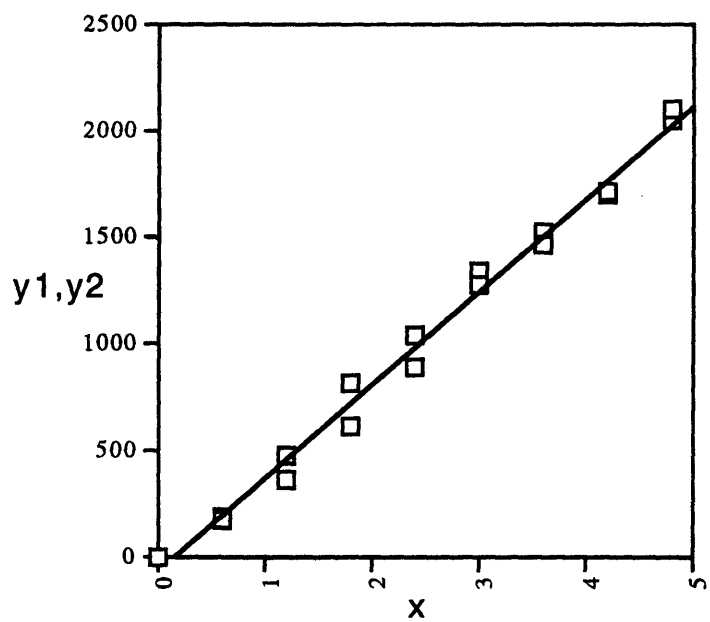

$y = 433.452x - 61.374 \quad r^2 = 0.991$

Gradient = $10^6\, k_{(obs)}$

$k_{(obs)} = 43.35(2.3) \times 10^{-5}\ s^{-1}$; $t_{1/2} = 26.6$ min

Appendix 3.8. Kinetic Data for the Thermolysis of $Cp^*_2ThPh_2$ in the presence of DMAP (≈ 6 equiv) at 345.8 K; First Run: Experiment D1

time (x)	SM_{int}	P_{int}	IS_{int}	$[SM]_t$	$[P]_t$	SM_y (y^1)	P_y (y^2)
0.00	52043.08	0.00	49440.39	1.05	0.00	0.00	0.00
0.60	43264.89	1793.59	40204.36	1.08	0.04	-22.06	43.31
1.20	81258.87	4246.65	75037.30	1.08	0.06	-28.35	55.26
1.80	93799.94	9272.29	90996.77	1.03	0.10	20.96	101.81
2.40	37643.49	5135.76	37350.72	1.01	0.14	43.50	139.98
3.00	35676.55	7088.65	37173.54	0.96	0.19	92.41	199.86
3.60	64503.94	15034.00	72508.15	0.89	0.21	168.28	219.37
4.20	42231.74	12080.49	50595.55	0.83	0.24	232.00	257.25
4.80	30159.00	10409.03	36852.15	0.82	0.28	251.73	312.42

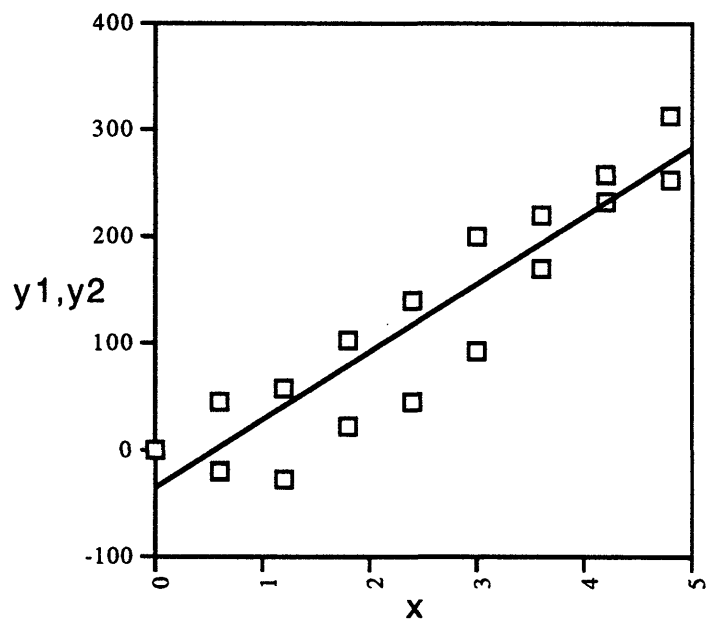

$y = 63.217x - 35.735 \quad r^2 = 0.854$

Gradient = $10^6\, k_{(obs)}$

$k_{(obs)} = 6.32(1.3) \times 10^{-5}\ s^{-1}$; $t_{1/2} = 182.7$ min

Appendix 3.9. Kinetic Data for the Thermolysis of $Cp^*_2ThPh_2$ in the presence of DMAP (≈ 6 equiv) at 345.8 K; Second Run: Experiment D2

time (x)	SM_{int}	P_{int}	IS_{int}	$[SM]_t$	$[P]_t$	SM_y (y^1)	P_y (y^2)
0.00	85063.95	209.69	87062.51	0.98	0.00	0.00	0.00
0.66	71670.94	2333.55	70625.98	1.01	0.03	-37.91	31.93
1.20	62256.92	3819.34	66357.91	0.94	0.06	40.57	58.25
1.80	66292.99	6759.66	70466.14	0.94	0.10	37.83	100.87
2.40	53235.64	7992.74	61074.62	0.87	0.13	114.15	141.34
3.06	53162.70	9527.96	65889.08	0.81	0.14	191.39	157.70
3.60	56494.88	12971.75	64933.42	0.87	0.20	115.99	226.27
4.20	47377.26	13395.37	63281.91	0.75	0.21	266.23	241.71
4.80	53873.51	17227.78	74013.41	0.73	0.23	294.38	269.65

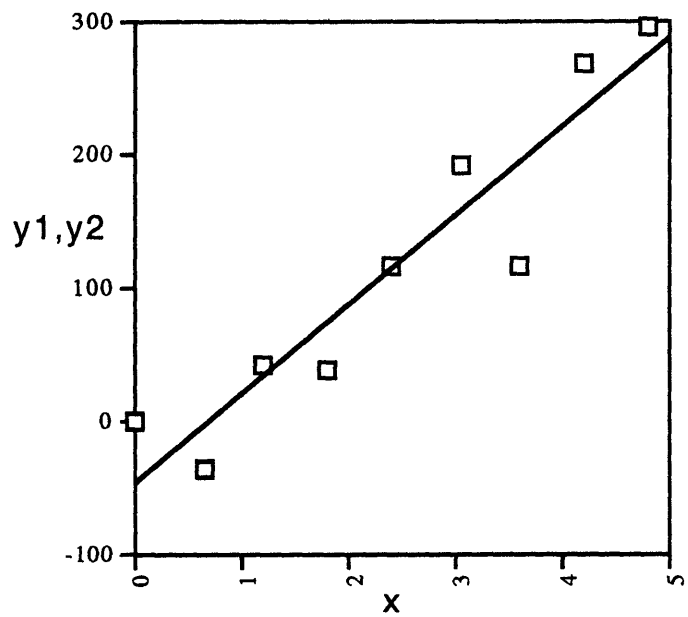

$y = 66.733x - 47.424 \quad r^2 = 0.877$

Gradient = $10^6\, k_{(obs)}$

$k_{(obs)} = 6.26(1.1) \times 10^{-5}\ s^{-1}$; $t_{1/2} = 184.5$ min

Appendix 3.10. Arrhenius Plot for Data for Experiments A1, A2, B1, B2, C1 and C2

Experiment	1/T (K^{-1}) (x)	ln $k_{(obs)}$ (y)
A1	0.00289157	-9.6163406
A2	0.00289157	-9.8679853
B1	0.00284665	-8.7371169
B2	0.00284665	-8.7961402
C1	0.00276184	-7.7555839
C2	0.00276184	-7.7437295

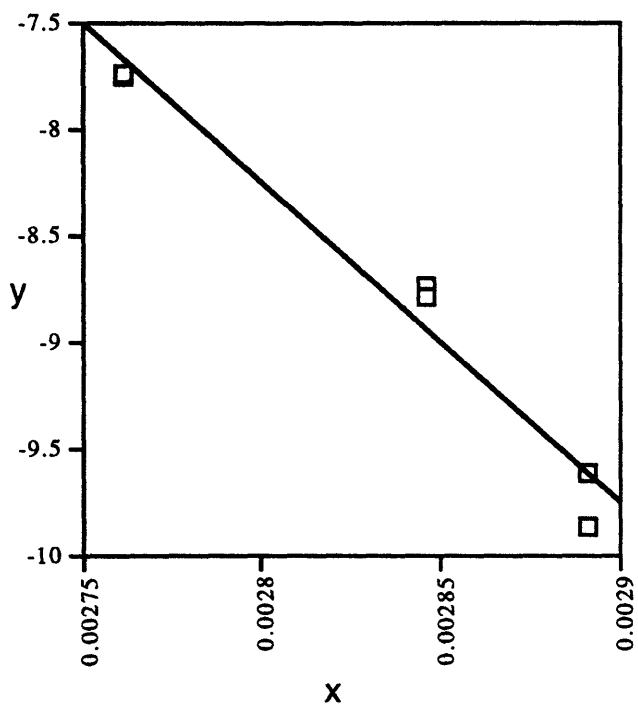

$y = -14921.353x + 33.525 \quad r^2 = 0.965$

Gradient = - E_a/R = -14921.353

Appendix 3.11. Eyring Plot for Experiments A1, A2, B1, B2, C1 and C2

Experiment	1/T (K^{-1}) (x)	ln ($k_{(obs)}$/T) (y)
A1	0.00289157	-15.462295
A2	0.00289157	-15.71394
B1	0.00284665	-14.598728
B2	0.00284665	-14.657752
C1	0.00276184	-13.647441
C2	0.00276184	-13.635587

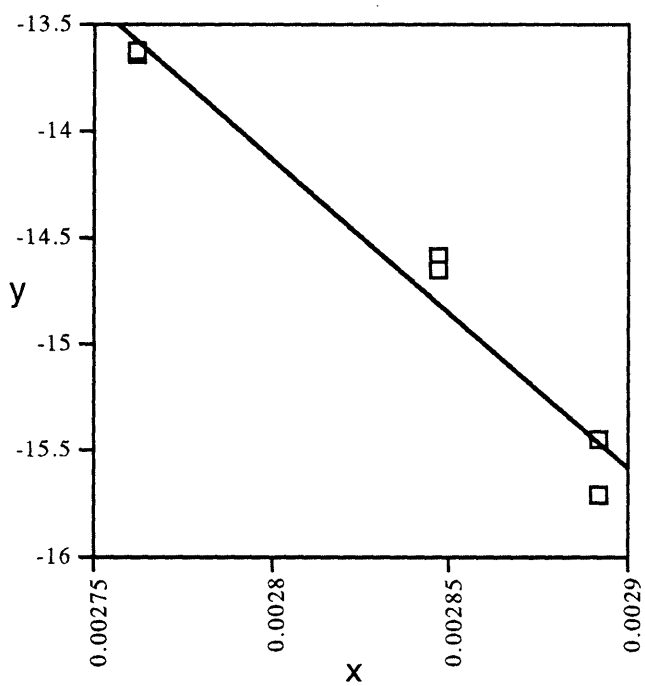

$y = -14567.156x + 26.655 \quad r^2 = 0.964$

Gradient = - $\Delta H/R$ = -14567.156

Appendix. 3.12. Crystal Data Collection and Refinement Parameters for $Cp^*_2Th(o\text{-}C_6H_4C(C_2H_5)=C(C_2H_5))$ (1) and $Cp^*_2Th(Ph)(2\text{-}CH_2\text{-}6\text{-}MeC_5H_3N)$ (3)

compound	1	3
chemical formula	$C_{32}H_{44}Th$	$C_{33}H_{43}NTh$
color, habit	yellow, variable	colorless plates
crystal size (mm)	0.27 x 0.51 x 0.80	0.15 x 0.26 x 0.40
crystal system	orthorhombic	monoclinic
space group	$P2_12_12_1$	$P2_1$
a (Å)	9.851 (2)	9.586 (2)
b (Å)	15.621 (4)	16.890 (3)
c (Å)	17.788 (5)	9.644 (2)
α (deg)	90	90
β (deg)	90	111.95(3)
γ (deg)	90	90
V (Å^3)	2737.27	1448.31(0)
Z	4	2
density (calcd) (g/cm^3)	1.603	1.572
μ (cm^{-1})	41.836	51.68
temerature (K)	102	193
radiation	Mo Kα	Mo Kα
wavelength (Å)	0.71069	0.71073
monochromator	HOGcrystal	HOGcrystal
min/max transmission	0.155/0.351	0.255/0.742
abs cor	semi-empirical	semi-empirical
diffractometer	Picker	Siemens R3m/V
2Θ range (deg)	6-45	0-0
index ranges	$0 \leq h \leq 12$,	$-10 \leq h \leq 9$,
	$0 \leq k \leq 20$,	$-18 \leq k \leq 18$,
	$-23 \leq l \leq 23$	$0 \leq l \leq 10$
no. rflns measured	10710	3782
no. indep. rflns	6289	3782
R_{int} (%)	7.4	0.0
R_w (%)	4.33	8.46
R (%)	4.31	5.37
solution	direct methods	direct methods

Appendix 3.13. Crystal Data Collection and Refinement Parameters for $Cp^*_2Th(Ph)(o\text{-}C_6H_4P(O)Ph_2)$ (4) and $Cp^*_2Th(OMe)(o\text{-}C_6H_4P(O)(OMe)_2)$ (5)

compound	4	5
chemical formula	$C_{44}H_{49}OPTh$	$C_{29}H_{43}O_4PTh$
color, habit	colorless plates	colorless prisms
crystal size (mm)	0.12 x 0.18 x 0.34	0.26 x 0.56 x 0.72
crystal system	triclinic	monoclinic
space group	$P\bar{1}$	$P2_1/n$
a (Å)	10.389(3)	10.049 (2)
b (Å)	16.920(5)	17.794 (3)
c (Å)	21.720(5)	16.460 (3)
α (deg)	98.22(2)	90
β (deg)	91.47(2)	91.58(0)
γ (deg)	93.67(3)	90
V (Å^3)	3768(2)	2942.01
Z	4	4
density (calcd) (g/cm^3)	1.510	1.623
μ (cm^{-1})	40.31	39.596
temerature (K)	193	103
radiation	Mo Kα	Mo Kα
wavelength (Å)	0.71073	0.71069
monochromator	HOG crystal	HOG crystal
min/max transmission	N/A	0.108/0.378
abs cor	none	semi-empirical
diffractometer	Siemens R3m/V	Picker
2Θ range (deg)	3-45	6-50
index ranges	$0 \le h \le 11$,	$0 \le h \le 9$,
	$-18 \le k \le 18$,	$0 \le k \le 21$,
	$-23 \le l \le 23$	$-19 \le l \le 19$
no. rflns measured	10408	8106
no. indep. rflns	9759	5170
R_{int} (%)	4.45	5.8
R_W (%)	8.61	3.72
R (%)	6.41	3.94
solution	direct methods	direct methods

Appendix 3.14. Fractional Coordinates and Isotropic Thermal Parameters for $Cp^*_2Th(o\text{-}C_6H_4C(C_2H_5)=C(C_2H_5))$ (1)

atom	x	y	z	$B_{iso}/Å^2 \times 10^4$
Th	0.48212(3)	0.4900(2)	0.41713(2)	10
C(1)	0.6922(11)	0.5528(7)	0.3263(6)	17
C(2)	0.7535(8)	0.4893(7)	0.3710(5)	15
C(3)	0.7019(10)	0.4077(7)	0.3502(6)	15
C(4)	0.6066(9)	0.4206(7)	0.2884(5)	15
C(5)	0.6024(9)	0.5101(7)	0.2739(5)	17
C(6)	0.3626(9)	0.4768(7)	0.5588(5)	18
C(7)	0.5063(9)	0.4804(6)	0.5725(4)	17
C(8)	0.5484(9)	0.5648(7)	0.5556(5)	17
C(9)	0.4350(10)	0.6112(7)	0.5307(5)	17
C(10)	0.3225(10)	0.5579(6)	0.5335(5)	14
C(11)	0.7137(11)	0.6463(9)	0.3273(7)	25
C(12)	0.8616(8)	0.5033(8)	0.4293(5)	21
C(13)	0.7475(10)	0.3256(7)	0.3813(7)	20
C(14)	0.5373(10)	0.3538(6)	0.2425(6)	19
C(15)	0.5284(11)	0.5508(7)	0.2097(5)	21
C(16)	0.2723(11)	0.4027(7)	0.5780(7)	24
C(17)	0.5952(11)	0.4093(8)	0.6027(6)	25
C(18)	0.6873(11)	0.6026(9)	0.5722(8)	32
C(19)	0.4375(13)	0.7060(7)	0.5146(6)	26
C(20)	0.1755(11)	0.5840(8)	0.5204(6)	24
C(21)	0.3121(10)	0.5769(7)	0.3476(6)	15
C(22)	0.3091(10)	0.6615(7)	0.3332(6)	15
C(23)	0.2018(11)	0.7017(7)	0.2953(5)	17
C(24)	0.0951(10)	0.6507(7)	0.2698(5)	17
C(25)	0.0959(9)	0.5635(6)	0.2831(5)	14
C(26)	0.2012(9)	0.5232(6)	0.3223(5)	13
C(27)	0.4166(10)	0.2584(7)	0.4320(6)	22
C(28)	0.2877(10)	0.2949(7)	0.3963(6)	17
C(29)	0.2954(9)	0.3896(6)	0.3808(5)	12
C(30)	0.1983(10)	0.4284(6)	0.3373(6)	12
C(31)	0.0863(10)	0.3782(6)	0.2999(5)	14
C(32)	0.1201(11)	0.3607(7)	0.2166(6)	18

Appendix 3.15. Bond Distances for $Cp^*_2Th(o\text{-}C_6H_4C(C_2H_5)=C(C_2H_5))$ (1)

atom	atom	distance/Å	atom	atom	distance/Å
Th	C(1)	2.803(9)	C(5)	C(15)	1.496(12)
Th	C(2)	2.796(7)	C(6)	C(7)	1.437(12)
Th	C(3)	2.785(9)	C(6)	C(10)	1.401(13)
Th	C(4)	2.816(9)	C(6)	C(16)	1.500(13)
Th	C(5)	2.828(9)	C(7)	C(8)	1.415(13)
Th	C(6)	2.789(9)	C(7)	C(17)	1.514(12)
Th	C(7)	2.778(7)	C(8)	C(9)	1.404(13)
Th	C(8)	2.804(9)	C(8)	C(10)	1.519(13)
Th	C(9)	2.808(9)	C(9)	C(18)	1.387(14)
Th	C(10)	2.808(9)	C(9)	C(19)	1.508(14)
Th	C(21)	2.486(10)	C(10)	C(20)	1.522(13)
Th	C(29)	2.502(9)	C(21)	C(22)	1.346(14)
Th	Ct(1)	2.528	C(21)	C(26)	1.448(12)
Th	Ct(2)	2.528	C(22)	C(23)	1.403(13)
C(1)	C(2)	1.408(14)	C(23)	C(24)	1.394(14)
C(1)	C(5)	1.448(13)	C(24)	C(25)	1.383(14)
C(1)	C(11)	1.477(15)	C(25)	C(26)	1.400(12)
C(2)	C(3)	1.421(14)	C(26)	C(30)	1.505(12)
C(2)	C(12)	1.503(10)	C(30)	C(31)	1.508(12)
C(3)	C(4)	1.460(13)	C(29)	C(30)	1.371(13)
C(3)	C(13)	1.467(14)	C(31)	C(32)	1.543(13)
C(4)	C(5)	1.423(15)	C(28)	C(29)	1.507(13)
C(4)	C(14)	1.490(13)	C(27)	C(28)	1.530(13)

Appendix 3.16. Bond Angles for $Cp^*_2Th(o\text{-}C_6H_4C(C_2H_5)=C(C_2H_5))$ (1)

atom	atom	atom	angle/degree
C(21)	Th	C(29)	73.6(3)
C(2)	C(1)	C(5)	107.6(8)
C(2)	C(1)	C(11)	129.0(10)
C(5)	C(1)	C(11)	123.4(10)
C(1)	C(2)	C(3)	109.3(8)
C(1)	C(2)	C(12)	126.3(9)
C(3)	C(2)	C(12)	124.3(9)
C(2)	C(3)	C(4)	107.6(8)
C(2)	C(3)	C(13)	125.2(9)
C(4)	C(3)	C(13)	127.0(9)
C(3)	C(4)	C(5)	106.9(8)
C(3)	C(4)	C(14)	127.6(9)
C(5)	C(4)	C(14)	125.1(8)
C(1)	C(5)	C(4)	108.5(8)
C(1)	C(5)	C(15)	126.4(9)
C(4)	C(5)	C(15)	124.8(9)
C(7)	C(6)	C(10)	107.3(8)
C(7)	C(6)	C(16)	125.1(9)
C(10)	C(6)	C(16)	127.1(8)
C(6)	C(7)	C(8)	106.8(8)
C(6)	C(7)	C(17)	127.0(9)
C(8)	C(7)	C(17)	126.1(9)
C(7)	C(8)	C(9)	108.4(8)
C(7)	C(8)	C(18)	125.8(10)
C(9)	C(8)	C(18)	125.3(10)
C(8)	C(9)	C(10)	108.3(9)
C(8)	C(9)	C(19)	123.6(9)
C(10)	C(9)	C(19)	127.5(9)
C(6)	C(10)	C(9)	109.2(8)
C(6)	C(10)	C(20)	124.0(9)
C(9)	C(10)	C(20)	126.4(9)
Th	C(21)	C(22)	130.1(7)
Th	C(21)	C(26)	110.2(6)
C(22)	C(21)	C(26)	119.6(9)
C(21)	C(22)	C(23)	123.2(9)
C(22)	C(23)	C(24)	117.9(9)
C(23)	C(24)	C(25)	120.2(9)
C(24)	C(25)	C(26)	122.2(8)
C(21)	C(26)	C(25)	116.9(8)
C(21)	C(26)	C(30)	122.0(8)
C(25)	C(26)	C(30)	121.1(8)
C(26)	C(30)	C(31)	116.6(8)
C(26)	C(30)	C(29)	121.4(8)
C(31)	C(30)	C(29)	122.0(8)
C(30)	C(31)	C(32)	110.9(8)
Th	C(29)	C(30)	112.4(6)
Th	C(29)	C(28)	127.2(6)
C(30)	C(29)	C(28)	120.1(8)
C(29)	C(28)	C(27)	113.6(8)
C(21)	Th	Ct(1)	102.15
C(21)	Th	Ct(2)	100.35
C(29)	Th	Ct(1)	108.38
C(29)	Th	Ct(2)	107.07
Ct(1)	Th	Ct(2)	142.06

Appendix 3.17. Fractional Coordinates and Isotropic Thermal Parameters for $Cp^*_2Th(Ph)(2\text{-}CH_2\text{-}6\text{-}MeC_5H_3N)$ (3)

atom	x	y	z	$U_{eq} \times 10^3$
Th	0.1120(1)	0.0000	0.7680(1)	17(1)
N	0.1358(15)	0.1329(8)	0.6190(16)	31(3)
C(1)	0.1780(21)	0.0792(12)	0.6763(22)	45(4)
C(2)	0.2048(13)	0.0058(14)	0.6485(13)	24(3)
C(3)	0.1712(17)	0.0487(10)	0.7832(18)	29(3)
C(4)	0.1051(13)	0.0101(10)	0.9030(13)	20(3)
C(5)	0.1099(19)	0.0783(10)	0.8438(19)	29(3)
C(6)	0.3554(19)	0.0907(10)	0.9530(18)	30(3)
C(7)	0.2404(20)	0.1353(11)	0.9273(20)	41(4)
C(8)	0.1784(19)	0.1584(11)	0.7634(19)	37(3)
C(9)	0.2676(19)	0.1168(10)	0.6947(18)	34(3)
C(10)	0.3852(26)	0.0769(16)	0.8017(26)	68(5)
C(11)	0.2178(21)	0.1434(10)	0.5756(25)	45(4)
C(12)	0.2853(20)	0.0430(15)	0.5026(23)	68(4)
C(13)	0.1894(30)	0.1228(14)	0.8066(26)	80(4)
C(14)	0.0648(18)	0.0014(17)	1.0671(16)	55(3)
C(15)	0.0890(21)	0.1664(11)	0.9209(20)	41(4)
C(16)	0.4764(25)	0.0618(14)	1.1179(26)	73(4)
C(17)	0.1952(21)	0.1752(12)	1.0421(20)	49(4)
C(18)	0.0639(30)	0.2119(17)	0.6990(31)	96(4)
C(19)	0.2727(26)	0.1251(16)	0.5336(27)	86(4)
C(20)	0.5197(18)	0.0392(11)	0.8080(25)	51(4)
C(21)	0.2937(23)	0.0941(13)	0.9672(22)	45(4)
C(22)	0.4199(20)	0.1269(11)	0.9424(20)	35(4)
C(23)	0.5212(22)	0.1800(12)	1.0413(21)	48(4)
C(24)	0.5064(24)	0.1956(13)	1.1764(24)	59(4)
C(25)	0.3864(27)	0.1585(14)	1.2094(21)	45(4)
C(26)	0.2881(28)	0.1113(10)	1.1046(18)	32(3)
C(27)	0.0510(16)	0.0128(10)	0.4809(15)	33(3)
C(28)	0.1507(18)	0.0811(10)	0.5097(19)	31(3)
C(29)	0.2657(25)	0.0959(14)	0.4510(26)	59(4)
C(30)	0.3375(23)	0.1611(12)	0.4872(23)	51(4)
C(31)	0.3150(24)	0.2188(14)	0.5862(24)	61(4)
C(32)	0.2037(20)	0.2034(10)	0.6465(19)	38(4)
C(33)	0.1750(21)	0.2628(12)	0.7449(21)	48(4)

Appendix 3.18. Bond Distances for $Cp^*_2Th(Ph)(2\text{-}CH_2\text{-}6\text{-}MeC_5H_3N)$ (3)

atom	atom	distance/Å	atom	atom	distance/Å
Th	N	2.721(14)	Th	C(1)	2.909(19)
Th	C(2)	2.818(11)	Th	C(3)	2.893(18)
Th	C(4)	2.842(14)	Th	C(5)	2.823(20)
Th	C(6)	2.804(15)	Th	C(7)	2.771(18)
Th	C(8)	2.754(19)	Th	C(9)	2.722(19)
Th	C(10)	2.832(26)	Th	C(21)	2.597(19)
Th	C(28)	2.985(19)	Th	C(27)	2.617(15)
N	C(32)	1.335(22)	N	C(28)	1.418(24)
C(1)	C(2)	1.464(30)	C(1)	C(5)	1.500(26)
C(1)	C(11)	1.409(28)	C(2)	C(3)	1.416(23)
C(2)	C(12)	1.469(25)	C(3)	C(4)	1.476(21)
C(3)	C(13)	1.294(30)	C(4)	C(5)	1.278(24)
C(4)	C(14)	1.496(19)	C(5)	C(15)	1.643(25)
C(6)	C(7)	1.280(26)	C(6)	C(10)	1.606(34)
C(6)	C(16)	1.653(25)	C(7)	C(8)	1.517(25)
C(7)	C(17)	1.493(31)	C(8)	C(9)	1.444(29)
C(8)	C(18)	1.378(32)	C(9)	C(10)	1.386(26)
C(9)	C(19)	1.579(34)	C(10)	C(20)	1.419(33)
C(21)	C(22)	1.430(32)	C(21)	C(26)	1.377(30)
C(22)	C(23)	1.401(25)	C(23)	C(24)	1.386(34)
C(24)	C(25)	1.446(33)	C(25)	C(26)	1.354(24)
C(32)	C(31)	1.416(35)	C(32)	C(33)	1.476(29)
C(31)	C(30)	1.437(34)	C(30)	C(29)	1.276(31)
C(29)	C(28)	1.438(34)	C(28)	C(27)	1.819(23)
Th	Ct(1)	2.587	Th	Ct(2)	2.489

Appendix 3.19. Bond Angles for $Cp^*_2Th(Ph)(2\text{-}CH_2\text{-}6\text{-}MeC_5H_3N)$ (3)

atom	atom	atom	angle/degree
N	Th	C(1)	73.7(5)
C(1)	Th	C(2)	29.6(6)
C(1)	Th	C(3)	48.5(5)
N	Th	C(4)	114.4(5)
C(2)	Th	C(4)	47.8(3)
N	Th	C(5)	88.3(5)
C(2)	Th	C(5)	47.2(5)
C(4)	Th	C(5)	26.1(5)
C(1)	Th	C(6)	156.6(6)
C(3)	Th	C(6)	112.7(5)
C(5)	Th	C(6)	128.3(5)
C(1)	Th	C(7)	136.4(6)
C(2)	Th	C(7)	88.2(5)
C(4)	Th	C(7)	117.7(6)
N	Th	C(8)	136.7(6)
C(2)	Th	C(8)	100.4(6)
C(4)	Th	C(8)	106.2(6)
C(6)	Th	C(8)	48.5(4)
N	Th	C(9)	107.4(5)
C(2)	Th	C(9)	118.7(5)
C(4)	Th	C(9)	136.8(5)
C(6)	Th	C(9)	50.4(5)
C(8)	Th	C(9)	30.6(6)
C(1)	Th	C(10)	169.7(7)
C(3)	Th	C(10)	135.2(6)
C(5)	Th	C(10)	159.9(6)
C(7)	Th	C(10)	50.1(7)
C(9)	Th	C(10)	28.8(6)
C(1)	Th	C(21)	104.1(6)
C(3)	Th	C(21)	121.3(7)
C(5)	Th	C(21)	83.3(6)
C(7)	Th	C(21)	93.3(6)
C(9)	Th	C(21)	110.8(6)
N	Th	C(28)	28.3(5)
C(2)	Th	C(28)	97.2(4)
C(4)	Th	C(28)	134.0(4)
C(6)	Th	C(28)	116.6(5)
C(8)	Th	C(28)	109.3(5)
C(10)	Th	C(28)	84.7(6)
N	Th	C(27)	62.5(6)
C(2)	Th	C(27)	77.5(4)
C(4)	Th	C(27)	125.3(4)
C(6)	Th	C(27)	115.6(5)
C(8)	Th	C(27)	82.2(5)
C(10)	Th	C(27)	85.1(6)
C(28)	Th	C(27)	37.2(5)
N	Th	C(2)	95.9(5)
N	Th	C(3)	121.8(4)
C(2)	Th	C(3)	28.7(5)
C(1)	Th	C(4)	48.1(5)
C(3)	Th	C(4)	29.8(4)
C(1)	Th	C(5)	30.3(5)
C(3)	Th	C(5)	46.2(5)
N	Th	C(6)	125.0(5)
C(2)	Th	C(6)	139.0(6)
C(4)	Th	C(6)	108.6(5)
N	Th	C(7)	149.9(5)
C(2)	Th	C(7)	112.7(6)
C(4)	Th	C(7)	92.6(6)
C(6)	Th	C(7)	26.5(5)
C(1)	Th	C(8)	130.0(5)
C(3)	Th	C(8)	87.2(5)

atom	atom	atom	angle/degree
C(5)	Th	C(8)	131.3(6)
C(7)	Th	C(8)	31.9(5)
C(1)	Th	C(9)	144.0(5)
C(3)	Th	C(9)	115.0(5)
C(5)	Th	C(9)	161.1(5)
C(7)	Th	C(9)	51.2(6)
N	Th	C(10)	100.5(6)
C(2)	Th	C(10)	147.2(7)
C(4)	Th	C(10)	141.2(6)
C(6)	Th	C(10)	33.1(7)
C(8)	Th	C(10)	49.2(7)
N	Th	C(21)	73.8(5)
C(2)	Th	C(21)	130.2(7)
C(4)	Th	C(21)	91.6(6)
C(6)	Th	C(21)	72.2(6)
C(8)	Th	C(21)	120.7(5)
C(10)	Th	C(21)	81.9(7)
C(1)	Th	C(28)	86.4(6)
C(3)	Th	C(28)	125.8(4)
C(5)	Th	C(28)	110.0(5)
C(7)	Th	C(28)	132.3(6)
C(9)	Th	C(28)	82.2(5)
C(21)	Th	C(28)	94.5(6)
C(1)	Th	C(27)	84.6(5)
C(3)	Th	C(27)	100.8(5)
C(5)	Th	C(27)	114.9(5)
C(7)	Th	C(27)	113.3(6)
C(9)	Th	C(27)	65.9(5)
C(21)	Th	C(27)	131.0(6)
Th	N	C(28)	86.3(9)
Th	C(1)	C(2)	71.8(9)
C(2)	C(1)	C(5)	99.4(14)
C(2)	C(1)	C(11)	130.0(16)

atom	atom	atom	angle/degree
Th	C(2)	C(1)	78.6(9)
C(1)	C(2)	C(3)	111.7(14)
C(1)	C(2)	C(12)	126.0(17)
Th	C(3)	C(2)	72.7(9)
C(2)	C(3)	C(4)	104.9(15)
C(2)	C(3)	C(13)	131.0(18)
Th	N	C(32)	139.6(11)
C(32)	N	C(28)	121.4(17)
Th	C(1)	C(5)	71.7(10)
Th	C(1)	C(11)	123.0(16)
C(5)	C(1)	C(11)	130.3(17)
Th	C(1)	C(3)	78.6(8)
Th	C(2)	C(12)	120.4(12)
C(3)	C(2)	C(12)	121.1(19)
Th	C(2)	C(4)	73.2(8)
Th	C(3)	C(13)	118.3(16)
C(4)	C(3)	C(13)	124.1(17)
Th	C(4)	C(3)	77.0(9)
C(3)	C(4)	C(5)	108.9(13)
C(3)	C(4)	C(14)	127.3(17)
Th	C(5)	C(1)	78.0(12)
C(1)	C(5)	C(4)	114.8(15)
C(1)	C(5)	C(15)	114.1(14)
Th	C(6)	C(7)	75.3(10)
C(7)	C(6)	C(10)	110.0(16)
C(7)	C(6)	C(16)	127.2(19)
Th	C(7)	C(6)	78.1(11)
C(6)	C(7)	C(8)	109.1(19)
C(6)	C(7)	C(17)	126.1(16)
Th	C(8)	C(7)	74.7(10)
C(7)	C(8)	C(9)	106.5(14)
C(7)	C(8)	C(18)	125.1(21)
Th	C(9)	C(8)	75.9(11)

atom	atom	atom	angle/degree
C(8)	C(9)	C(10)	110.5(18)
C(8)	C(9)	C(19)	130.6(16)
Th	C(10)	C(6)	72.5(12)
C(6)	C(10)	C(9)	103.6(20)
C(6)	C(10)	C(20)	119.6(18)
Th	C(21)	C(22)	119.3(15)
C(22)	C(21)	C(26)	114.7(16)
C(22)	C(23)	C(24)	118.2(21)
C(24)	C(25)	C(26)	118.7(19)
N	C(32)	C(31)	118.0(19)
C(31)	C(32)	C(33)	119.3(17)
C(31)	C(30)	C(29)	124.6(25)
Th	C(28)	N	65.5(9)
N	C(28)	C(29)	119.4(15)
N	C(28)	C(27)	117.3(15)
Th	C(27)	C(28)	82.5(8)
Th	C(4)	C(5)	76.2(11)
Th	C(4)	C(14)	122.2(9)
C(5)	C(4)	C(14)	122.8(17)
Th	C(5)	C(4)	77.8(11)
Th	C(5)	C(15)	124.4(12)
C(4)	C(5)	C(15)	129.6(16)
Th	C(6)	C(10)	74.4(10)
Th	C(6)	C(16)	124.6(12)

atom	atom	atom	angle/degree
C(10)	C(6)	C(16)	122.1(17)
Th	C(7)	C(8)	73.4(9)
Th	C(7)	C(17)	126.3(13)
C(8)	C(7)	C(17)	123.2(16)
Th	C(8)	C(9)	73.5(10)
Th	C(8)	C(18)	119.7(15)
C(9)	C(8)	C(18)	128.3(20)
Th	C(9)	C(10)	80.0(14)
Th	C(9)	C(19)	122.8(12)
C(10)	C(9)	C(19)	117.4(20)
Th	C(10)	C(9)	71.2(13)
Th	C(10)	C(20)	125.8(16)
C(9)	C(10)	C(20)	136.4(25)
Th	C(21)	C(26)	125.8(15)
C(21)	C(22)	C(23)	123.3(20)
C(23)	C(24)	C(25)	119.6(18)
C(21)	C(26)	C(25)	125.2(19)
N	C(32)	C(33)	122.6(19)
C(32)	C(31)	C(30)	118.1(20)
C(30)	C(29)	C(28)	117.2(23)
Th	C(28)	C(29)	139.6(11)
Th	C(28)	C(27)	60.4(7)
C(29)	C(28)	C(27)	121.8(16)
Ct(1)	Th	Ct(2)	133.5

Appendix 3.20. Fractional Coordinates and Isotropic Thermal Parameters for $Cp^*_2Th(Ph)(o\text{-}C_6H_4)P(O)Ph_2$) (4)

atom	x	y	z	U_{eq} /Å^2 x 10^3
Molecule A				
Th_a	0.2315(1)	0.3278(1)	0.6154(1)	22(1)
P_a	0.3786(5)	0.1621(3)	0.6632(2)	31(2)
O_a	0.2945(13)	0.1923(7)	0.6140(6)	40(4)
$C(1)_a$	0.2997(21)	0.4441(10)	0.5349(8)	37(6)
$C(2)_a$	0.2630(22)	0.3723(12)	0.4939(9)	45(7)
$C(3)_a$	0.3560(23)	0.3190(14)	0.5017(9)	52(8)
$C(4)_a$	0.4522(21)	0.3510(13)	0.5469(10)	49(8)
$C(5)_a$	0.4191(19)	0.4305(10)	0.5666(8)	32(6)
$C(6)_a$	0.0255(18)	0.4167(12)	0.6592(9)	38(6)
$C(7)_a$	-0.0088(18)	0.3372(12)	0.6760(9)	38(7)
$C(8)_a$	0.0756(25)	0.3262(12)	0.7238(10)	54(8)
$C(9)_a$	0.1624(19)	0.3945(11)	0.7394(9)	36(6)
$C(10)_a$	0.1334(19)	0.4506(11)	0.6994(8)	35(6)
$C(11)_a$	0.2476(23)	0.5238(12)	0.5366(12)	57(8)
$C(12)_a$	0.1569(28)	0.3672(14)	0.4457(10)	78(9)
$C(13)_a$	0. 3606(29)	0.2334(13)	0.4659(12)	77(9)
$C(14)_a$	0.5720(26)	0.3125(16)	0.5600(13)	77(9)
$C(15)_a$	0.5056(22)	0.4970(13)	0.6049(10)	53(7)
$C(16)_a$	-0.520(25)	0.4579(16)	0.6159(11)	72(9)
$C(17)_a$	-0.1192(23)	0.2861(18)	0.6593(13)	79(9)
$C(18)_a$	0.0640(31)	0.2561(15)	0.7601(13)	89(10)
$C(19)_a$	0.2430(22)	0.4149(15)	0.7977(9)	60(8)
$C(20)_a$	0.1943(25)	0.5371(12)	0.7052(11)	59(8)
$C(21)_a$	0.4258(17)	0.3223(10)	0.6946(8)	25(6)
$C(22)_a$	0.4936(19)	0.3870(12)	0.7266(8)	37(6)
$C(23)_a$	0.5947(20)	0. 3814(13)	0.7707(9)	46(7)
$C(24)_a$	0.6267(20)	0.3060(12)	0.7842(10)	44(7)
$C(25)_a$	0.5650(20)	0.2368(12)	0.7516(9)	40(7)
$C(26)_a$	0.4634(18)	0.2464(11)	0.7089(8)	35(6)
$C(27)_a$	0.2739(20)	0.1056(11)	0.7096(10)	41(7)

atom	x	y	z	U_{eq} /Å^2 x 10^3
C(28)$_a$	0.1545(21)	0.0678(15)	0.6801(11)	57(8)
C(29)$_a$	0.0706(24)	0.0276(14)	0.7123(14)	67(9)
C(30)$_a$	0.1044(28)	0.0193(16)	0.7719(14)	75(10)
C(31)$_a$	0.2105(32)	0.0575(20)	0.8026(14)	100(11)
C(32)$_a$	0.3007(25)	0.1026(16)	0.7707(12)	68(9)
C(33)$_a$	0.4875(20)	0.0927(11)	0.6291(10)	45(7)
C(34)$_a$	0.4538(36)	0.0173(17)	0. 6085(21)	156(12)
C(35)$_a$	0.5303(44)	-0.0322(18)	0.5737(29)	259(13)
C(36)$_a$	0.6638(35)	-0.0089(16)	0.5727(19)	124(11)
C(37)$_a$	0.7066(25)	0.0675(14)	0.5940(11)	64(8)
C(38)$_a$	0.6150(20)	0.1193(11)	0.6195(10)	45(7)
C(39)$_a$	0.0670(17)	0.2340(13)	0.5430(9)	37(6)
C(40)$_a$	-0.0413(21)	0.2653(17)	0.5179(11)	69(9)
C(41)$_a$	-0.1355(24)	0.2191(18)	0.4744(13)	81(10)
C(42)$_a$	-0.1220(23)	0.1353(15)	0.4580(13)	72(9)
C(43)$_a$	-0.0150(25)	0.1030(15)	0.4792(10)	60(8)
C(44)$_a$	0.0763(19)	0.1484(11)	0.5218(9)	37(6)
Molecule B				
Th$_b$	0.2059(1)	0.2857(1)	0.1004(1)	52(1)
P$_b$	0.3071(10)	0.1432(8)	0.1940(3)	137(5)
O$_b$	0.3215(25)	0.1812(15)	0.1359(8)	152(9)
C(1)$_b$	0.1017(54)	0.1483(33)	0.0064(25)	182(17)
C(1')$_b$	-0.1131(42)	0.2748(25)	0.872(20)	137(13)
C(2)$_b$	0.1232(38)	0.2150(23)	-0.0255(18)	39(9)
C(2')$_b$	-0.0523(36)	0.3177(22)	0.0465(17)	34(9)
C(3)$_b$	0.0189(24)	0.2687(14)	-0.0003(11)	60(6)
C(4)$_b$	-0.0250(45)	0.2436(28)	0.0408(21)	51(11)
C(4')$_b$	0.0069(38)	0.1845(23)	0.0227(18)	33(9)
C(5)$_b$	-0.0307(35)	0.1900(22)	0.0714(17)	107(10)
C(6)$_b$	0.3890(24)	0.4206(18)	0.1113(11)	83(9)
C(6')$_b$	-0.1793(47)	0.3030(29)	0.1470(22)	61(12)
C(7)$_b$	0.2657(27)	0.4523(17)	0.0955(15)	86(10)
C(7')$_b$	-0.0833(46)	0.4008(28)	0.0408(21)	59(12)

atom	x	y	z	$U_{eq} \times 10^3$
C(8)$_b$	0.2164(26)	0.4359(15)	0.1625(20)	114(10)
C(9)$_b$	0.2990(49)	0.4077(26)	0.2002(15)	145(13)
C(10)$_b$	0.4014(25)	0.3958(26)	0.1666(13)	116(11)
C(11)$_b$	0.1905(49)	0.833(29)	0.0080(22)	64(12)
C(12)$_b$	0.1883(51)	0.2127(31)	-0.0863(24)	70(13)
C(13)$_b$	0.0328(40)	0.3185(24)	-0.0534(19)	131(12)
C(15)$_b$	-0.0719(39)	0.1209(24)	0.1080(18)	129(12)
C(16)$_b$	0.5086(28)	0.4296(29)	0.0696(16)	145(12)
C(17)$_b$	0.2346(27)	0.4950(17)	0.0436(17)	87(10)
C(18)$_b$	0.0756(36)	0.4844(17)	0.1711(28)	207(12)
C(19)$_b$	0.2564(50)	0.4127(25)	0.2662(14)	207(12)
C(20)$_b$	0.5114(32)	0.3652(39)	0.1947(20)	214(13)
C(21)$_b$	0.1243(19)	0.2431(11)	0.2043(10)	46(7)
C(22)$_b$	0.0279(23)	0.2795(14)	0.2397(16)	84(10)
C(23)$_b$	-0.-132(27)	0.2609(15)	0.2954(17)	97(10)
C(24)$_b$	0.0395(22)	0.2027(15)	0.3225(12)	68(8)
C(25)$_b$	0.1409(21)	0.1660(19)	0.2932(10)	76(9)
C(26)$_b$	0.1769(22)	0.1880(17)	0.2365(10)	66(9)
C(27)$_b$	0.2503(23)	0.0250(12)	0.1728(13)	124(12)
C(28)$_b$	0.2122	-0.0051	0.1114	151(14)
C(29)$_b$	0.1753	-0.0863	0.0950	174(16)
C(30)$_b$	0.1765	-0.01374	0.1400	325(24)
C(31)$_b$	0.2147	-0.01073	0.2014	105(10)
C(32)$_b$	0.2515	-0.0262	0.2178	108(10)
C(33)$_b$	0.4697(29)	0.1506(22)	0.2375(16)	212(19)
C(34)$_b$	0.5916	0.1204	0.2360	219(19)
C(35)$_b$	0.6831	0.1477	0.2837	98(9)
C(36)$_b$	0.6527	0.2052	0.3329	213(19)
C(37)$_b$	0.5308	0.2353	0.3344	427(27)
C(38)$_b$	0.4393	0.2080	0.2867	243(21)
C(39)$_b$	0.3383(24)	0.2301(16)	0.0144(10)	62(12)
C(39')$_b$	0.4208(19)	0.2719(14)	0.0245(10)	32(8)
C(40)$_b$	0.4144	0.1650	0.0139	48(10)

atom	x	y	z	$U_{eq} \times 10^3$
C(40')$_b$	0.5317	0.2332	0.0361	44(10)
C(41)$_b$	0.4965	0.1458	-0.0350	59(11)
C(41')$_b$	0.6378	0.2394	-0.0015	51(11)
C(42)$_b$	0.5025	0.1917	-0.0835	46(10)
C(42')$_b$	0.6330	0.2842	-0.0505	39(9)
C(43)$_b$	0.4264	0.2567	-0.0830	53(11)
C(43')$_b$	0.5221	0.3229	-0.0621	48(10)
C(44)$_b$	0.3443	0.2759	-0.0341	38(9)
C(44')$_b$	0.4160	0.3167	-0.0245	41(9)

Appendix 3.21. Bond Distances for $Cp^*_2Th(Ph)(o\text{-}C_6H_4)P(O)Ph_2$) (4)

atom	atom	distance/Å
Th_a	O_a	2.421(12)
Th_a	$C(1)_a$	2.880(19)
Th_a	$C(2)_a$	2.866(21)
Th_a	$C(3)_a$	2.807(21)
Th_a	$C(4)_a$	2.802(23)
Th_a	$C(5)_a$	2.853(19)
Th_a	$C(6)_a$	2.802(19)
Th_a	$C(7)_a$	2.854(19)
Th_a	$C(8)_a$	2.894(23)
Th_a	$C(9)_a$	2.894(19)
Th_a	$C(10)_a$	2.822(18)
Th_a	$C(39)_a$	2.591(18)
Th_a	$C(21)_a$	2.634(17)
Th_b	O_b	2.405(26)
Th_b	$C(6)_b$	2.854(27)
Th_b	$C(7)_b$	2.865(28)
Th_b	$C(8)_b$	2.696(27)
Th_b	$C(9)_b$	2.873(35)
Th_b	$C(10)_b$	2.875(30)
Th_b	$C(1)_b$	2.992(50)
Th_b	$C(2)_b$	2.908(37)
Th_b	$C(3)_b$	2.857(24)
Th_b	$C(4)_b$	2.700(45)
Th_b	$C(5)_b$	2.860(35)
Th_b	$C(2')_b$	3.010(38)
Th_b	$C(4')_b$	2.931(36)
Th_b	$C(39)_b$	2.461(23)
Th_b	$C(39')_b$	2.810(21)
Th_b	$C(21)_b$	2.611(23)
P_a	O_a	1.526(14)
P_a	$C(26)_a$	1.784(17)
P_a	$C(27)_a$	1.820(22)
P_a	$C(33)_a$	1.781(21)
P_b	O_b	1.503(23)
P_b	$C(26)_b$	1.802(25)
P_b	$C(33)_b$	1.902(32)
P_b	$C(27)_b$	2.034(23)
$C(1)_a$	$C(2)_a$	1.425(25)
$C(1)_a$	$C(5)_a$	1.450(28)
$C(1)_a$	$C(11)_a$	1.481(28)
$C(2)_a$	$C(3)_a$	1.385(34)
$C(2)_a$	$C(12)_a$	1.492(34)
$C(3)_a$	$C(4)_a$	1.409(30)
$C(3)_a$	$C(13)_a$	1.547(31)
$C(4)_a$	$C(5)_a$	1.418(27)
$C(4)_a$	$C(14)_a$	1.481(36)
$C(5)_a$	$C(15)_a$	1.526(26)
$C(6)_a$	$C(7)_a$	1.468(30)
$C(6)_a$	$C(10)_a$	1.439(26)
$C(6)_a$	$C(16)_a$	1.496(34)
$C(7)_a$	$C(8)_a$	1.383(30)
$C(7)_a$	$C(17)_a$	1.399(31)
$C(8)_a$	$C(9)_a$	1.416(28)
$C(8)_a$	$C(18)_a$	1.515(36)
$C(9)_a$	$C(10)_a$	1.416(28)
$C(9)_a$	$C(19)_a$	1.486(27)
$C(10)_a$	$C(20)_a$	1.544(27)
$C(6)_b$	$C(7)_b$	1.471(39)
$C(6)_b$	$C(10)_b$	1.334(43)
$C(6)_b$	$C(16)_b$	1.570(41)
$C(7)_b$	$C(8)_b$	1.610(53)
$C(7)_b$	$C(17)_b$	1.463(48)

atom	atom	distance/Å
C(8)$_b$	C(9)$_b$	1.328(57)
C(8)$_b$	C(18)$_b$	1.724(45)
C(9)$_b$	C(10)$_b$	1.315(54)
C(9)$_b$	C(19)$_b$	1.503(48)
C(10)$_b$	C(20)$_b$	1.440(56)
C(1)$_b$	C(2)$_b$	1.415(71)
C(1)$_b$	C(11)$_b$	1.485(78)
C(1)$_b$	C(4')$_b$	1.226(69)
C(2)$_b$	C(3)$_b$	1.521(47)
C(2)$_b$	C(12)$_b$	1.496(66)
C(2)$_b$	C(4')$_b$	1.722(57)
C(3)$_b$	C(4)$_b$	1.135(55)
C(3)$_b$	C(13)$_b$	1.527(50)
C(3)$_b$	C(2')$_b$	1.466(43)
C(3)$_b$	C(4')$_b$	1.575(48)
C(4)$_b$	C(5)$_b$	1.198(63)
C(4)$_b$	C(1')$_b$	1.446(63)
C(4)$_b$	C(2')$_b$	1.293(61)
C(4)$_b$	C(4')$_b$	1.096(60)
C(5)$_b$	C(15)$_b$	1.550(57)
C(5)$_b$	C(1')$_b$	1.715(57)
C(5)$_b$	C(4')$_b$	1.130(53)
C(1')$_b$	C(2')$_b$	1.363(59)
C(1')$_b$	C(6')$_b$	1.515(64)
C(2')$_b$	C(7')$_b$	1.484(63)
C(39)$_a$	C(40)$_a$	1.403(32)
C(39)$_a$	C(44)$_a$	1.467(27)
C(40)$_a$	C(41)$_a$	1.451(34)
C(41)$_a$	C(42)$_a$	1.429(39)
C(42)$_a$	C(43)$_a$	1.367(37)
C(43)$_a$	C(44)$_a$	1.415(29)
C(39)$_b$	C(39')$_b$	1.073(32)
Th$_a$	Ct(1)$_a$	2.573
Th$_a$	Ct(2)$_a$	2.583

atom	atom	distance/Å
C(39)$_b$	C(44')$_b$	1.938(35)
C(40)$_b$	C(39')$_b$	1.787(35)
C(40)$_b$	C(40')$_b$	1.637(32)
C(41)$_b$	C(40')$_b$	1.988(30)
C(43)$_b$	C(43')$_b$	1.462(32)
C(43)$_b$	C(44')$_b$	1.518(30)
C(44)$_b$	C(39')$_b$	1.495(31)
C(44)$_b$	C(44')$_b$	0.979(32)
C(26)$_a$	C(21)$_a$	1.439(26)
C(26)$_a$	C(25)$_a$	1.419(28)
C(21)$_a$	C(22)$_a$	1.354(23)
C(22)$_a$	C(23)$_a$	1.420(28)
C(23)$_a$	C(24)$_a$	1.407(31)
C(24)$_a$	C(25)$_a$	1.387(26)
C(27)$_a$	C(28)$_a$	1.448(29)
C(27)$_a$	C(32)$_a$	1.357(33)
C(28)$_a$	C(29)$_a$	1.343(36)
C(29)$_a$	C(30)$_a$	1.361(43)
C(30)$_a$	C(31)$_a$	1.351(41)
C(31)$_a$	C(32)$_a$	1.428(42)
C(33)$_a$	C(34)$_a$	1.311(34)
C(33)$_a$	C(38)$_a$	1.403(29)
C(34)$_a$	C(35)$_a$	1.356(58)
C(35)$_a$	C(36)$_a$	1.419(57)
C(36)$_a$	C(37)$_a$	1.351(35)
C(37)$_a$	C(38)$_a$	1.405(32)
C(26)$_b$	C(21)$_b$	1.374(35)
C(26)$_b$	C(25)$_b$	1.391(34)
C(21)$_b$	C(22)$_b$	1.399(33)
C(22)$_b$	C(23)$_b$	1.366(50)
C(23)$_b$	C(24)$_b$	1.354(41)
C(24)$_b$	C(25)$_b$	1.379(34)
Th$_b$	Ct(1)$_b$	2.567
Th$_b$	Ct(2)$_b$	2.581

Appendix 3.22. Bond Angles for $Cp^*_2Th(Ph)(o\text{-}C_6H_4)P(O)Ph_2$) (4)

atom	atom	atom	angle/degree
O_a	Th_a	$C(1)_a$	130.3(5)
O_a	Th_a	$C(2)_a$	108.8(5)
$C(1)_a$	Th_a	$C(2)_a$	28.7(5)
O_a	Th_a	$C(3)_a$	84.2(6)
$C(1)_a$	Th_a	$C(3)_a$	46.7(6)
$C(2)_a$	Th_a	$C(3)_a$	28.2(7)
O_a	Th_a	$C(4)_a$	85.7(5)
$C(1)_a$	Th_a	$C(4)_a$	48.6(6)
$C(2)_a$	Th_a	$C(4)_a$	48.4(7)
$C(3)_a$	Th_a	$C(4)_a$	29.1(6)
O_a	Th_a	$C(5)_a$	113.7(5)
$C(1)_a$	Th_a	$C(5)_a$	29.3(6)
$C(2)_a$	Th_a	$C(5)_a$	47.5(5)
$C(3)_a$	Th_a	$C(5)_a$	46.6(6)
$C(4)_a$	Th_a	$C(5)_a$	29.0(6)
O_a	Th_a	$C(6)_a$	136.9(5)
$C(1)_a$	Th_a	$C(6)_a$	90.2(6)
$C(2)_a$	Th_a	$C(6)_a$	102.2(6)
$C(3)_a$	Th_a	$C(6)_a$	130.4(7)
$C(4)_a$	Th_a	$C(6)_a$	137.3(6)
$C(5)_a$	Th_a	$C(6)_a$	109.2(6)
O_a	Th_a	$C(7)_a$	106.8(5)
$C(1)_a$	Th_a	$C(7)_a$	118.5(6)
$C(2)_a$	Th_a	$C(7)_a$	121.8(6)
$C(3)_a$	Th_a	$C(7)_a$	146.2(6)
$C(4)_a$	Th_a	$C(7)_a$	167.0(6)
$C(5)_a$	Th_a	$C(7)_a$	139.2(6)
$C(6)_a$	Th_a	$C(7)_a$	30.1(6)
O_a	Th_a	$C(8)_a$	94.7(5)
$C(1)_a$	Th_a	$C(8)_a$	135.0(6)
$C(2)_a$	Th_a	$C(8)_a$	148.6(7)
$C(3)_a$	Th_a	$C(8)_a$	172.8(6)
$C(4)_a$	Th_a	$C(8)_a$	158.0(6)
$C(5)_a$	Th_a	$C(8)_a$	139.4(5)
$C(6)_a$	Th_a	$C(8)_a$	47.5(6)
$C(7)_a$	Th_a	$C(8)_a$	27.8(6)
O_a	Th_a	$C(9)_a$	110.4(5)
$C(1)_a$	Th_a	$C(9)_a$	114.9(5)
$C(2)_a$	Th_a	$C(9)_a$	140.7(6)
$C(3)_a$	Th_a	$C(9)_a$	157.9(6)
$C(4)_a$	Th_a	$C(9)_a$	132.2(5)
$C(5)_a$	Th_a	$C(9)_a$	111.4(5)
$C(6)_a$	Th_a	$C(9)_a$	47.8(6)
$C(7)_a$	Th_a	$C(9)_a$	47.1(5)
$C(8)_a$	Th_a	$C(9)_a$	28.3(5)
O_a	Th_a	$C(10)_a$	138.9(5)
$C(1)_a$	Th_a	$C(10)_a$	89.0(5)
$C(2)_a$	Th_a	$C(10)_a$	112.4(6)
$C(3)_a$	Th_a	$C(10)_a$	135.7(6)
$C(4)_a$	Th_a	$C(10)_a$	123.1(6)
$C(5)_a$	Th_a	$C(10)_a$	95.1(5)
$C(6)_a$	Th_a	$C(10)_a$	29.6(5)
$C(7)_a$	Th_a	$C(10)_a$	48.5(5)
$C(8)_a$	Th_a	$C(10)_a$	47.2(6)
$C(9)_a$	Th_a	$C(10)_a$	28.7(6)
O_a	Th_a	$C(39)_a$	72.5(6)
$C(1)_a$	Th_a	$C(39)_a$	100.1(6)
$C(2)_a$	Th_a	$C(39)_a$	74.6(6)
$C(3)_a$	Th_a	$C(39)_a$	79.1(6)
$C(4)_a$	Th_a	$C(39)_a$	107.2(6)
$C(5)_a$	Th_a	$C(39)_a$	121.4(6)
$C(6)_a$	Th_a	$C(39)_a$	88.2(6)

atom	atom	atom	angle/degree
C(7)$_a$	Th$_a$	C(39)$_a$	74.3(5)
C(8)$_a$	Th$_a$	C(39)$_a$	93.8(6)
C(9)$_a$	Th$_a$	C(39)$_a$	120.4(5)
C(10)$_a$	Th$_a$	C(39)$_a$	117.5(6)
O$_a$	Th$_a$	C(21)$_a$	68.6(5)
C(1)$_a$	Th$_a$	C(21)$_a$	108.9(6)
C(2)$_a$	Th$_a$	C(21)$_a$	123.3(6)
C(3)$_a$	Th$_a$	C(21)$_a$	101.9(6)
C(4)$_a$	Th$_a$	C(21)$_a$	75.4(6)
C(5)$_a$	Th$_a$	C(21)$_a$	80.3(5)
C(6)$_a$	Th$_a$	C(21)$_a$	116.9(5)
C(7)$_a$	Th$_a$	C(21)$_a$	111.9(5)
C(8)$_a$	Th$_a$	C(21)$_a$	84.2(6)
C(9)$_a$	Th$_a$	C(21)$_a$	70.2(5)
C(10)$_a$	Th$_a$	C(21)$_a$	89.4(5)
C(39)$_a$	Th$_a$	C(21)$_a$	140.8(6)
O$_b$	Th$_b$	C(6)$_b$	104.9(8)
O$_b$	Th$_b$	C(7)$_b$	134.3(8)
C(6)$_b$	Th$_b$	C(7)$_b$	29.8(8)
O$_b$	Th$_b$	C(8)$_b$	122.6(9)
C(6)$_b$	Th$_b$	C(8)$_b$	45.3(8)
C(7)$_b$	Th$_b$	C(8)$_b$	33.5(11)
O$_b$	Th$_b$	C(9)$_b$	95.2(11)
C(6)$_b$	Th$_b$	C(9)$_b$	45.2(10)
C(7)$_b$	Th$_b$	C(9)$_b$	52.1(10)
C(8)$_b$	Th$_b$	C(9)$_b$	27.4(12)
O$_b$	Th$_b$	C(10)$_b$	86.5(10)
C(6)$_b$	Th$_b$	C(10)$_b$	26.9(9)
C(7)$_b$	Th$_b$	C(10)$_b$	49.5(10)
C(8)$_b$	Th$_b$	C(10)$_b$	43.8(9)
C(9)$_b$	Th$_b$	C(10)$_b$	26.4(11)
O$_b$	Th$_b$	C(1)$_b$	81.1(12)
C(6)$_b$	Th$_b$	C(1)$_b$	140.2(12)

atom	atom	atom	angle/degree
C(7)$_b$	Th$_b$	C(1)$_b$	133.5(13)
C(8)$_b$	Th$_b$	C(1)$_b$	155.8(13)
C(9)$_b$	Th$_b$	C(1)$_b$	174.1(14)
C(10)$_b$	Th$_b$	C(1)$_b$	156.2(12)
O$_b$	Th$_b$	C(2)$_b$	102.3(9)
C(6)$_b$	Th$_b$	C(2)$_b$	116.2(9)
C(7)$_b$	Th$_b$	C(2)$_b$	105.9(10)
C(8)$_b$	Th$_b$	C(2)$_b$	133.7(12)
C(9)$_b$	Th$_b$	C(2)$_b$	158.0(12)
C(10)$_b$	Th$_b$	C(2)$_b$	141.1(10)
C(1)$_b$	Th$_b$	C(2)$_b$	27.7(14)
O$_b$	Th$_b$	C(3)$_b$	126.9(7)
C(6)$_b$	Th$_b$	C(3)$_b$	117.1(7)
C(7)$_b$	Th$_b$	C(3)$_b$	93.7(8)
C(8)$_b$	Th$_b$	C(3)$_b$	110.1(9)
C(9)$_b$	Th$_b$	C(3)$_b$	137.4(11)
C(10)$_b$	Th$_b$	C(3)$_b$	142.7(9)
C(1)$_b$	Th$_b$	C(3)$_b$	45.9(12)
C(2)$_b$	Th$_b$	C(3)$_b$	30.6(9)
O$_b$	Th$_b$	C(4)$_b$	117.5(12)
C(6)$_b$	Th$_b$	C(4)$_b$	135.9(12)
C(7)$_b$	Th$_b$	C(4)$_b$	107.9(12)
C(8)$_b$	Th$_b$	C(4)$_b$	112.0(12)
C(9)$_b$	Th$_b$	C(4)$_b$	134.8(14)
C(10)$_b$	Th$_b$	C(4)$_b$	155.0(13)
C(1)$_b$	Th$_b$	C(4)$_b$	45.3(15)
C(2)$_b$	Th$_b$	C(4)$_b$	45.2(12)
C(3)$_b$	Th$_b$	C(4)$_b$	23.3(11)
O$_b$	Th$_b$	C(5)$_b$	95.3(10)
C(6)$_b$	Th$_b$	C(5)$_b$	159.7(10)
C(7)$_b$	Th$_b$	C(5)$_b$	130.2(10)
C(8)$_b$	Th$_b$	C(5)$_b$	122.9(9)
C(9)$_b$	Th$_b$	C(5)$_b$	135.1(12)

atom	atom	atom	angle/degree
C(10)$_b$	Th$_b$	C(5)$_b$	161.2(9)
C(1)$_b$	Th$_b$	C(5)$_b$	41.6(13)
C(2)$_b$	Th$_b$	C(5)$_b$	56.7(11)
C(3)$_b$	Th$_b$	C(5)$_b$	46.1(9)
C(4)$_b$	Th$_b$	C(5)$_b$	24.7(13)
O$_b$	Th$_b$	C(2')$_b$	141.9(9)
C(6)$_b$	Th$_b$	C(2')$_b$	113.2(9)
C(7)$_b$	Th$_b$	C(2')$_b$	83.8(9)
C(8)$_b$	Th$_b$	C(2')$_b$	87.5(9)
C(9)$_b$	Th$_b$	C(2')$_b$	112.7(12)
C(10)$_b$	Th$_b$	C(2')$_b$	129.6(10)
C(1)$_b$	Th$_b$	C(2')$_b$	68.7(13)
C(2)$_b$	Th$_b$	C(2')$_b$	59.3(10)
C(3)$_b$	Th$_b$	C(2')$_b$	28.8(8)
C(4)$_b$	Th$_b$	C(2')$_b$	25.4(12)
C(5)$_b$	Th$_b$	C(2')$_b$	46.5(10)
O$_b$	Th$_b$	C(4')$_b$	98.2(10)
C(6)$_b$	Th$_b$	C(4')$_b$	147.1(9)
C(7)$_b$	Th$_b$	C(4')$_b$	125.0(10)
C(8)$_b$	Th$_b$	C(4')$_b$	134.0(10)
C(9)$_b$	Th$_b$	C(4')$_b$	154.9(12)
C(10)$_b$	Th$_b$	C(4')$_b$	174.0(11)
C(1)$_b$	Th$_b$	C(4')$_b$	23.9(13)
C(2)$_b$	Th$_b$	C(4')$_b$	34.3(11)
C(3)$_b$	Th$_b$	C(4')$_b$	31.5(9)
C(4)$_b$	Th$_b$	C(4')$_b$	22.0(12)
C(5)$_b$	Th$_b$	C(4')$_b$	22.5(10)
C(2')$_b$	Th$_b$	C(4')$_b$	46.9(10)
O$_b$	Th$_b$	C(39)$_b$	72.6(8)
C(6)$_b$	Th$_b$	C(39)$_b$	84.6(8)
C(7)$_b$	Th$_b$	C(39)$_b$	98.5(9)
C(8)$_b$	Th$_b$	C(39)$_b$	128.8(10)
C(9)$_b$	Th$_b$	C(39)$_b$	124.2(11)

atom	atom	atom	angle/degree
C(10)$_b$	Th$_b$	C(39)$_b$	97.7(8)
C(1)$_b$	Th$_b$	C(39)$_b$	59.2(12)
C(2)$_b$	Th$_b$	C(39)$_b$	51.3(10)
C(3)$_b$	Th$_b$	C(39)$_b$	80.2(7)
C(4)$_b$	Th$_b$	C(39)$_b$	96.3(11)
C(5)$_b$	Th$_b$	C(39)$_b$	100.7(9)
C(2')$_b$	Th$_b$	C(39)$_b$	108.3(9)
C(4')$_b$	Th$_b$	C(39)$_b$	80.3(9)
O$_b$	Th$_b$	C(39')$_b$	75.3(7)
C(6)$_b$	Th$_b$	C(39')$_b$	63.1(7)
C(7)$_b$	Th$_b$	C(39')$_b$	81.4(8)
C(8)$_b$	Th$_b$	C(39')$_b$	108.2(8)
C(9)$_b$	Th$_b$	C(39')$_b$	102.2(10)
C(10)$_b$	Th$_b$	C(39')$_b$	75.8(7)
C(1)$_b$	Th$_b$	C(39')$_b$	81.4(11)
C(2)$_b$	Th$_b$	C(39')$_b$	70.2(9)
C(3)$_b$	Th$_b$	C(39')$_b$	95.4(6)
C(4)$_b$	Th$_b$	C(39')$_b$	115.2(10)
C(5)$_b$	Th$_b$	C(39')$_b$	122.8(8)
C(2')$_b$	Th$_b$	C(39')$_b$	120.3(8)
C(4')$_b$	Th$_b$	C(39')$_b$	101.7(9)
C(39)$_b$	Th$_b$	C(39')$_b$	22.2(7)
O$_b$	Th$_b$	C(21)$_b$	66.0(7)
C(6)$_b$	Th$_b$	C(21)$_b$	116.5(6)
C(7)$_b$	Th$_b$	C(21)$_b$	118.6(7)
C(8)$_b$	Th$_b$	C(21)$_b$	85.1(10)
C(9)$_b$	Th$_b$	C(21)$_b$	72.2(9)
C(10)$_b$	Th$_b$	C(21)$_b$	91.2(8)
C(1)$_b$	Th$_b$	C(21)$_b$	102.0(11)
C(2)$_b$	Th$_b$	C(21)$_b$	127.2(9)
C(3)$_b$	Th$_b$	C(21)$_b$	115.8(7)
C(4)$_b$	Th$_b$	C(21)$_b$	92.6(11)
C(5)$_b$	Th$_b$	C(21)$_b$	72.7(9)

atom	atom	atom	angle/degree
C(2')$_b$	Th$_b$	C(21)$_b$	97.4(8)
C(4')$_b$	Th$_b$	C(21)$_b$	94.1(9)
C(39)$_b$	Th$_b$	C(21)$_b$	136.9(8)
C(39')$_b$	Th$_b$	C(21)$_b$	139.9(7)
O$_a$	P$_a$	C(26)$_a$	108.4(8)
O$_a$	P$_a$	C(27)$_a$	108.0(9)
C(26)$_a$	P$_a$	C(27)$_a$	112.3(9)
O$_a$	P$_a$	C(33)$_a$	111.9(9)
C(26)$_a$	P$_a$	C(33)$_a$	111.1(9)
C(27)$_a$	P$_a$	C(33)$_a$	105.1(9)
O$_b$	P$_b$	C(26)$_b$	107.8(15)
O$_b$	P$_b$	C(33)$_b$	109.3(16)
C(26)$_b$	P$_b$	C(33)$_b$	116.3(13)
O$_b$	P$_b$	C(27)$_b$	110.8(13)
C(26)$_b$	P$_b$	C(27)$_b$	105.5(12)
C(33)$_b$	P$_b$	C(27)$_b$	107.3(15)
Th$_a$	O$_a$	P$_a$	126.4(6)
Th$_b$	O$_b$	P$_b$	129.9(14)
Th$_a$	C(1)$_a$	C(2)$_a$	75.1(11)
Th$_a$	C(1)$_a$	C(5)$_a$	74.3(10)
C(2)$_a$	C(1)$_a$	C(5)$_a$	106.6(17)
Th$_a$	C(1)$_a$	C(11)$_a$	126.1(14)
C(2)$_a$	C(1)$_a$	C(11)$_a$	128.3(19)
C(5)$_a$	C(1)$_a$	C(11)$_a$	123.8(16)
Th$_a$	C(2)$_a$	C(1)$_a$	76.2(11)
Th$_a$	C(2)$_a$	C(3)$_a$	73.5(12)
C(1)$_a$	C(2)$_a$	C(3)$_a$	106.7(18)
Th$_a$	C(2)$_a$	C(12)$_a$	124.3(15)
C(1)$_a$	C(2)$_a$	C(12)$_a$	122.5(19)
C(3)$_a$	C(2)$_a$	C(12)$_a$	129.9(18)
Th$_a$	C(3)$_a$	C(2)$_a$	78.2(13)
Th$_a$	C(3)$_a$	C(4)$_a$	75.2(12)
C(2)$_a$	C(3)$_a$	C(4)$_a$	112.6(19)

atom	atom	atom	angle/degree
Th$_a$	C(3)$_a$	C(13)$_a$	114.8(16)
C(2)$_a$	C(3)$_a$	C(13)$_a$	126.2(20)
C(4)$_a$	C(3)$_a$	C(13)$_a$	121.2(22)
Th$_a$	C(4)$_a$	C(3)$_a$	75.7(13)
Th$_a$	C(4)$_a$	C(5)$_a$	77.5(12)
C(3)$_a$	C(4)$_a$	C(5)$_a$	104.7(19)
Th$_a$	C(4)$_a$	C(14)$_a$	120.7(17)
C(3)$_a$	C(4)$_a$	C(14)$_a$	125.0(20)
C(5)$_a$	C(4)$_a$	C(14)$_a$	129.3(19)
Th$_a$	C(5)$_a$	C(1)$_a$	76.4(11)
Th$_a$	C(5)$_a$	C(4)$_a$	73.5(12)
C(1)$_a$	C(5)$_a$	C(4)$_a$	109.3(15)
Th$_a$	C(5)$_a$	C(15)$_a$	125.6(13)
C(1)$_a$	C(5)$_a$	C(15)$_a$	123.6(16)
C(4)$_a$	C(5)$_a$	C(15)$_a$	126.1(18)
Th$_a$	C(6)$_a$	C(7)$_a$	76.9(11)
Th$_a$	C(6)$_a$	C(10)$_a$	75.9(11)
C(7)$_a$	C(6)$_a$	C(10)$_a$	106.7(17)
Th$_a$	C(6)$_a$	C(16)$_a$	120.4(14)
C(7)$_a$	C(6)$_a$	C(16)$_a$	125.2(17)
C(10)$_a$	C(6)$_a$	C(16)$_a$	127.5(19)
Th$_a$	C(7)$_a$	C(6)$_a$	73.0(11)
Th$_a$	C(7)$_a$	C(8)$_a$	77.7(13)
C(6)$_a$	C(7)$_a$	C(8)$_a$	107.2(17)
Th$_a$	C(7)$_a$	C(17)$_a$	125.3(15)
C(6)$_a$	C(7)$_a$	C(17)$_a$	129.4(21)
C(8)$_a$	C(7)$_a$	C(17)$_a$	122.1(22)
Th$_a$	C(8)$_a$	C(7)$_a$	74.5(12)
Th$_a$	C(8)$_a$	C(9)$_a$	75.8(12)
C(7)$_a$	C(8)$_a$	C(9)$_a$	110.2(19)
Th$_a$	C(8)$_a$	C(18)$_a$	123.3(16)
C(7)$_a$	C(8)$_a$	C(18)$_a$	124.4(21)
C(9)$_a$	C(8)$_a$	C(18)$_a$	124.9(21)

atom	atom	atom	angle/degree
Th$_a$	C(9)$_a$	C(8)$_a$	75.9(11)
Th$_a$	C(9)$_a$	C(10)$_a$	72.9(10)
C(8)$_a$	C(9)$_a$	C(10)$_a$	108.0(17)
Th$_a$	C(9)$_a$	C(19)$_a$	130.3(14)
C(8)$_a$	C(9)$_a$	C(19)$_a$	126.0(19)
C(10)$_a$	C(9)$_a$	C(19)$_a$	123.8(17)
Th$_a$	C(10)$_a$	C(6)$_a$	74.4(10)
Th$_a$	C(10)$_a$	C(9)$_a$	78.5(11)
C(6)$_a$	C(10)$_a$	C(9)$_a$	107.9(16)
Th$_a$	C(10)$_a$	C(20)$_a$	120.2(13)
C(6)$_a$	C(10)$_a$	C(20)$_a$	126.4(18)
C(9)$_a$	C(10)$_a$	C(20)$_a$	125.1(17)
Th$_b$	C(6)$_b$	C(7)$_b$	75.5(15)
Th$_b$	C(6)$_b$	C(10)$_b$	77.4(19)
C(7)$_b$	C(6)$_b$	C(10)$_b$	117.8(25)
Th$_b$	C(6)$_b$	C(16)$_b$	125.9(21)
C(7)$_b$	C(6)$_b$	C(16)$_b$	120.4(27)
C(10)$_b$	C(6)$_b$	C(16)$_b$	121.0(25)
Th$_b$	C(7)$_b$	C(6)$_b$	74.7(16)
Th$_b$	C(7)$_b$	C(8)$_b$	67.5(13)
C(6)$_b$	C(7)$_b$	C(8)$_b$	88.1(22)
Th$_b$	C(7)$_b$	C(17)$_b$	126.0(18)
C(6)$_b$	C(7)$_b$	C(17)$_b$	128.6(26)
C(8)$_b$	C(7)$_b$	C(17)$_b$	141.9(25)
Th$_b$	C(8)$_b$	C(7)$_b$	79.0(16)
Th$_b$	C(8)$_b$	C(9)$_b$	83.7(20)
C(7)$_b$	C(8)$_b$	C(9)$_b$	117.7(29)
Th$_b$	C(8)$_b$	C(18)$_b$	118.7(17)
C(7)$_b$	C(8)$_b$	C(18)$_b$	104.4(30)
C(9)$_b$	C(8)$_b$	C(18)$_b$	135.8(39)
Th$_b$	C(9)$_b$	C(8)$_b$	68.9(19)
Th$_b$	C(9)$_b$	C(10)$_b$	76.9(20)
C(8)$_b$	C(9)$_b$	C(10)$_b$	104.0(32)

atom	atom	atom	angle/degree
Th$_b$	C(9)$_b$	C(19)$_b$	124.6(29)
C(8)$_b$	C(9)$_b$	C(19)$_b$	113.7(42)
C(10)$_b$	C(9)$_b$	C(19)$_b$	141.3(41)
Th$_b$	C(10)$_b$	C(6)$_b$	75.7(16)
Th$_b$	C(10)$_b$	C(9)$_b$	76.7(21)
C(6)$_b$	C(10)$_b$	C(9)$_b$	112.2(32)
Th$_b$	C(10)$_b$	C(20)$_b$	119.4(32)
C(6)$_b$	C(10)$_b$	C(20)$_b$	129.4(29)
C(9)$_b$	C(10)$_b$	C(20)$_b$	118.2(33)
Th$_b$	C(1)$_b$	C(2)$_b$	72.8(25)
Th$_b$	C(1)$_b$	C(11)$_b$	106.9(31)
C(2)$_b$	C(1)$_b$	C(11)$_b$	125.2(47)
Th$_b$	C(1)$_b$	C(4')$_b$	75.3(28)
C(2)$_b$	C(1)$_b$	C(4')$_b$	81.0(41)
C(11)$_b$	C(1)$_b$	C(4')$_b$	153.6(55)
Th$_b$	C(2)$_b$	C(1)$_b$	79.5(26)
Th$_b$	C(2)$_b$	C(3)$_b$	72.9(16)
C(1)$_b$	C(2)$_b$	C(3)$_b$	102.0(34)
Th$_b$	C(2)$_b$	C(12)$_b$	131.9(28)
C(1)$_b$	C(2)$_b$	C(12)$_b$	124.6(40)
C(3)$_b$	C(2)$_b$	C(12)$_b$	128.1(37)
Th$_b$	C(2)$_b$	C(4')$_b$	73.6(17)
C(1)$_b$	C(2)$_b$	C(4')$_b$	44.7(29)
C(3)$_b$	C(2)$_b$	C(4')$_b$	57.7(21)
C(12)$_b$	C(2)$_b$	C(4')$_b$	153.9(33)
Th$_b$	C(3)$_b$	C(2)$_b$	76.6(17)
Th$_b$	C(3)$_b$	C(4)$_b$	70.5(25)
C(2)$_b$	C(3)$_b$	C(4)$_b$	108.4(34)
Th$_b$	C(3)$_b$	C(13)$_b$	121.4(19)
C(2)$_b$	C(3)$_b$	C(13)$_b$	91.9(26)
C(4)$_b$	C(3)$_b$	C(13)$_b$	159.0(36)
Th$_b$	C(3)$_b$	C(2')$_b$	81.4(17)
C(2)$_b$	C(3)$_b$	C(2')$_b$	157.3(28)

atom	atom	atom	angle/degree
C(4)$_b$	C(3)$_b$	C(2')$_b$	58.0(30)
C(13)$_b$	C(3)$_b$	C(2')$_b$	104.5(26)
Th$_b$	C(3)$_b$	C(4')$_b$	76.8(16)
C(2)$_b$	C(3)$_b$	C(4')$_b$	67.6(23)
C(4)$_b$	C(3)$_b$	C(4')$_b$	44.1(28)
C(13)$_b$	C(3)$_b$	C(4')$_b$	149.7(25)
C(2')$_b$	C(3)$_b$	C(4')$_b$	102.0(25)
Th$_b$	C(4)$_b$	C(3)$_b$	86.1(27)
Th$_b$	C(4)$_b$	C(5)$_b$	85.1(29)
C(3)$_b$	C(4)$_b$	C(5)$_b$	147.1(49)
Th$_b$	C(4)$_b$	C(1')$_b$	101.6(26)
C(3)$_b$	C(4)$_b$	C(1')$_b$	132.6(45)
C(5)$_b$	C(4)$_b$	C(1')$_b$	80.3(36)
Th$_b$	C(4)$_b$	C(2')$_b$	90.8(27)
C(3)$_b$	C(4)$_b$	C(2')$_b$	74.0(35)
C(5)$_b$	C(4)$_b$	C(2')$_b$	137.7(45)
C(1')$_b$	C(4)$_b$	C(2')$_b$	59.4(31)
Th$_b$	C(4)$_b$	C(4')$_b$	90.9(33)
C(3)$_b$	C(4)$_b$	C(4')$_b$	89.7(41)
C(5)$_b$	C(4)$_b$	C(4')$_b$	58.8(37)
C(1')$_b$	C(4)$_b$	C(4')$_b$	136.0(50)
C(2')$_b$	C(4)$_b$	C(4')$_b$	163.4(54)
Th$_b$	C(5)$_b$	C(4)$_b$	70.2(27)
Th$_b$	C(5)$_b$	C(15)$_b$	121.9(24)
C(4)$_b$	C(5)$_b$	C(15)$_b$	166.8(41)
Th$_b$	C(5)$_b$	C(1')$_b$	89.0(19)
C(4)$_b$	C(5)$_b$	C(1')$_b$	56.2(30)
C(15)$_b$	C(5)$_b$	C(1')$_b$	115.6(30)
Th$_b$	C(5)$_b$	C(4')$_b$	82.3(26)
C(4)$_b$	C(5)$_b$	C(4')$_b$	56.1(35)
C(15)$_b$	C(5)$_b$	C(4')$_b$	127.1(37)
C(1')$_b$	C(5)$_b$	C(4')$_b$	110.5(37)
C(4)$_b$	C(1')$_b$	C(5)$_b$	43.5(26)

atom	atom	atom	angle/degree
C(4)$_b$	C(1')$_b$	C(2')$_b$	54.7(30)
C(5)$_b$	C(1')$_b$	C(2')$_b$	97.4(32)
C(4)$_b$	C(1')$_b$	C(6')$_b$	165.7(43)
C(5)$_b$	C(1')$_b$	C(6')$_b$	126.7(37)
C(2')$_b$	C(1')$_b$	C(6')$_b$	130.2(38)
Th$_b$	C(2')$_b$	C(3)$_b$	69.8(17)
Th$_b$	C(2')$_b$	C(4)$_b$	63.8(25)
C(3)$_b$	C(2')$_b$	C(4)$_b$	48.1(26)
Th$_b$	C(2')$_b$	C(1')$_b$	90.2(26)
C(3)$_b$	C(2')$_b$	C(1')$_b$	113.5(33)
C(4)$_b$	C(2')$_b$	C(1')$_b$	65.9(33)
Th$_b$	C(2')$_b$	C(7')$_b$	120.2(25)
C(3)$_b$	C(2')$_b$	C(7')$_b$	122.8(34)
C(4)$_b$	C(2')$_b$	C(7')$_b$	169.7(41)
C(1')$_b$	C(2')$_b$	C(7')$_b$	121.9(37)
Th$_b$	C(4')$_b$	C(1)$_b$	80.9(29)
Th$_b$	C(4')$_b$	C(2)$_b$	72.1(17)
C(1)$_b$	C(4')$_b$	C(2)$_b$	54.3(33)
Th$_b$	C(4')$_b$	C(3)$_b$	71.7(15)
C(1)$_b$	C(4')$_b$	C(3)$_b$	108.5(39)
C(2)$_b$	C(4')$_b$	C(3)$_b$	54.7(21)
Th$_b$	C(4')$_b$	C(4)$_b$	67.1(29)
C(1)$_b$	C(4')$_b$	C(4)$_b$	143.6(49)
C(2)$_b$	C(4')$_b$	C(4)$_b$	97.9(38)
C(3)$_b$	C(4')$_b$	C(4)$_b$	46.1(31)
Th$_b$	C(4')$_b$	C(5)$_b$	75.2(25)
C(1)$_b$	C(4')$_b$	C(5)$_b$	123.9(48)
C(2)$_b$	C(4')$_b$	C(5)$_b$	147.1(36)
C(3)$_b$	C(4')$_b$	C(5)$_b$	110.6(34)
C(4)$_b$	C(4')$_b$	C(5)$_b$	65.1(38)
Th$_a$	C(39)$_a$	C(40)$_a$	119.9(16)
Th$_a$	C(39)$_a$	C(44)$_a$	126.6(13)
C(40)$_a$	C(39)$_a$	C(44)$_a$	113.5(18)

atom	atom	atom	angle/degree
C(39)$_a$	C(40)$_a$	C(41)$_a$	124.4(25)
C(40)$_a$	C(41)$_a$	C(42)$_a$	118.5(25)
C(41)$_a$	C(42)$_a$	C(43)$_a$	119.0(22)
C(42)$_a$	C(43)$_a$	C(44)$_a$	121.9(22)
C(39)$_a$	C(44)$_a$	C(43)$_a$	122.5(19)
Th$_b$	C(39)$_b$	C(40)$_b$	126.3(6)
Th$_b$	C(39)$_b$	C(44)$_b$	113.4(6)
Th$_b$	C(39)$_b$	C(39')$_b$	97.5(18)
C(40)$_b$	C(39)$_b$	C(39')$_b$	91.8
C(44)$_b$	C(39)$_b$	C(39')$_b$	73.3
Th$_b$	C(39)$_b$	C(44')$_b$	109.3(13)
C(40)$_b$	C(39)$_b$	C(44')$_b$	114.0
C(44)$_b$	C(39)$_b$	C(44')$_b$	28.7
C(39')$_b$	C(39)$_b$	C(44')$_b$	44.6
C(39)$_b$	C(40)$_b$	C(39')$_b$	36.9
C(41)$_b$	C(40)$_b$	C(39')$_b$	103.7
C(39)$_b$	C(40)$_b$	C(40')$_b$	84.5
C(41)$_b$	C(40)$_b$	C(40')$_b$	81.5
C(39')$_b$	C(40)$_b$	C(40')$_b$	47.8
C(40)$_b$	C(41)$_b$	C(40')$_b$	54.5
C(42)$_b$	C(41)$_b$	C(40')$_b$	98.7
C(42)$_b$	C(43)$_b$	C(43')$_b$	100.5
C(44)$_b$	C(43)$_b$	C(43')$_b$	94.7
C(42)$_b$	C(43)$_b$	C(44')$_b$	121.2
C(44)$_b$	C(43)$_b$	C(44')$_b$	39.0
C(43')$_b$	C(43)$_b$	C(44')$_b$	55.8
C(39)$_b$	C(44)$_b$	C(39')$_b$	43.4
C(43)$_b$	C(44)$_b$	C(39')$_b$	106.4
C(39)$_b$	C(44)$_b$	C(44')$_b$	108.1
C(43)$_b$	C(44)$_b$	C(44')$_b$	77.3
C(39')$_b$	C(44)$_b$	C(44')$_b$	64.8
Th$_b$	C(39')$_b$	C(39)$_b$	60.3(16)
Th$_b$	C(39')$_b$	C(40)$_b$	95.6(12)

atom	atom	atom	angle/degree
C(39)$_b$	C(39')$_b$	C(40)$_b$	51.3
Th$_b$	C(39')$_b$	C(44)$_b$	94.1(13)
C(39)$_b$	C(39')$_b$	C(44)$_b$	63.3
C(40)$_b$	C(39')$_b$	C(44)$_b$	94.4
Th$_b$	C(39')$_b$	C(40')$_b$	126.1(5)
C(39)$_b$	C(39')$_b$	C(40')$_b$	111.4
C(40)$_b$	C(39')$_b$	C(40')$_b$	60.4
C(44)$_b$	C(39')$_b$	C(40')$_b$	132.0
Th$_b$	C(39')$_b$	C(44')$_b$	113.4(5)
C(39)$_b$	C(39')$_b$	C(44')$_b$	102.7
C(40)$_b$	C(39')$_b$	C(44')$_b$	123.6
C(44)$_b$	C(39')$_b$	C(44')$_b$	39.4
C(40)$_b$	C(40')$_b$	C(41)$_b$	43.9
C(40)$_b$	C(40')$_b$	C(39')$_b$	71.7
C(41)$_b$	C(40')$_b$	C(39')$_b$	94.3
C(40)$_b$	C(40')$_b$	C(41')$_b$	119.4
C(41)$_b$	C(40')$_b$	C(41')$_b$	75.5
C(43)$_b$	C(43')$_b$	C(42')$_b$	103.3
C(43)$_b$	C(43')$_b$	C(44')$_b$	64.2
C(39)$_b$	C(44')$_b$	C(43)$_b$	87.8
C(39)$_b$	C(44')$_b$	C(44)$_b$	43.2
C(43)$_b$	C(44')$_b$	C(44)$_b$	63.7
C(39)$_b$	C(44')$_b$	C(39')$_b$	32.7
C(43)$_b$	C(44')$_b$	C(39')$_b$	105.2
C(44)$_b$	C(44')$_b$	C(39')$_b$	75.8
C(39)$_b$	C(44')$_b$	C(43')$_b$	133.1
C(43)$_b$	C(44')$_b$	C(43')$_b$	60.1
C(44)$_b$	C(44')$_b$	C(43')$_b$	123.7
P$_a$	C(26)$_a$	C(21)$_a$	113.9(13)
P$_a$	C(26)$_a$	C(25)$_a$	121.4(15)
C(21)$_a$	C(26)$_a$	C(25)$_a$	124.5(16)
Th$_a$	C(21)$_a$	C(26)$_a$	120.0(11)
Th$_a$	C(21)$_a$	C(22)$_a$	125.1(13)

atom	atom	atom	angle/degree
C(26)$_a$	C(21)$_a$	C(22)$_a$	114.8(16)
C(21)$_a$	C(22)$_a$	C(23)$_a$	123.3(19)
C(22)$_a$	C(23)$_a$	C(24)$_a$	120.1(18)
C(23)$_a$	C(24)$_a$	C(25)$_a$	120.0(19)
C(26)$_a$	C(25)$_a$	C(24)$_a$	117.2(18)
P$_a$	C(27)$_a$	C(28)$_a$	117.4(17)
P$_a$	C(27)$_a$	C(32)$_a$	122.1(16)
C(28)$_a$	C(27)$_a$	C(32)$_a$	120.4(21)
C(27)$_a$	C(28)$_a$	C(29)$_a$	120.5(22)
C(28)$_a$	C(29)$_a$	C(30)$_a$	118.2(23)
C(29)$_a$	C(30)$_a$	C(31)$_a$	123.2(28)
C(30)$_a$	C(31)$_a$	C(32)$_a$	120.0(27)
C(27)$_a$	C(32)$_a$	C(31)$_a$	117.2(22)
P$_a$	C(33)$_a$	C(34)$_a$	123.7(22)
P$_a$	C(33)$_a$	C(38)$_a$	119.6(14)
C(34)$_a$	C(33)$_a$	C(38)$_a$	116.5(23)
C(33)$_a$	C(34)$_a$	C(35)$_a$	123.7(33)
C(34)$_a$	C(35)$_a$	C(36)$_a$	118.2(33)
C(35)$_a$	C(36)$_a$	C(37)$_a$	119.8(30)

atom	atom	atom	angle/degree
C(36)$_a$	C(37)$_a$	C(38)$_a$	117.1(25)
C(33)$_a$	C(38)$_a$	C(37)$_a$	122.6(18)
P$_b$	C(26)$_b$	C(21)$_b$	110.1(17)
P$_b$	C(26)$_b$	C(25)$_b$	121.6(21)
C(21)$_b$	C(26)$_b$	C(25)$_b$	128.3(23)
Th$_b$	C(21)$_b$	C(26)$_b$	126.2(15)
Th$_b$	C(21)$_b$	C(22)$_b$	124.7(18)
C(26)$_b$	C(21)$_b$	C(22)$_b$	108.8(22)
C(21)$_b$	C(22)$_b$	C(23)$_b$	126.2(25)
C(22)$_b$	C(23)$_b$	C(24)$_b$	121.2(26)
C(23)$_b$	C(24)$_b$	C(25)$_b$	117.4(26)
C(26)$_b$	C(25)$_b$	C(24)$_b$	117.9(26)
P$_b$	C(33)$_b$	C(34)$_b$	143.4(10)
P$_b$	C(33)$_b$	C(38)$_b$	96.6(11)
P$_b$	C(27)$_b$	C(28)$_b$	118.6(8)
P$_b$	C(27)$_b$	C(32)$_b$	121.4(8)
Ct(1)$_a$	Th$_a$	Ct(2)$_a$	135.5
Ct(1)$_b$	Th$_b$	Ct(2)$_b$	144.7

Appendix 3.23. Fractional Coordinates and Isotropic Thermal Parameters for $Cp^*_2Th(OMe)(o\text{-}C_6H_4P(O)(OMe)_2)$ (5)

atom	x	y	z	$B_{iso}/Å^2 \times 10^4$
Th	0.07289(3)	0.25129(3)	0.33243(2)	11
P	-0.1382(3)	0.4067(2)	0.2861(2)	14
O(1)	-0.1218(8)	0.3348(5)	0.3319(5)	16
O(2)	-0.1372(8)	0.4716(4)	0.3496(5)	19
O(3)	-0.2724(8)	0.4154(5)	0.2343(5)	19
O(4)	0.2623(7)	0.2219(4)	0.2856(5)	14
C(1)	-0.0395(11)	0.1035(6)	0.3313(7)	15
C(2)	0.0409(11)	0.1052(6)	0.2641(7)	16
C(3)	-0.0174(11)	0.1551(6)	0.2064(7)	15
C(4)	-0.1366(12)	0.1847(6)	0.2379(7)	16
C(5)	-0.1524(11)	0.1531(7)	0.3158(7)	15
C(6)	0.2213(11)	0.2368(6)	0.4773(6)	17
C(7)	0.0926(10)	0.2432(8)	0.5053(6)	18
C(8)	0.0462(11)	0.3167(7)	0.4916(6)	16
C(9)	0.1487(11)	0.3577(6)	0.4555(7)	15
C(10)	0.2592(11)	0.3084(6)	0.4483(6)	13
C(11)	0.0236(13)	0.0495(7)	0.4017(8)	22
C(12)	0.1617(13)	0.0578(7)	0.2513(8)	22
C(13)	0.0329(13)	0.1722(7)	0.1232(7)	22
C(14)	-0.2331(11)	0.2332(6)	0.1932(7)	19
C(15)	-0.2641(12)	0.1684(7)	0.3722(8)	20
C(16)	0.3104(12)	0.1680(7)	0.4820(8)	19
C(17)	0.0161(13)	0.1850(7)	0.5528(8)	22
C(18)	-0.0852(13)	0.3475(7)	0.5170(7)	21
C(19)	0.1546(13)	0.4411(7)	0.4369(8)	22
C(20)	0.3904(12)	0.3310(7)	0.4143(7)	20
C(21)	0.0897(10)	0.3608(7)	0.2247(7)	14
C(22)	0.1947(11)	0.3661(7)	0.1682(8)	18
C(23)	0.1917(12)	0.4189(7)	0.1068(7)	20
C(24)	0.0876(12)	0.4706(7)	0.0994(7)	19
C(25)	-0.0134(13)	0.4674(7)	0.1520(8)	24
C(26)	-0.0108(11)	0.4142(6)	0.2142(7)	16
C(27)	-0.1529(15)	0.5497(7)	0.3264(9)	30
C(28)	-0.3981(12)	0.4121(8)	0.2759(9)	27
C(29)	0.3857(12)	0.2026(8)	0.2559(8)	24

Appendix 3.24. Bond Distances for $Cp^*_2Th(OMe)(o\text{-}C_6H_4P(O)(OMe)_2)$ (5)

atom	atom	distance/Å	atom	atom	distance/Å
Th	O(1)	2.456(8)	C(24)	C(25)	1.353(17)
Th	O(4)	2.138(7)	C(25)	C(26)	1.395(18)
Th	C(21)	2.644(12)	C(1)	C(2)	1.389(16)
Th	C(1)	2.861(11)	C(1)	C(5)	1.455(16)
Th	C(2)	2.848(11)	C(1)	C(11)	1.510(16)
Th	C(3)	2.820(10)	C(2)	C(3)	1.415(15)
Th	C(4)	2.842(11)	C(2)	C(12)	1.498(17)
Th	C(5)	2.866(10)	C(3)	C(4)	1.420(16)
Th	C(6)	2.790(9)	C(3)	C(13)	1.505(17)
Th	C(7)	2.851(10)	C(4)	C(5)	1.414(17)
Th	C(8)	2.886(10)	C(4)	C(14)	1.479(15)
Th	C(9)	2.861(10)	C(5)	C(15)	1.500(17)
Th	C(10)	2.825(10)	C(6)	C(7)	1.390(15)
P	O(1)	1.494(8)	C(6)	C(10)	1.417(15)
P	O(3)	1.583(8)	C(6)	C(16)	1.517(16)
P	O(2)	1.558(9)	C(7)	C(8)	1.404(17)
P	C(26)	1.771(11)	C(7)	C(17)	1.519(18)
O(3)	C(28)	1.455(15)	C(8)	C(9)	1.407(16)
O(2)	C(27)	1.448(16)	C(8)	C(18)	1.500(18)
O(4)	C(29)	1.388(14)	C(9)	C(10)	1.423(15)
C(21)	C(22)	1.429(16)	C(9)	C(19)	1.517(17)
C(21)	C(26)	1.394(16)	C(10)	C(20)	1.500(16)
C(22)	C(23)	1.379(17)	Th	Ct(1)	2.579
C(23)	C(24)	1.396(18)	Th	Ct(2)	2.578

Appendix 3.25. Bond Angles for $Cp^*_2Th(OMe)(o\text{-}C_6H_4P(O)(OMe)_2)$ (5)

atom	atom	atom	angle/degree
O(1)	Th	O(4)	149.7(3)
O(1)	Th	C(21)	67.5
O(1)	Th	C(1)	104.0
O(1)	Th	C(2)	118.0
O(1)	Th	C(3)	97.1
O(1)	Th	C(4)	70.9
O(1)	Th	C(5)	75.0
O(1)	Th	C(6)	117.8
O(1)	Th	C(7)	93.9
O(1)	Th	C(8)	70.5
O(1)	Th	C(9)	78.4
O(1)	Th	C(10)	107.3
O(4)	Th	C(21)	82.2
O(4)	Th	C(1)	97.4
O(4)	Th	C(2)	74.1
O(4)	Th	C(3)	81.9
O(4)	Th	C(4)	110.8
O(4)	Th	C(5)	121.7
O(4)	Th	C(6)	79.9
O(4)	Th	C(7)	108.0
O(4)	Th	C(8)	122.1
O(4)	Th	C(9)	101.2
O(4)	Th	C(10)	75.6
C(21)	Th	C(1)	134.9
C(21)	Th	C(2)	114.6
C(21)	Th	C(3)	88.8
C(21)	Th	C(4)	90.0
C(21)	Th	C(5)	116.8
C(21)	Th	C(6)	126.8
C(21)	Th	C(7)	134.6
C(21)	Th	C(8)	108.7
C(21)	Th	C(9)	88.1
C(21)	Th	C(10)	97.7
C(1)	Th	C(2)	28.2
C(1)	Th	C(3)	47.0
C(1)	Th	C(4)	47.7
C(1)	Th	C(5)	29.4
C(1)	Th	C(6)	97.0
C(1)	Th	C(7)	88.7
C(1)	Th	C(8)	109.2
C(1)	Th	C(9)	135.2
C(1)	Th	C(10)	126.1
C(2)	Th	C(3)	28.9
C(2)	Th	C(4)	47.9
C(2)	Th	C(5)	47.6
C(2)	Th	C(6)	107.8
C(2)	Th	C(7)	110.6
C(2)	Th	C(8)	135.6
C(2)	Th	C(9)	155.4
C(2)	Th	C(10)	131.4
C(3)	Th	C(4)	29.0(3)
C(3)	Th	C(5)	47.4(3)
C(3)	Th	C(6)	136.6(3)
C(3)	Th	C(7)	135.7(3)
C(3)	Th	C(8)	151.2(3)
C(3)	Th	C(9)	175.5(3)
C(3)	Th	C(10)	155.4(3)
C(4)	Th	C(5)	28.7(3)
C(4)	Th	C(6)	143.1(3)
C(4)	Th	C(7)	123.8(3)
C(4)	Th	C(8)	125.4(3)
C(4)	Th	C(9)	147.7(3)
C(4)	Th	C(10)	170.7(3)
C(5)	Th	C(6)	115.3(3)

atom	atom	atom	angle/degree
C(5)	Th	C(7)	95.6(3)
C(5)	Th	C(8)	103.8(3)
C(5)	Th	C(9)	131.7(3)
C(5)	Th	C(10)	142.2(3)
C(6)	Th	C(7)	28.5(3)
C(6)	Th	C(8)	47.3(3)
C(6)	Th	C(9)	47.9(3)
C(6)	Th	C(10)	29.2(3)
C(7)	Th	C(8)	28.3(3)
C(7)	Th	C(9)	46.9(3)
C(7)	Th	C(10)	47.0(3)
C(8)	Th	C(9)	28.3(3)
C(8)	Th	C(10)	47.0(3)
C(9)	Th	C(10)	29.0(3)
O(1)	P	O(3)	115.9(5)
O(1)	P	O(2)	107.3(5)
O(1)	P	C(26)	109.3(5)
O(3)	P	O(2)	106.2(4)
O(3)	P	C(26)	104.7(5)
O(2)	P	C(26)	113.6(5)
Th	O(1)	P	126.6(5)
P	O(3)	C(28)	118.6(8)
P	O(2)	C(27)	122.4(9)
Th	O(4)	C(29)	179.5(8)
Th	C(21)	C(22)	123.2(8)
Th	C(21)	C(26)	121.7(8)
C(22)	C(21)	C(26)	114.8(11)
C(21)	C(22)	C(23)	121.3(11)
C(22)	C(23)	C(24)	120.9(11)
C(23)	C(24)	C(25)	119.4(12)
C(24)	C(25)	C(26)	119.9(12)
P	C(26)	C(21)	113.6(9)
P	C(26)	C(25)	122.8(9)
C(21)	C(26)	C(25)	123.5(11)
C(2)	C(1)	C(5)	108.4(10)
C(2)	C(1)	C(11)	125.0(11)

atom	atom	atom	angle/degree
C(5)	C(1)	C(11)	125.9(11)
C(1)	C(2)	C(3)	108.0(10)
C(1)	C(2)	C(12)	126.2(11)
C(3)	C(2)	C(12)	125.6(11)
C(2)	C(3)	C(4)	109.1(10)
C(2)	C(3)	C(13)	126.5(11)
C(4)	C(3)	C(13)	124.4(10)
C(3)	C(4)	C(5)	107.5(10)
C(3)	C(4)	C(14)	125.7(11)
C(5)	C(4)	C(14)	126.5(11)
C(1)	C(5)	C(4)	107.1(10)
C(1)	C(5)	C(15)	126.5(11)
C(4)	C(5)	C(15)	126.4(11)
C(7)	C(6)	C(10)	107.4(10)
C(7)	C(6)	C(16)	127.1(11)
C(10)	C(6)	C(16)	125.4(10)
C(6)	C(7)	C(8)	109.3(10)
C(6)	C(7)	C(17)	127.1(12
C(8)	C(7)	C(17)	123.1(10)
C(7)	C(8)	C(9)	107.9(10)
C(7)	C(8)	C(18)	125.9(11)
C(9)	C(8)	C(18)	126.0(11)
C(8)	C(9)	C(10)	107.3(10)
C(8)	C(9)	C(19)	128.8(11)
C(10)	C(9)	C(19)	123.4(11)
C(6)	C(10)	C(9)	107.9(10)
C(6)	C(10)	C(20)	127.9(11)
C(9)	C(10)	C(20)	124.2(11)
O(4)	Th	Ct(2)	97.94
O(4)	Th	Ct(1)	97.59
O(1)	Th	Ct(2)	93.52
O(1)	Th	Ct(1)	93.13
Ct(1)	Th	Ct(2)	136.33
Ct(2)	Th	C(21)	112.27
Ct(1)	Th	C(21)	110.13

Appendix 3.26. Selected Bond Lengths for Common Atoms of 1, 3, 4 and 5

atom	atom	1	3	4	5
Arene Ring					
Th	C(21)	2.486(10)	2.597(19)	2.634(17)	2.644(12)
C(21)	C(22)	1.346(14)	1.430(32)	1.354(23)	1.429(16)
C(21)	C(26)	1.448(12)	1.377(30)	1.439(26)	1.394(17)
C(22)	C(23)	1.403(13)	1.401(25)	1.420(28)	1.379(17)
C(23)	C(24)	1.394(14)	1.386(34)	1.407(31)	1.396(18)
C(24)	C(25)	1.383(14)	1.446(33)	1.387(26)	1.353(17)
C(25)	C(26)	1.400(12)	1.354(24)	1.419(28)	1.395(18)
Thorium-Cp*(Centroid)					
Th	Ct(1)	2.528	2.587	2.573	2.579
Th	Ct(2)	2.528	2.489	2.583	2.578
Thorium-Cp*(sp2-C)					
Th	C(1)	2.803(9)	2.909(19)	2.880(19)	2.861(11)
Th	C(2)	2.796(7)	2.818(11)	2.866(21)	2.848(11)
Th	C(3)	2.785(9)	2.893(18)	2.807(21)	2.820(10)
Th	C(4)	2.816(9)	2.842(14)	2.802(23)	2.842(11)
Th	C(5)	2.828(9)	2.823(20)	2.853(19)	2.866(10)
Th	C(6)	2.789(9)	2.804(15)	2.802(19)	2.790(9)
Th	C(7)	2.778(7)	2.771(18)	2.854(19)	2.851(10)
Th	C(8)	2.804(9)	2.754(19)	2.894(23)	2.886(10)
Th	C(9)	2.808(9)	2.722(19)	2.894(19)	2.861(10)
Th	C(10)	2.808(9)	2.832(26)	2.822(18)	2.825(10)

Appendix 3.27. Selected Bond Angles for Common Atoms of 1, 3, 4 and 5

atom	atom	atom	1	3	4	5
Cp*(Centroid)-Thorium-Cp*(Centroid)						
Ct(1)	Th	Ct(2)	142.06	133.5	135.5	136.33
Arene Ring						
Th	C(21)	C(22)	130.1(7)	119.3(15)	125.1(13)	123.2(8)
Th	C(21)	C(26)	110.2(6)	125.8(15)	120.0(11)	121.7(8)
C(22)	C(21)	C(26)	119.6(9)	114.7(16)	114.8(16)	114.8(11)
C(21)	C(22)	C(23)	123.2(9)	123.3(20)	123.3(19)	121.3(11)
C(22)	C(23)	C(24)	117.9(9)	118.2(21)	120.1(18)	120.9(11)
C(23)	C(24)	C(25)	120.2(9)	119.6(18)	120.0(19)	119.4(12)
C(24)	C(25)	C(26)	122.2(8)	118.7(19)	117.2(18)	119.9(12)
C(21)	C(26)	C(25)	116.9(8)	125.2(19)	124.5(16)	123.5(11)

APPENDIX TO CHAPTER FOUR

Appendix 4.1. Crystal Data Collection and Refinement Parameters for $(^tBuO)_2Ce(NTMS_2)_2$ (1) and $(tBuO)_2Ce(N(TMS)(o\text{-}MeOC_6H_4))_2$ (2)

compound	1	2
chemical formula	$C_{20}H_{54}CeN_2O_2Si_4$	$C_{28}H_{48}CeN_2O_4Si_2$
color, habit	red, irregular	dark purple block
crystal size (mm)	0.23 x 0.25 x 0.33	0.45 x 0.47 x 0.55
crystal system	tetragonal	triclinic
space group	$I4_1/acd$	$P1$
a (Å)	18.955 (3)	9.9597 (5)
b (Å)	18.955 (3)	10.6794 (5)
c (Å)	35.555 (7)	18.6174 (8)
α (deg)	90	89.857 (4)
β (deg)	90	76.222 (3)
γ (deg)	90	62.456 (3)
V (Å^3)	12775(4)	1694.73(17)
Z	16	2
density (calcd) (g/cm^3)	1.263	1.319
μ (cm^{-1})	15.92	1.445
temerature (K)	101	173
radiation	Mo Kα	Mo Kα
wavelength (Å)	0.71073	0.71073
monochromator	HOG crystal	HOG crystal
diffractometer	Picker	Picker
2Θ range (deg)	6-45	4-65
index ranges	$0 \le h \le 20$,	$0 \le h \le 14$,
	$-11 \le k \le 20$,	$-14 \le k \le 16$,
	$-21 \le l \le 38$	$-27 \le l \le 28$
no. rflns measured	5986	13069
no. indep. rflns	2089	12161
R_{int} (%)	5.52	1.46
R_w (%)	4.00	3.85
R (%)	4.40	3.17
solution	direct methods	direct methods

Appendix 4.2. Crystal Data Collection and Refinement Parameters for $(^tBuO)_3Ce(N(TMS)(2,6\text{-}^iPr_2C_6H_3)$ (3) and $Ce_3(O^tBu)_{10}(NO_3)$ (4)

compound	3	4
chemical formula	$C_{27}H_{53}CeNO_3Si$	$C_{45}H_{102}Ce_3NO_{13}$
color, habit	red	yellow-brown
crystal size (mm)	0.20 x 0.27 x 0.27	0.27 x 0.27 x 0.30
crystal system	monoclinic	monoclinic
space group	$P2_1/n$	$P2_1/c$
a (Å)	11.681(3)	18.042(3)
b (Å)	16.279(4)	17.051(3)
c (Å)	17.050(4)	19.800(4)
α (deg)	90	90
β (deg)	93.11(1)	104.26(1)
γ (deg)	90	90
V (Å^3)	3237.32	5903.42
Z	4	4
density (calcd) (g/cm^3)	1.247	1.449
μ (cm^{-1})	14.87	23.629
temerature (K)	99	99
radiation	MoKα	MoKα
wavelength (Å)	0.71069	0.71069
monochromator	HOG crystal	HOG crystal
diffractometer	Picker	Picker
2Θ range (deg)	6-45	6-45
index ranges	$0 \le h \le 12$,	$0 \le h \le 14$,
	$-17 \le k \le 18$,	$0 \le k \le 18$,
	$-18 \le l \le 18$	$-21 \le l \le 20$
no. rflns measured	4665	9105
no. indep. rflns	4236	7698
R_{int} (%)	3.90	2.00
R_w (%)	6.27	2.97
R (%)	6.68	2.89
solution	direct methods	direct methods

Appendix 4.3. Fractional Coordinates and Isotropic Thermal Parameters for $(^tBuO)_2Ce(N(TMS_2)_2$ (1)

atom	x	y	z	$U_{eq}/Å^2 \times 10^3$
Ce	0.2500	0.2646(1)	0.0000	14(1)
O	0.3357(3)	0.3303(3)	-0.0040(1)	19(2)
N	0.2570(4)	0.2125(4)	0.0571(2)	16(3)
Si(1)	0.3205(1)	0.1488(1)	0.0603(1)	17(1)
Si(2)	0.2064(1)	0.2439(1)	0.0944(1)	20(1)
C(1)	0.3882(4)	0.3809(5)	0.0064(2)	18(3)
C(2)	0.3507(6)	0.4446(5)	0.0219(3)	31(4)
C(3)	0.4304(5)	0.4014(6)	-0.0280(3)	28(3)
C(4)	0.4351(6)	0.3487(5)	0.0367(3)	32(4)
C(5)	0.3616(5)	0.1422(5)	0.0126(3)	22(3)
C(6)	0.3934(5)	0.1676(6)	0.0943(3)	23(4)
C(7)	0.2840(6)	0.0607(5)	0.0717(3)	27(3)
C(8)	0.1110(5)	0.2307(7)	0.0839(3)	31(4)
C(9)	0.2242(6)	0.3404(6)	0.1011(3)	33(4)
C(10)	0.2249(7)	0.1992(6)	0.1401(3)	35(4)

Appendix 4.4 Bond Distances for (^{t}BuO)$_2$Ce(N(TMS$_2$)$_2$ (1)

atom	atom	distance/Å
Ce	N	2.260(7)
Ce	N'	2.260(7)
N	Si(1)	1.708(7)
Si(1)	C(5)	1.874(11)
N	C(7)	1.852(10)
Si(2)	C(8)	1.866(11)
Si(2)	C(10)	1.867(11)
O	C(1)	1.431(11)
C(1)	C(3)	1.517(13)
Ce	O	2.052(6)
Ce	O'	2.052(6)
N	Si(2)	1.744(7)
Si(1)	C(6)	1.868(10)
Si(2)	C(9)	1.871(11)
C(1)	C(2)	1.503(14)
C(1)	C(4)	1.517(14)

Appendix 4.5. Bond Angles for (^{t}BuO)$_2$Ce(N(TMS$_2$)$_2$ (1)

atom	atom	atom	angle/degree
N	Ce	N'	128.1(4)
O	Ce	O'	105.3(3)
Ce	N	Si(1)	114.3(3)
Si(1)	N	Si(2)	125.3(4)
C(5)	Si(1)	C(6)	106.8(5)
N	Si(1)	C(7)	112.7(4)
C(6)	Si(1)	C(7)	108.3(5)
C(8)	Si(2)	C(9)	109.8(5)
N	Si(2)	C(10)	113.9(4)
C(9)	Si(2)	C(10)	107.1(5)
O	C(1)	C(2)	107.6(7)
C(2)	C(1)	C(3)	109.7(8)
C(2)	C(1)	C(4)	109.4(8)
N	Ce	O	106.4(2)
O	Ce	N'	104.5(2)
N	Ce	O'	104.5(2)
N'	Ce	O'	106.4(2)
Ce	N	Si(2)	120.0(4)
N	Si(1)	C(5)	106.0(4)
N	Si(1)	C(6)	115.5(4)
C(5)	Si(1)	C(7)	107.1(5)
N	Si(2)	C(8)	109.7(4)
N	Si(2)	C(9)	109.5(4)
C(8)	Si(2)	C(10)	106.8(5)
Ce	O	C(1)	159.9(5)
O	C(1)	C(3)	108.9(7)
O	C(1)	C(4)	108.5(7)
C(3)	C(1)	C(4)	112.7(8)

Appendix 4.6. Fractional Coordinates and Isotropic Thermal Parameters for $(^tBuO)_2Ce(N(TMS)(o\text{-}MeOC_6H_4))_2$ (2)

atom	x	y	z	$U_{eq}/Å^2 \times 10^4$
Ce	0.9115(1)	-0.0081(16)	0.7600(1)	164(1)
N(1)	0.9287(21)	0.1651(19)	0.8266(10)	210(5)
N(2)	1.0829(22)	-0.1977(18)	0.6670(10)	215(5)
Si(1)	0.7566(8)	0.3132(7)	0.8747(4)	276(2)
Si(2)	1.0225(9)	-0.3186(7)	0.6461(4)	304(3)
O(1)	0.7460(19)	0.1128(17)	0.7042(9)	243(5)
O(2)	0.8446(20)	-0.1091(18)	0.8454(9)	263(5)
O(3)	1.1681(18)	-0.0981(16)	0.7990(9)	241(5)
O(4)	1.1068(19)	0.0391(16)	0.6620(9)	230(5)
C(1)	0.6818(29)	0.1711(27)	0.6436(14)	300(6)
C(2)	0.5443(40)	0.1500(41)	0.6458(21)	561(8)
C(3)	0.6335(49)	0.3270(36)	0.6497(24)	646(8)
C(4)	0.8102(41)	0.0965(45)	0.5710(18)	621(8)
C(5)	0.8274(30)	-0.1658(26)	0.9146(13)	296(6)
C(6)	0.6679(36)	-0.1618(35)	0.9348(18)	447(7)
C(7)	0.9573(37)	-0.3186(31)	0.9045(18)	435(7)
C(8)	0.8398(43)	-0.0747(35)	0.9731(16)	489(8)
C(9)	0.5904(28)	0.2746(28)	0.8793(16)	341(7)
C(10)	0.7130(37)	0.4784(28)	0.8281(22)	482(7)
C(11)	0.7567(35)	0.3497(37)	0.9729(18)	510(8)
C(12)	0.8108(34)	-0.2479(29)	0.6977(16)	364(7)
C(13)	1.0397(43)	-0.3421(39)	0.5442(18)	549(8)
C(14)	1.1322(43)	-0.4973(31)	0.6754(26)	631(8)
C(15)	1.0752(25)	0.1465(23)	0.8298(12)	220(6)
C(16)	1.2047(24)	0.0082(24)	0.8149(12)	228(6)
C(17)	1..3544(27)	-0.0195(29)	0.8151(14)	313(6)
C(18)	1.3807(30)	0.0935(32)	0.8314(16)	375(7)
C(19)	1.2582(32)	0.2300(30)	0.8467(16)	354(7)
C(20)	1..1078(29)	0.2560(27)	0.8459(14)	295(6)

atom	x	y	z	$U_{eq}/Å^2 \times 10^4$
C(21)	1.2897(30)	-0.2429(26)	0.7910(16)	343(6)
C(22)	1.2243(25)	-0.2067(22)	0.6274(12)	222(6)
C(23)	1.2419(25)	-0.0823(23)	0.6250(12)	220(6)
C(24)	1.3815(29)	-0.0830(28)	0.5902(14)	308(6)
C(25)	1.5124(30)	-0.2110(32)	0.5545(16)	379(7)
C(26)	1.5000(31)	-0.3344(30)	0.5544(16)	396(7)
C(27)	1.3586(30)	-0.3320(26)	0.5901(15)	326(6)
C(28)	1.1066(31)	0.1730(24)	0.6532(15)	314(6)

Appendix 4.7. Bond Distances for $(^tBuO)_2Ce(N(TMS)(o\text{-}MeOC_6H_4))_2$ (2)

atom	atom	distance/Å	atom	atom	distance/Å
Ce	O(1)	2.074(2)	Ce	O(2)	2.073(2)
Ce	O(3)	2.567(2)	Ce	O(4)	2.564(2)
Ce	N(1)	2.326(2)	Ce	N(2)	2.333(2)
Si(1)	N(1)	1.736(2)	Si(1)	C(9)	1.868(4)
Si(1)	C(10)	1.878(3)	Si(1)	C(11)	1.870(4)
Si(2)	N(2)	1.737(3)	Si(2)	C(12)	1.872(3)
Si(2)	C(13)	1.870(4)	Si(2)	C(14)	1.869(3)
O(1)	C(1)	1.429(3)	O(2)	C(5)	1.430(3)
O(3)	C(16)	1.396(4)	O(3)	C(21)	1.439(3)
O(4)	C(23)	1.385(2)	O(4)	C(28)	1.440(3)
N(1)	C(15)	1.394(3)	N(2)	C(22)	1.383(3)
C(1)	C(2)	1.504(6)	C(1)	C(3)	1.503(5)
C(1)	C(4)	1.529(4)	C(5)	C(6)	1.524(5)
C(5)	C(7)	1.521(3)	C(5)	C(8)	1.527(5)
C(15)	C(16)	1.412(3)	C(15)	C(20)	1.403(4)
C(16)	C(16)	1.381(4)	C(17)	C(18)	1.398(5)
C(18)	C(19)	1.375(3)	C(19)	C(20)	1.395(5)
C(22)	C(23)	1.420(4)	C(22)	C(27)	1.404(3)
C(23)	C(24)	1.384(4)	C(24)	C(25)	1.399(3)
C(25)	C(26)	1.381(5)	C(26)	C(27)	1.395(4)

Appendix 4.8. Bond Angles for $(^tBuO)_2Ce(N(TMS)(o\text{-}MeOC_6H_4))_2$ (2)

atom	atom	atom	angle/degree
O(1)	Ce	O(2)	117.4(1)
O(2)	Ce	O(3)	86.1(1)
O(2)	Ce	O(4)	155.5(1)
O(1)	Ce	N(1)	102.1(1)
O(3)	Ce	N(1)	65.7(1)
O(1)	Ce	N(2)	99.7(1)
N(1)	Ce	N(2)	79.0(1)
N(1)	Ce	N(2)	135.9(1)
N(1)	Si(1)	C(10)	113.7(1)
C(10)	Si(1)	C(11)	111.8(1)
N(2)	Si(2)	C(11)	109.2(2)
N(2)	Si(2)	C(13)	111.3(2)
N(2)	Si(2)	C(14)	113.7(2)
C(13)	Si(2)	C(14)	108.5(2)
Ce	O(2)	C(5)	161.9(2)
Ce	O(3)	C(21)	127.1(2)
Ce	O(4)	C(23)	114.4(1)
C(23)	O(4)	C(28)	117.2(2)
Ce	N(1)	C(15)	120.0(1)
Ce	N(2)	Si(2)	118.1(1)
Si(2)	N(2)	C(22)	122.2(1)
O(1)	C(1)	C(3)	108.9(3)
O(1)	C(1)	C(4)	108.0(2)
C(3)	C(1)	C(4)	109.1(3)
O(2)	C(5)	C(7)	108.6(2)
O(2)	C(5)	C(8)	108.0(3)
C(15)	C(16)	C(17)	123.2(3)
C(17)	C(18)	C(19)	119.9(2)
C(15)	C(20)	C(19)	122.2(2)
N(2)	C(22)	C(27)	125.4(3)
O(4)	C(23)	C(22)	113.5(2)
C(22)	C(23)	C(24)	123.1(2)
C(24)	C(25)	C(26)	119.5(3)
C(22)	C(27)	C(26)	122.4(3)
O(1)	Ce	O(3)	155.9(1)
O(1)	Ce	O(4)	86.3(1)
O(3)	Ce	O(4)	71.1(1)
O(2)	Ce	N(1)	101.1(1)
O(4)	Ce	N(1)	78.3(1)
O(2)	Ce	N(2)	102.1(1)
O(4)	Ce	N(2)	65.4(1)
N(2)	Si(1)	C(9)	107.6(1)
C(9)	Si(1)	C(10)	106.6(2)
C(9)	Si(1)	C(11)	107.7(2)
N(2)	Si(2)	C(12)	108.3(1)
C(12)	Si(2)	C(13)	108.0(2)
C(12)	Si(2)	C(14)	106.8(2)
Ce	O(1)	C(1)	159.1(1)
Ce	O(3)	C(16)	14.4(1)
C(16)	O(3)	C(21)	117.2(2)
Ce	O(4)	C(28)	127.0(1)
Ce	N(1)	Si(1)	118.8(1)
Si(1)	N(1)	C(15)	121.1(2)
Ce	N(2)	C(22)	119.7(2)
O(1)	C(1)	C(2)	109.3(3)
C(2)	C(1)	C(3)	111.3(3)
C(2)	C(1)	C(4)	110.1(3)
O(2)	C(5)	C(6)	107.9(2)
C(6)	C(5)	C(7)	109.8(3)
C(6)	C(5)	C(8)	111.7(2)
N(1)	C(15)	C(16)	119.3(2)
C(16)	C(15)	C(20)	115.5(2)

atom	atom	atom	angle/degree
O(3)	C(16)	C(17)	122.9(2)
C(16)	C(17)	C(18)	119.1(2)
C(18)	C(19)	C(20)	120.2(3)
N(2)	C(22)	C(23)	119.4(2)

atom	atom	atom	angle/degree
C(23)	C(22)	C(27)	115.2(2)
O(4)	C(23)	C(24)	123.4(2)
C(23)	C(24)	C(25)	119.4(3)
C(25)	C(26)	C(27)	120.4(2)

Appendix 4.9. Fractional Coordinates and Isotropic Thermal Parameters for $(^tBuO)_3Ce(N(TMS)(2, 6\text{-}^iPr_2C_6H_3)$ (3)

atom	x	y	z	$B_{iso}/Å^2 x\ 10^4$
Ce	0.1142(1)	0.2216(1)	0.33719(5)	15
N	0.2724(10)	0.2109(8)	0.4180(7)	22
Si	0.3598(4)	0.1253(3)	0.4283(2)	18
O(1)	0.0241(8)	0.3312(6)	0.3332(5)	21
O(2)	-0.0030(8)	0.1322(6)	0.3618(6)	24
O(3)	0.1640(8)	0.2015(6)	0.2247(5)	20
C(1)	-0.0327(12)	0.4063(9)	0.3343(8)	18
C(2)	0.0149(13)	0.4543(10)	0.4036(10)	30
C(3)	-0.0142(17)	0.4518(13)	0.2596(12)	47
C(4)	-0.1573(14)	0.3904(11)	0.3442(11)	37
C(5)	-0.1040(13)	0.0867(10)	0.3654(9)	25
C(6)	-0.0740(21)	-0.0015(15)	0.3704(25)	115
C(7)	-0.1661(15)	0.1088(13)	0.4376(12)	48
C(8)	-0.1767(20)	0.1007(27)	0.2939(15)	129
C(9)	0.1704(11)	0.1883(9)	0.1419(8)	18
C(10)	0.1901(14)	0.2711(12)	0.1040(9)	35
C(11)	0.2673(14)	0.1301(10)	0.1302(10)	30
C(12)	0.0558(14)	0.1534(11)	0.1128(10)	35
C(13)	0.2766(12)	0.0417(9)	0.3805(9)	23
C(14)	0.3942(14)	0.1003(10)	0.5334(9)	30
C(15)	0.4998(14)	0.1364(9)	0.3814(10)	30
C(16)	0.2822(14)	0.2863(9)	0.4557(8)	27
C(17)	0.2309(11)	0.3023(10)	0.5268(9)	26
C(18)	0.2436(11)	0.3813(10)	0.5595(8)	18
C(19)	0.3042(12)	0.4438(9)	0.5258(9)	19
C(20)	0.3561(13)	0.4291(9)	0.4562(8)	18
C(21)	0.3482(11)	0.3526(9)	0.4191(8)	17
C(22)	0.1618(14)	0.2389(10)	0.5640(8)	27
C(23)	0.1981(15)	0.2296(12)	0.6525(9)	36
C(24)	0.0344(14)	0.2584(11)	0.5544(10)	34
C(25)	0.4074(12)	0.3411(9)	0.3426(8)	20
C(26)	0.5314(14)	0.3600(10)	0.3489(10)	32
C(27)	0.3437(14)	0.3904(10)	0.2772(9)	27

Appendix 4.10. Bond Distances for (^{t}BuO)$_3$Ce(N(TMS)(2, 6-^{i}Pr$_2$C$_6$H$_3$) (3)

atom	atom	distance/Å	atom	atom	distance/Å
Ce	N	2.250(12)	C(5)	C(8)	1.465(28)
Ce	O(1)	2.070(10)	C(9)	C(10)	1.518(23)
Ce	O(2)	2.058(10)	C(9)	C(11)	1.497(21)
Ce	O(3)	2.060(9)	C(9)	C(12)	1.513(20)
N	C(16)	1.387(18)	C(16)	C(17)	1.405(21)
N	Si	1.731(13)	C(16)	C(21)	1.482(21)
Si	C(13)	1.837(15)	C(17)	C(18)	1.407(21)
Si	C(14)	1.861(16)	C(17)	C(22)	1.475(21)
Si	C(15)	1.867(17)	C(18)	C(19)	1.382(20)
O(1)	C(1)	1.392(17)	C(19)	C(20)	1.382(20)
O(2)	C(5)	1.396(17)	C(20)	C(21)	1.397(20)
O(3)	C(9)	1.434(16)	C(21)	C(25)	1.521(19)
C(1)	C(2)	1.497(21)	C(22)	C(23)	1.553(21)
C(1)	C(3)	1.500(24)	C(22)	C(24)	1.521(22)
C(1)	C(4)	1. 497(21)	C(25)	C(26)	1.478(21)
C(5)	C(6)	1.480(3)	C(25)	C(27)	1.533(20)
C(5)	C(7)	1.506(23)			

Appendix 4.11. Bond Angles for (^{t}BuO)$_3$Ce(N(TMS)(2, 6-^{i}Pr$_2$C$_6$H$_3$) (3)

atom	atom	atom	angle/degree
O(1)	Ce	O(2)	105.9(4)
O(1)	Ce	O(3)	106.0(4)
O(1)	Ce	N	119.1(4)
O(2)	Ce	O(3)	107.6(4)
O(2)	Ce	N	110.7(4)
O(3)	Ce	N	107.1(4)
N	Si	C(13)	104.9(6)
N	Si	C(14)	111.7(7)
N	Si	C(15)	113.9(7)
C(13)	Si	C(14)	110.2(8)
C(13)	Si	C(15)	109.6(7)
C(14)	Si	C(15)	106.6(8)
Ce	O(1)	C(1)	176.7(8)
Ce	O(2)	C(5)	163.2(10)
Ce	O(3)	C(9)	166.6(8)
Ce	N	Si	125.8(7)
Ce	N	C(16)	105.8(9)
Si	N	C(16)	129.2(10)
N	C(16)	C(17)	122.4(14)
N	C(16)	C(21)	118.7(13)
C(17)	C(16)	C(21)	119.0(13)
C(16)	C(17)	C(18)	118.1(14)
C(16)	C(17)	C(22)	120.7(14)
C(18)	C(17)	C(22)	121.2(14)
C(17)	C(18)	C(19)	123.6(13)
C(18)	C(19)	C(20)	119.2(13)
C(19)	C(20)	C(21)	121.4(14)
C(16)	C(21)	C(20)	118.8(13)
C(16)	C(21)	C(25)	122.9(13)
C(20)	C(21)	C(25)	118.3(13)
C(17)	C(22)	C(23)	111.0(13)
C(17)	C(22)	C(24)	111.2(13)
C(23)	C(22)	C(26)	109.8(13)
C(21)	C(25)	C(26)	113.7(12)
C(21)	C(25)	C(27)	109.5(12)
C(26)	C(25)	C(27)	112.3(13)
O(1)	C(1)	C(2)	108.2(11)
O(1)	C(1)	C(3)	109.4(13)
O(1)	C(1)	C(4)	108.4(13)
C(2)	C(1)	C(3)	110.4(14)
C(2)	C(1)	C(4)	108.9(13)
C(3)	C(1)	C(4)	111.5(14)
O(2)	C(5)	C(6)	108.6(15)
O(2)	C(5)	C(7)	110.8(13)
O(2)	C(5)	C(8)	109.5(15)
C(6)	C(5)	C(7)	107.8(19)
C(6)	C(5)	C(8)	108.9(25)
C(7)	C(5)	C(8)	111.1(19)
O(3)	C(9)	C(10)	107.6(12)
O(3)	C(9)	C(11)	107.9(12)
O(3)	C(9)	C(12)	106.7(11)
C(10)	C(9)	C(11)	111.9(13)
C(10)	C(9)	C(12)	110.2(13)
C(11)	C(9)	C(12)	112.3(13)

Appendix 4.12. Fractional Coordinates and Isotropic Thermal Parameters for $Ce_3(^tBuO)_{10}(NO_3)$ (4)

atom	x	y	z	$B_{iso}/Å^2 x\ 10^4$
Ce(1)	0.27421(2)	0.14912(2)	0.33138(1)	15
Ce(2)	0.13444(2)	-0.01391(2)	0.32327(1)	16
Ce(3)	0.24464(2)	-0.00057(2)	0.18999(1)	16
N	0.2507(3)	0.3228(3)	0.3191(2)	28
O(1)	0.2898(2)	0.2871(2)	0.2832(2)	32
O(2)	0.2155(2)	0.2822(2)	0.3526(2)	27
O(3)	0.2494(3)	0.3945(2)	0.3205(2)	40
O(4)	0.1606(2)	0.0845(2)	0.2397(2)	16
O(5)	0.2698(2)	0.0005(2)	0.3200(2)	16
O(6)	0.3748(2)	0.1726(2)	0.4116(2)	20
O(7)	0.1754(2)	0.0945(2)	0.3887(2)	18
O(8)	0.1470(2)	-0.1081(2)	0.3919(2)	23
O(9)	0.0174(2)	-0.0010(2)	0.3060(2)	22
O(10)	0.1514(2)	-0.0790(2)	0.2225(2)	19
O(11)	0.3212(2)	-0.0878(2)	0.1807(2)	27
O(12)	0.2038(2)	0.0240(2)	0.0847(2)	20
O(13)	0.3151(2)	0.1085(2)	0.2246(2)	19
C(1)	0.1023(3)	0.1337(3)	0.1967(3)	19
C(2)	0.0458(3)	0.0817(3)	0.1456(3)	25
C(3)	0.0606(3)	0.1783(3)	0.2431(3)	25
C(4)	0.1390(3)	0.1925(3)	0.1568(3)	23
C(5)	0.3335(3)	-0.0420(3)	0.3660(3)	19
C(6)	0.4079(3)	-0.0141(3)	0.3516(3)	24
C(7)	0.3336(3)	-0.0243(3)	0.4411(3)	22
C(8)	0.3228(3)	-0.1295(3)	0.3516(3)	27
C(9)	0.4378(3)	0.2029(3)	0.4625(3)	22
C(10)	0.4414(3)	0.1632(4)	0.5323(3)	32
C(11)	0.4253(4)	0.2910(4)	0.4679(3)	38
C(12)	0.5113(3)	0.1867(4)	0.4420(3)	32
C(13)	0.1561(3)	0.1249(3)	0.4502(3)	22
C(14)	0.0950(3)	0.1887(3)	0.4285(3)	26

atom	x	y	z	$B_{iso}/Å^2 x\ 10^4$
C(15)	0.2278(3)	0.1601(4)	0.4983(3)	27
C(16)	0.1262(3)	0.0586(4)	0.4872(3)	30
C(17)	0.1420(3)	-0.1701(3)	0.4401(3)	30
C(18)	0.2091(5)	-0.1665(6)	0.5005(5)	94
C(19)	0.0691(6)	-0.1588(6)	0.4634(6)	89
C(20)	0.1378(7)	-0.2449(5)	0.4060(5)	95
C(21)	-0.0645(3)	-0.0007(3)	0.3006(3)	28
C(22)	-0.1054(3)	0.0270(4)	0.2278(3)	37
C(23)	0.0902(4)	-0.0830(4)	0.3129(4)	40
C(24)	0.0804(3)	0.0538(4)	0.3552(3)	37
C(25)	0.1144(3)	-0.1495(3)	0.1905(3)	25
C(26)	0.1624(4)	-0.2202(4)	0.2233(4)	42
C(27)	0.1103(4)	-0.1460(4)	0.1134(3)	36
C(28)	0.0354(4)	-0.1539(3)	0.2026(3)	33
C(29)	0.3727(4)	-0.1426(4)	0.1601(3)	36
C(30)	0.4520(4)	-0.1336(4)	0.2091(4)	47
C(31)	0.3746(5)	-0.1255(5)	0.0861(4)	63
C(32)	0.3453(4)	-0.2254(4)	0.1674(4)	51
C(33)	0.1865(3)	0.0322(3)	0.0099(3)	28
C(34)	0.2592(5)	0.0534(6)	-0.0114(4)	74
C(35)	0.1616(5)	-0.0451(5)	-0.0229(4)	64
C(36)	0.1285(7)	0.0938(6)	-0.0128(4)	96
C(37)	0.3718(3)	0.1464(3)	0.1957(3)	25
C(38)	0.4346(3)	0.1787(4)	0.2540(3)	33
C(39)	0.4062(3)	0.0851(4)	0.1556(3)	33
C(40)	0.3340(4)	0.2104(4)	0.1463(3)	36
C(41)	0.6361(8)	0.1358(7)	0.1171(6)	107
C(42)	0.6651(8)	0.1038(8)	0.1772(6)	113
C(43)	0.6411(5)	0.0643(5)	0.2328(5)	125
C(44)	0.6691(12)	0.0337(12)	0.2968(6)	193
C(45)	0.6460(6)	-0.0002(7)	0.3481(5)	90

Appendix 4.13. Bond Distances for $Ce_3(^tBuO)_{10}(NO_3)$ (4)

atom	atom	distance/Å
Ce(1)	O(1)	2.580(4)
Ce(1)	O(2)	2.582(4)
Ce(1)	O(4)	2.623(3)
Ce(1)	O(5)	2.544(3)
Ce(1)	O(6)	2.134(3)
Ce(1)	O(7)	2.516(3)
Ce(1)	O(13)	2.501(3)
Ce(2)	O(4)	2.482(3)
Ce(2)	O(5)	2.471(3)
Ce(2)	O(7)	2.273(3)
Ce(2)	O(8)	2.080(3)
Ce(2)	O(9)	2.066(3)
Ce(2)	O(10)	2.368(3)
Ce(3)	O(4)	2.470(3)
Ce(3)	O(5)	2.501(3)
Ce(3)	O(10)	2.360(3)
Ce(3)	O(11)	2.068(3)
Ce(3)	O(12)	2.077(3)
Ce(3)	O(13)	2.263(3)
N	O(1)	1.274(6)
N	O(2)	1.238(5)
N	O(3)	1.223(6)
O(4)	C(1)	1.448(6)
O(5)	C(5)	1.469(6)
O(6)	C(9)	1.417(6)
O(7)	C(13)	1.443(6)
O(8)	C(17)	1.442(6)
O(9)	C(21)	1.454(6)
O(10)	C(25)	1.443(6)
O(11)	C(29)	1.445(7)
O(12)	C(33)	1.443(6)
O(13)	C(37)	1.443(6)
C(1)	C(2)	1.531(7)
C(1)	C(3)	1.526(7)
C(1)	C(4)	1.524(7)
C(5)	C(6)	1.515(7)
C(5)	C(7)	1.517(7)
C(5)	C(8)	1.523(8)
C(9)	C(10)	1.525(8)
C(9)	C(11)	1.528(8)
C(9)	C(12)	1.506(8)
C(13)	C(14)	1.534(8)
C(13)	C(15)	1.528(7)
C(13)	C(16)	1.515(8)
C(17)	C(18)	1.480(9)
C(17)	C(19)	1.509(10)
C(17)	C(20)	1.437(11)
C(21)	C(22)	1.523(8)
C(21)	C(23)	1.515(8)
C(21)	C(24)	1.508(8)
C(25)	C(26)	1.532(8)
C(25)	C(27)	1.510(8)
C(25)	C(28)	1.507(8)
C(29)	C(30)	1.527(9)
C(29)	C(31)	1.503(9)
C(29)	C(32)	1.516(10)
C(33)	C(34)	1.517(10)
C(33)	C(35)	1.488(9)
C(33)	C(36)	1.472(9)
C(37)	C(38)	1.509(8)
C(37)	C(39)	1.532(8)
C(37)	C(40)	1.510(8)
C(41)	C(42)	1.316(14)
C(42)	C(43)	1.411(14)
C(43)	C(44)	1.310(14)
C(44)	C(45)	1.380(17)

Appendix 4.14. Bond Angles for $Ce_3(^tBuO)_{10}(NO_3)$ (4)

atom	atom	atom	angle/degree
O(1)	Ce(1)	O(2)	49.15(12)
O(1)	Ce(1)	O(6)	87.34(13)
O(1)	Ce(1)	O(13)	81.83(11)
O(1)	Ce(1)	O(7)	131.20(11)
O(2)	Ce(1)	O(6)	91.22(12)
O(2)	Ce(1)	O(13)	126.81(11)
O(2)	Ce(1)	O(7)	83.52(11)
O(4)	Ce(1)	O(5)	61.17(10)
O(4)	Ce(1)	O(1)	105.39(12)
O(4)	Ce(1)	O(2)	101.56(11)
O(4)	Ce(1)	O(6)	165.95(12)
O(4)	Ce(1)	O(13)	69.01(10)
O(4)	Ce(1)	O(7)	68.71(10)
O(5)	Ce(1)	O(1)	151.57(11)
O(5)	Ce(1)	O(2)	152.22(11)
O(5)	Ce(1)	O(6)	104.79(12)
O(5)	Ce(1)	O(13)	70.05(10)
O(5)	Ce(1)	O(7)	70.18(10)
O(6)	Ce(1)	O(13)	107.86(12)
O(6)	Ce(1)	O(7)	107.52(12)
O(13)	Ce(1)	O(7)	131.90(10)
O(4)	Ce(2)	O(5)	64.13(10)
O(4)	Ce(2)	O(7)	75.04(11)
O(4)	Ce(2)	O(8)	161.67(12)
O(4)	Ce(2)	O(9)	99.95(12)
O(4)	Ce(2)	O(10)	70.69(11)
O(5)	Ce(2)	O(7)	75.49(11)
O(5)	Ce(2)	O(8)	98.28(12)
O(5)	Ce(2)	O(9)	164.07(12)
O(7)	Ce(2)	O(8)	106.76(13)
O(7)	Ce(2)	O(9)	100.56(13)
O(7)	Ce(2)	O(10)	140.33(11)
O(8)	Ce(2)	O(9)	97.64(13)
O(8)	Ce(2)	O(10)	99.92(13)
O(9)	Ce(2)	O(10)	104.43(13)
O(4)	Ce(3)	O(5)	63.87(10)
O(4)	Ce(3)	O(13)	75.58(11)
O(4)	Ce(3)	O(10)	71.04(11)
O(4)	Ce(3)	O(11)	161.06(12)
O(4)	Ce(3)	O(12)	100.42(12)
O(5)	Ce(3)	O(13)	74.68(11)
O(5)	Ce(3)	O(10)	71.60(11)
O(5)	Ce(3)	O(11)	98.06(12)
O(5)	Ce(3)	O(12)	164.10(12)
O(10)	Ce(3)	O(11)	98.82(14)
O(10)	Ce(3)	O(12)	106.74(12)
O(11)	Ce(3)	O(12)	97.82(14)
O(13)	Ce(3)	O(10)	140.22(12)
O(13)	Ce(3)	O(11)	106.28(14)
O(13)	Ce(3)	O(12)	99.93(12)
O(1)	N	O(2)	17.4(4)
O(1)	N	O(3)	120.4(5)
O(2)	N	O(3)	122.1(5)
Ce(1)	O(1)	N	95.9(3)
Ce(1)	O(2)	N	96.8(3)
Ce(1)	O(4)	Ce(2)	93.85(10)
Ce(1)	O(4)	Ce(3)	94.08(10)
Ce(1)	O(4)	C(1)	119.54(27)
Ce(2)	O(4)	Ce(3)	96.06(11)
Ce(2)	O(4)	C(1)	123.64(27)
Ce(3)	O(4)	C(1)	122.35(26)
Ce(1)	O(5)	Ce(2)	96.09(11)
Ce(1)	O(5)	Ce(3)	95.28(10)
Ce(1)	O(5)	C(5)	115.67(26)
Ce(2)	O(5)	Ce(3)	95.52(11)
Ce(2)	O(5)	C(5)	124.21(27)
Ce(3)	O(5)	C(5)	123.39(26)
Ce(1)	O(6)	C(9)	169.5(3)
Ce(1)	O(7)	Ce(2)	102.19(12)
Ce(1)	O(7)	C(13)	126.34(28)
Ce(2)	O(7)	C(13)	131.4(3)
Ce(2)	O(8)	C(17)	169.7(3)

atom	atom	atom	angle/degree
Ce(2)	O(9)	C(21)	172.2(3)
Ce(2)	O(10)	Ce(3)	102.29(12)
Ce(2)	O(10)	C(25)	128.3(3)
Ce(3)	O(10)	C(25)	129.4(3)
Ce(3)	O(11)	C(29)	168.3(3)
Ce(1)	O(12)	C(33)	169.6(3)
Ce(1)	O(13)	Ce(3)	102.88(12)
Ce(1)	O(13)	C(37)	126.7(3)
Ce(3)	O(13)	C(37)	130.4(3)
O(4)	C(1)	C(2)	108.7(4)
O(4)	C(1)	C(3)	109.3(4)
O(4)	C(1)	C(4)	110.0(4)
C(2)	C(1)	C(3)	109.8(4)
C(2)	C(1)	C(4)	109.9(4)
C(3)	C(1)	C(4)	109.0(4)
O(5)	C(5)	C(6)	108.8(4)
O(5)	C(5)	C(7)	108.8(4)
O(5)	C(5)	C(8)	108.8(4)
C(6)	C(5)	C(7)	109.6(4)
C(6)	C(5)	C(8)	110.4(4)
C(7)	C(5)	C(8)	110.3(4)
O(6)	C(9)	C(10)	109.4(4)
O(6)	C(9)	C(11)	107.5(4)
O(6)	C(9)	C(12)	110.2(4)
C(10)	C(9)	C(11)	110.4(5)
C(10)	C(9)	C(12)	108.7(5)
C(11)	C(9)	C(12)	110.6(5)
O(7)	C(13)	C(14)	108.9(4)
O(7)	C(13)	C(15)	109.0(4)
O(7)	C(13)	C(16)	109.2(4)
C(14)	C(13)	C(15)	109.6(5)
C(14)	C(13)	C(16)	110.3(4)
C(15)	C(13)	C(16)	109.9(4)
O(8)	C(17)	C(18)	109.5(5)
O(8)	C(17)	C(19)	108.2(5)
O(8)	C(17)	C(20)	110.1(5)

atom	atom	atom	angle/degree
C(18)	C(17)	C(19)	110.5(7)
C(18)	C(17)	C(20)	110.6(8)
C(19)	C(17)	C(20)	107.9(8)
O(9)	C(21)	C(22)	108.7(4)
O(9)	C(21)	C(23)	109.3(5)
O(9)	C(21)	C(24)	108.5(4)
C(22)	C(21)	C(23)	110.1(5)
C(22)	C(21)	C(24)	110.7(5)
C(23)	C(21)	C(24)	109.5(5)
O(10)	C(25)	C(26)	108.6(4)
O(10)	C(25)	C(27)	108.3(4)
O(10)	C(25)	C(28)	108.9(4)
C(26)	C(25)	C(27)	110.0(5)
C(26)	C(25)	C(28)	110.5(5)
C(27)	C(25)	C(28)	110.5(5)
O(11)	C(29)	C(30)	108.8(5)
O(11)	C(29)	C(31)	108.7(5)
O(11)	C(29)	C(32)	109.2(5)
C(30)	C(29)	C(31)	110.9(6)
C(30)	C(29)	C(32)	108.0(6)
C(31)	C(29)	C(32)	111.2(6)
O(12)	C(33)	C(34)	109.0(5)
O(12)	C(33)	C(35)	109.2(5)
O(12)	C(33)	C(36)	109.9(5)
C(34)	C(33)	C(35)	106.2(6)
C(34)	C(33)	C(36)	110.2(7)
C(35)	C(33)	C(36)	112.5(7)
O(13)	C(37)	C(38)	109.3(4)
O(13)	C(37)	C(39)	108.5(4)
O(13)	C(37)	C(40)	109.3(4)
C(38)	C(37)	C(39)	108.8(5)
C(38)	C(37)	C(40)	111.5(5)
C(39)	C(37)	C(40)	109.5(5)
C(41)	C(42)	C(43)	141.7(14)
C(42)	C(43)	C(44)	141.7(13)
C(43)	C(44)	C(45)	139.1(17)

5895-3